



Universidad de Valladolid

ESCUELA DE INGENIERÍAS INDUSTRIALES
DEPARTAMENTO DE INGENIERÍA ENERGÉTICA Y FLUIDOMECÁNICA

Experimental Characterization of a Microtubular Solid Oxide Fuel Cell fueled with Hydrogen, Methane and Hydrogen Sulfide

presentada por:

Carlos ANDRÉS LOZANO

PARA OPTAR AL GRADO DE DOCTOR POR LA
UNIVERSIDAD DE VALLADOLID

dirigida por

Dr. D. Francisco V. TINAUT FLUIXÁ

Dr. D. John W. VAN ZEE

Valladolid, marzo 2012

Me gustaría aprovechar estas primeras líneas para mostrar mi agradecimiento a todas aquellas personas que han hecho posible la realización de esta Tesis Doctoral.

Al *Grupo de Motores Térmicos y Energías Renovables* del *Departamento de Ingeniería Energética y Fluidomecánica* de la *Universidad de Valladolid*, por darme la oportunidad de realizar este proyecto dentro de su área de investigación y apoyarme en todos los sentidos. Al departamento de *Ingeniería Química* de la *Universidad de South Carolina*, con especial mención al *Grupo de Pilas de Combustible del Dr. Van Zee*, por acogerme durante mi estancia en los Estados Unidos y darme la oportunidad de usar sus instalaciones. También me gustaría dar las gracias a todas las personas integrantes de estos dos grupos de investigación, por su compañerismo y su disposición para ayudar en cualquier momento, haciendo inolvidables todos los momentos compartidos con ellos.

A los profesores Francisco Tinaut y John Van Zee, mis directores de tesis, por guiarme con su experiencia, conocimientos, dedicación y paciencia a través de todo el desarrollo de la tesis doctoral.

A la *Comisión Fulbright*, la *Universidad de Valladolid* y la *Fundación CIDAUT*, por su apoyo financiero a lo largo del desarrollo de la tesis.

A todos los compañeros y amigos que me han acompañado a lo largo de esta larga travesía, por compartir mis preocupaciones y alegrías.

A mi padre y mi hermano, por estar siempre ahí, incluso en los momentos más difíciles, apoyándome y animándome a continuar.

A Fátima, mi mujer, por su incondicional apoyo en todo momento, su paciencia y su cariño, haciéndolo todo más fácil.

A mi madre, Teresa, a la que siempre recordaremos con cariño.

A todos, de corazón,

Muchas Gracias.

I would like to use these first lines of the dissertation to thank everybody that made this PhD possible.

The *Group of Combustion Engines and Renewable Energies* of the *Department of Energy and Fluidmechanics Engineering* of the *University of Valladolid*, for giving me the chance to do this project inside their research area and supporting me in every sense. The *Department of Chemical Engineering* of the *University of South Carolina*, with special mention to *Dr. Van Zee's Fuel Cells Group* for admitting me during my stay at the United States of America and for giving me the chance of using their facilities. Also, I would like to thank everyone at these two research groups for their companionship and their willingness to help any time, making all the moments we shared unforgettable.

The Professors Francisco Tinaut and John Van Zee, my advisors, for guiding me with their experience, knowledge, dedication and patience.

The *Spanish Fulbright Commission*, the *University of Valladolid* and *CIDAUT Foundation*, for their financial support during this time.

All the friends I made along this long journey, they shared my worries and happiness.

My father and brother, for always being there when I needed them, even in the most difficult moments, supporting me and encouraging me to go on.

Fátima, my wife, for her unconditional support, her patience and her affection making everything easier.

My mother, Teresa. We will always remember her with affection.

To all of you, deep from my heart,

Thank you very much.

En memoria de mi madre, Teresa.

GENERAL INDEX

1. Introducción.....	3
1.1. Contexto Energético.....	3
1.2. Antecedentes	6
1.3. Objetivos	7
1.3.1. Objetivos Generales	7
1.3.2. Objetivos Particulares.....	8
1.4. Estructura del Documento.....	9
1.5. Referencias.....	11
1. Introduction.....	17
1.1. Energy Context	17
1.2. Previous Work.....	19
1.3. Objectives	20
1.3.1. General Objectives	20
1.3.2. Specific Objectives	21
1.4. Structure of the Document.....	22
1.5. References.....	24

2. Fuel Cells and SOFCs: Current Situation	29
2.1. Introduction.....	29
2.2. Fuel cells.....	30
2.2.1. Introduction.....	30
2.2.2. Types of Fuel Cells.....	34
2.2.3. Solid Oxide Fuel Cells (SOFCs)	36
2.2.3.1. Electrolyte Materials	38
2.2.3.2. Anode Materials.....	39
2.2.3.3. Cathode Materials	39
2.3. Techniques and Methods of Characterization.....	40
2.3.1. Electrochemical Techniques	42
2.3.1.1. Polarization Curves	43
2.3.1.2. Cyclic Voltammetry (CV).....	43
2.3.1.3. Transitory Analysis	44
2.3.1.4. Electrochemical Impedance Spectroscopy (EIS).....	44
2.3.2. Other Techniques	44
2.4. Summary in English.....	45
2.5. Summary in Spanish.....	46
2.6. References	48

3. Experimental Facility and Electrochemical Techniques.....	63
3.1. Introduction	63
3.2. Solid Oxide Fuel Cell	64
3.3. Experimental Facility	67
3.4. Experimental Electrochemical Techniques	72
3.4.1. Introduction.....	72
3.4.2. Polarization Curve	77
3.4.3. Electrochemical Impedance Spectroscopy	79
3.4.4. Cyclic Voltammetry	81
3.4.5. Transient Analysis	82
3.4.6. Mass Balance	84
3.5. Summary in English	86
3.6. Summary in Spanish	86
3.7. References.....	87

4. Experimental Characterization of the SOFC Using Hydrogen.....	95
4.1. Introduction.....	95
4.2. Effect of Dilution on the Current.....	96
4.3. Polarization Curves.....	104
4.4. Electrochemical Impedance Spectroscopy.....	107
4.5. Electrochemical Reactions	111
4.6. Analysis of the Results: Fuel Cell Structure.....	114
4.7. Summary in English.....	116
4.8. Summary in Spanish.....	117
4.9. References	118
5. Experimental Characterization of the SOFC Using Methane	123
5.1. Introduction.....	123
5.2. Effect of Methane and Dilution on the Current.....	125
5.3. Polarization Curves.....	135
5.4. Electrochemical Impedance Spectroscopy.....	140
5.5. Carbon Mass Balance.....	146
5.6. Electrochemical Reactions	152
5.7. Summary in English.....	158
5.8. Summary in Spanish.....	160
5.9. References	161

6. Preliminary Characterization of the SOFC	
Contamination with Hydrogen Sulfide.....	167
6.1. Introduction	167
6.2. Effect of Hydrogen Sulfide on the Current.....	169
6.3. Polarization Curves	177
6.4. Electrochemical Impedance Spectroscopy	179
6.5. Summary in English	181
6.6. Summary in Spanish	183
6.7. References.....	185
7. Conclusions and Future Research.....	191
7.1. Conclusions	191
7.1.1. General Conclusions.....	191
7.1.2. Specific Conclusions.....	192
7.2. Future Research.....	196
7. Conclusiones y Trabajo Futuro.....	201
7.1. Conclusiones	201
7.1.1. Conclusiones Generales.....	201
7.1.2. Conclusiones Particulares	202
7.2. Trabajo Futuro.....	206
References.....	211

A1. Limiting Current Calculation.....	233
A1.1. Introduction	233
A1.2. Model Used	233
A1.3. Calculation and Results.....	235
A1.4. References.....	239
A2. Reaction Potential Calculation.....	243
A2.1. Introduction	243
A2.2. Procedure.....	243
A2.3. References.....	245

ÍNDICE GENERAL (EN ESPAÑOL)

1. Introducción.....	3
1.1. Contexto Energético.....	3
1.2. Antecedentes	6
1.3. Objetivos	7
1.3.1. Objetivos Generales	7
1.3.2. Objetivos Particulares.....	8
1.4. Estructura del Documento.....	9
1.5. Referencias.....	11
1. Introducción.....	17
1.1. Contexto Energético.....	17
1.2. Antecedentes	19
1.3. Objetivos	20
1.3.1. Objetivos Generales	20
1.3.2. Objetivos Particulares.....	21
1.4. Estructura del Documento.....	22
1.5. Referencias	24

2. Pilas de Combustible y SOFCs: Situación Actual	29
2.1. Introducción	29
2.2. Pilas de Combustible	30
2.2.1. Introducción	30
2.2.2. Tipos de Pilas de Combustible	34
2.2.3. Pilas de Combustible de Óxido Sólido (SOFCs)	36
2.2.3.1. Materiales para el Electrolito.....	38
2.2.3.2. Materiales para el Ánodo.....	39
2.2.3.3. Materiales para el Cátodo.....	39
2.3. Métodos y Técnicas de Caracterización	40
2.3.1. Técnicas Electroquímicas	42
2.3.1.1. Curvas de Polarización.....	43
2.3.1.2. Voltametría Cíclica (CV).....	43
2.3.1.3. Análisis del Transitorio.....	44
2.3.1.4. Espectroscopía de Impedancia Electroquímica (EIS)	44
2.3.2. Otras Técnicas.....	44
2.4. Resumen en Inglés	45
2.5. Resumen en Español.....	46
2.6. Referencias	48

3. Instalación Experimental y Técnicas Electroquímicas	63
3.1. Introducción.....	63
3.2. La Pila de Óxido Sólido.....	64
3.3. Instalación Experimental	67
3.4. Técnicas Electroquímicas Experimentales.....	72
3.4.1. Introducción	72
3.4.2. Curva de Polarización.....	77
3.4.3. Espectroscopía de Impedancia Electroquímica	79
3.4.4. Voltametría Cíclica	81
3.4.5. Análisis del Transitorio.....	82
3.4.6. Balance de Masa	84
3.5. Resumen en Inglés.....	86
3.6. Resumen en Español	86
3.7. Referencias.....	87

4. Caracterización Experimental de la SOFC	
 Utilizando Hidrógeno	95
4.1. Introducción	95
4.2. Efecto de la Dilución en la Corriente Eléctrica	96
4.3. Curvas de Polarización	104
4.4. Espectroscopía de Impedancia Electroquímica	107
4.5. Reacciones Electroquímicas	111
4.6. Análisis de los Resultados: Estructura de la Pila	114
4.7. Resumen en Inglés	116
4.8. Resumen en Español.....	117
4.9. Referencias	118
5. Caracterización Experimental de la SOFC	
 Utilizando Metano.....	123
5.1. Introducción	123
5.2. Efecto del Metano y la Dilución en la Corriente	125
5.3. Curvas de Polarización	135
5.4. Espectroscopía de Impedancia Electroquímica	140
5.5. Balance de Masa del Carbono	146
5.6. Reacciones Electroquímicas	152
5.7. Resumen en Inglés	158
5.8. Resumen en Español.....	160
5.9. Referencias	161

6. Caracterización Prelimiar de la Contaminación de la SOFC con Ácido Sulfídrico	167
6.1. Introducción.....	167
6.2. Efecto del Ácido Sulfídrico en la Corriente Eléctrica	169
6.3. Curvas de Polarización	177
6.4. Espectroscopía de Impedancia Electroquímica.....	179
6.5. Resumen en Inglés.....	181
6.6. Resumen en Español	183
6.7. Referencias.....	185
7. Conclusiones y Trabajo Futuro	191
7.1. Conclusiones	191
7.1.1. Conclusiones Generales.....	191
7.1.2. Conclusiones Particulares	192
7.2. Trabajo Futuro.....	196
7. Conclusiones y Trabajo Futuro	201
7.1. Conclusiones	201
7.1.1. Conclusiones Generales.....	201
7.1.2. Conclusiones Particulares	202
7.2. Trabajo Futuro.....	206
Referencias.....	211

A1. Cálculo de la Corriente Límite	233
A1.1. Introducción.....	233
A1.2. Modelo Empleado	233
A1.3. Cálculos y Resultados	235
A1.4. Referencias.....	239
A2. Cálculo del Potencial de Reacción.....	243
A2.1. Introducción.....	243
A2.2. Procedimiento	243
A2.3. Referencias.....	245

LIST OF FIGURES

Figure 2.1: Working principle for different kinds of fuel cells (adapted from [59]).	31
Figure 3.1: Schematic of the MTEC SOFC structure, from [17].	65
Figure 3.2: SOFC picture immediately after the drying process.	67
Figure 3.3: Experimental setup at the University of South Carolina, from [16].	68
Figure 3.4: SOFC mechanical support and air blower for the cathode side.	68
Figure 3.5: Picture of the experimental setup at the University of South Carolina.	70
Figure 3.6: Example of polarization curves for PEMFC, from [9].	78
Figure 3.7: Example of EIS test for different systems, from [10].	80
Figure 3.8: Example of CV test for PEM with different catalyst loading, from [11].	81
Figure 4.1: Expected ideal transient H ₂ dilution with Ar. Current scale arbitrary and depends on whether electrodes operate under kinetic or mass transport regimes.	97
Figure 4.2: Transient 1 st fuel cell, 50% H ₂ in Ar.	98
Figure 4.3: Transient 2 nd fuel cell, 10% H ₂ in Ar.	99
Figure 4.4: Transient 1 st fuel cell, 50% H ₂ in Ar, adjusted to exponential expression.	102
Figure 4.5: Transient 2 nd fuel cell, 10% H ₂ in Ar, adjusted to exponential expression.	103
Figure 4.6: Polarization curves 1 st fuel cell, 50% H ₂ in Ar.	105
Figure 4.7: Polarization curves 2 nd fuel cell, 10% H ₂ in Ar.	106
Figure 4.8: Impedance test 1 st fuel cell, 50% H ₂ in Ar.	108
Figure 4.9: Impedance test 2 nd fuel cell, 10% H ₂ in Ar.	109
Figure 4.10: Expected reactions (not corrected w/ activities, E ^o _{900°C}), H ₂ fuel, from [12].	112
Figure 4.11: Expected reactions (corrected with activities, E _{900°C}), H ₂ fuel, from [12].	113
Figure 5.1: Transient expected for the diluted methane case.	127
Figure 5.2: Transient expected for the pure methane case.	128
Figure 5.3: Transient 1 st fuel cell, 50% H ₂ /CH ₄ in Ar.	128
Figure 5.4: Transient 2 nd fuel cell, 10% H ₂ /CH ₄ in Ar.	129
Figure 5.5: Transient 3 rd fuel cell, no dilution with Ar.	129
Figure 5.6: C-H-O equilibrium diagram at 750°C, from [1].	130
Figure 5.7: Transient adjusted with exponential function, 1 st cell.	133
Figure 5.8: Transient adjusted with exponential function, 2 nd cell.	134
Figure 5.9: Transient adjusted with exponential function, 3 rd cell.	134
Figure 5.10: Polarization curves 1 st fuel cell, 50% H ₂ /CH ₄ in Ar.	137

Figure 5.11: Polarization curves 2 nd fuel cell, 10% H ₂ /CH ₄ in Ar.	137
Figure 5.12: Polarization curves 3 rd fuel cell, no dilution with Ar.	138
Figure 5.13: Impedance test 1 st fuel cell, 50% H ₂ /CH ₄ in Ar.	141
Figure 5.14: Impedance test 2 nd fuel cell, 10% H ₂ /CH ₄ in Ar.	142
Figure 5.15: Impedance test 3 rd fuel cell, no dilution with Ar.	143
Figure 5.16: SOFC anode: Input and outputs.	147
Figure 5.17: Expected reactions (E ⁰ _{900°C} , not corrected w/ activities), CH ₄ fuel, [14].	153
Figure 5.18: Expected reactions (E _{900°C} , corrected with activities), CH ₄ fuel, from [14].	154
Figure 6.1: Ideal transient expected for H ₂ S contamination at 0.9V.	168
Figure 6.2: Transient during 25ppm H ₂ S cyclic contamination.	170
Figure 6.3: Transient during 25ppm H ₂ S cyclic contamination (adjusted).	172
Figure 6.4: Polarization curves and power showing the irreversible effect of H ₂ S.	177
Figure 6.5: Impedance curves showing the irreversible effect of H ₂ S.	179
Figure A1.1: Flow pattern for the correlation used (anode side).	234
Figure A1.2: Real flow pattern of the fuel cell (anode side).	234

LIST OF TABLES

Table 2.1: Main Fuel Cell Types.	35
Table 2.2: Main Electrolyte Materials for SOFC. Adapted from [6].	38
Table 3.1: Characteristics of the SOFC fabricated by the MTEC in Thailand.	67
Table 3.2: Models used in experimental setup at the University of South Carolina.	71
Table 4.1: Flow conditions of the tests carried out.	96
Table 4.2: Summary of the results obtained with the transients.	104
Table 4.3: Minimum stoichiometry while performing polarization curves.	105
Table 4.4: Expected reactions when H ₂ is used as fuel.	112
Table 5.1: Flow conditions of the tests carried out.	124
Table 5.2: Summary of the results obtained with the transient analysis.	132
Table 5.3 Minimum stoichiometry while performing polarization curves.	136
Table 5.4: Conditions of each sample collected (2 nd cell, 10% dilution in Ar).	147
Table 5.5: Results obtained for each sample.	149
Table 5.6: Reactions when CH ₄ is used as fuel.	152
Table 5.7: Percentage of reaction from outlet composition (for CH ₄ fuel, 0.6V).	158
Table 5.8: Concentration of each species found at the outlet of the SOFC at 0.6V.	158
Table 6.1: Flow conditions of the tests carried out.	169
Table 6.2: Summary of the results obtained with the transient analysis (0.9V).	176
Table A1.1: Kinematic viscosity (ν) at 900°C for all different species, in m ² /s.	236
Table A1.2: Averaged molecule diameter (σ) in Å.	237
Table A1.3: Calculated diffusivities (Chapman-Enskog Theory).	237
Table A1.4: Geometric characteristics of the fuel cell.	238
Table A1.5: Limiting currents calculated for all different reactions.	238

LIST OF SYMBOLS

Latin Symbols:

c	Concentration
C_p	Constant Pressure Heat Capacity
D	Diffusivity
d_e	Characteristic Diameter
F	Faraday's Constant
G	Gibbs Free Energy
H	Enthalpy
i	Current Density
I	Electric Current
i_0	Exchange Current Density
I_0	Initial Electric Current (at $t = t_0$)
i_L	Limiting Current Density
I_{ss}	Current at Steady State
L	Characteristic Length
M	Molar mass of an Element
m	Mass
n	Number of Electrons Involved in a Half-Reaction.
P	Pressure
Q	Volumetric Flux
R	Ideal Gas Constant
Re	Reynolds Number
S	Entropy
Sc	Schmidt Number
Sh	Sherwood Number
T	Temperature

t	Time
t_0	Initial Time
V	Potential
V_{avg}	Average Velocity of the Flow
Z	Total Electric Charge

Greek Symbols:

α	Tafel Constant
Γ	Time Constant
η	Overpotential
σ	Averaged Collision Diameter
ν	Kinematic viscosity
Ω	Collision Integral Parameter

CAPÍTULO 1

Introducción

Contenido

1.1. Contexto Energético.....	3
1.2. Antecedentes	6
1.3. Objetivos	7
1.3.1. Objetivos Generales	7
1.3.2. Objetivos Particulares.....	8
1.4. Estructura del Documento.....	9
1.5. Referencias.....	11

1. Introducción

1.1. Contexto Energético

Vivimos en un mundo con una gran demanda energética, que crece día a día. Desde los tiempos de la Revolución Industrial en los siglos XVIII y XIX nos vamos haciendo más y más dependientes de la energía en nuestra vida cotidiana. La humanidad consume en la actualidad un promedio de 16TJ cada segundo (o lo que es lo mismo, una potencia media de 16TW), lo que es varios órdenes de magnitud menor de la potencia promedio que recibimos del sol en forma de radiación electromagnética - sobre 170,000TW, de los cuales aproximadamente la mitad llegan a la superficie de la Tierra [7]. Obviamente una parte de dicha energía se consume en los distintos fenómenos naturales, como el ciclo del agua o el viento. A pesar de ello, el resto de energía no usada en los ciclos naturales es tan grande que debería, en principio, cubrir la demanda energética actual holgadamente. Sin embargo el problema aparece a la hora de cómo transformarla en otra forma de energía que podamos aprovechar para nuestras necesidades (principalmente, energía eléctrica). Los combustibles fósiles fueron la primera forma de energía que se aprovechó a gran escala e incluso hoy en día siguen siendo nuestra principal fuente de energía. Los combustibles fósiles se forman a partir de materia orgánica muerta que fue enterrada bajo la superficie de la Tierra. En ellos la energía del Sol fue transformándose en energía química a lo largo de millones de años. Por ello presentan una densidad energética extraordinariamente alta (tanto en términos volumétricos como en términos másicos) que los hacen candidatos ideales para la mayoría de nuestras aplicaciones.

El problema que presentan los combustibles fósiles es que requieren de un periodo de tiempo extremadamente largo - millones de años - bajo determinadas condiciones de presión y temperatura para ser obtenidos. Considerando este hecho queda claro que unas pocas generaciones están

consumiendo unos recursos que pertenecían a millones de generaciones, dado que ese fue el tiempo que llevó producirlos. Por lo tanto se puede decir de forma contundente que llevamos bastante tiempo viviendo por encima de nuestras posibilidades. Sin embargo, dado que nadie está dispuesto a cambiar el estilo de vida actual, se necesitan fuentes de energía alternativas así como un empleo más eficiente de la energía disponible.

Estos problemas también se pueden considerar desde el punto de vista de la sostenibilidad. Se dice que una fuente de energía es renovable cuando puede ser usada de forma continua, esto es, cuando puede ser producida tan rápidamente como es consumida. Un buen ejemplo de este tipo de energía es la energía hidroeléctrica, donde la energía cinética y/o potencial del agua de un río (que proviene del ciclo del agua, esto es, del sol) se transforma en energía mecánica a través de una hidroturbina. Después esta energía se transforma en energía mecánica usando un alternador. Los combustibles fósiles, por otra parte, no son considerados fuentes de energía renovables dado que el tiempo que lleva obtenerlos es mucho mayor que lo que lleva consumirlos. Por ello, la única solución a largo plazo para el problema energético es el empleo de energías renovables como única fuente de energía para nuestras actividades.

Dado que el problema energético es probablemente el mayor reto al que la humanidad se enfrenta en este siglo, se está realizando un grandísimo esfuerzo en todos los sentidos para desarrollar nuevas fuentes de energía renovables. El problema que presentan la mayoría de estas fuentes de energía es su carácter intermitente con dificultad en la predicción de su producción, además de una baja densidad energética. Por ello, una forma de almacenamiento eficiente es un punto crítico a la hora de su implementación. Las baterías eléctricas son capaces de almacenar electricidad - de hecho, en forma de energía electroquímica - pero presentan grandes problemas que parecen ser difíciles de resolver con la tecnología actual. Estos problemas incluyen una baja densidad de energía y potencia específica, se descargan al estar tiempo sin emplearse y presentan una alta degradación ante repetidos ciclos de carga/descarga (baja vida útil).

En este sentido, el hidrógeno como vector energético (esto es, como medio para almacenar y transportar la energía), parece tener un mayor potencial que las baterías tradicionales y muchos expertos esperan que sea el principal vector energético en el futuro a largo plazo, ya que tiene propiedades muy interesantes como una energía y potencia específicas mucho mayor a la de las baterías. Hay diversos modos para aprovechar energéticamente el hidrógeno, siendo las tecnologías más prometedoras los motores de combustión interna (mezclado con otros combustibles) y las pilas de combustible.

En primer lugar, los motores de combustión interna transforman la energía química contenida en el hidrógeno en calor, que es posteriormente transformado en trabajo mecánico. Según la Segunda Ley de la Termodinámica, no todo el calor generado puede ser completamente transformado en trabajo mecánico. Esto significa que la eficiencia de los motores de combustión está limitada por un rendimiento teórico máximo llamado rendimiento de Carnot. El rendimiento con el que los motores actuales funcionan varía entre un 20% y un 40% en función de las condiciones de operación.

Por otro lado, las pilas de combustibles ofrecen una transformación electroquímica directa de la energía química del hidrógeno en electricidad, por lo que no presentan tan limitación y por ello tienen la capacidad de presentar mayores rendimientos [1]. Sin embargo, otras limitaciones - que serán discutidas a lo largo de esta memoria - causan que las pilas de combustible reales tengan rendimientos de alrededor del 50% cuando funcionan de forma autónoma [2]. Las pilas de combustible de alta temperatura (como las pilas de Óxido Sólido - SOFC por sus siglas en inglés), presentan unos rendimientos globales mucho mayores cuando se emplean en conjunción con ciclos de cogeneración [3-5], esto es, cuando el calor sobrante se emplea para otros propósitos.

Al comparar las pilas con los motores de combustión [6], las pilas de combustible presentan la ventaja adicional de no tener partes móviles (excepto aquellas relacionadas con el equipo auxiliar, como compresores, bombas y sopladores), lo que les da el potencial de una vida útil muy

larga si otros problemas que presentan son superados. También, el hecho de no tener partes móviles las convierte en un aparato extremadamente silencioso incluso a máxima potencia, lo que ciertamente se adecua a determinadas aplicaciones donde el ruido debe ser minimizado, como por ejemplo aplicaciones militares.

Por todas estas razones, las pilas de combustible parecen ser la alternativa energética más prometedora a largo plazo. Sus propiedades las convierten en el candidato perfecto para resolver los problemas que las fuentes de energía renovables presentan y por tanto el estudio de sus limitaciones para superarla es una prioridad en la comunidad científica y justifica el interés del tema de esta tesis doctoral.

1.2. Antecedentes

La energía y la forma en que la usamos es uso de los principales problemas a los que la humanidad se enfrenta en este siglo. Desde la Revolución Industrial la demanda global de energía ha crecido de tal manera que las fuentes tradicionales de energía - en concreto los combustibles fósiles - parecen ser inadecuados dado que incrementan la contaminación del medioambiente y se agotarán en un futuro relativamente próximo. Dentro del *Grupo de Motores Térmicos y Energías Renovables* (MYER) de la Universidad de Valladolid - donde esta tesis doctoral ha sido desarrollada - siempre ha habido un gran interés en el campo energético. Los objetivos se encaminan a aumentar las eficiencias de los distintos procesos para reducir las emisiones contaminantes y el consumo energético, así como la búsqueda de combustibles alternativos y nuevos dispositivos de conversión energética.

El tema de esta tesis queda claramente dentro del campo de investigación del Grupo MYER, dado que las pilas de combustible son probablemente la tecnología más prometedora en el mundo energético en la actualidad. La producción de hidrógeno de diversas fuentes, en especial a partir de combustibles renovables, y su utilización en distintos dispositivos (motores, pilas de combustible), son objetivos del Grupo.

La parte experimental de la investigación fue llevada a cabo en la Universidad de South Carolina, en Columbia, South Carolina, USA, con una beca de la Comisión Fulbright. El Grupo del Dr. Van Zee, en el Departamento de Ingeniería Química de la Universidad de South Carolina es uno de los grupos de investigación líderes en este campo, y probablemente sea uno de los mejores lugares para estudiar y comprender estas tecnologías. Los resultados obtenidos durante mi estancia en la Universidad de South Carolina, así como los conocimientos adquiridos durante el tiempo que pasé haciendo esta tesis doctoral - tanto en la Universidad de Valladolid, como en la Universidad de South Carolina - se refleja en esta memoria de la tesis doctoral.

1.3. Objetivos

Los objetivos fundamentales de este trabajo se pueden clasificar en dos categorías atendiendo a su carácter: los objetivos generales y los objetivos particulares.

1.3.1. Objetivos Generales

El primer objetivo fundamental de este trabajo está relacionado con la carácter académico de la tesis doctoral. El doctorado es el estándar más alto del sistema educativo y persigue la excelencia a través de la educación. La investigación, como cualquier otra ciencia, requiere dedicación para poder alcanzar las habilidades para llegar a desarrollarla de forma satisfactoria. El doctorado es la mejor escuela para lograrlo, y por tanto un objetivo para esta tesis doctoral es la adquisición de la habilidades necesarias para llevar a cabo investigación al más alto nivel. Esto incluye identificación de problemas, diseño tanto de experimentos como de los bancos de ensayo y la construcción de los mismos, aprendizaje de procedimientos experimentales para poder llevar a cabo los experimentos requeridos y análisis de los resultados usando distintas

herramientas. A este respecto, la estancia en uno de los mejores centros de investigación del mundo ciertamente ayudó a la consecución de este objetivo.

Otro objetivo muy importante que está contenido en esta categoría es la adquisición de una extensa base de conocimiento relacionada con el campo de estudio, pilas de combustible, que debe incluir tanto conocimientos generales (como las bases de la electroquímica) y también un conocimiento más particular que solo es relevante a las pilas de combustible y no otros procesos electroquímicos (las particulares propiedades de las pilas de combustible, como los requerimientos del flujo, instrumentación...).

El último gran objetivo general está relacionado con la habilidad para aplicar las habilidades y conocimientos adquiridos en el laboratorio al mundo real. Esto incluye la aplicación de técnicas adquiridas a campos distintos de las pilas de combustible.

1.3.2. Objetivos Particulares

Los objetivos particulares de este proyecto están íntimamente ligados a la pila de combustible que fue empleada. El primer objetivo particular incluye la realización de una revisión bibliográfica que proporcione los conocimientos requeridos sobre pilas de combustible y su estado del arte actual.

El segundo objetivo particular está relacionado con la caracterización de la Pila de Combustible de Óxido Sólido (SOFC, de sus siglas en inglés). Esto requiere tanto habilidades experimentales como destreza a la hora de analizar los resultados, aplicadas a este caso concreto. Caracterizar la pila de combustible es muy importante, dado que permite su comparación con otras pilas y también influye en el diseño experimental que se debe realizar a continuación.

El tercer objetivo está relacionado con la metodología seguida para realizar los experimentos con la pila de Óxido Sólido. Es muy importante aprender la forma de realizar experimentos que sean significativos para poder explicar los fenómenos observados. Además de esto, los experimentos deberán perseguir la consecución de los objetivos marcados por el proyecto.

Una vez que esto ha sido logrado, todos los resultados deberán ser analizados. La compresión de los procesos que tiene lugar dentro de la pila de combustible, su modelado, y el uso de los conocimientos adquiridos para mejorar el diseño de la pila de combustible es el objetivo último de este proyecto.

1.4. Estructura del Documento

El documento está estructurado en siete capítulos y un apéndice. El primero de los capítulos proporciona una descripción del fondo del doctorando, así como del grupo. También describe las particularidades del trabajo que ha sido llevado a cabo y la razón por la que es importante y relevante para la comunidad científica. Además, también se incluyen los objetivos del trabajo, tanto los generales como los particulares del proyecto dentro del cual se realizó la tesis doctoral.

El segundo capítulo contiene la revisión bibliográfica llevada a cabo para poder realizar el proyecto. Se centra fundamentalmente en las pilas de combustible, sus propiedades, tipos y particularidades. Hace un hincapié especial en las Pilas de Combustible de Óxido Sólido (SOFC), dado que el proyecto estaba ligado a este tipo de pilas. También se hace describen brevemente las técnicas más empleadas en la bibliografía para el estudio y caracterización de pilas de combustible.

El tercer capítulo describe la instalación experimental de la Universidad de South Carolina (donde los experimentos fueron llevados a cabo) así como las técnicas experimentales usadas a lo largo del proyecto.

Los tres siguientes capítulos (cuarto, quinto y sexto) presentan y analizan los resultados obtenidos durante este proyecto. El cuarto capítulo está relacionado con la caracterización de la pila de combustible con hidrógeno como combustible. Emplea hidrógeno, y argón para los experimentos con dilución. Dichos resultados han sido analizados en dicho capítulo.

El quinto capítulo contiene los resultados obtenidos cuando el metano se emplea como combustible. Emplea los resultados del capítulo anterior para comprender y analizar los resultados obtenidos en dicho capítulo. El argón sigue siendo utilizado para llevar a cabo la dilución del combustible

El sexto capítulo presenta los resultados preliminares obtenidos cuando el hidrógeno es contaminado con pequeñas cantidades de ácido sulfídrico. Para tener una imagen más clara de los resultados, los experimentos sólo se llevaron a cabo antes y después de la contaminación, pero no durante la misma. Aunque se requiere de estudios futuros para poder comprender completamente los fenómenos encontrados durante dichos experimentos, los resultados preliminares son extremadamente prometedores y muy interesantes.

Las conclusiones y el trabajo futuro de este proyecto se incluyen en el séptimo capítulo. Como los objetivos, las conclusiones también se dividen dos clases: generales y particulares.

Por último, el apéndice incluido al final del documento recoge el cálculo de la corriente eléctrica límite para todas las reacciones que están implicadas a lo largo del documento. Usa las ecuaciones correspondientes y los resultados han sido tabulados para facilitar su lectura. Se debe remarcar que dado que la estructura del flujo de los gases del ánodo es

extremadamente complicada, no se ha modelado el flujo real. El problema se ha simplificado con una geometría más sencilla con la que calcular la corriente eléctrica límite. Dos casos distintos se han estudiado con ese enfoque y se ha determinado que el caso real corresponde a un caso intermedio a los dos. Por ello, los dos casos estudiados nos dan el rango donde la corriente eléctrica límite real debe estar contenida, los límites inferior y superior de la misma.

1.5. Referencias

- [1] Lutz, A. E., Larson, R. S., Keller, J. O., "Thermodynamic comparison of fuel cells to the Carnot cycle", International Journal of Hydrogen Energy, Vol. 27, pages 1103-1111, 2002.
- [2] Appleby, A. J., Foulkes, F. R., *Fuel Cell Handbook*, Van Nostrand Reinhold, New York, NY, 1989.
- [3] Alston, T., Kendall, K., Palin, M., Prica, M., Windibank, P., "A 1000-cell SOFC reactor for domestic cogeneration", Journal of Power Sources, Vol. 71, pages 271-274, 1998.
- [4] Lee, K. H., Strand, R. K., "SOFC cogeneration system for building applications, part 1: Development of SOFC system-level model and the parametric study", Renewable Energy, Vol. 34, pages 2831-2838, 2008.
- [5] Barrera, R., De Biase, S., Ginocchio, S., Bedogni, S., Montelatici, L., "Performance and life time test on a 5kW SOFC system for distributed cogeneration", International Journal of Hydrogen Energy, Vol. 33, pages 3193-3196, 2008.

- [6] Heywood, J. B., Internal Combustion Engine Fundamentals, McGraw-Hill, 1988.
- [7] Zidansek, A., Ambrozic, M., Milfelner, M., Blinc, R., Lior, N., "Solar orbital power: Sustainability analysis", Energy, Vol. 36, pages 1986-1995, 2011.

CHAPTER 1

Introduction

Contents

1.1. Energy Context	17
1.2. Previous Work.....	19
1.3. Objectives	20
1.3.1. General Objectives	20
1.3.2. Specific Objectives	21
1.4. Structure of the Document.....	22
1.5. References.....	24

1. Introduction

1.1. Energy Context

We live in a world with an enormous energy demand, which is increasing day by day. Since the times of the Industrial Revolution in the 18th and 19th Centuries, we are becoming more and more dependent on energy for our everyday life. Currently human beings consume an average energy rate of about 16TW, which is several orders of magnitude smaller to the one we constantly receive from the sun as electromagnetic radiation - about 170,000TW on average, from which about half reaches the surface of the Earth [7]. Obviously some part of this energy is used in natural phenomena such as the water cycle, wind, etc. In spite of it, that energy should, in principle, cover our current demand easily. However, the problem lies on how we transform this radiation into a form of energy that we can actually use for our needs (mainly electricity). Fossil fuels have been the first form of energy that we have used, and they are still our main source of energy. They are dead organic matter, that was buried under the surface of the Earth and which have been transforming the energy of the Sun into chemical energy for millions of years. The present an extraordinarily high energy density (both in volumetric terms and also in terms of mass) that makes them perfect for most of our applications.

The problem that fossil fuels present is that it takes an extremely long period of time - millions of years - under certain conditions of temperature and pressure to be obtained. Considering this, it should be clear that a few generations are consuming resources that belonged to millions of generations, as it took millions of years to be produced. Therefore, it can definitely be said that we have been living over our possibilities, but nobody is willing to give up on their current lifestyle so alternative and more efficient ways to use the energy are needed.

This issue can also be seen from a renewability point of view. It is said that a source of energy is renewable when it is used continuously, that is,

it can be produced as quickly as it is consumed. A good example of this kind of energy is the hydroelectric energy, where the kinetic and/or potential energy of the water in a river (that comes from the water cycle, i.e. from the sun) is transformed into mechanical energy by means of a hydroturbine. Afterwards, this energy is transformed into electrical energy using an alternator. Fossil fuels, on the other hand, are not considered as renewable sources of energy, since the time that it takes to obtain them is much longer than the one it takes for them to be consumed. Thus the only long term solution to the energy problem is using renewable energies as the source of all the energy that is used for our activities.

Since the energy problem is probably the biggest challenge the humanity is facing in this century, a huge effort has been put into developing new sources of energy that are renewable. The problem that most of these sources of energy have is that they are intermittent and non-predictable with a low energy density. Thus a way to store this energy in an efficient way is critical when they are implemented. Electric batteries are able to store electricity - in fact electrochemical energy - but they have important issues that seem to be difficult to overcome with the current technology, such as having a low specific energy and power, discharging over time, and degrading over charge/discharge cycles.

With this respect, hydrogen as an energy vector (i.e. as a way to store and transport energy) seems to have a bigger potential and many experts expect it to be the main energy carrier in the long term-future, for it has some interesting properties such as a larger specific energy and power. There are several ways to energetically use hydrogen, being the most promising ones combustion engines (mixed with other fuels) and fuel cells.

Combustion engines transform the chemical energy contained in the hydrogen firstly into heat, which is transformed into mechanical work afterwards. According to the Second Law of Thermodynamics, not all the heat produced can be transformed into mechanical work. This means that the efficiency of the heat engine is limited by the Carnot efficiency. Actual efficiencies of real heat engines vary between 20% and 40%, depending on the engine size and operating conditions.

On the other hand, in fuel cells a direct electrochemical transformation of the chemical energy of the hydrogen into electricity takes place, so no such limitation is found, and thus they present much higher efficiencies [1]. However, other limitations - that will be discussed throughout this dissertation - cause that real fuel cells present efficiencies of around 50% on their own [2]. High temperature fuel cells (like Solid Oxide Fuel Cells), show much higher global efficiencies when they are coupled in a cogeneration cycle [3-5] - when the spare heat is used for other purposes.

Compared to combustion engines [6], fuel cells also present the advantage of not having moving parts (apart from those associated to the auxiliary elements, such as compressors, pumps and blowers), which promises a potential for longer expected lifetime, if other issues associated to fuel cells are overcome. Also, the fact that they have no moving parts makes them an extremely low-noise device even at full power, which certainly suits some applications where noise needs to be minimized, like military applications.

For all the reasons mentioned above, fuel cells seem most promising alternative for energy generation in the long term future. Their properties make them the perfect candidate to solve the issues that renewable sources of energy present, thus the study of their limitations in order to overcome them is a priority for scientific community, and justifies the interest of the topic of this PhD.

1.2. Previous Work

Energy and the way we use it is one of the main issues that humanity is facing in this century. From the Industrial Revolution global energy demand has increased in such a way that traditional energy sources - fossil fuels concretely - seem to be inadequate for they increase the pollution of the environment and will be over in a few years. Inside the *Combustion Engines and Renewable Energies Group* (MYER, from its initials in Spanish) of the University of Valladolid - where this PhD had been developed - there has always been a great interest in the energy field.

Objectives are aimed to increase efficiencies in order to reduce pollutant emissions and energy consumption, as well as the search for alternative fuels, and energy devices.

The topic of this thesis is clearly within the MYER Group research field, as fuel cells are probably the most promising technology in the energy world at the moment. Hydrogen production from different sources, especially renewable fuels, and its utilization in different devices (engines, fuel cells) are objectives of the Group.

The experimental work related to this research was carried out at the University of South Carolina, in Columbia, South Carolina, USA, with a grant supported by the Spanish Fulbright Commission. Dr. Van Zee's Group, in the Chemical Engineering Department at the University of South Carolina, is one of the leading groups in this field in the world, and it is probably one of the best places to learn about this technologies. The results obtained during my stay at the University of South Carolina, as well as the knowledge which I acquired during the time I was doing the PhD - both at the University of Valladolid and the University of South Carolina - is reflected in this dissertation.

1.3. Objectives

The main objectives of this work can be classified into two types according to their character: the general objectives and the specific objectives.

1.3.1. General Objectives

The first main objective of this work is related to the academic character of the PhD. PhD is the highest standard in our educational system and it pursues excellence in education. Research, as any other science, requires dedication in order to achieve the abilities and skills to develop it in a satisfactory way. PhD is the best method to achieve it, and therefore a

really important objective for this PhD is the acquisition of the abilities and skills to develop research at the highest level. This includes problem identification, experimental design, apparatus design, construction and data collection in order to carry out the required experiments, and analysis of the results using several tools. With this respect, the stay at one of the best fuel cell research centers in the world certainly helped achieving this objective.

Another very important objective that lies into this category is the acquisition of an important knowledge base related to the field of study, fuel cells, which includes both general knowledge (as electrochemistry) and also a more particular knowledge that is only relevant to fuel cells and no other electrochemical processes (fuel cell particular properties like flow requirements, instrumentation...)

The last general objective is related to the ability of applying the skills and the knowledge acquired in the laboratory to the real world. This includes practical application of the techniques learnt in fields not limited to fuel cells.

1.3.2. Specific Objectives

The specific objectives of this project are intimately related to the fuel cell that was used. The first specific objective is to carry out a literature review in order to acquire the required knowledge about fuel cells and their current state of the art.

The second specific objective is related to the characterization of the Solid Oxide Fuel Cell. This will require both experimental skills and analysis abilities applied to this concrete case. Characterizing the fuel cell is really important as it allows comparing it with other cells and also it influences in the experimental design that should follow.

The third objective is related to methodology to perform the SOFC experiments. It is important to learn how to carry out meaningful experiments that enlighten and explain the phenomena observed. In addition to this, they should be in accordance with the objectives of the project.

Once this is achieved, all the results should be analyzed. Understanding the processes that take place inside the fuel, modeling them and using the knowledge to improve the design of the fuel cell is the ultimate objective of the project.

1.4. Structure of the Document

The document is structured into seven chapters and one appendix. The first one gives a description of the background of the PhD student as well as the group. It also describes the particularities of the work carried out and the reason why it is important and relevant for the scientific community. In addition to this, it also describes the objectives that the work pursues, both general and particular to the project in which the PhD was developed.

The second chapter contains the literature review performed for the project. It focuses mainly on fuel cells its properties, types and particularities. It has a special emphasis on Solid Oxide Fuel Cells (SOFC) since the project was linked to this type of fuel cell. It also briefly describes the most widely used techniques to study and characterize fuel cells, found in the literature.

The third chapter describes the experimental facility at the University of South Carolina (where the experiments were carried out) as well as the experimental procedures used throughout the project.

The next three chapters (fourth, fifth and sixth) present and analyze the results obtained during this project. The fourth chapter is related to the characterization of the fuel cell when hydrogen is used as the fuel. It uses hydrogen, and argon to perform the dilution experiments. Those results are also analyzed in the fourth chapter.

The fifth chapter contains the results obtained when methane is used as the fuel. It also uses the results from the previous chapter to understand and analyze the new results produced in this chapter. Argon is used again as the gas to perform the dilution of the fuel.

The sixth chapter presents the preliminary results obtained when hydrogen is contaminated with hydrogen sulfide. In order to get a clearer image of the final results, experiments were only carried out before and after the contamination process, but not during it. Although further studies are required to completely understand the phenomenon found in those experiments, the preliminary results are extremely promising and really interesting.

The conclusions and the future work of this project are included in the seventh chapter. Like the objectives, the conclusions are also divided into two types: general and particular conclusions.

Finally, the appendix included reflects the calculation of the limiting currents for all the reactions that appear throughout the document. It uses the correspondent equations and the results are tabulated for a clearer viewing. It must be remarked that since the flow pattern in the anode of the fuel cell is extremely complicated the real flow has not been modeled. The problem was simplified using an easier geometry that allowed calculating the limiting current. Two different cases were studied with this approach and it was determined that the real case was an intermediate case between the other two. For this reason, the two cases studied

provide the range where the real limiting current should be contained, the upper and lower limits.

1.5. References

- [1] Lutz, A. E., Larson, R. S., Keller, J. O., "Thermodynamic comparison of fuel cells to the Carnot cycle", International Journal of Hydrogen Energy, Vol. 27, pages 1103-1111, 2002.
- [2] Appleby, A. J., Foulkes, F. R., Fuel Cell Handbook, Van Nostrand Reinhold, New York, NY, 1989.
- [3] Alston, T., Kendall, K., Palin, M., Prica, M., Windibank, P., "A 1000-cell SOFC reactor for domestic cogeneration", Journal of Power Sources, Vol. 71, pages 271-274, 1998.
- [4] Lee, K. H., Strand, R. K., "SOFC cogeneration system for building applications, part 1: Development of SOFC system-level model and the parametric study", Renewable Energy, Vol. 34, pages 2831-2838, 2008.
- [5] Barrera, R., De Biase, S., Ginocchio, S., Bedogni, S., Montelatici, L., "Performance and life time test on a 5kW SOFC system for distributed cogeneration, International Journal of Hydrogen Energy, Vol. 33, pages 3193-3196, 2008.
- [6] Heywood, J. B., *Internal Combustion Engine Fundamentals*, McGraw-Hill, 1988.
- [7] Zidansek, A., Ambrozic, M., Milfelner, M., Blinc, R., Lior, N., "Solar orbital power: Sustainability analysis", Energy, Vol. 36, pages 1986-1995, 2011.

CHAPTER 2

Fuel Cells and SOFCs: Current Situation

Contents

2.1. Introduction	29
2.2. Fuel cells	30
2.2.1. Introduction.....	30
2.2.2. Types of Fuel Cells.....	34
2.2.3. Solid Oxide Fuel Cells (SOFCs)	36
2.2.3.1. Electrolyte Materials	38
2.2.3.2. Anode Materials.....	39
2.2.3.3. Cathode Materials	39
2.3. Techniques and Methods of Characterization	40
2.3.1. Electrochemical Techniques	42
2.3.1.1. Polarization Curves	43
2.3.1.2. Cyclic Voltammetry (CV).....	43
2.3.1.3. Transitory Analysis	44
2.3.1.4. Electrochemical Impedance Spectroscopy (EIS).....	44
2.3.2. Other Techniques	44
2.4. Summary in English	45
2.5. Summary in Spanish	46
2.6. References.....	48

2. Fuel Cells and SOFCs: Current Situation

2.1. Introduction

As it was pointed out in previous chapters, energy is one of the biggest issues that humanity is facing in this century. With this respect, fuel cells, as a device that transforms the chemical energy of a fuel into electrical energy by means of an electrochemical reaction, are a promising technology for the mid-term future.

The issues that are currently preventing them from being a commercially competitive technology are related to cost and durability [20]. Although the targets set by the US Department of Energy (DOE) are being met with recent developments [22] and [21], still the sensitivity of the catalyst used in most types of fuel cells (platinum mainly), makes it impossible to use them with any other fuel apart from pure hydrogen. The reason for this is that hydrogen is a simple molecule with a relatively simple chemistry

An exception to this is the SOFC, which operates at higher temperatures and uses a different catalyst (nickel generally). This particularity makes it more tolerant to impurities in the hydrogen [24] and [25], and this fact converts this kind of fuel cell in a good candidate to use hydrogen from different sources (alternative and renewable fuels) and even other kind of fuels - like methane or other kind of hydrocarbons - directly.

This higher tolerance to impurities compared with other kind of fuel cells does not mean that SOFC are complete immune to contaminants. Therefore, certain standards - as the limits of each contaminant that this kind of fuel cells are able to tolerate without significant performance drop -

must be established. For this reason, in this chapter, the literature review focuses on the different kind of fuel cells, its particularities.

Finally, it must be remarked that the project in which this PhD has been involved studied the viability of using a specific kind of SOFC with coal gas. To do so, the performance drop of the fuel cell with different levels of contamination and with different contaminants was evaluated using several techniques.

2.2. Fuel cells

2.2.1. Introduction

According to Webster Dictionary, a fuel cell is “a device that continuously changes the chemical energy of a fuel (as hydrogen) and an oxidant directly into electrical energy” [18].

In more colloquial words, a fuel cell is a device that transforms the chemical energy contained inside a fuel (generally hydrogen) into electrical energy directly. Batteries also transform chemical energy into electricity directly, but unlike fuel cells, the source of energy is not supplied externally (as a fuel), but it is stored inside of them. This way, batteries discharge while they are used until they cannot produce any more electricity. Fuel cells, on the contrary, are able to produce electricity continuously as long as fuel is supplied to them [15].

The concept of fuel cells has been known for a long time. The working principle was discovered back in 1838 by Christian Friedrich Schönbein, a German scientist, who published it in the January issue of 1839 of Philosophical Magazine [12]. However limitations in the technology and the material science have delayed its development. Recent awareness of global warming issues and fossil fuel dependence have launched the interest over this kind of technology over the last twenty years, although

improvements and developments are still needed in order to make fuel cells commercially viable.

There are several different types of fuel cells, but all of them rely on the same working principle: fuel and oxidant enter the fuel cell through two different channels that are separated by the electrolyte. At the electrode, where the catalyst is located (it may be the same for both sides, or each side can have a different one, that depends on the technology used), a chemical reaction happens, and ions are produced. One kind of ions (either the ones produced in the anode, or the ones produced in the cathode, depending on the fuel cell), are transported to the other side through the electrolyte, where they meet the other kind of ions, forming the products of the reaction. To close the internal charge balance, electrons are transferred accordingly by an external circuit, producing the electric energy. Figure 2.1 shows the working explained before for the most common fuel cells used nowadays.

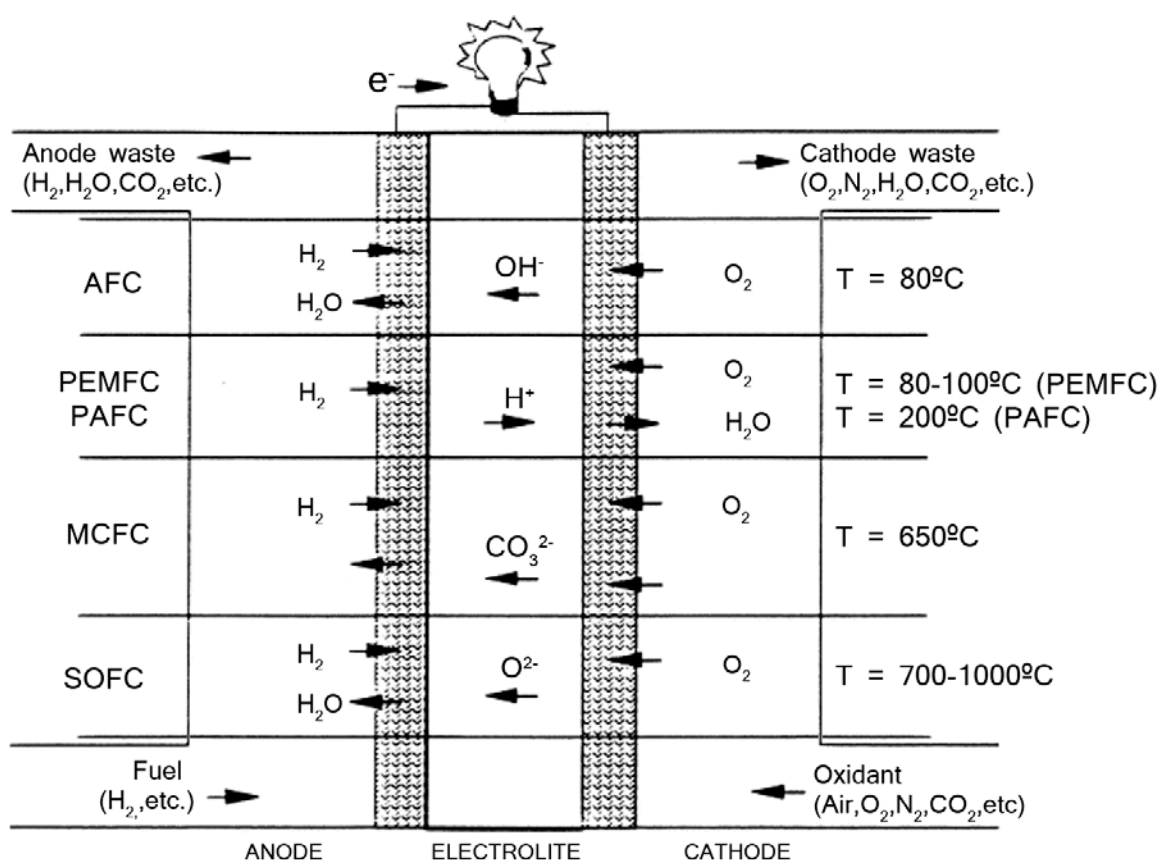


Figure 2.1: Working principle for different kinds of fuel cells (adapted from [59]).

From the previous description it is clear that there are certain **elements** which are key in a **fuel cell** so it can work properly. They must also have certain properties to allow all the processes that have to take place inside the fuel cell to happen. The main parts inside the fuel cell are:

- **Electrolyte/membrane:** Separates the anode and cathode side. It must present a high ion conductivity (of the type of ions that are transported inside the fuel cell) with an extremely low electric conductivity. This way, ions can easily cross over, while electrons must go through the electric circuit connected to the electrodes, not through the electrolyte. It must also have an extremely low permeability to both the fuel and the oxidant, so that the crossover of the gas from one side to the other is minimized. This is important because if one of the gases crosses over to the other side, it would cause a local chemical reaction, not electrochemical, that would reduce the efficiency of the fuel cell. Multiple studies [1] [2] [3], show the negative effect of fuel/oxidant crossover, the most noticeable is probably the reduction in the open circuit potential (OCV) of the fuel cell.
- **Catalysts:** they usually are precious metals/alloys [11]. Reactions take place by their action, although they remain unaltered during the fuel cell operation. As in other types of reactions, catalysts cause the reaction to happen in more steps (and they are present in the intermediate sub-products), lowering the activation energy and making it possible for the reaction to happen under the given conditions [4]. At the electrodes, a surface reaction takes place, thus the rates at which reactions happen do not depend on the amount of the catalyst present in the cell (volume or weight), but on its surface area inside the fuel cell [10]. As catalysts are usually precious metals or precious alloys, to make fuel cells more cost-effective, the objective is to produce as much surface area using the smallest possible amount of catalyst. This is highly affected by the electrode disposition and structure, as it will be explained.
- **Electrodes:** they have two important functions inside the fuel cell. They collect the electrons travelling from one side to the other, so it is

where the potential difference is created, and they are connected to the external electric circuit that closes the electron balance. For that reason electrodes must be made of conductive material, with an electric conductivity as high as possible. At the same time, electrodes are the support for the catalyst at each side. Therefore, for the reasons pointed out before, electrodes are usually made of materials which show an extremely high surface area - like porous materials - with a high electric conductivity. When the catalyst is deposited over the electrode (usually by painting or spraying), it is assured that it will have an extremely large surface to volume ratio, increasing the efficiency of the use of the catalyst. [7], [8], [74].

- **Seals and gaskets:** they prevent all gaseous products to cross through a joint of the fuel cell. All of the parts of the different types of fuel cells are made of different materials, thus ensuring that seals and joints are in a good condition over the lifetime of the fuel cell is critical to ensure proper working conditions inside the fuel cell. This is critical for low temperature fuel cells, where materials used are typically silicones and elastomers [5], [9], but also for high temperature fuel cells (like solid oxide fuel cells), where the differences in the expansion coefficients of the different materials that form the fuel cell make it even more difficult to find an adequate solution. Materials used for this kind of fuel cells range from ceramic pastes, glass, or mica-based materials (when the joint is close to the high temperature area) to silicon seals (where the joint is not affected by the heat) and glass [6].

It is clear from the description of the different parts that integrate fuel cells that Material Science plays an extremely important role in the development of this kind of technologies. Also Chemistry and Chemical Engineering are really important for fuel cells, as they rely on catalysts to work, and the study of all different reactions is key for a proper understanding of their working principles.

Finally, Mechanical Engineering also plays an important role for fuel cell development, as assembly and sealing procedures must be carefully

studied to prevent leaks and gas crossover. Also, specific problems of each fuel cell demand specific solutions that may involve other disciplines. For example, for low temperature fuel cells, water management inside the flow fields is a critical issue. Membranes used as electrolytes are only able to conduct the ions when they have a certain level of humidity but too much water would block the flow field, preventing the fuel and the oxidizer to reach the catalysts. Fluid Dynamics are required to understand this specific problem. Therefore, it can be said that the technology of fuel cells is extremely multidisciplinary, and every single aspect of it must be considered in order to achieve optimum performances in terms of specific energy and power, durability, cost, robustness, etc.

2.2.2. Types of Fuel Cells

Fuel cells are generally classified according to the type of electrolyte that they use [14], which also characterizes the ions that are transported through it [26], and the working temperature of the fuel cell. According to this criterion we can distinguish five basic types of fuel cells that are shown in Table 2.1 (adapted from [14]).

Different characteristics showed in Table 2.1 cause each fuel cell to adapt in a better way to one kind of application or another. For example, high temperature fuel cells (SOFC or MCFC) need a long startup procedure to rise the temperature to such high temperatures with a minimal thermal expansion and thus are not adequate for applications that require a short startup time (like automotive applications). On the other hand, the lower the operating temperature is, the less tolerant to fuel contaminant the fuel cell becomes. For instance, CO quickly poisons the catalyst of a PEMFC or a PAFC [16], [17], [19], whereas it can even be used as a fuel in a

SOFC, making the later more suitable to work with alternative fuels like coal gas or biomass gas.

Table 2.1: Main Fuel Cell Types.

Abbreviation	PEMFC	PAFC	AFC	MCFC	SOFC
Name	Polymer Electrolyte Membrane Fuel Cell	Phosphoric Acid Fuel Cell	Alkaline Fuel Cell	Molten Carbonate Fuel Cell	Solid Oxide Fuel Cell
Ions	H ⁺	H ⁺	OH ⁻	CO ₃ ²⁻	O ²⁻
Electrolyte	Polymer (Nafion)	Liquid H ₃ PO ₄	Liquid KOH	Molten Carbonate	Perovskites (YSZ)
Typical catalysts	Platinum	Platinum	Platinum	Nickel	Nickel/Silver
Operating Temperature	80°C	200°C	60-220°C	650°C	600-1000°C
Typical Fuel	H ₂ , CH ₃ OH	H ₂	H ₂	H ₂ , CH ₄ ,	H ₂ , CH ₄ , CO
Typical applications	Automotive applications, APUs, Emergency power systems	Distributed power generation	Space and marine applications	Stationary power generation, cogeneration	Stationary power generation, cogeneration, alternative fuels.

Different characteristics showed in Table 2.1 cause each fuel cell to adapt in a better way to one kind of application or another. For example, high temperature fuel cells (SOFC or MCFC) need a long startup procedure to rise the temperature to such high temperatures with a minimal thermal expansion and thus are not adequate for applications that require a short startup time (like automotive applications). On the other hand, the lower the operating temperature is, the less tolerant to fuel contaminant the fuel cell becomes. For instance, CO quickly poisons the catalyst of a PEMFC or a PAFC [16], [17], [19], whereas it can even be used as a fuel in a

SOFC, making the later more suitable to work with alternative fuels like coal gas or biomass gas.

To summarize, each different kind of fuel cell presents different properties that made them more suitable for certain applications. Currently, the ones that seem to have more advantages, and that are being more carefully studied are the Polymer Electrolyte Membrane Fuel Cell (PEMFC) and the Solid Oxide Fuel Cell (SOFC). The first one with a lower temperature of operation, and a short startup time, seems to be adequate for automotive applications, while the SOFC would be more suitable for stationary power generation, either fuelled with hydrogen or with alternative fuels.

In this dissertation, the focus has been put on SOFC. A microtubular kind of these fuel cells, was studied and characterized with hydrogen and also with methane (CH_4) as well as the presence of certain contaminants (like H_2S) in order to study the viability of using them with alternative fuels.

2.2.3. Solid Oxide Fuel Cells (SOFCs)

A particular type of Solid Oxide Fuel Cell was used in the project in which this PhD was involved. It was manufactured by the *National Metal and Materials Technology Center* (MTEC) in Thailand and had the geometry of an electrolyte supported tubular cell [73]. The particularities that this concrete cell presented are described in Chapter 3. The general characteristics of this kind of fuel cells have are presented here.

Solid Oxide Fuel Cells are the latest kind of fuel cells that have appeared. They are based on a doped perovskite-type material that acts as the electrolyte. This solid material is able to conduct ions at high temperatures (650-900°C).

This way, oxygen molecules reach the cathode catalyst, where they are dissociated into two oxygen ions. Those ions are transported from cathode

to the anode side, where they meet the hydrogen ions (the protons) that had been produced from the hydrogen molecules in the anode catalyst. In the anode catalyst, electrons are also produced. Those electrons are transported to the cathode side by means of an external electric circuit that closes the system. Equation 2.1 shows the reaction in the cathode side, while equations 2.2 and 2.3 show the reactions taking place in the anode side.



In addition to the usual characteristics that are demanded for every fuel cell, Solid Oxide Fuel Cells also requires an additional aspect related to the high temperatures at which they operate. They require that all the different materials that compose the fuel cell have similar thermal expansion coefficients [27]. If that was not the case internal thermal stress would cause internal cell cracking and eventual cell failure.

Being such a recent innovation, different materials for the electrolyte as well as the catalysts, electrodes and current collectors are used currently in SOFCs. The objective is finding materials that showing similar thermal expansion coefficients, also show high catalytic activity (catalysts), good ion conductivity (electrolyte), and low electric resistivity (both the current collectors and the elements that electrically connect the catalyst (where the reaction takes place) to the current collector [70]. Another important objective is finding materials that allow reducing the operating temperature of the SOFC [25]. In the following sections a description of the most common materials currently used is given.

2.2.3.1. Electrolyte Materials

Table 2.2: Main Electrolyte Materials for SOFC. Adapted from [6].

Material	Chemical Formulas	
Zirconia electrolytes		
YSZ	$(\text{ZrO}_2)_{1-x} (\text{Y}_2\text{O}_3)_x$	(with $x \sim 0.08-0.1$)
SSZ	$(\text{ZrO}_2)_x (\text{Sc}_2\text{O}_3)_{1-x}$	(with $x \sim 0.8$)
CaSZ	$\text{Zr}_{0.85}\text{Ca}_{0.15}\text{O}_{1.85}$	
Ceria electrolytes		
GDC	$\text{Ce}_x\text{Gd}_{1-x}\text{O}_y$	(with $x \sim 0.8$, $y \sim 1.8$)
SDC	$\text{Ce}_x\text{Sm}_{1-x}\text{O}_y$	(with $x \sim 0.8$, $y \sim 1.9$)
YDC	$\text{Ce}_x\text{Y}_{1-x}\text{O}_y$	(with $x \sim 0.8$, $y \sim 1.96$)
CDC	$\text{Ce}_x\text{Ca}_{1-x}\text{O}_y$	(with $x \sim 0.9$, $y \sim 1.8$)
Lanthanum electrolytes		
LSGM	$\text{La}_x\text{Sr}_{1-x}\text{Ga}_y\text{Mg}_{1-y}\text{O}_3$	(with $x \sim 0.9$, $y \sim 0.8$)
LSGMC	$\text{La}_x\text{Sr}_{1-x}\text{Ga}_y\text{Mg}_{1-y-z}\text{Co}_z\text{O}_3$	(with $x \sim 0.8$, $y \sim 0.8$, $z \sim 0.085$)
LSGMF	$\text{La}_x\text{Sr}_{1-x}\text{Ga}_y\text{Mg}_{1-y-z}\text{Fe}_z\text{O}_3$	(with $x \sim 0.8$, $y \sim 0.5$, $z \sim 0.4$)
LSGMCF	$\text{La}_{0.8}\text{Sr}_{0.2}\text{Ga}_{0.32}\text{Mg}_{0.08}\text{Co}_{0.2}\text{Fe}_{0.4}\text{O}_3$	
LaAlO ₃ -based	$\text{La}_{1-x}\text{Ca}_x\text{AlO}_3$	(with $x = 0.0027-0.008$)
	$\text{La}_{1-x}\text{Ba}_x\text{AlO}_3$	(with $x = 0.1$)
Others		
BCY	$\text{BaCe}_x\text{Y}_{1-x}\text{O}_3$	(with $x \sim 0.25$)
YSTh	$(\text{ThO}_2)_{1-x}(\text{Y}_2\text{O}_3)_x$	(with $x \sim 0.08-0.1$)
YSHa	$(\text{HfO}_2)_{1-x}(\text{Y}_2\text{O}_3)_x$	(with $x \sim 0.08-0.1$)
Bismuth oxide-based	$(\text{Bi}_2\text{O}_3)_x(\text{Nb}_2\text{O}_5)_{1-x}$	(with $x \sim 0.25$)
Pyrochlorores-based	YZr_2O_7 $\text{Gd}_2\text{Ti}_2\text{O}_7$	
Barium brownmillerites	BaZrO_3 $\text{Ba}_2\text{In}_2\text{O}_5$ $\text{Ba}_3\text{In}_x\text{AO}_y$ $\text{Ba}_3\text{Sc}_2\text{ZrO}_8$	(with A = Ti, Zr, Ce, Hf)
Strontium brownmillerites	$\text{Sr}_2\text{ScAl}_x\text{A}_y\text{O}_z$ $\text{Sr}_2\text{ScAlO}_5$ $\text{Sr}_3\text{In}_2\text{HfO}_8$	(with A = Mg, Zn)

As it was pointed out before, the electrolyte materials used for Solid Oxide Fuel Cells are generally perovskite-type material doped in a way that it allows the material to conduct ions at high temperatures while it behaves as an electric insulator for electrons.

The first material to be used was Yttria Stabilized Zirconia (YSZ). It is obtained adding a certain amount of yttrium oxide (Y_2O_3) to zirconium oxide (ZrO_2). This produces that some of the zirconia ions (Zr^{4+}) in the zirconia lattice are replaced with yttria ions (Y^{+3}), causing oxygen vacancies. These oxygen vacancies are the ones allowing for ion conductivity at high temperatures [28].

Table 2.2 shows a summary of the main electrolyte materials currently used, adapted from [6]

2.2.3.2. Anode Materials

As the anode catalyst, the most widely used material is nickel, especially for its cheap price compared to other catalysts [51]. Platinum is also used in other studies as the anode catalyst. It shows a higher activity and stability (especially to oxidation at high temperatures), although it is much more expensive than nickel, so it is not as widely used.

Also any copper content in the anode catalyst seems to increase the resistance of the catalyst towards coking with hydrocarbons, thus the new trends to produce carbon resistant catalysts for SOFC using hydrocarbon fuels include using Ni-Cu alloys [32].

2.2.3.3. Cathode Materials

The first material to be used as the cathode catalyst was Lanthanum Strontium Manganite (LSM or LSMO). Its general formula is: $\text{La}_{1-x}\text{Sr}_x\text{MnO}_3$ (with $x \sim 0.1-0.2$). It shows good catalytic activity, stability at high temperatures, reasonably good electric conductivity and a similar thermal

expansion coefficient compared to the other elements of the fuel cell. However, according to the literature [27], cobalt oxides with different lanthanides and alkali-earth metals in the A-site position produce higher activities and stabilities. Examples of this kind of catalysts are: $\text{Ba}_{0.5}\text{Sr}_{0.5}\text{Co}_{0.8}\text{Fe}_{0.2}\text{O}_{3-\delta}$ (BSCF) [68], $\text{La}_{0.6}\text{Sr}_{0.4}\text{Co}_{0.2}\text{Fe}_{0.8}\text{O}_{3-\delta}$ (LSFC) [69] and $\text{Pr}_{0.8}\text{Sr}_{0.2}\text{Fe}\text{O}_{3-\delta}$ (PSF) [67]. However, these materials have a larger thermal expansion coefficient compared with the rest of elements of the fuel cell, so further research is necessary in order to overcome those drawbacks.

Finally, silver is a typical current collector material for the cathode side, since it shows a high electric conductivity, high resistance to corrosion at high temperatures and also it enhances the kinetic activity of the catalyst in the cathode side [72].

2.3. Techniques and Methods of Characterization

Fuel Cells are technologically viable devices, as has been proved by the wide variety of prototypes already implemented [53, 54, 55,]. However, in order to become commercially viable, their design needs to be improved in terms of durability and cost, as it was pointed out before. So that this is achieved, a deeper knowledge of the processes taking place inside the device must be acquired [30].

The scientific method provides with several tools that make this studies possible. Attending to their nature, they can basically be classified into two different categories: experimental methods - those involved with the actual physical device - and modeling methods - those where the actual device is not physically used. Although each of them could be used by itself, they generally produce better results when they are used together, as they complement one another [29].

The approach that generally produces better results in the engineering field is the following one [30, 31]: some experiments are carried out with the device. From those results and the knowledge base acquired previously, several models that explain the results obtained can be derived. Then, a new set of experiments must be designed in order to determine which of the models fits the system in a better way. Once the new experiments are completed, the analysis can be done, and it will usually lead to further questions, more refined models and new experiments proposed until a model that explains the phenomena found in a satisfactory way is developed. When this is achieved, the model can be used to predict the device behavior under new working conditions, as well as to improve the design of the device. Once the improved device is ready for testing, new experiments should be carried out, and base on the results of those experiments and the previous knowledge, a new model can be derived, starting the whole process all over again.

In the literature plenty of models proposed for the SOFC, as well as different modeling strategies can be found, both involving both the macroscale [33, 34, 35] (which use the conservation equations and the electrochemical theory to model the processes that happen inside the fuel cell) and the microscale [36, 37] (where approaches that consider the grain boundary diffusivities and microscopic structure are used to derive new models).

There are also plenty of experimental studies that involve SOFC in the literature [56, 57, 58]. However, unlike what happens with PEM fuel cells, there are really few studies that use an electrochemical approach (describing the possible reactions and their potentials) to characterize the SOFC. One of the unique features of this thesis is the attempt to apply electrochemical engineering analysis techniques used in PEM fuel cell research [23, 50, 52] to explain and characterize SOFC behavior during

contamination. This electrochemical engineering approach, rather than the material-technology approach that the majority of the studies related to SOFC use, presents a new and alternative point of view for this type of fuel cells. This new approach, together with the particular fuel cell structure, is what makes this project unique and different from the studies found in the literature.

For those reasons a mainly experimental project was chosen, which was obviously complemented with the analysis of the results obtained during those experiments. Therefore, in this section a review of the main experimental methods used in the literature is presented as well as a brief description of them.

Attending to the character of the technique they have been classified into three different groups: electrochemical techniques, surface techniques and complementary techniques. Since the objective of the thesis was to characterize the fuel cell from an electrochemical point of view, the description will focus on this type of techniques.

A more detailed explanation of the methods that have been used in the project is presented in Chapter 3.

2.3.1. Electrochemical Techniques

Electrochemical techniques cover a set of different procedures. Since they are based in various electrochemical principles, they can be applied to any electrochemical device, like batteries and fuel cells, including SOFC. The main ones are:

2.3.1.1. Polarization Curves

Polarization curves analyze the behavior of the device at different levels of polarization when it has reached steady state. There are two different ways of performing it: Constant current or constant voltage; both provide measured values of the voltage or the current respectively from which voltage-current (V-I) diagrams are elaborated. They show useful information about the way the fuel cell works at different levels of load or power. Several studies in the bibliography use this approach to characterize SOFC [38, 39, 40].

2.3.1.2. Cyclic Voltammetry (CV)

Cyclic Voltammetry is similar to polarization curves in the sense that it analyzes the effect of different polarization levels on the fuel cell. The main difference with polarization curves is that it does not wait for steady state. Instead, it quickly sweeps (50-200mV/s) from one potential to another (set points) a certain number of times, without letting the cell reach steady state and constantly recording the measured current. It also produces a V-I diagram with a closed shape over the cycle. This shape would show several peaks in the current at different voltages, where each peak corresponds to a certain reaction that takes place at that particular voltage.

The problem with this technique and SOFC is that this device presents a really strong electric resistance (from the electrolyte) that makes it difficult to see anything when the technique is applied to the full cell. However, several authors use this technique with only certain parts of the cell (specially the catalyst of the cathode side) to see its behavior and properties [41, 42].

2.3.1.3. Transitory Analysis

Transitory analysis is another electrochemical technique based on polarization principles. The main difference with the previous ones is that it only focuses on one potential. Then, once steady state has been reached, a certain parameter is changed, and the transient response of the device is recorded. It provides useful information about that process, like how fast it occurs, if it is reversible or not, and with all that data a better characterization of the device can be done. Many authors use this technique to characterize certain aspects of the SOFC [43, 44, 45]

2.3.1.4. Electrochemical Impedance Spectroscopy (EIS)

Unlike all the previous techniques, which were based on polarization principles, Electrochemical Impedance Spectroscopy uses the frequency domain to extract valuable information from the device. This way, at a constant voltage or current, a small sinusoidal perturbation is induced with different frequencies (from 65kHz to 0.01Hz for the SOFC used in this project). The response of the device is recorded and the results are plotted in a Nyquist or Bode Diagram. It offers information about the time response of the device and its general properties. It is widely used in the study of SOFC [46-49].

2.3.2. Other Techniques

Other techniques currently used to study the characteristics and behavior of the fuel cells include surface techniques, and other complementary techniques.

The surface techniques can produce magnified images of the surface of interest so that microscopic properties can be revealed, like Scanning

Electron Microscopy (SEM), or they can provide a spectrum from a certain property that relates to the structure of the surface. The most widely used techniques of this type are probably SEM [60, 61, 62] and X-ray Photoelectron Spectroscopy (XPS) [63, 64, 65], although other techniques, like Temperature-Programmed Reduction (TPR) [66] and Thermal Desorption Spectroscopy (TPD) [13] are also used.

Regarding the complementary techniques, they include any technique that, although it is not applied on the cell directly, contributes to understanding the processes of the fuel cell by giving external information about a certain process. Good examples of this kind of techniques are the mass spectrometer and the gas chromatographer used to determine the composition of the samples at the outlet of the fuel cell when it was working with methane.

2.4. Summary in English

The current situation of the fuel cells, with a special emphasis on the Solid Oxide Fuel Cells has been briefly reviewed in this chapter. In general, it can be said that fuel cells are a promising technology for energy conversion. Given the current global energy situation, they might be a key device in the coming years for humanity.

Among the fuel cells, the ones that are becoming more promising for energy applications are Proton Exchange Membrane Fuel Cells and the Solid Oxide Fuel Cells. The first ones operate at lower temperatures with a relatively low startup time, which make them the perfect candidate for automotive applications.

On the other hand, Solid Oxide Fuel Cells operate at much higher temperatures, which causes them to have longer startup times. This fact

does not make them suitable for portable applications. However, given the high operation temperatures and their really high efficiencies - especially if they are used in combined cycles with heat recovery - they are a perfect candidate for stationary applications (power generation, etc.). However, in order to become a commercially competitive technology they need to overcome their main two issues - like the rest of fuel cells - their high costs, and their durability.

Also, a quick view over the main electrochemical techniques used in literature to characterize fuel cells has been given here. Most of them will be used in this project, and a more exhaustive description of them can be found in Chapter 3.

The main contribution of this PhD lies on the electrochemical approach taken to characterize the Solid Oxide Fuel Cell. Most of studies found in the literature use a material-science approach, and really few focus on the reactions, and the potentials at which they occur. Also, the particular flow field distribution of the anode gives a unique character to the results presented here.

2.5. Summary in Spanish

La situación actual de las pilas de combustible ha sido brevemente revisada en este capítulo, con un énfasis especial en las Pilas de Combustible de Óxido Sólido (SOFC, de sus siglas en inglés). En general, se puede decir que las pilas de combustible son una tecnología prometedora para convertir la energía. Dada la situación energética global, las pilas de combustible podrían ser un elemento clave en los próximos años para la humanidad.

Entre todas las tecnologías de pilas de combustibles, las más prometedoras en la actualidad son las de Membrana de Intercambio de Protones (PEMFC, de sus siglas en inglés) y las de Óxido Sólido. Las primeras operan a bajas temperaturas con tiempos de encendido relativamente cortos, lo que las convierte en un candidato perfecto para aplicaciones de automoción.

Por otro lado, las pilas de Óxido Sólido operan a temperaturas mucho mayores, lo que provoca que tengan tiempos de encendido mucho más largos. Esto hace que no sean apropiadas para aplicaciones en automoción. Sin embargo, por las altas temperaturas a las que operan y las altas eficiencias que son capaces de alcanzar - especialmente si se emplean en ciclos combinados con recuperación de calor - son unas buenas candidatas para aplicaciones estacionarias (como la generación de energía eléctrica). De todos modos, deberán superar sus actuales limitaciones - iguales a las del resto de pilas, alto coste y corta vida útil - para llegar a ser comercialmente competitivas.

También se ha dado una rápida visión de las principales técnicas electroquímicas usadas en la literatura para caracterizar las pilas de combustible. La mayoría de ellas serán empleadas en este proyecto y por tanto se ha dado una descripción más exhaustiva de las mismas en el Capítulo 3.

La principal contribución de esta tesis es el enfoque electroquímico usado para caracterizar la Pila de Óxido Sólido. La mayoría de los estudios encontrados en la literatura usan un enfoque centrado en la ciencia de materiales, y muy poco se fijan en las reacciones y los potenciales a los que tienen lugar. Además, la particular distribución del flujo de combustible en el ánodo da un carácter único a los resultados presentados aquí.

2.6. References

- [1] Vilekar, S. A., Datta, R., "The effect of hydrogen crossover on open-circuit voltage in polymer electrolyte membrane fuel cells", *Journal of Power Sources*, Vol. 195, pages 2241-2247, 2010.
- [2] Francia, C., Ijeri, V. S., Specchia, S., Spinelli, P., "Estimation of hydrogen crossover through Nafion(R) membranes in PEMFCs", *Journal of Power Sources*, Vol. 196, pages 1833-1839, 2011.
- [3] Chao Xu, C., Faghri, A., Li, X., Ward, T., "Methanol and water crossover in a passive liquid-feed direct methanol fuel cell", *International Journal of Hydrogen Energy*, Vol. 35, pages 1769-1777, 2010.
- [4] Masel, R. I., "Chemical Kinetics and Catalysis" Wiley-Interscience, New York, 2001.
- [5] Tan, J., Chao, Y. J., Van Zee, J. W., Lee, W. K., "Degradation of elastomeric gasket materials in PEM fuel cells", *Materials Science and Engineering: A*, Vols. 445-446, pages 669-675, 2007.
- [6] Wincewicz, K. C., Cooper, J. S., "Taxonomies of SOFC material and manufacturing alternatives", *Journal of Power Sources*, Vol. 140, pages 280-296, 2005.
- [7] Piao, J., Sun, K., Chen, X., "Compatibility between glass sealants and electrode materials of solid oxide fuel cells", *Rare Metals*, Vol. 27, pages 378-383, 2008.

- [8] Maheshwari, P. H., Mathur, R. B., Dhami, T. L., "The influence of the pore size and its distribution in a carbon paper electrode on the performance of a PEM Fuel cell", *Electrochimica Acta*, Vol. 54, pages 655-659, 2008.
- [9] Lin, C.-W., Chien, C.-H., Tan, J., Chao, Y. J., Van Zee, J. W., "Chemical degradation of five elastomeric seal materials in a simulated and an accelerated PEM fuel cell environment", *Journal of Power Sources*, Vol. 196, pages 1955-1966, 2011.
- [10] Beard, K. D., Schaal, M. T., Van Zee, J. W., Monnier, J. R., "Preparation of highly dispersed PEM fuel cell catalysts using electroless deposition methods", *Applied Catalysis B: Environmental*, Vol. 72, pages 262-271, 2007.
- [11] Antolini, E., Salgado, J. R. C., Gonzalez, E. R., "The stability of Pt-M (M = first row transition metal) alloy catalysts and its effect on the activity in low temperature fuel cells: A literature review and tests on a Pt-Co catalyst", *Journal of Power Sources*, Vol. 160, pages 957-968, 2006.
- [12] Andújar, J. M., Segura, F., "Fuel cells: History and updating. A walk along two centuries", *Renewable and Sustainable Energy Reviews*, Vol. 13, pages 2309-2322, 2009.
- [13] Yan, A., Maragou, V., Arico, A., Cheng, M., "Panagiotis Tsiakaras, Investigation of a $\text{Ba}_{0.5}\text{Sr}_{0.5}\text{Co}_{0.8}\text{Fe}_{0.2}\text{O}_{3-\delta}$ based cathode SOFC: II. The effect of CO₂ on the chemical stability", *Applied Catalysis B: Environmental*, Vol. 76, pages 320-327, 2007.
- [14] O'Hare, R., Cha, S.W., Colella, W., Prinz, F. B., *Fuel Cell Fundamentals*. Wiley, Cap. 1. (2009).

- [15] Hirschenhofer, J.H., Stauffer, D.B., Engleman, R.R., and Klett, M.G., *Fuel Cell Handbook*. DOE/FETC-99/1076, Cap 1. (2008).
- [16] Gasteiger, H. A., Markovic, N. M., Ross Jr., P. N., "Electrooxidation of CO and H₂/CO Mixtures on a Well-Characterized Pt₃Sn Electrode Surface", *J. Phys. Chem.* Vol. 99, pages 8945-8949, 1995.
- [17] Springer, T. E., Rockward, T., Zawodzinski, T. A., Gottesfeld, S., "Model for Polymer Electrolyte Fuel Cell Operation on Reformate Feed. Effects of CO, H₂ Dilution and High Fuel Utilization", *J. Electrochem. Soc.*, Vol. 148, pages A11-A23, 2001.
- [18] Merriam Webster online dictionary. <http://www.merriam-webster.com>
Consulted on 02/22/2011.
- [19] Song, R.-H., Shin, D. R., "Influence of CO concentration and reactant gas pressure on cell performance in PAFC", *International Journal of Hydrogen Energy*, Vol. 26, pages 1259-1262, 2001.
- [20] Zegers, P., "Fuel cell commercialization: The key to a hydrogen economy", *Journal of Power Sources*, Vol. 154, pages 497-502, 2006.
- [21] Satyapal, S., FY 2010 Annual Progress Report, DOE Hydrogen Program.
http://www.hydrogen.energy.gov/pdfs/progress10/i_introduction.pdf
Consulted on 15/11/2011.
- [22] Milliken, J. FY 2007 Annual Progress Report, DOE Hydrogen Program.
http://www.hydrogen.energy.gov/pdfs/progress07/i_introduction.pdf
Consulted on 15/02/2009.

- [23] Mohtadi, R., Lee, W.-K., Van Zee, J. W., "The effect of temperature on the adsorption rate of hydrogen sulfide on Pt anodes in a PEMFC", Applied Catalysis B: Environmental, Vol. 56, pages 37-42, 2005.
- [24] Kirubakaran, A., Jain, S., Nema, R. K., "A review on fuel cell technologies and power electronic interface", J. of Renewable and Sustainable Energy Reviews, Vol. 13, pages 2430-2440, 2009.
- [25] Huijsmans, J. P. P., van Berkel, F. P. F., Christie, G. M., "Intermediate temperature SOFC - a promise for the 21st century", Journal of Power Sources, Vol. 71, pages 107-110, 1998.
- [26] Mekhilef S, Saidur, R., Safari, A., "Comparative study of different fuel cell technologies", Renew. Sustain. Energy Rev., 2011.
- [27] Vert, V. B., Serra, J. M., Jordá, J. L., "Electrochemical characterization of $\text{MBaCo}_3\text{ZnO}_{7+d}$ ($\text{M} = \text{Y}, \text{Er}, \text{Tb}$) as SOFC cathode material with low thermal expansion coefficient", Electrochemistry Communications, Vol. 12, pages 278-281, 2010.
- [28] Minh, N. Q., "Ceramic Fuel-Cells", Journal of the American Ceramic Society, Vol. 76, pages 563-588, 1993
- [29] Carvalho, L., Scott, L., Jeffery, R., "An exploratory study into the use of qualitative research methods in descriptive process modeling", Information and Software Technology, Vol. 47, pages 113-127, 2005.
- [30] Studer, R., Benjamins, V. R., Fensel, D., "Knowledge engineering: Principles and methods, Data & Knowledge Engineering", Vol. 25, pages 161-197, 1998.

- [31] Donckels, B. M. R., De Pauw, D. J. W., Vanrolleghem, P. A., De Baets, B., "An ideal point method for the design of compromise experiments to simultaneously estimate the parameters of rival mathematical models", Chemical Engineering Science, Vol. 65, pages 1705-1719, 2010.
- [32] Park, E. W., Moon, H., Park, M.-S., Hyun, S. H., "Fabrication and characterization of Cu-Ni-YSZ SOFC anodes for direct use of methane via Cu-electroplating", International Journal of Hydrogen Energy, Vol. 34, pages 5537-5545, 2009
- [33] Zhu, H., Kee, R. J., Janardhanan, V. M., Deutschmann, O., Goodwin, D. G., "Modeling Elementary Heterogeneous Chemistry and Electrochemistry in Solid-Oxide Fuel Cells", J. Electrochem. Soc., Vol. 152, pages A2427-A2440, 2005.
- [34] Bessler, W. G., "Rapid Impedance Modeling via Potential Step and Current Relaxation Simulations", J. Electrochem. Soc., Vol. 154 pages B1186-B1191, 2007.
- [35] Recknagle, K. P., Ryan, E. M., Koeppel, B. J., Mahoney, L. A., Khaleel, M. A., "Modeling of electrochemistry and steam-methane reforming performance for simulating pressurized solid oxide fuel cell stacks", J. Power Sources, Vol. 195 pages 6637-6644, 2010.
- [36] Maier, J., "Ionic transport in nano-sized systems", Solid State Ionics, Vol.175, pages 7-12, 2004.
- [37] Zhao, F., Virkar, A. V., "Effect of morphology and space charge on conduction through porous doped ceria", Journal of Power Sources, Vol. 195, pages 6268-6279, 2010.

- [38] Bedogni, S., Campanari, S., Iora, P., Montelatici, L., Silva, P., "Experimental analysis and modeling for a circular-planar type IT-SOFC", Journal of Power Sources, Vol. 171, pages 617-625, 2007.
- [39] Suzuki, T., Yamaguchi, T., Fujishiro, Y., Awano, M., "Improvement of SOFC Performance Using a Microtubular, Anode-Supported SOFC", J. Electrochem. Soc., Vol. 153, pages A925-A928, 2006.
- [40] Peña-Martínez, J., Marrero-López, D., Pérez-Coll, D., Ruiz-Morales, J. C., Núñez, P., "Performance of XSCoF (X = Ba, La and Sm) and LSCrX' (X' = Mn, Fe and Al) perovskite-structure materials on LSGM electrolyte for IT-SOFC", Electrochimica Acta, Vol. 52, pages 2950-2958, 2007.
- [41] Kournoutis, V. Ch., Tietz, F., Bebelis, S., "Cyclic voltammetry characterization of a $\text{La}_{0.8}\text{Sr}_{0.2}\text{Co}_{0.2}\text{Fe}_{0.8}\text{O}_{3-\delta}$ electrode interfaced to CGO/YSZ", Solid State Ionics, Vol. 197, pages 13-17, 2011.
- [42] Mangalaraja, R. V., Ananthakumar, S., Paulraj, M., Pesenti, H., López, M., Camurri, C. P., Barcos, L. A., Avila, R. E., "Electrical and thermal characterization of Sm^{3+} doped ceria electrolytes synthesized by combustion technique", Journal of Alloys and Compounds, Vol. 510, pages 134-140, 2012.
- [43] Channa K, De Silva, R., Kaseman, B. J., Bayless, D. J., "Accelerated anode failure of a high temperature planar SOFC operated with reduced moisture and increased PH_3 concentrations in coal syngas", International Journal of Hydrogen Energy, Vol. 36, pages 9945-9955, 2011.

- [44] Marina, O. A., Pederson, L. R., Thomsen, E. C., Coyle, C. A., Yoon, K. J., "Reversible poisoning of nickel/zirconia solid oxide fuel cell anodes by hydrogen chloride in coal gas", *Journal of Power Sources*, Vol. 195, pages 7033-7037, 2010.
- [45] Hofmann, Ph., Panopoulos, K. D., Aravind, P. V., Siedlecki, M., Schweiger, A., Karl, J., Ouweltjes, J. P., Kakaras, E., "Operation of solid oxide fuel cell on biomass product gas with tar levels >10 g Nm⁻³", *International Journal of Hydrogen Energy*, Vol. 34, pages 9203-9212, 2009.
- [46] Fu, C., Sun, K., Zhang, N., Chen, X., Zhou, D., "Electrochemical characteristics of LSCF-SDC composite cathode for intermediate temperature SOFC", *Electrochimica Acta*, Vol. 52, pages 4589-4594, 2007.
- [47] Huang, Q.-A., Hui, R., Wang, B., Zhang, J., "A review of AC impedance modeling and validation in SOFC diagnosis", *Electrochimica Acta*, Vol. 52, pages 8144-8164, 2007.
- [48] Morel, B., Roberge, R., Savoie, S., Napporn, T. W., Meunier, M., "Catalytic activity and performance of LSM cathode materials in single chamber SOFC", *Applied Catalysis A: General*, Vol. 323, pages 181-187, 2007.
- [49] Rambabu, B., Ghosh, S., Zhao, W., Jena, H., "Innovative processing of dense LSGM electrolytes for IT-SOFC's", *Journal of Power Sources*, Vol. 159, pages 21-28, 2006.
- [50] Kim, S.-H., Shimpalee, S., Van Zee, J. W., "The Effect of Flow Field Design and Voltage Change Range on the Dynamic Behavior of a PEMFC", *J. of Electrochem. Soc.*, Vol. 152, pages A1265-A1271, 2005.

- [51] Sumi, H., Puengjinda, P., Muroyama, H., Matsui, T., Eguchi, K., "Effects of crystal Structure of yttria- and scandia-stabilized zirconia in nickel-based SOFC anodes on carbon deposition and oxidation behavior", *Journal of Power Sources*, Vol. 196, pages 6048-6054, 2011.
- [52] Kim, S-H., Shimpalee, S., and Van Zee, J. W., "The effect of stoichiometry on dynamic behavior of a PEMFC during load change", *J. of Power Source*, Vol. 135, pages 110-121, 2004.
- [53] Li, X., Li, J., Xu, L., Yang, F., Hua, J., Ouyang, M., "Performance analysis of proton-exchange membrane fuel cell stacks used in Beijing urban-route buses trial project", *International Journal of Hydrogen Energy*, Vol. 35, pages 3841-3847, 2010.
- [54] Haraldsson, K., Folkesson, A., Alvfors, P., "Fuel cell buses in the Stockholm CUTE project—First experiences from a climate perspective", *Journal of Power Sources*, Vol. 145, pages 620-631, 2005.
- [55] Shang, J. L., Pollet, B. G., "Hydrogen fuel cell hybrid scooter (HFCHS) with plug-in features on Birmingham campus", *International Journal of Hydrogen Energy*, Vol. 35, pages 12709-12715, 2010.
- [56] Hernández, A. M., Mogni, L., Caneiro, A., "La₂NiO_{4+δ} as cathode for SOFC: Reactivity study with YSZ and CGO electrolytes", *International Journal of Hydrogen Energy*, Vol. 35, pages 6031-6036, 2010.
- [57] Calì, M., Santarelli, M. G. L., Leone, P., "Design of experiments for fitting regression models on the tubular SOFC: Screening test, response surface analysis and optimization", *International Journal of Hydrogen Energy*, Vol. 32, pages 343-358, 2007.

- [58] Santori, G., Brunetti, E., Polonara, F., "Experimental characterization of an anode-supported tubular SOFC generator fueled with hydrogen, including a principal component analysis and a multi-linear regression", International Journal of Hydrogen Energy, Vol. 36, pages 8435-8449, 2011.
- [59] Joon, K., "Fuel cells - a 21st century power system", Journal of Power Sources, Vol. 71, pages 12-18, 1998.
- [60] He, H., Vohs, J. M., Gorte, R. J., "Carbonaceous deposits in direct utilization hydrocarbon SOFC anode", Journal of Power Sources, Vol. 144, pages 135-140, 2005.
- [61] Vivet, N., Chupin, S., Estrade, E., Richard, A., Bonnamy, S., Rochais, D., Bruneton, E., "Effect of Ni content in SOFC Ni-YSZ cermets: A three-dimensional study by FIB-SEM tomography", Journal of Power Sources, Vol. 196, pages 9989-9997, 2011.
- [62] Panteix, P. J., Baco-Carles, V., Tailhades, Ph., Rieu, M., Lenormand, P., Ansart, F., Fontaine, M. L., "Elaboration of metallic compacts with high porosity for mechanical supports of SOFC", Solid State Sciences, Vol. 11, pages 444-450, 2009.
- [63] Gansor, P., Xu, C., Sabolsky, K., Zondlo, J. W., Sabolsky, E. M., "Phosphine impurity tolerance of Sr₂MgMoO_{6-δ} composite SOFC anodes", Journal of Power Sources, Vol. 198, pages 7-13, 2012.
- [64] Jardiel, T., Caldes, M. T., Moser, F., Hamon, J., Gauthier, G., Joubert, O., "New SOFC electrode materials: The Ni-substituted LSCM-based compounds (La_{0.75}Sr_{0.25})(Cr_{0.5}Mn_{0.5-x}Ni_x)O_{3-δ} and (La_{0.75}Sr_{0.25})(Cr_{0.5-x}Ni_xMn_{0.5})O_{3-δ}" Solid State Ionics, Vol. 181, pages 894-901, 2010.

- [65] Lay, E., Gauthier, G., Dessemond, L., "Preliminary studies of the new Ce-doped La/Sr chromo-manganite series as potential SOFC anode or SOEC cathode materials", Solid State Ionics, Vol. 189, pages 91-99, 2011.
- [66] Fiúza, R. da P., da Silva, M. A., Boaventura, J. S.;, "Development of Fe-Ni/YSZ-GDC electrocatalysts for application as SOFC anodes: XRD and TPR characterization and evaluation in the ethanol steam reforming reaction", International Journal of Hydrogen Energy, Vol. 35, pages 11216-11228, 2010.
- [67] Tikhonovich, V. N., Kharton, V. V., Naumovich, E. N., Savitsky, A. A., "Surface modification of La(Sr)MnO₃ electrodes" Solid State Ionics, Vol. 106, pages 197-206, 1998.
- [68] Shao, Z., Haile, S. M., "A High Performance Cathode for the Next Generation Solid-Oxide Fuel Cells", Nature, Vol. 431, pages 170-173, 2004.
- [69] Esquirol, A., Brandon, N. P., Kilner, J. A., Mogensen, M., "Electrochemical Characterization of La_{0.6}Sr_{0.4}Co_{0.2}Fe_{0.8}O₃ Cathodes for Intermediate-Temperature SOFCs", J. Electrochem. Soc., Vol. 151, pages A1847-A1855, 2004.
- [70] Stöver, D., Buchkremer, H. P., Uhlenbruck, S., "Processing and properties of the ceramic conductive multilayer device solid oxide fuel cell (SOFC)", Ceramics International, Vol. 30, pages 1107-1113, 2004.
- [72] Simner, S. P., Anderson, M. D., Coleman, J. E., Stevenson, J. W., "Performance of a novel La(Sr)Fe(Co)O₃-Ag SOFC cathode", Journal of Power Sources, Vol. 161, pages 115-122, 2006.

- [73] Aungkavattana, P., Timakul, P., Atong, D., Mongkolkachit, C., Wanakitti, S., Lertwittayanon, K., Hills, M., Henson, M., "Component Materials and Design for Tubular Solid Oxide Fuel Cell", Annual Meeting of The Ceramic Society of Japan, Invited lecture, Nagaoka, Japan, 2008.
- [74] Pérez-Flores, J. C., Ritter, C., Pérez-Coll, D., Mather, G. C., Canales-Vázquez, J., Gálvez-Sánchez, M., García-Alvarado, F., Amador, U., "Structural and electrochemical characterization of $\text{La}_{2-x}\text{Sr}_x\text{NiTiO}_{6-\delta}$ ", International Journal of Hydrogen Energy, Available online 25 November 2011.

CHAPTER 3

Experimental Facility and Electrochemical Techniques

Contents

3.1. Introduction	63
3.2. Solid Oxide Fuel Cell	64
3.3. Experimental Facility	67
3.4. Experimental Electrochemical Techniques	72
3.4.1. Introduction.....	72
3.4.2. Polarization Curve	77
3.4.3. Electrochemical Impedance Spectroscopy	79
3.4.4. Cyclic Voltammetry	81
3.4.5. Transient Analysis	82
3.4.6. Mass Balance	84
3.5. Summary in English	86
3.6. Summary in Spanish	86
3.7. References.....	87

3. Experimental Facility and Electrochemical Techniques

3.1. Introduction

Although the main reasons that have prevented fuel cells from being commercially competitive so far are well known: low durability and high cost [1] [2] [3], further research is still needed to completely understand the processes that take place inside the fuel cell, the **mechanisms that cause degradation**, so that they can be overcome in order to extend their lifetime. Therefore, a precise characterization of the electrochemical processes that take place inside the fuel cell is the key point to understand and develop the technology.

Microtubular Solid Oxide Fuel Cells (SOFCs) also present these issues, so it is important to characterize them. As they have a small size, they produce reduced amounts of current and power, thus they operate assembled in racks and stacks to produce the desired voltage and current [4]. However, for characterization purposes, it is more convenient to use only one cell. As all the devices used, such as potentiostats, galvanostats, frequency analyzers, load boxes, etc., are generally only able to work with low current and power, it is easier to implement and interpret the electrochemical techniques that are necessary for its characterization when only one cell is used. Also, information obtained from one cell is generally more relevant and accurate than the one obtained for the full stack.

The experimental test station used to carry out all the experiments presented in this document as well as the manufacturing characteristics of the SOFC tested in this project is presented here. The microtubular Solid Oxide Fuel Cells were **tested individually** for the reasons explained above and so the experimental facility was designed to fit this purpose.

3.2. Solid Oxide Fuel Cell

The Solid Oxide Fuel Cells that were tested in the experimental facility that will be described in the next section were manufactured by the *National Metal and Materials Technology Center (MTEC)* in Thailand. Similarly to other cells reported in the literature [18-20], it is an **electrolyte-supported microtubular fuel cell**. Other authors report anode-supported microtubular fuel cells [21] and cathode supported microtubular fuel cells [22] that show different properties. The electrolyte tube is composed by Yttria Stabilized Zirconia, where the percentage of zirconia is 8% by mole basis (8YSZ). The anode is located in the internal surface of this tube and consists of a **Nickel/YSZ coating**. The cathode, consequently, is located in the external surface of the tube and it is composed of a layer of **Lanthanum strontium manganate** (its empiric formula is: $\text{La}_{0.8}\text{Sr}_{0.2}\text{MnO}_3$, and it is abbreviated as LSM or LSMO).

A schematic drawing of the fuel cell structure can be seen in Figure 3.1. As can be seen, hydrogen gas is fed to the anode side while air is fed to the cathode side and oxygen ions (O^{2-}) travel from the cathode to the anode through the electrolyte so that the global reaction (equation 3.1) for the fuel cell is satisfied. The half-cell reactions are shown by equations 3.2 (anode) and 3.3 (cathode).



A **concentric copper tube** inside the electrolyte delivers the gaseous fuel to the anode. It serves a double function. In addition to **delivering the fuel** to the anode of the fuel cell, it acts as the **anode current collector**, that is, it collects the electrons generated at the anode side, to close the electric circuit. A layer of nickel oxide foam separates the electrolyte from

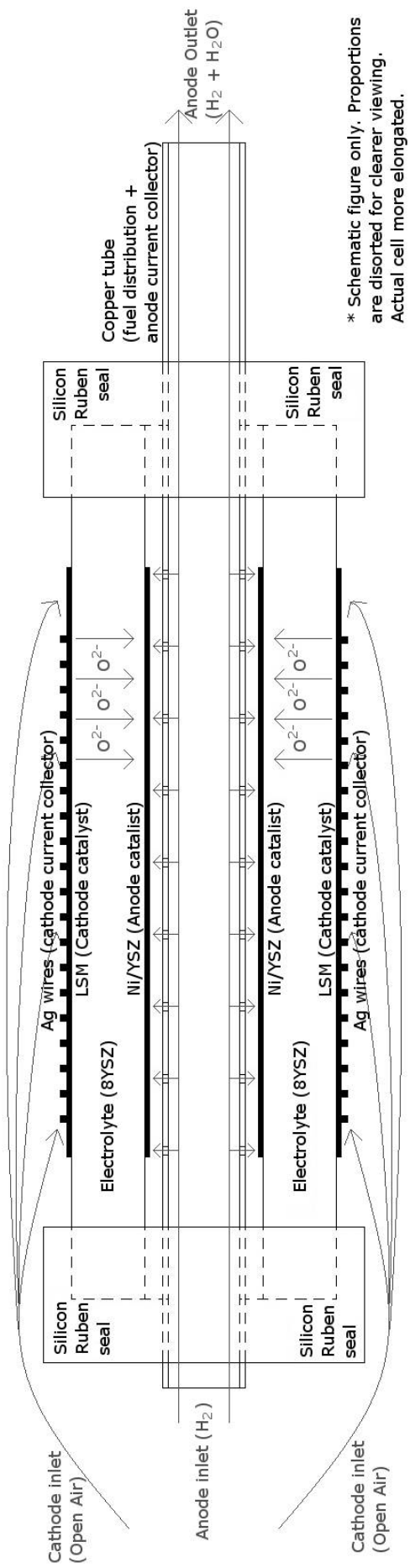


Figure 3.1: Schematic of the MTEC SOFC structure, from [17].

the copper tube. As it is very tightly packed, a good electric contact between the anode catalyst (the nickel particles) and the copper tube is achieved.

So that the fuel is delivered in a consistent way from the inside of the copper tube to the nickel catalyst just outside of it, the copper tube presents four different rows of evenly distributed small holes in the longitudinal direction. That ensures that the fuel is able to flow at a uniform rate towards the nickel catalyst. At both ends of the microtubular YSZ electrolyte, **high temperature silicon rubber seals** are placed to prevent leakage from the anode side. In the experimental facility used, the silicon seals were replaced by ceramic glue seals because the furnace had a larger size than the fuel cell itself, and the seals lied inside of it. Thus, a high temperature resistive material - a **ceramic paste** - was used to replace the silicon rubber seals.

Like in many other solid oxide fuel cells, the cathode current collector is a silver wire [8]. In this case, the **silver wire** is rolled around the LSM catalyst of the cathode. It also serves a double function: it **collects the electrons** at the cathode side (working as the cathode current collector) and also **enhances the catalytic activity** of the LSM paste deposited over the electrolyte.

The fabrication process that the *MTEC* follows to prepare their fuel cells is the following one. Firstly, the **electrolyte is formed by extrusion** of the 8% mol $\text{Y}_2\text{-O}_3$ Stabilized Zirconia. This material is **sintered** at constant temperature (1600°C) for four hours. Cooling process follow, and then the internal surface of the tube - where the anode is located - is **coated with Ni/YSZ Cermet by slide casting**. Then, the cathode catalyst located at the external surface of the electrolyte is coated over the tube with **LSM paste using a painting technique**. After that, the whole structure is **dried** inside an oven at 100°C for thirty minutes.

The **silver wire is rolled** over the LSM cathode catalyst then and a further layer of LSM is painted over the wire. The anode current collector - the internal copper tube - covered with a NiO conductive foam is inserted inside the electrolyte then. The conductive foam is compressed between

the electrolyte and the copper tube, tightening the current collector to the electrolyte. Finally, the two silicon rubber seals are placed at the extremes of the electrolyte to prevent leakage from the anode, and give the structure the required rigidity.



Figure 3.2: SOFC picture immediately after the drying process.

Table 3.1 shows a summary of the characteristics that the Solid Oxide Fuel Cell produced by the MTEC has while Figure 3.2 shows how the cells look like right after the drying process and before the silver wires are rolled over the cathode side.

Table 3.1: Characteristics of the SOFC fabricated by the MTEC in Thailand.

Component	Material	Thickness (mm)	Fabrication
Anode	NiO/YSZ, NiO/GDC	0.20	Slip coating
Electrolyte	YSZ, doped-CeO ₂	0.30	Extrusion
Cathode	LSM, doped-LSM	0.30	Painting
Anode Current C.	Copper	N/A	Insertion
Cathode Current C.	Silver	N/A	Wiring

3.3. Experimental Facility

A schematic drawing of the experimental test station used is shown in Figure 3.3. It consists of a furnace which is able to rise the temperature to the desired value. The fuel cell is located inside the furnace. Several gas cylinders located at the back of the laboratory supply all the

necessary gases to the fuel cell through the corresponding tubing. The amount of gas supplied is controlled by using electronic mass flow controllers which are commanded by the load box.

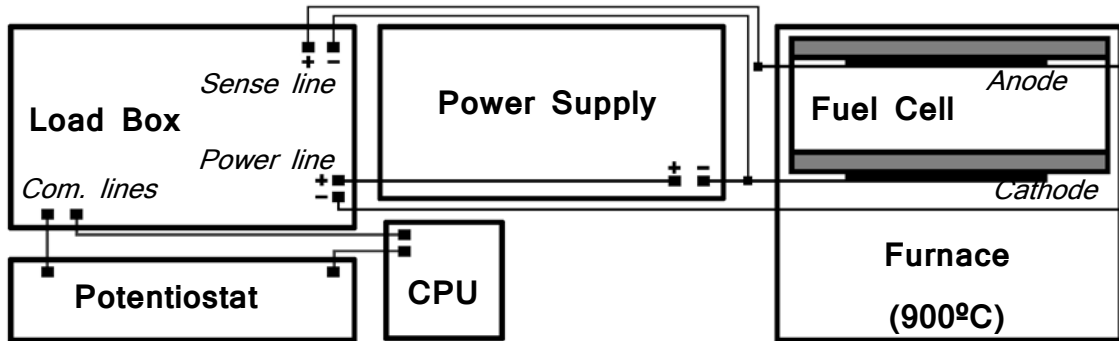


Figure 3.3: Experimental setup at the University of South Carolina, from [16].

Although the anode gas flows through the tubing all the time, on the cathode side, air is simply blown on the surface. Also, ambient air is able to flow into the furnace through the holes left between the insulation wall and the tubing of the fuel cell. This kind of setup is generally called “breathing fuel cell” in the literature [6] [7], and theoretically it should not need an external air supply to work. Air is supplied in great excess because the flow patterns are difficult to establish, and to ensure a proper characterization the anode side should be the limiting section of the test cell and thus, air excess should be warranted. A picture of the air blower can be seen in Figure 3.4.



Figure 3.4: SOFC mechanical support and air blower for the cathode side.

The load box is the central unit of control of the test station. It controls the mass flow both for the anode and cathode sides, also allowing making mixtures of the available gases. It also controls the potential (or current depending on the mode chosen) between the terminals of the fuel cell, making it possible to carry out different tests (like polarization curves) without the aid of any other equipment. It is connected to a personal computer to extend its possibilities, facilitating its control and data saving. The program used to control it in the CPU is the *FuelCell 3.91* by *Scribner and Associates*.

As the power that a single cell is able to produce is quite limited, the ohmic losses on the connecting wires can become relevant, thus an auxiliary power supply is connected to the electric circuit, in order to compensate for them.

For more specific tests, such as impedance analysis or cyclic voltammetry, it is necessary to use more specific apparatus. A potentiostat/galvanostat is a device that is able to either maintain a constant voltage between two electrodes (working and counter electrodes) - when it works as a potentiostat - or supply a constant current - when it functions as a galvanostat. The potentiostat/galvanostat is also connected to a personal computer, so that the control of the fuel cell can be done more easily and the results can be saved in electronic format. To control the potentiostat/galvanostat programs developed by *Scribner and Associates* were used as well. Specifically, for the cyclic voltammetry test, the *CorrWare* and *CorrView* software was used. For the impedance tests *ZPlot* and *ZView* software was used.

These actions can also be carried out by the load box. The main difference is that the potentiostat/galvanostat has the power supply integrated inside it, and so it presents a more accurate control loop which usually leads to better results and a faster response. Although cyclic voltammetry could also be theoretically done with the load box too, the fact that these tests are usually done with a rapid change in the voltage (up to 0.2 V/s), make it impossible to carry them out with the load box.

The main limitation of the potentiostat/galvanostat device is that unlike the load box, it does not support high currents. In fact, the maximum current supported by the equipment used was 1A.

For the impedance test, a frequency analyzer, coupled to the load box (for the high current analysis) or potentiostat/galvanostat (for the low current analysis) needed to be used.

Finally, at the outlet of the anode of the fuel cell, there is a valve located that allows the user to switch the outlet flow between a hood and a plastic bag, where samples of the outlet gas can be collected in order to study its composition, making it possible to close certain mass balances inside the fuel cell. Those gas bags were analyzed using a mass spectrometer and a gas chromatographer (model Buck Scientific 910 GC) in order to determine its composition.

A picture of the complete installation can be found in Figure 3.5, and Table 3.2 shows the concrete models of all the different parts that composed the experimental facility.

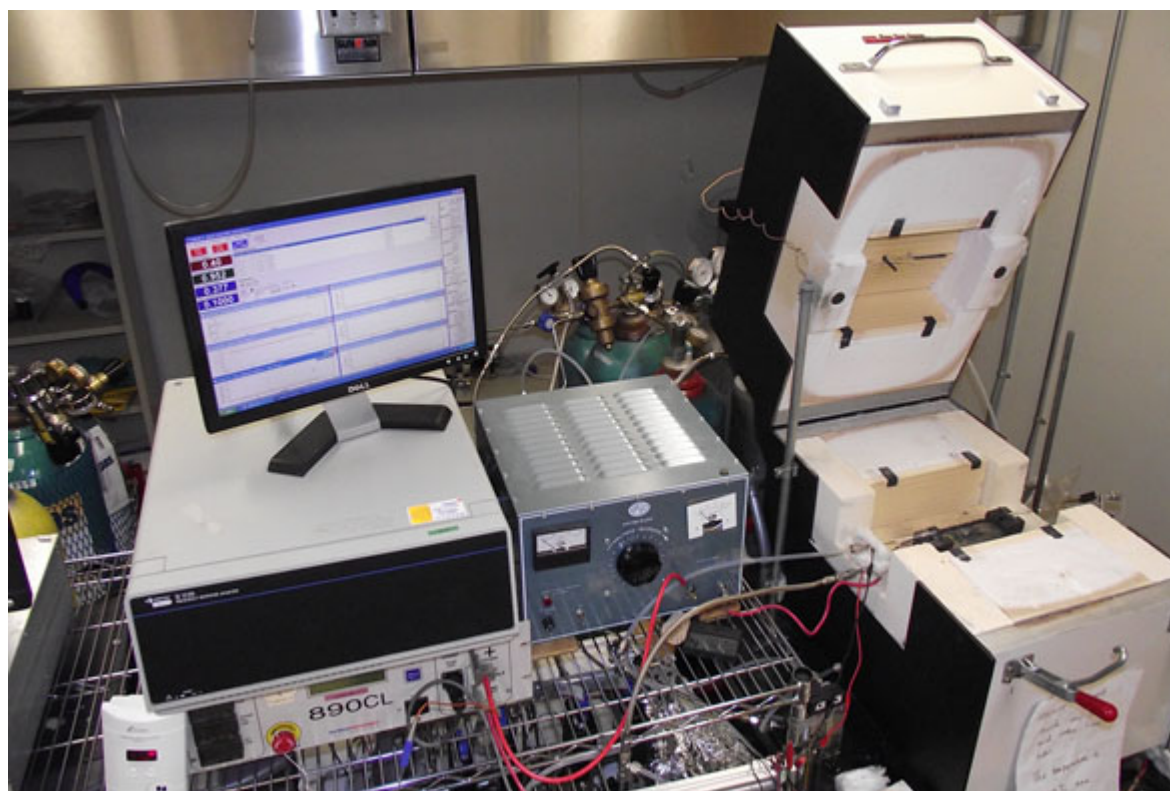


Figure 3.5: Picture of the experimental setup at the University of South Carolina.

Table 3.2: Models used in experimental setup at the University of South Carolina.

Aparatus	Model
Potentiostat/galvanostat	Princeton Applied Research, model 273A
Load Box	Scribner and Associates, model 890CL
Furnace	Springfield Technologies
Frequency analyzer	Solartron 1250
Power Supply	EPSCO Electro-plater
Personal computer	Dell, Intel Core 2 Duo Processor.
Mass Flow Controllers	MKS 1179A

For all tests, hydrogen flow was set to 50 standard cubic centimeters per minute (sccm) and air flow to 300sccm. The correspondent stoichiometry depends on the performance of the SOFC and it is reported here.

Stoichiometry, in the electrochemical context, is an extremely important concept for the study of the fuel cells. It is defined as the ratio of molar flow rate of reactant gas to the molar flow rate of consumed gas based on the device electric current and the assumed number of electrons of the reaction. . For this reason there will be two different stoichiometries for a fuel cell: the anode stoichiometry (where hydrogen is flowing) and the cathode stoichiometry (where the oxygen is flowing).

With this definition it is clear that stoichiometry is an important parameter to determine the working conditions of a fuel cell. If it is a large number, it means that more gas than necessary is being used. However, if it is small (but never below one), it means that the amount of gas which is used is close to the required value to complete the reaction and thus it could happen that the cell is working with less gas than it should. If this is the case, there will be areas of catalyst where no reactant reaches (it would be consumed first), and this could damage the catalyst causing cell deterioration and eventual failure. This phenomenon is known as “fuel cell starvation”.

To prevent cell starvation, the stoichiometry, both for the anode and cathode sides, should be carefully controlled so that it is never below a certain level. For PEM fuel cells typical levels are 1.2 and 1.5 for the anode and cathode sides respectively. As SOFC is new technology still in

a development stage, it is not clear yet which values of stoichiometry would be adequate for them. Since the objective of the project is to characterize the fuel cell, and not optimize its performance, it was chosen to use high values of stoichiometry both for the anode and the cathode side to ensure that cell failure did not occur for this reason.

The value chosen for this case was that the minimum stoichiometry was always over 3 even in the most unfavorable conditions for the anode side. For the cathode side, since the flow distribution is impossible to calculate, it was decided to use even higher stoichiometry.

3.4. Experimental Electrochemical Techniques

3.4.1. Introduction

Electrochemistry, as a branch of the chemistry, is a science that studies the chemical reactions that occur at an interface of two different materials: one of them being ion-conductive, and the other one being electron-conductive. This means that the electrons which are exchanged in the reaction are not directly transferred to the molecules of the products (as in an oxidation/reduction reaction) but they are forced to move through the electron-conductive material while the ions move through the ion-conductive material, closing the electric circuit.

Electrochemistry is an important science, as it gives a scientific support to modern energy technologies such as batteries and fuel cells. The first ones are present in multitude of devices widely used currently, such as cell phones, laptops, cameras, music players, and so on. The second ones, as was explained in previous chapters, are one of the most promising technologies to help humanity overcome the energy issues that we are currently facing. From another point of view, electrochemistry also provides a scientific background to other issues related with important product degradation, as corrosion of the metals certainly is.

From the definition of electrochemistry, another important characteristic of electrochemical reactions that must be pointed out is that, as the reactants

are separated, all reactions can be split into two half-reactions each of which occurs at one side of the interface where reaction takes place. The side that loses the electrons - that is, where the reactant is oxidized - is called the anode, whereas the side that receives the electrons - where the reactant is reduced - is called the cathode. Thus there will always be two half-cell reactions in any electrochemical reaction: the anodic half-reaction, and the cathodic half-reaction.

By definition, electric current is the movement of electrons. Electric current is a form of energy that is broadly extended nowadays, and that can be easily transformed into mechanical energy by means of an electric engine. This electric energy produced clearly contrasts with the result of an oxidation/reduction reaction: heat. This is so, because for an oxidation/reduction reaction electrons are transferred directly - together with the ions - to the new molecules that are being formed. The energy produced by that kind of reaction (which is the difference in the Gibbs free energy of the products and the reactants) is released as heat. If the desired type of energy is mechanical (like that of a car), a device that transforms it - a heat engine - is necessary.

According to the Second Law of Thermodynamics [13], it is impossible to completely transform heat into mechanical energy, no matter how efficient the device used is. The maximum fraction of transformation - given by the ideal device - depends on the temperature at which the heat is released, and the temperature of the environment. The higher the difference between the two temperatures is, the higher the efficiency of the transformation would be. This higher limit for the efficiency in any heat engine is also called Carnot efficiency, and it explains the reason why fuel cells - as electrochemical device - have the potential of producing higher efficiencies in fuel utilization than the heat engines which are currently used for transport and other energy-related sectors, like it was pointed out in previous sections.

From the definition of electrochemistry, it is clear that the laws that govern this kind of reactions are not the same as those that govern the general electrochemical reactions (oxidation/reduction). In the second case, the

Gibbs free energy determines the thermodynamic equilibrium of a certain reaction and it determines if will take place in one direction or in the opposite under certain conditions. However, for the electrochemical reactions, it is the potential difference - given in the electrochemical potential series and the Nernst equation - that accounts for the equilibrium of both half-cell reactions, and if the reaction will take place in a certain direction or the opposite.

Michael Faraday established in 1832 a universal relationship between the Gibbs free energy of a certain reaction and the potential difference that it would generate. These two quantities are linked by the number of electrons that are involved in the reaction and a constant which was named after Michael Faraday as *Faraday's constant*. These equations have been reproduced and rewritten in more convenient units afterwards by several authors like Strong [14] and can be summarized by equation 3.4, where it is shown that the total mass that reacts (m) is directly proportional to the total electric charge that passes through it (Z - calculated as the integral of the electric current over time). The constant that relates these two quantities considers the total number of electrons involved in the reaction (n), the molar mass of the substance (M) and Faraday's constant (F) as shown in equation 3.4.

$$m = \frac{Z}{F} \cdot \frac{M}{n} \quad (3.4)$$

Even if that equilibrium laws seem to be effectively the same for both kinds of reactions, the laws that govern the kinetics of one kind of reaction and the other show bigger differences. While oxidation/reduction reaction kinetic traditional laws usually depend on the concentration of reactants and products elevated to different powers - and that marks the order of the reaction, in the electrochemical reaction different models have been developed to explain all behaviors found. Obviously electrical current plays an extremely important role in all of them.

It is clear from equation 3.4, that if the current produced is zero, no global net reaction can take place, as the charge balance cannot be violated.

Instead a potential difference will be generated, but no global kinetic activity is seen. The exception to this is a corrosion reaction where no measurable net current is observed in the external circuit because the electrons produced by the oxidation reaction are consumed by the reduction reaction which occurs on the same surface. For the rest of electrochemical reactions, if current is allowed to circulate, two kinds of limitations can occur. As the reactants must reach the surface where reaction is taking place (and thus, where they are consumed), if the mass transport is not quick enough, no more current can be produced which leads to the first possible limitation: mass transport limitation.

Even if enough reactant was supplied to the reacting surface, the reaction would take a certain time to occur, which will also limit the reaction rate, leading to the second possible limitation: charge transfer limitation. The reactions that follow this behavior are also known as kinetic limited reactions. Either of the two will be dominant and will determine the rate - and therefore the current - at which the reaction will take place.

For the most favorable conditions - that is, when the electric circuit is closed and the separator provides no resistance - the current observed is controlled by one of the electrodes which may operate at either mass transfer or kinetic limitations. Depending on the structure, the materials used in the device and the working conditions, the current can be controlled by either the mass transfer or by the charge transfer.

The charge transfer limitation has been successfully modeled by the Butler-Volmer equation [12]. It relates the overpotential applied (the actual potential difference of the electrodes compared to the equilibrium potential of those electrodes for the given conditions) to the current measured, through several variables - like the exchange current density and the symmetry factor - that depend on the reactants and the conditions of operation, as shown by equation 3.5:

$$i = i_0 \cdot \left(\exp\left[\frac{\alpha_a \cdot n \cdot F \cdot \eta}{R \cdot T} \right] - \exp\left[-\frac{\alpha_c \cdot n \cdot F \cdot \eta}{R \cdot T} \right] \right) \quad (3.5)$$

The Butler-Volmer equation presents two limiting cases. When the current is small - that is, when the overpotential is small, which happens when the actual potential is close to the equilibrium potential - a linear region can be seen, with the current increasing linearly with the overpotential. This can also be called, polarization resistance. When current is large - that is, when the overpotential is big - the Butler-Volmer equation can be simplified to an exponential dependence of the current with the overpotential, called the Tafel equation [15], given by equation 3.6 and 3.7. As it can be seen in equation 3.7, it is a linear relationship between the overpotential (η) and the logarithm of the current density (i), exactly as the empirical equation proposed initially by Tafel when he started studying this phenomenon. Also, for electrochemical reactions, this relationship is applied for the anodic and cathodic reactions separately, as the constants that appear in the exponential relationship, which are called Tafel constants, are usually different for the anodic reaction and the cathodic reaction. These conditions are usually the ones taking place when corrosion occurs, and thus are the key to understand the corrosion processes.

$$i = i_0 \cdot \exp\left(\frac{\alpha \cdot n \cdot F \cdot \eta}{R \cdot T}\right) \quad (3.6)$$

$$\eta = \frac{2.303 \cdot R \cdot T}{\alpha \cdot n \cdot F} \cdot \log(i) - \frac{2.303 \cdot R \cdot T}{\alpha \cdot n \cdot F} \cdot \log(i_0) \quad (3.7)$$

A more detailed explanation of all these processes and the equations governing them can be found in the literature [5]. Given the high temperatures at which Solid Oxide Fuel Cells operate, it is a reasonable hypothesis that they are limited by mass transfer rather than charge transfer, which generally involves the diffusion process hydrogen from the bulk (the center of the tube) to the catalyst or for the oxygen to be transported across the diffusion boundary layer on the outside of the tube. Thus, in order to compute a theoretical limiting current, the flow field of the fuel inside the anode should be solved, but often mass or heat transfer analogies can be used to estimate the value of the limiting

current. This is described with more detail further in the dissertation, and Appendix A1 shows the calculation of this limiting current for the two extreme cases.

In this section the most common techniques used to characterize electrochemical devices are explained. All of them were used in the experiments carried out during the experiments to characterize the solid oxide fuel cell.

3.4.2. Polarization Curve

The polarization curve is an experiment that can be carried out on fuel cells and that provides information about its behavior towards polarization. It generally consists of a series of experiments where the voltage (or the current) is hold at a certain value for a certain period of time - until steady state is reached. Then, the current (or the voltage) is measured. By doing this at different voltages or currents a certain number of points are obtained, and when they are plotted in a V-I diagram, they produce the polarization curve. Figure 3.6 - taken from [9] - is included as an example of polarization curves with PEM fuel cells.

To obtain the polarization curve, the load box was used to control the potential/current of the fuel cell. Firstly, an open circuit voltage experiment was set for the first and the last experiments. Open circuit voltage is an important magnitude of the fuel cell. It is obtained by setting the current equal to zero, and thus represents the equilibrium potential of the cell, and should coincide with the one predicted by the Nernst equation.

For the rest of the experiments, constant voltage control was chosen. Although both methods (voltage-controlled and current-controlled) should yield to the same result, from what was explained before, current is intimately related to the kinetic of the reaction, so imposing it, means imposing the rate of the reaction, which forces a reaction to occur and may lead to electrode damage if there is insufficient transport of reactant at the reaction site.

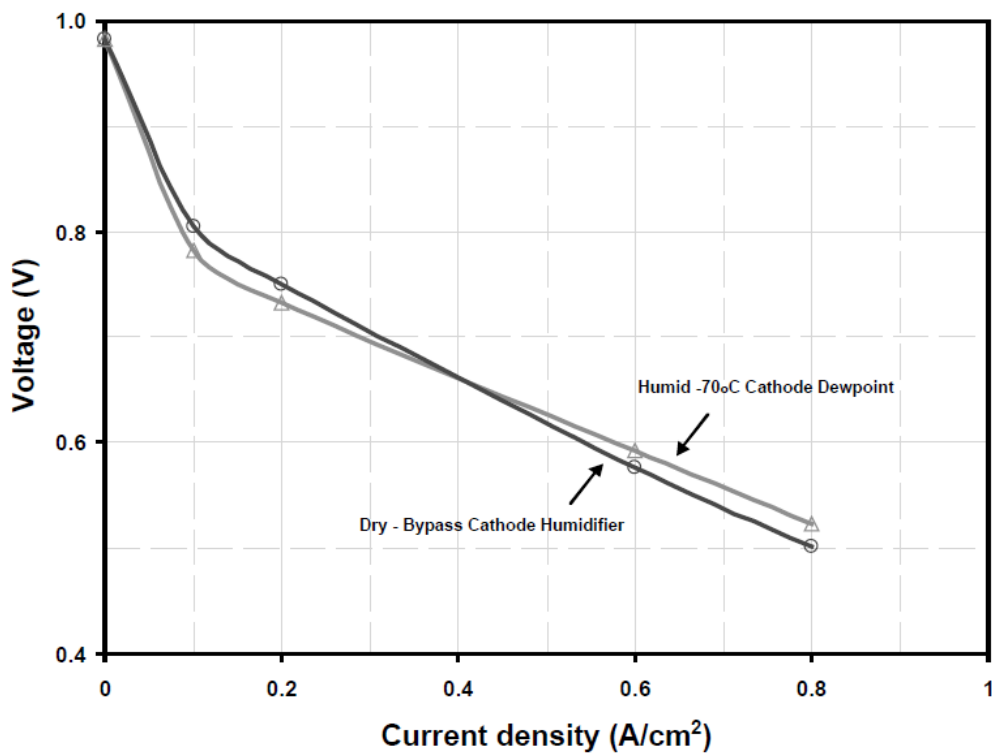


Figure 3.6: Example of polarization curves for PEMFC, from [9].

The constant voltage experiments started at 1.1V. Voltages higher than this did not produce stable current, even though the open circuit voltage of the MTEC SOFC was always higher than that (around 1.23V generally). Although the reason for these oscillations was not completely determined, it is believed that a voltage of 0.1V was not sufficient to overcome the ohmic limitations of the electrolyte.

This explanation also agrees with the peak in the current that was observed during when transitions from open circuit voltage to any lower voltage were set. This peak is explained by the amount of hydrogen accumulated in the foam, that reacts quickly when the circuit is closed, but then the cell is not able to maintain it for the hydrogen diffusion is too slow to maintain it.

Therefore, experiments start at 1.1V and they go down to 0.35V. Then the same experiments are repeated in the reverse order. This way two polarization curves for the system are obtained (one with decreasing potentials, and another one with increasing potentials), which should not show hysteresis. The average of the two values is presented here as the

polarization curve. By using this approach, it can be verified if the hold time for each level of polarization is long enough so that steady state is reached and more consistent results are produced, and also if the fuel cell is working correctly.

However, if hysteresis is actually seen, it means that no steady state was reached and so the hold time for the experiment should be increased. It was found that a set time that was adequate for the response of the fuel cell was 183 seconds and this was the value used in all experiments. During each experiment, one point was recorded every 10 seconds and then, the average of the last six points was taken as the value for the set voltage.

3.4.3. Electrochemical Impedance Spectroscopy

Electrochemical Impedance Spectroscopy (EIS) is a test in the frequency domain that can be carried out on certain physical systems, like fuel cells, and that evaluates the response of the system in the frequency domain.

It is carried out by setting a constant voltage (or current) in the fuel cell and introducing small sinusoidal perturbations in the current (or voltage) for a wide range of frequencies. The response of fuel cell is recorded using a frequency analyzer and important data can be obtained from its analysis. Figure 3.7, from [10], is an example of the kind of plots that EIS techniques can produce for three different systems.

These results are generally plotted in a complex plane (Z -imaginary, Z -real) plot, where Z is the impedance of the fuel cell. The module of the impedance is the ratio between the peak values of the voltage and the current at each frequency, while the angle is calculated by the delay in the response of the output signal.

When the values and the shape of the curve produced is analyzed, many properties of the fuel cell can be estimated, like the internal resistance, mass transfer estimates, the frequency response, etc.

The approach used for the experiments was setting a controlled voltage (0.6V) which produced a stable current. Then this current was perturbed, with a sinusoidal profile. The best results were always obtained with larger perturbations, and the results presented here included a perturbation of $\pm 20\%$ of DC current. The frequency used ranged from 32kHz to 0.01Hz.

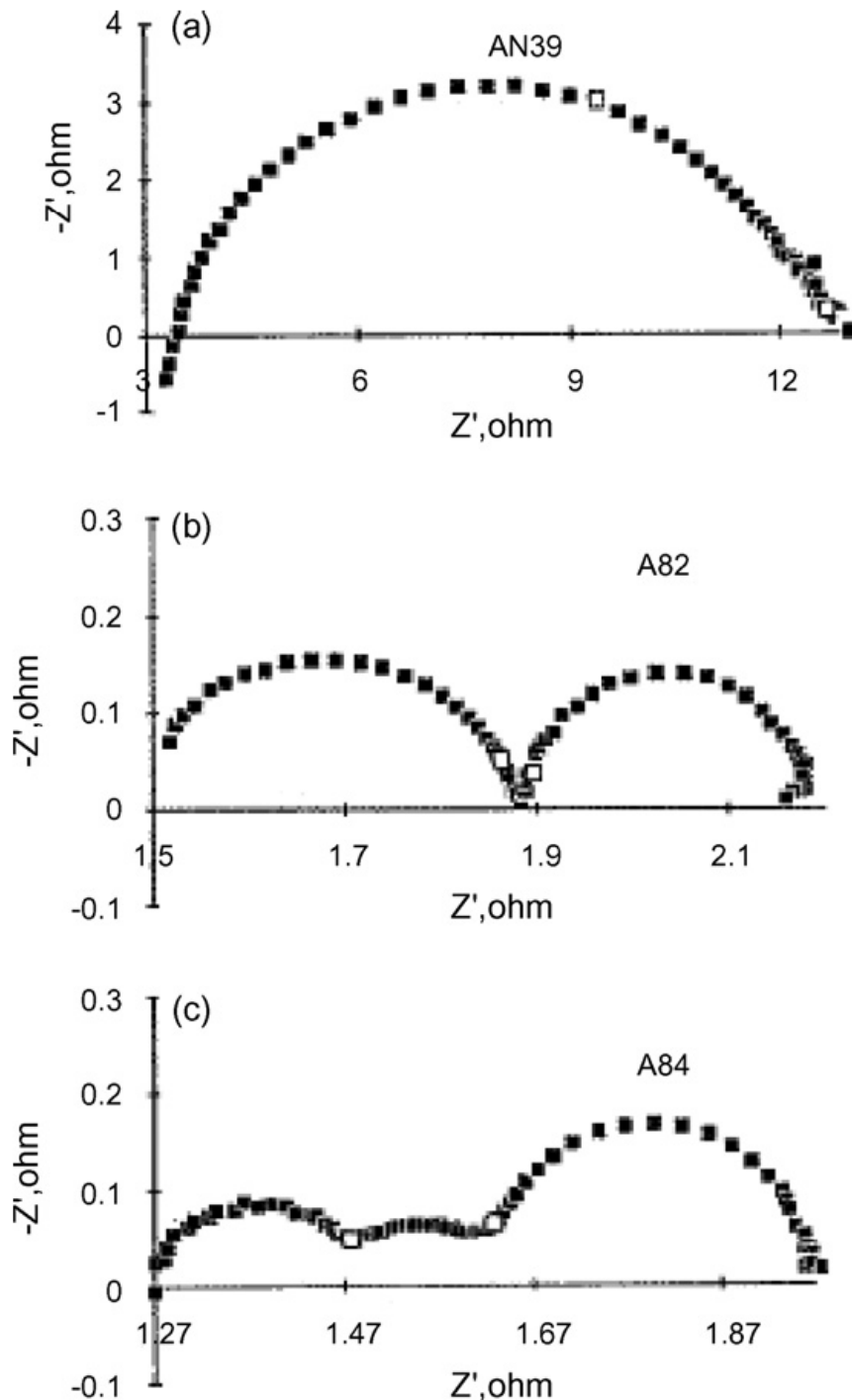


Figure 3.7: Example of EIS test for different systems, from [10].

3.4.4. Cyclic Voltammetry

Cyclic voltammetry (CV) consist of sweeping the voltage of the cell between two defined points, at a certain rate. This cyclic sweep produces a certain hysteresis in the curve and also certain peaks at the potentials where the catalyst is oxidized and reduced. The peaks and the hysteresis only appear when the sweeping is done at a high rate, and so it can only be done with a potentiostat/galvanostat, not with the load box. An example of the results obtained with this technique with a PEM fuel cell is shown in Figure 3.8.

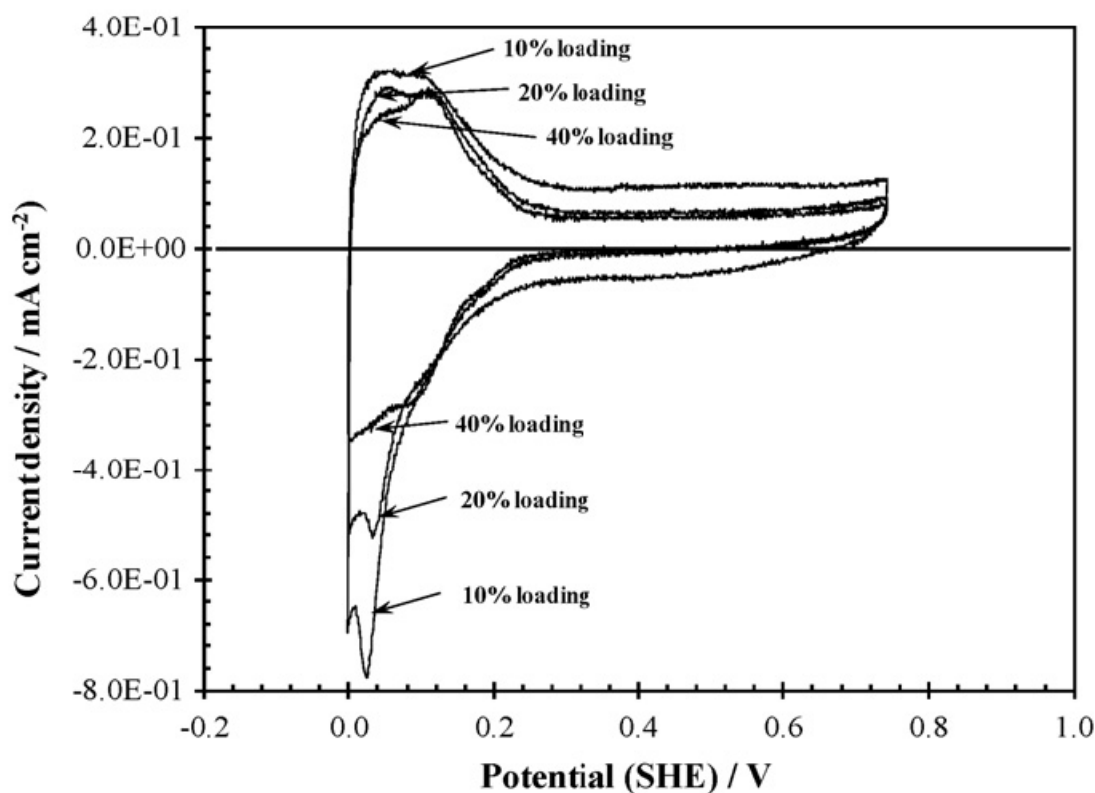


Figure 3.8: Example of CV test for PEM with different catalyst loading, from [11].

From the area of the peaks observed, the surface area of catalyst that is present and chemically active can be estimated, to characterize the cell. Also, comparing cases with no contamination, with cases when certain contaminants are flown before the test, show the effect that the

contaminant has on the catalyst (compacting it and thus reducing its surface area, reacting with it, etc.), and so it is a really powerful technique to study the behavior of the catalyst *in situ*. It can also account the recovery rate after the contamination.

In traditional CV-tests in PEM fuel cells, the cathode flow is set to nitrogen while the anode flow is set to hydrogen. However, Solid Oxide Fuel Cells present oxygen ion conductivity, rather than proton conductivity in the electrolyte, thus oxygen (or air) should be used on the cathode side, and nitrogen on the anode side. This approach cannot be used in a breathing fuel cell, because oxygen molecules will enter the anode side, and since there is no fuel to react with, they will react with the nickel catalyst oxidizing it, and quickly ruining the fuel cell.

The few papers that show cyclic voltammetry in SOFC in the literature always have platinum - that will not corrode - as the anode catalyst. Since one of the objectives of these cells is creating a cheap technology to benefit from the coal reserves of a developing country, the idea of changing the anode catalyst was discarded.

To try to overcome this problem, a new CV technique was developed. It consisted of using fuel in the anode with air in the cathode, same as regular conditions. However, after a few trials, it appeared absolutely clear that the main loss was the ohmic loss in the electrolyte, which made it impossible to observe any peak in the diagram. In a way, it was like doing a fast polarization curve, so the technique was abandoned.

3.4.5. Transient Analysis

Transient analysis is also a powerful tool to study the behavior of the cells. It consists of keeping all the variables constant except for a single parameter that is changed. The response is recorded, and from the shape of the response (time constant, final value), several interesting parameters can be calculated, such as diffusion coefficients, impact of the contaminant, etc.

For these experiments, two different transients were performed. For both of them the cells were kept at constant voltage (0.6V) while the fuel conditions were changed, and the current was recorded in order to see the changes induced (the transient). Hydrogen dilution with argon was used for first transient. Pure hydrogen was always flowing at the start of all experiments. Argon was added to hydrogen into the anode once steady state was reached. The dilution level was maintained until steady state was reached again, when argon was removed to see the recovery. Hydrogen flow was kept constant throughout the experiment.

The start of the second transient was exactly the same way as the first one: keeping the flow of hydrogen constant, a transition from pure hydrogen to diluted hydrogen with argon was induced. Then, instead of removing the argon to see the recovery, hydrogen was replaced by methane maintaining the same proportion fuel to argon. However, in order to keep the stoichiometry similar in both cases, the flow of fuel was reduced by a factor three. A molecule of hydrogen produces two electrons while a molecule of methane produces eight for full oxidation (to H₂O and CO₂) and six for partial oxidation (to H₂O and CO) and the initial results with the mass spectrometer showed that the main product at the outlet was CO rather than CO₂, so in order to keep the stoichiometry approximately constant (in other words, to keep the number of available electrons flown constant), the flow should be reduced by a factor of 6/2, that is, three.

Then, the process is reversed to see the recovery, always waiting for the fuel cell to reach steady state. This way, after steady state was reached methane was replaced again by hydrogen (with the consequent increase in the flow, by a factor of three) keeping the ratio fuel to argon constant. Once steady state was reached again, argon was removed in order to record the final transient.

It has to be remarked that during each set of conditions, and after steady state was reached, a set of experiments (polarization curves and impedance spectroscopy tests) was carried out to characterize the state of

the fuel cell. The blank gaps that can be seen in the transients presented in this dissertation correspond to those periods.

3.4.6. Mass Balance

Although this is not technically an electrochemical method, it has been included here because it is a complementary technique that helps analyzing the results obtained from the electrochemical tests by giving light over the composition at the outlet of the fuel cell.

This technique was applied only when methane was used as a fuel. The objective was trying to close the carbon balance inside the fuel cell, to get an estimate of the carbon deposition that took place during the flowing of methane.

The approach used was the following one: gas samples were collected at the outlet of the fuel cell while methane was flown (for different conditions of potential and current applied, and also for different stages: beginning of contamination, end of contamination, etc.). Those bags were analyzed using a mass spectrometer that had been previously calibrated, so it produced the ratio in which the following molecules were present at the outlet: Ar, H₂, CH₄, CO and CO₂.

Obviously neither H₂O (it condensed at room temperature), nor C (as a solid) could be appropriately measured. Since the most interesting result of these experiments was to estimate the amount of coking (the amount of carbon that deposited in the fuel cell) during operation, two different methods were used.

The first one was based on the Ar/C ratio. Since the anode of the fuel cell is a closed system for carbon and hydrogen (only oxygen ions can enter it if there are no leaks) this ratio should remain constant. This ratio was known at the inlet of the fuel cell, so, with the proportions of CH₄, CO, CO₂ and Ar at the outlet (from the mass spectrometer), the amount of C could be estimated.

The second one was based on the H/C ratio. It should also remain constant as the anode of the fuel cell is also a closed system for the hydrogen. The problem that this method presented was that there were two unknowns: C and H₂O. However, there is an additional equation that has not been considered yet. As this an electrochemical system, the rate of reaction and the current produced are linked by Faraday's Law. In other words, the current (electrons moving at a certain rate) is related to the number of molecules that have reacted. The current generated by the cell was constantly recorded. By integrating it over the sample-taking period of time, the number of electrons that have been produced by the reaction can be calculated. As the number of electrons that the molecules of each species generate is known, both the amount of carbon deposited and also the amount of water generated can be calculated, by solving the system of equations.

In principle, the first method should be more accurate, as it uses fewer variables than the second one. However, there are certain experiments (like those without dilution with argon) where the first method cannot be applied, so it is interesting to do both of them in order to have a comparison of the two.

Finally, the inert gas used to dilute the fuel was argon rather than nitrogen. The reason for this, as it was pointed out in previous chapters, was to facilitate the operation of the mass spectrometer that was used to analyze the samples collected at the outlet of the anode of fuel cell. CO was expected to be one of the main products at the outlet when methane fueled the fuel cell. CO has approximately the same molecular weight as N₂ (both around 28), so their peaks would overlap in the mass spectrometer unless the device has a really large resolution - like the one used for the experiments. Even if the resolution of the mass spectrometer is extremely high, in order to get a good separation between the peaks of CO and N₂, low amounts of nitrogen concentration should be used. This reason justifies the use argon instead of nitrogen. It is believed that nitrogen should behave as an inert gas for the conditions of the fuel cell, so argon should not change the behavior of the cell compared to the one it has with nitrogen.

3.5. Summary in English

A description of the experimental facility used to perform all the different tests on a single fuel cell has been presented in this chapter. In addition to this, the techniques and methods used to characterize the fuel cell and to obtain its physical and electrochemical properties has also been described here.

The techniques are based on different electrochemical principles. Polarization Curves and Transient Analysis are based on the principles of polarization, while Electrochemical Impedance Spectroscopy is based on the response of the fuel cell in the frequency domain. The mass and carbon balance analysis carried out during the use of methane as the fuel provides additional information that complements the previous results offering a new perspective.

The objective of all the different tests that have been described in this chapter is to understand the processes that take place inside the fuel cell, in order to characterize them and use this knowledge to improve the characteristics and the design of the fuel cell. Each technique produces different kind of information about the fuel cell, and so they are all relevant in order to understand the fuel cell behavior.

3.6. Summary in Spanish

En este capítulo se ha realizado una descripción del banco de ensayo experimental donde se realizaron las diferentes pruebas sobre cada pila de óxido sólido, de forma individual. Además, también se han descrito las distintas técnicas y métodos empleados para caracterizar la pila de combustible y obtener sus propiedades físicas y electroquímicas.

Cada técnica está basada en un principio electroquímico distinto. Las curvas de polarización y el análisis de los transitorios están basados en los principios de polarización mientras que la espectroscopía electroquímica de la impedancia está basada en la respuesta de la pila de

combustible de óxido sólido en el dominio de la frecuencia. El balance de masa y del carbono realizado durante el empleo de metano como combustible complementa los resultados anteriores ofreciendo una nueva perspectiva de los mismos.

El objetivo de los distintos ensayos descritos en este capítulo es la comprensión de los distintos procesos que ocurren dentro de la pila de combustible durante su funcionamiento, para poder caracterizarlos y emplear este nuevo conocimiento para mejorar las características y el diseño de la pila de combustible. Cada técnica produce un tipo distinto de información, por lo que todas ellas son relevantes al centrarse en aspectos distintos del comportamiento de la pila de combustible.

3.7. References

- [1] Zhang, S., Yuan, X., Wang, H., Mérida, W., Zhu, H., Shen, J., Wu, S., Zhang, J., "A review of accelerated stress tests of MEA durability in PEM fuel cells", International Journal of Hydrogen Energy, Vol. 34, pages 388-404, 2009.
- [2] Joon, K., "Fuel cells - a 21st century power system", Journal of Power Sources, Vol. 71, pages 12-18, 1998.
- [3] Stambouli, A. B., Traversa, E., "Fuel cells, an alternative to standard sources of energy", Renewable and Sustainable Energy Reviews, Vol. 6, pages 295-304, 2002.
- [4] Howe, K. S., Thompson, G. J., Kendall, K., "Micro-tubular solid oxide fuel cells and stacks", Journal of Power Sources, Vol. 196, pages 1677-1686, 2011.
- [5] Jones, D. A. *Principles and Prevention of Corrosion*. Ed. Prentice Hall, 1995.

- [6] Bussayajarn, N., Han Ming, H., Hoong, K. K., Stephen, W. Y. M., Hwa, C. S., "Planar air breathing PEMFC with self-humidifying MEA and open cathode geometry design for portable applications", International Journal of Hydrogen Energy, Vol. 34, pages 7761-7767, 2009.
- [7] Secanell, M., Djilali, N., Suleman, A., "Optimization of a planar self-breathing PEM fuel cell cathode". 11th AIAA/ISSMO Multidisciplinary Analysis and Optimization Conference, Portsmouth, Virginia, 2006.
- [8] De Silva, K. C. R., Kaseman, B. J., Bayless, D. J., "Silver (Ag) as anode and cathode current collectors in high temperature planar solid oxide fuel cells", International Journal of Hydrogen Energy, Vol. 36, pages 779-786, 2011.
- [9] Shimpalee, S., Greenway, S., Spuckler, D., Van Zee, J. W., "Predicting water and current distributions in a commercial-size PEMFC", Journal of Power Sources, Vol. 135, pages 79-87, 2004.
- [10] Huang, Q.-A., Hui, R., Wang, B., Zhang, J., "A review of AC impedance modeling and validation in SOFC diagnosis", Electrochimica Acta, Vol. 52, pages 8144-8164, 2007.
- [11] Punyawudho, K., Blom, D. A., Van Zee, J. W., Monnier, J. R., "Comparison of different methods for determination of Pt surface site concentrations for supported Pt electrocatalysts", Electrochimica Acta, Vol. 55, pages 5349-5356, 2010.
- [12] Bard, A., Faulkner, L., *Electrochemical Methods. Fundamentals and Applications*. 2nd edition, John Wiley and Sons, Inc., 2001.
- [13] Sonntag, R. E., Borgnakke, C., Van Wylen , G. J., *Fundamentals of Thermodynamics*, 6th edition, John Wiley and Sons, Inc., 2002.

- [14] Strong, F. C., "Faraday's laws in one equation", *J. Chem. Educ.*, Vol. 38, page 98, 1961.
- [15] Burstein, G. T., "A Century of Tafel's Equation: 1905-2005 A Commemorative Issue of Corrosion Science". *Corrosion Science*, Vol. 47, pages 2858-2870, 2005.
- [16] Andres Lozano, C., Ohashi, M., Shimpalee, S., Van Zee, J. W., Aungkavattana, P., "Electrochemical Analysis of Microtubular SOFC under Fuel Contaminants". *ECS Transactions*, Vol. 33, pages 149-160, 2010.
- [17] Andres Lozano, C., Ohashi, M., Shimpalee, S., Van Zee, J. W., Aungkavattana, P., "Comparison of Hydrogen and Methane as fuel in Micro-Tubular SOFC using Electrochemical Analysis". *J. Electrochem. Soc.*, Vol. 158, pages B1235-B1245, 2011.
- [18] Chen, K., Lü, Z., Ai, N., Huang, X., Zhang, Y., Ge, X., Xin, X., Chen, X., Su, W., "Fabrication and performance of anode-supported YSZ films by slurry spin coating", *Solid State Ionics*, Vol. 177, pages 3455-3460, 2007.
- [19] Will, J., Mitterdorfer, A., Kleinlogel, C., Perednis, D., Gauckler, L. J., "Fabrication of thin electrolytes for second-generation solid oxide fuel cells", *Solid State Ionics*, Vol. 131, pages 79-96, 2000.
- [20] Souza, S. de, Visco, S. J., Jonghe, L. C. De, "Reduced-Temperature Solid Oxide Fuel Cell Based on YSZ Thin-Film Electrolyte", *J. Electrochem. Soc.*, Vol. 144, pages L35-L37, 1997.
- [21] Campana, R., Merino, R. I., Larrea, A., Villarreal, I., Orera, V. M., "Fabrication, electrochemical characterization and thermal cycling of anode supported microtubular solid oxide fuel cells", *Journal of Power Sources*, Vol. 192, pages 120-125, 2009.

[22] Yamaguchi, T., Shimizu, S., Suzuki, T., Fujishiro, Y., Awano, M., "Fabrication and characterization of high performance cathode supported small-scale SOFC for intermediate temperature operation", Electrochemistry Communications, Vol. 10, pages 1381-1383, 2008.

CHAPTER 4

Experimental Characterization of the SOFC Using Hydrogen

Contents

4.1. Introduction	95
4.2. Effect of Dilution on the Current	96
4.3. Polarization Curves	104
4.4. Electrochemical Impedance Spectroscopy	107
4.5. Electrochemical Reactions	111
4.6. Analysis of the Results: Fuel Cell Structure	114
4.7. Summary in English	116
4.8. Summary in Spanish	117
4.9. References.....	118

4. Experimental Characterization of the SOFC Using Hydrogen

4.1. Introduction

Even though using alternative and renewable fuels should be the long term goal for fuel cells [1-4], for all the reasons explained in the previous chapters (difficulty to understand the processes that take place inside the fuel cell), in order to properly characterize the behavior of the fuel cell, a more standard fuel is required.

Hydrogen, due to its simpler chemistry and high reactivity, is the most suitable fuel for applications with fuel cells. In fact every fuel cell is capable of operating with it, even the most delicate ones. For those reasons, a characterization with hydrogen, using all the electrochemical techniques described in the previous chapter is vital in order to understand the processes that take place inside the fuel cell, analyze them and eventually improve the design of the fuel cell based on the results obtained with this analysis.

As it was explained in previous chapters, the fact that SOFC are a technology in development, without an established standardized method of production, causes that cells show different performance. This fact complicates the analysis of the results enormously. Some authors opted to perform a linear analysis with a big sample of results to get around this problem [5, 6, 9]. In this case, due to the limited amount of cells available to test it was decided to evaluate the effect of the different experiments establishing a baseline at the beginning of life for each fuel cell, and comparing the results to that baseline, as described in Chapter 3. Other authors also follow this procedure [7, 8 and 10].

The results that were obtained using pure hydrogen as the fuel are presented in this chapter, with a focus on analyzing the impact that the

dilution of hydrogen with an inert gas (argon) has on the performance and behavior of the fuel cell.

In order to analyze those effects, two different cases were considered. The first one, a small dilution case to 50% hydrogen and 50% argon, while in the second case 10% hydrogen and 90% argon was used. The summary of the flow conditions to every test can be found in Table 4.1. As it was discussed in previous chapters, special care was taken to make sure that both the stoichiometry of the anode and the cathode was high enough (always over 2) so that it would not have an effect on the tests carried out.

Table 4.1: Flow conditions of the tests carried out.

Fuel Cell #	1 st	2 nd
Anode flow H ₂ (set point, sccm)	50	50
Current (0.6V, A)	1.77	1.97
Anode stoich (0.6V)*	3.77	3.39
Anode flow Ar (set point, sccm)	50	450
Anode dilution (real %H ₂)*	53.15%	9.95%
Cathode flow Air (set point, sccm)	300	300
Cathode stoich (0.6V)**	~ 9.2	~ 8.28

*Min. stoichiometry for the anode side at 0.6V (max. current for these conditions used for the calculation).

** Cathode theoretical stoichiometry calculated for same conditions. Actual stoichiometry was impossible to calculate.

The results obtained with these techniques are presented and analyzed in this chapter.

4.2. Effect of Dilution on the Current

The effect of the dilution of hydrogen with argon was analyzed using the procedure indicated in the previous section that consists of a transitory

analysis. Two different levels of dilution were studied, and they are reflected on Table 4.1. In the first case the transition from 100% hydrogen in the anode to 50% hydrogen diluted with argon was performed, while in the second one the transition was from 100% to 10% hydrogen. As it was pointed out in the previous section, the flow of hydrogen remained constant during the experiment, while the argon flow increased to achieve the desired dilution.

Figure 4.1 shows the expected results for both transients when hydrogen is diluted with argon. It is idealized, since it reflects instantaneous processes (vertical lines), although in reality it is expected that an exponential decrease/increase will be seen for this case. Also, as it is shown by the figure, a decrease in the current is expected when hydrogen is diluted with argon. Obviously the descent in the performance when dilution occurs will be intimately related with the level of dilution used, the higher the dilution level, the higher the decrease in the current.

Expected transients with diluted H₂ (0.6V)

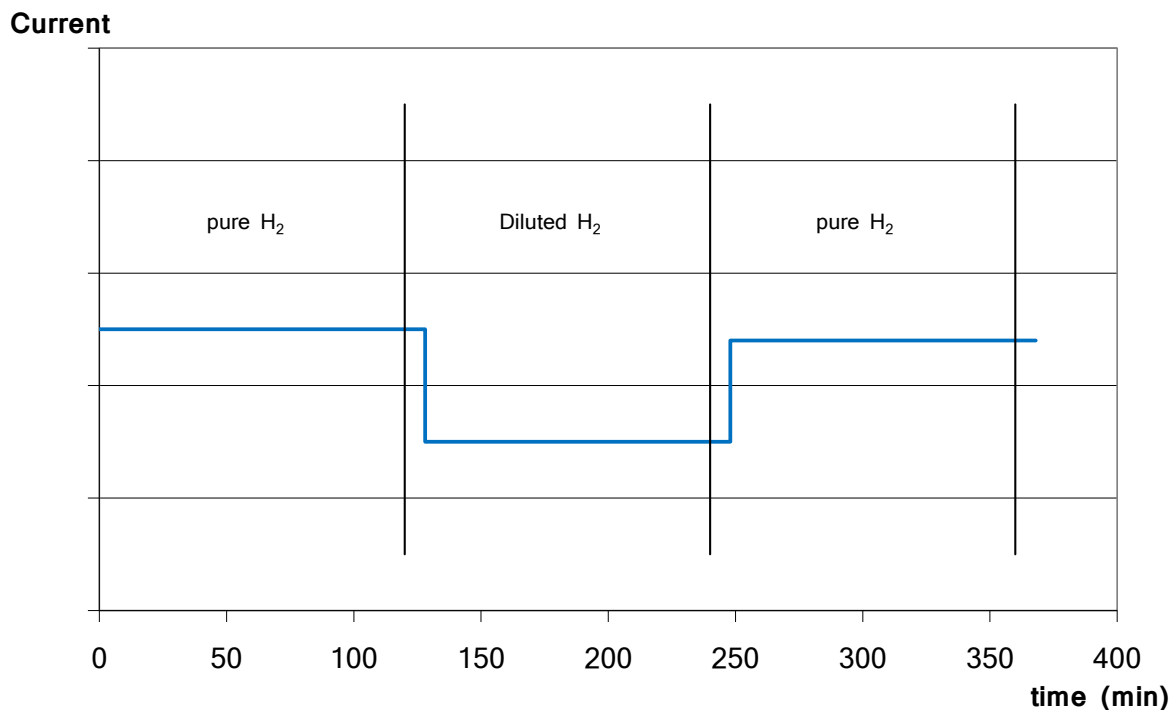


Figure 4.1: Expected ideal transient H₂ dilution with Ar. Current scale arbitrary and depends on whether electrodes operate under kinetic or mass transport regimes.

The actual results obtained for the experiment with the first cell (hydrogen diluted from 100% to 50%) are shown in Figure 4.2. This figure reflects both the decay with the dilution and the subsequent recovery when the argon was removed. The blank gaps that can be seen in the graphs correspond to other shorter experiments (polarization curves and impedance tests) that were carried out during this test, as it was explained in Chapter 3.

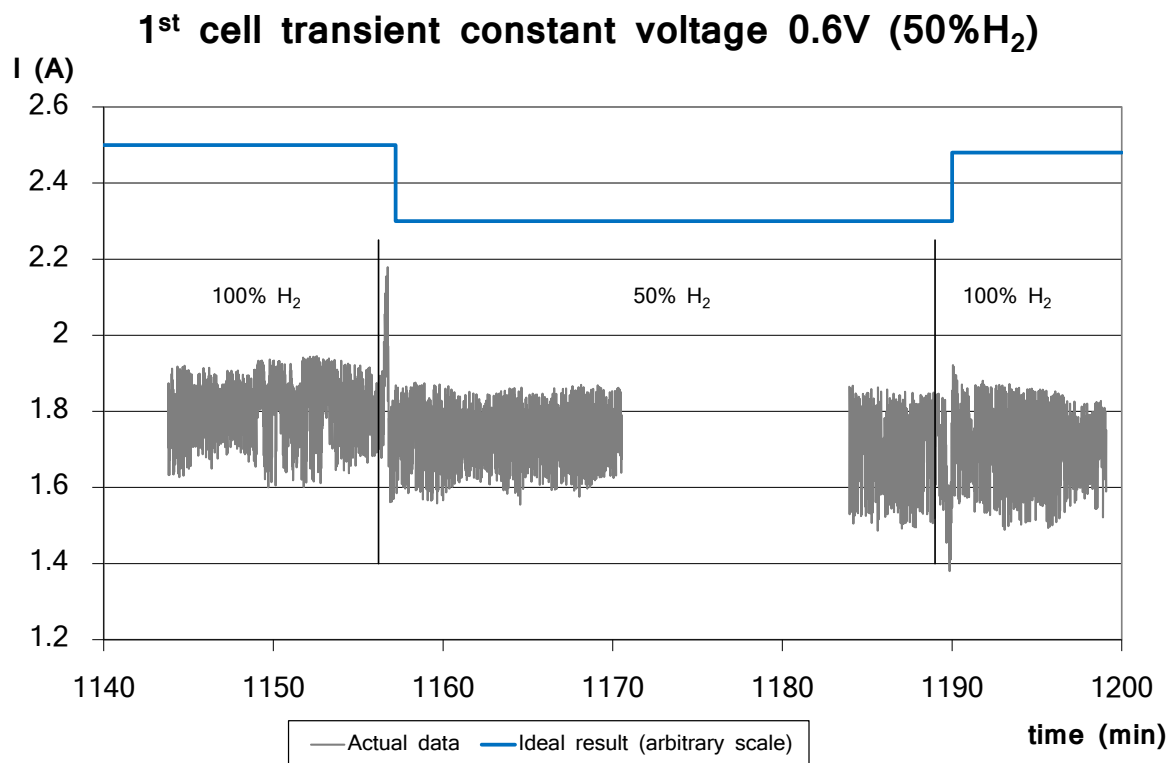


Figure 4.2: Transient 1st fuel cell, 50% H₂ in Ar.

Figure 4.3 reflects the actual results obtained for the experiment with the second cell (when hydrogen diluted from 100% to 10% with argon). Like the previous case, this figure shows both the decay with the dilution and the subsequent recovery when the argon was removed.

Also, like the previous figure, the blank gaps that can be seen in the graphs correspond to other shorter experiments (polarization curves and impedance tests) that were carried out during this test.

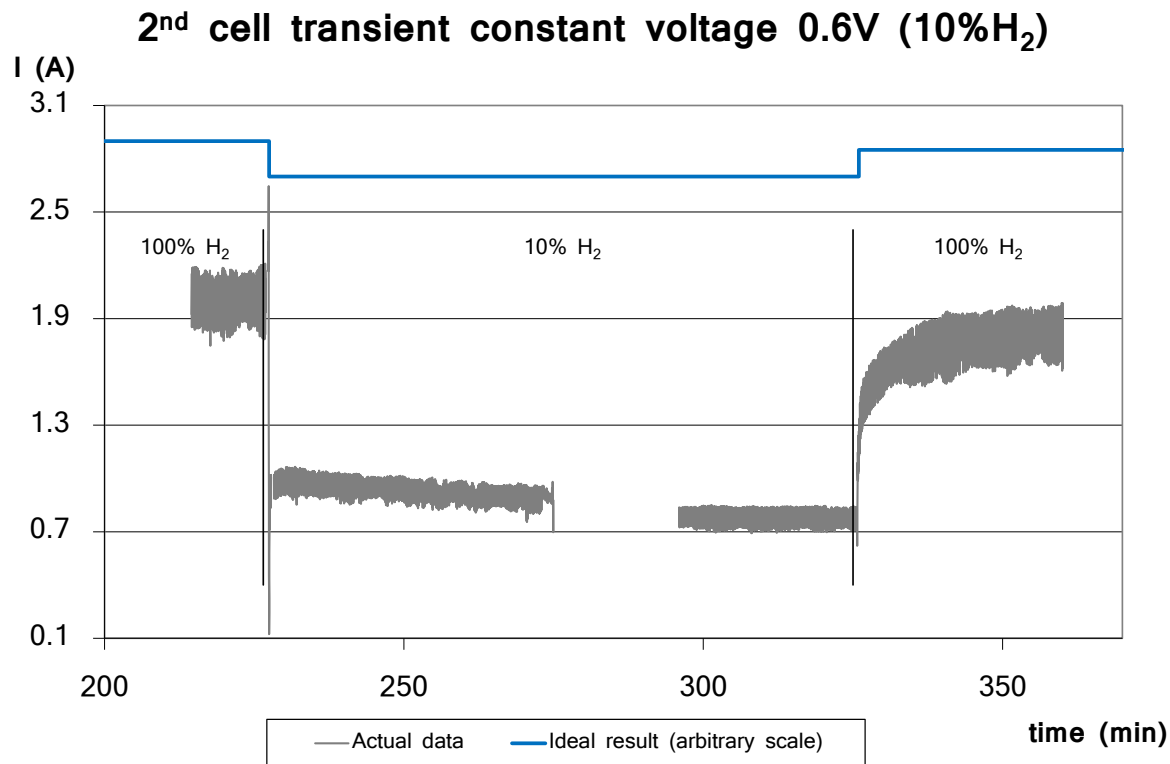


Figure 4.3: Transient 2nd fuel cell, 10% H₂ in Ar.

As it can be seen, both graphs (Figures 4.2 and 4.3) present similar trends, and their main difference lies on the steady state value of the current and the time constant (the velocity at which the changes take place).

The case where hydrogen was diluted to 50% with argon (second cell) showed an extremely small change in the current (see Figure 4.2). This particularity, added to the fact that the signal measured has quite a large quantity of noise, makes it difficult to distinguish both cases (diluted and non-diluted) for this level of dilution (50%) and adds imprecision to the fitting performed over the graph.

Regarding the trend of these transients, several transitory stages can be observed: First, a quick increase in the value of the current can be seen, followed by a sharp decrease and a slower increase to a maximum. After that, a much slower decrease to the steady state value takes place. These trends are more easily observed in the higher dilution case - 10%

hydrogen, Figure 4.3 - as the transients show much bigger changes than the low dilution case (Figure 4.2).

From all those trends observed, the first sharp increase observed should be completely disregarded as it is not caused by dilution. In fact, it is caused by the increase of the mass flow entering the fuel cell anode inherent to the dilution process. Since the flow of hydrogen is kept constant, dilution is achieved by adding the required argon flow to the existing hydrogen flow. Due to limitations in the test station used, even if both parameters (flow and composition) are changed at the same time, for a short period of time (the time that takes to flow the dead volume of hydrogen present in the tubing that connects the mass flow controller and the entrance of the fuel cell) pure hydrogen will be flowing at a higher rate - the rate that the dilution requires - than before, causing the current to increase during that extremely short period of time. For that reason, this transient should be disregarded, as it is not a true effect of the dilution but a limitation in the control of the flow [12].

Although this explanation seems to be the most reasonable for this phenomenon, it must be remarked that if the stoichiometry of the fuel cell is high enough, the current should not increase even if the flow of hydrogen is incremented. Therefore, this fact suggests that the actual (local) stoichiometry of the cell is lower than expected. The particular cell inner structure (described in Chapter 3), with such small holes in the copper tube that acts as the current collector, and a tightly packed nickel oxide foam seems to difficult the flow of the gas to the catalyst, which is probably causing local starvation of the catalyst located further from the holes. These facts will be discussed more in detail in section 4.6.

When dilution is removed, the same explanation can be used for the first quick transient observed. In that case, a quick decrease in the current can be seen followed by a steady increase. That first quick decrease, again, is caused by the dead volume of mixture (hydrogen and argon) present in the tubing that connects the mass flow controllers and the entrance of the fuel cell. When settings are changed to remove hydrogen dilution, the diluted mixture present in the dead volume will be flowing at a lower rate

- the correspondent to pure hydrogen - causing the decrease in the current. Again, as this transient is not caused by the dilution process, but rather by a change in the hydrogen flow, it should be disregarded.

Even though this transient is quite short compared with the rest of the transients, the fact that it would actually enhance the local fuel cell starvation may be increasing the fuel cell performance drop when dilution is removed. This fact is also discussed more in detail throughout this chapter.

The next transient that can be observed when dilution to 10% is applied (Figure 4.3) is a sharp decrease and quick recovery to a maximum that follows the quick increase. It might also be present in the 50% dilution case, but if it actually existed in that case, it must be so small and quick that it is hidden by the noise of the signal. Considering that this transient cannot be seen when dilution is removed (where just a steady increase can be seen, not a sharp one followed by a quick decrease to a minimum that should be observed if the response was exactly the opposite to that observed when dilution is applied), it seems to be caused by the transitory response of the mass flow controllers.

The mass flow controllers used are, apparently, an underdamped system, and thus they overreact when changes occur. That would cause an initial over flow of argon that is quickly reduced to the desired value, and it would perfectly suit the shape of the transient. However, when dilution is removed, no overreaction could be observed since the valve of the argon mass flow controller would simply be closed, not allowing for any overreaction.

Although other explanation could also be provided to explain this transient, if we take this one as the true explanation, this transient should also be disregarded, since it would not be caused by the dilution of the flow, but rather by the control system of the flow. Considering that, it must be remarked that the time constant calculated for the transient generated when dilution is removed should be more precise than the one calculated when dilution is applied, as it is less influenced by the control system.

The last transient associated to the dilution process is a slow decrease (slow increase when dilution is removed) to the steady state value and this represents the real effect of the dilution process, and thus it was the one fitted.

For those transients, percentage of decrease and the following recovery were calculated as well as a time constant for both process (one for the dilution and another for the recovery) using the graphs to fit the data to an exponential expression that satisfies equation 4.1.

$$I(t) = I_0 - (I_0 - I_{ss}) \cdot \exp\left(-\frac{\Gamma}{(t - t_0)}\right) \quad (4.1)$$

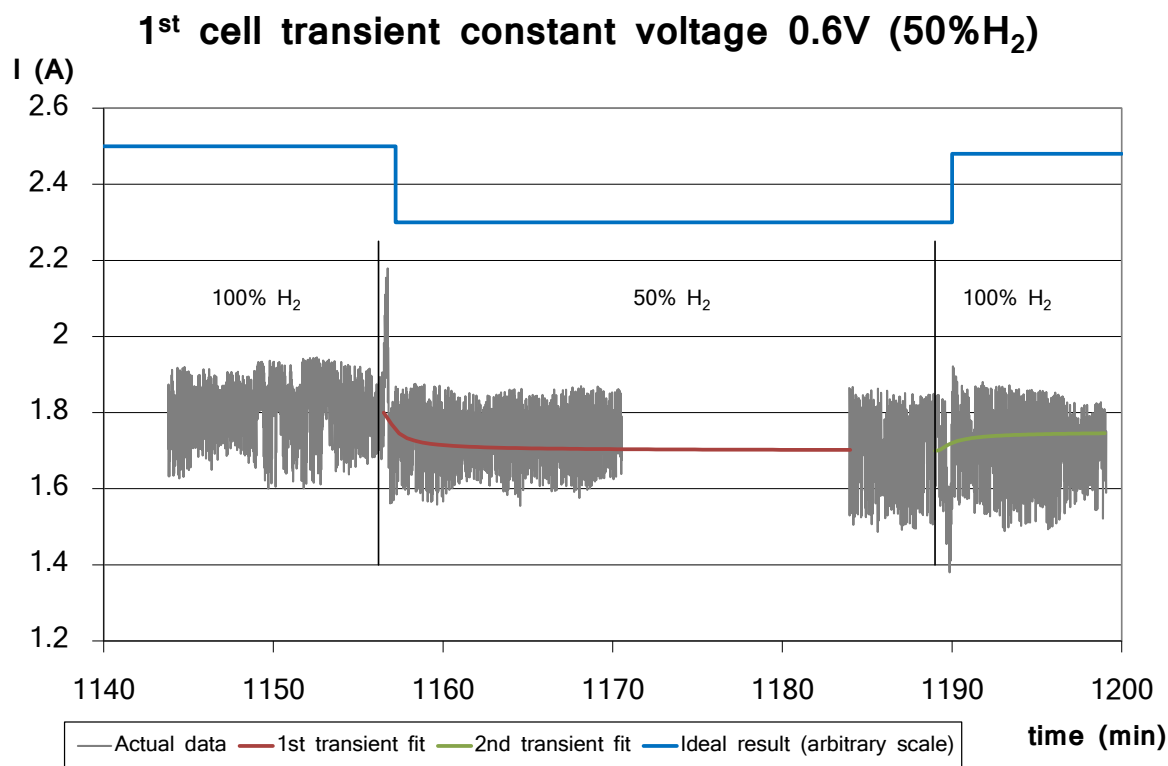


Figure 4.4: Transient 1st fuel cell, 50% H₂ in Ar, adjusted to exponential expression.

The time constant (Γ) and the percentage change (%change, which is calculated according to equation 4.2 once the graph is fitted), are both

relevant parameters in the equation, and therefore they are both shown in Table 4.2, for the dilution and for the recovery periods.

$$\%_{\text{change}} = \frac{I_0 - I_{ss}}{I_0} \quad (4.2)$$

Figures 4.4 and 4.5 show the data, fitted using the previous equations (4.1 and 4.2) for both cases (50% and 10% dilution). The results obtained with this fitting are reflected in Table 4.2.

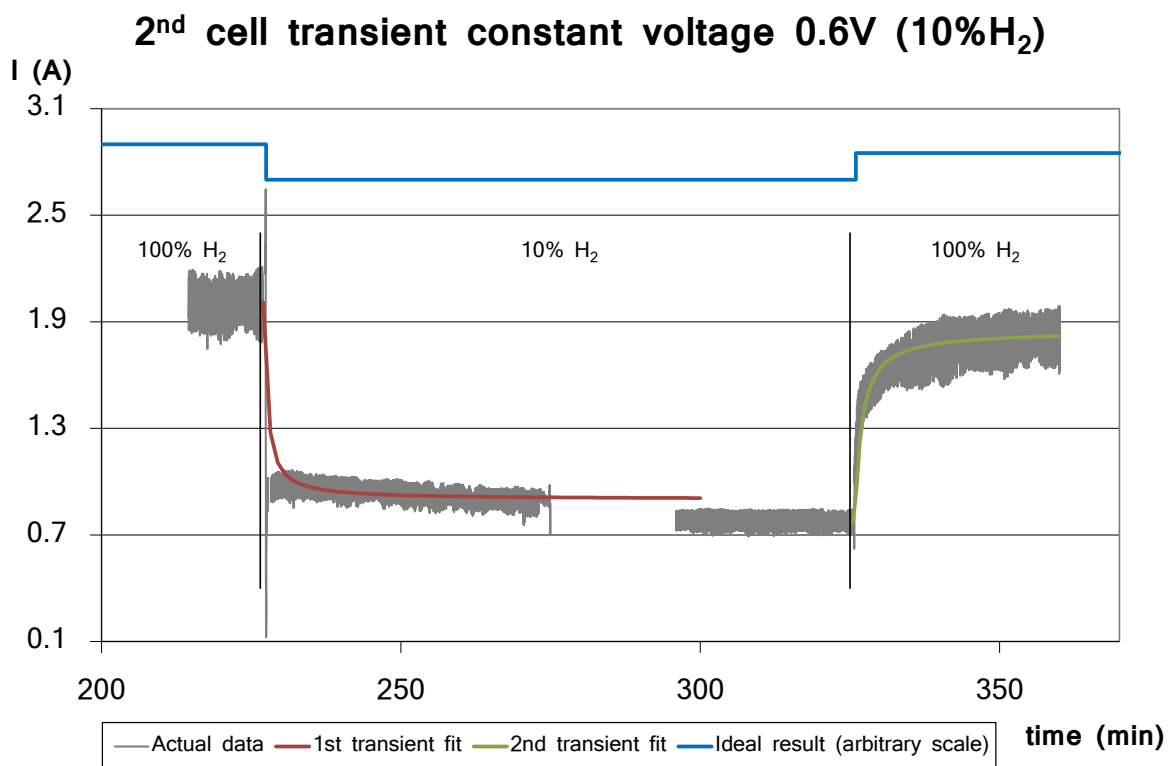


Figure 4.5: Transient 2nd fuel cell, 10% H₂ in Ar, adjusted to exponential expression.

Finally, when the two cases (10% hydrogen and 50% hydrogen) are compared, a much higher decrease can be observed with the higher value of dilution. For the case where hydrogen is diluted to 10% of the total flow (Figure 4.3), the current shows a much lower proportion than the case where hydrogen is diluted to 50% of the total flow (Figure 4.2) when those currents are compared to their respective 100% hydrogen current

value. While a change in the value current can hardly be observed for the 50% hydrogen case, current drops over 60% of its original value for the 10% case. After that, not a full recovery can be seen in none of the cases, but it is much acute in the 10% dilution case.

Regarding the time constants, they show that the response is quicker when dilution is applied compared to the response when dilution is removed (the time constant is multiplied by approximately two when dilution is removed, compared to its value when dilution is applied). The actual data for both cases can be found in Table 4.2.

Table 4.2: Summary of the results obtained with the transients.

Condition	1 st cell, 50%H ₂			2 nd cell, 10%H ₂		
	I (A)	change	Γ. (s)	I (A)	change	Γ. (s)
Pure H ₂	1.80	-	-	2.01	-	-
Diluted H ₂	1.70	-5.5%	~33*	0.77	-62%	30
Pure H ₂	1.73	-3.9%	~54*	1.80	-10%	60

* Imprecise value due to noise, fluctuations and small difference between the values.

4.3. Polarization Curves

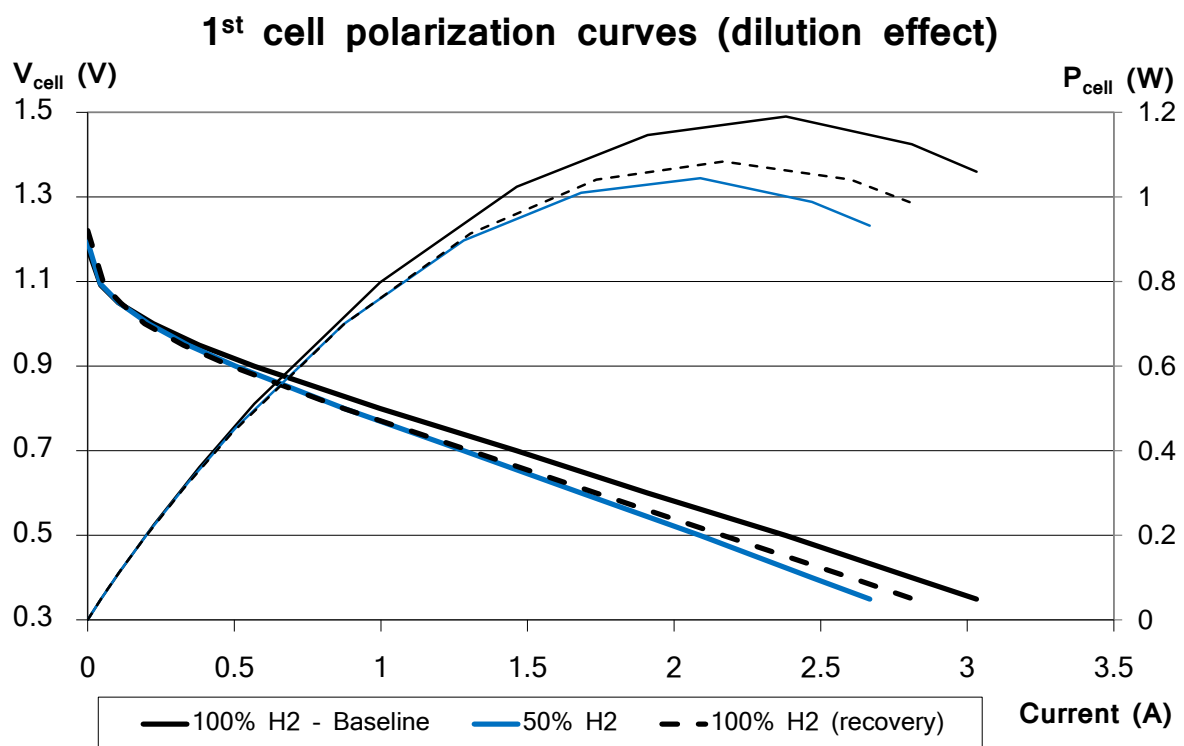
The polarization curves were performed following the procedure indicated in the previous chapter. The flow conditions for each polarization curve are identical to those used in the transient analysis and so they are reflected in Table 4.1. The minimum stoichiometry while performing the polarization curve is a bit lower, as the voltage is reduced to 0.35V, which increases the current and thus reduces the stoichiometry both for the anode and the cathode, as the flows are fixed. For those cases, the minimum stoichiometry - which occurred at 0.35V - are shown in table 4.3.

Figure 4.6 shows the polarization curve of the first cell. For this cell the hydrogen fuel was diluted with argon to 50% and three different curves can be observed: the one taken before diluting the hydrogen (baseline), the one taken during hydrogen dilution, and the one taken after hydrogen dilution (recovery).

Table 4.3: Minimum stoichiometry while performing polarization curves.

Fuel Cell #	1 st	2 nd
Minimum anode stoich. (0.35V)	2.25	2.5
Theoretical minimum cathode stoich. (0.35V)	~ 5.7	~ 6.3

Figure 4.7 shows the polarization curve for the second cell. In this case hydrogen was also diluted with argon, but to a much higher extent: 10% of hydrogen with 90% argon. Once again three different tests were performed - corresponding to the three different lines that can be seen in the figure - one before dilution (the baseline), one after dilution (the recovery) and one during dilution.

**Figure 4.6:** Polarization curves 1st fuel cell, 50% H₂ in Ar.

The results obtained are similar in both cases, and in accordance with what the transient analysis showed. Like before, the trends are really

similar, and also, the dilution has a bigger impact in the case where it is stronger (the one performed to 10% with the second cell).

It is apparent from both graphs that the effect of the hydrogen dilution is the same for every voltage, it reduces the current by a certain factor, and this factor is approximately the same for all voltages. This means that the cell behaves the same way for every potential when the fuel that it is using is diluted with argon.

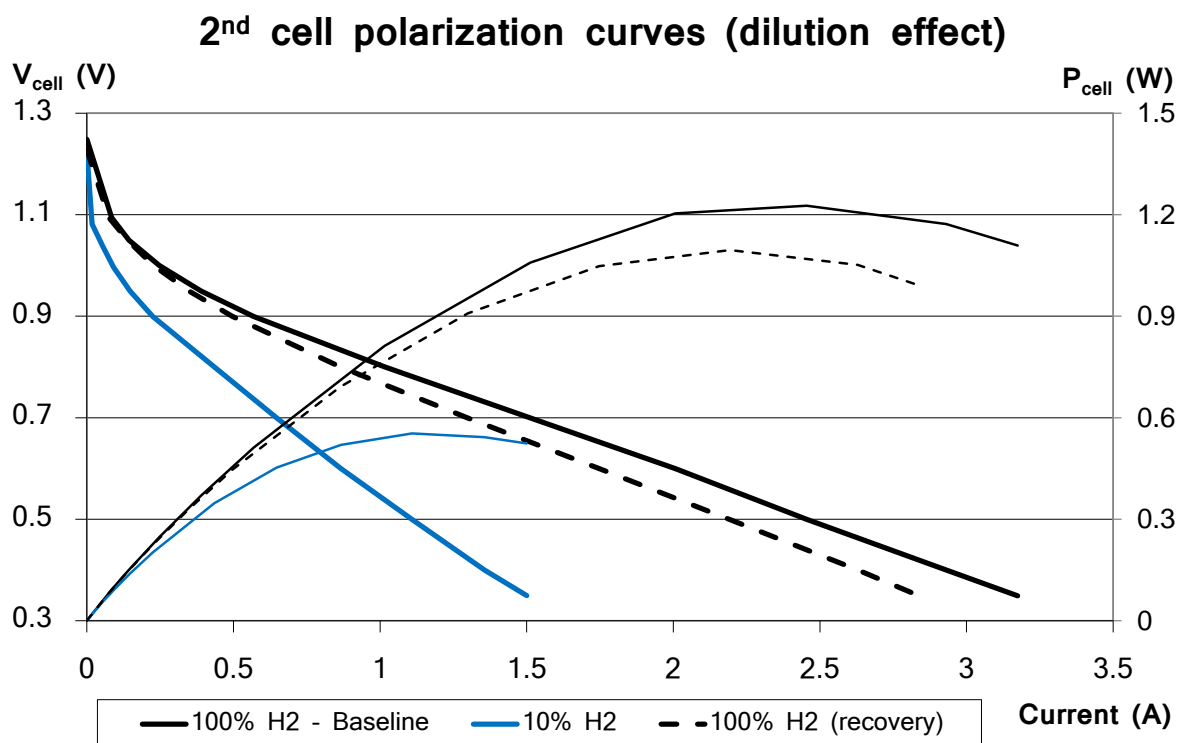


Figure 4.7: Polarization curves 2nd fuel cell, 10% H₂ in Ar.

Also, the open circuit voltage remains practically unaltered. From the Nernst equation, a decrease of 0.1V was expected to be found in the 10% H₂ dilution case while a 0.03V was expected to be found in the 50% H₂ dilution case. In the second case, the decrease is so small that it is difficult to measure. However, in the first case, this decrease should have been more noticeable, but it is really likely that this effect was hidden by the fluctuations in the measurement.

Finally, as was shown in the transitory analysis, a decrease in the performance can be observed in both cases when hydrogen was diluted with argon and this effect was much higher at stronger dilutions. After that, not a complete recovery can be observed in neither of the cases, although the performance loss is again more acute in the high dilution case. The values of this decrease in the performance, at 0.6V correspond exactly with the results that were obtained during the transitory analysis that was shown before.

4.4. Electrochemical Impedance Spectroscopy

Following the procedure described in the previous chapter impedance tests were performed on the cells to evaluate some of its characteristics. The conditions used were the same as the ones utilized for the transient analysis, and thus are reflected in Table 4.1.

The average voltage during these experiments was 0.6V (like the one kept to perform the transient experiments), with perturbations of 20% of the current - that correspond to perturbations a little smaller than 0.1V in the voltage, and so the actual stoichiometry both for the anode and the cathode sides was always above the values shown in Table 4.3, making sure that the cell was never lacking fuel or oxidant.

The results obtained are shown in Figures 4.8 and 4.9. Figure 4.8 shows the impedance test results for the first fuel cell, where only 50% dilution was applied, whereas Figure 4.9 shows the impedance test results for the second fuel cell, where 10% dilution was applied.

For both cases of dilution, three different lines can be observed. They correspond to the three different conditions that were tested during the experiments: one baseline performed before starting any dilution, another one measured during the dilution process and finally one performed right after the dilution of hydrogen was removed from the cell, to see its recovery.

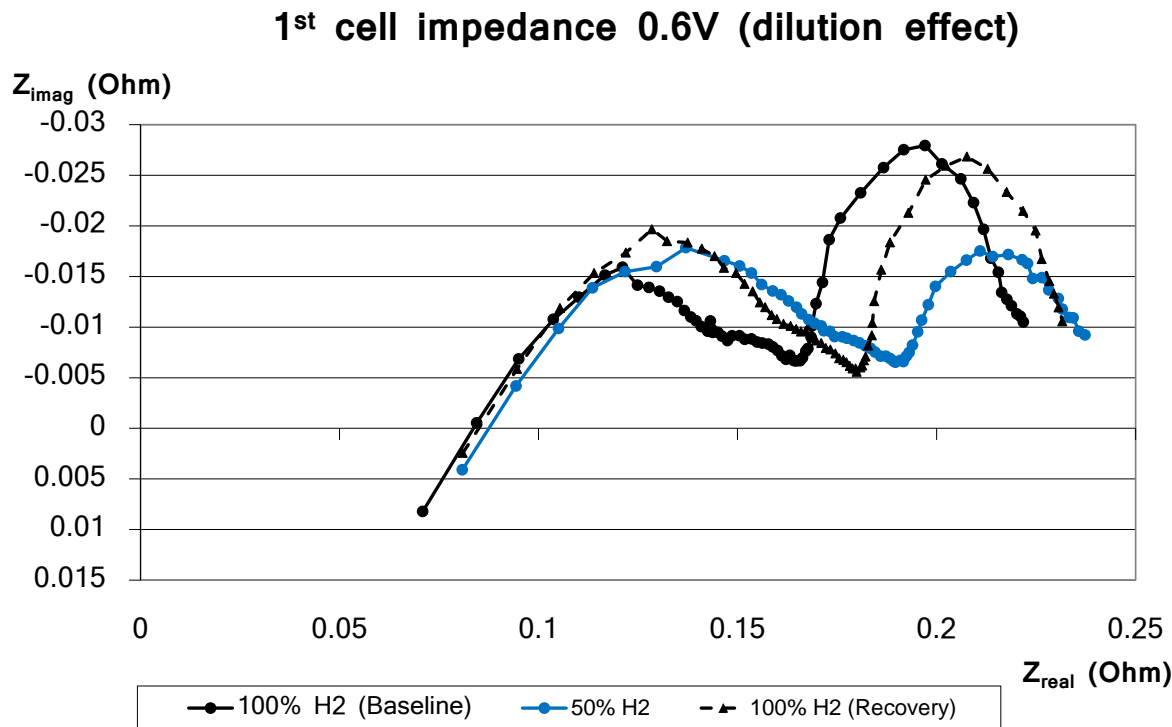


Figure 4.8: Impedance test 1st fuel cell, 50% H₂ in Ar.

Unlike transient analysis and polarization curves, which are based on the same basic principle (polarization to obtain a current), impedance testing uses a different approach to characterize the fuel cell, using a signal that oscillates at different frequencies. This way an analysis in the frequency domain is performed, and it provides information of different processes that can take place inside the fuel cell.

For those reasons, the trends that the impedance analysis shows in the case of small and strong dilution are completely different. In the case of the first fuel cell (50% dilution, that is, small dilution), Figure 4.8, no effect can be appreciated in the high frequency region (the intercept with the real axis where the resistance is smaller). This means that the total resistance of the fuel cell (which is mainly produced by the electrolyte ion transport) does not change in the case of small dilution (50%).

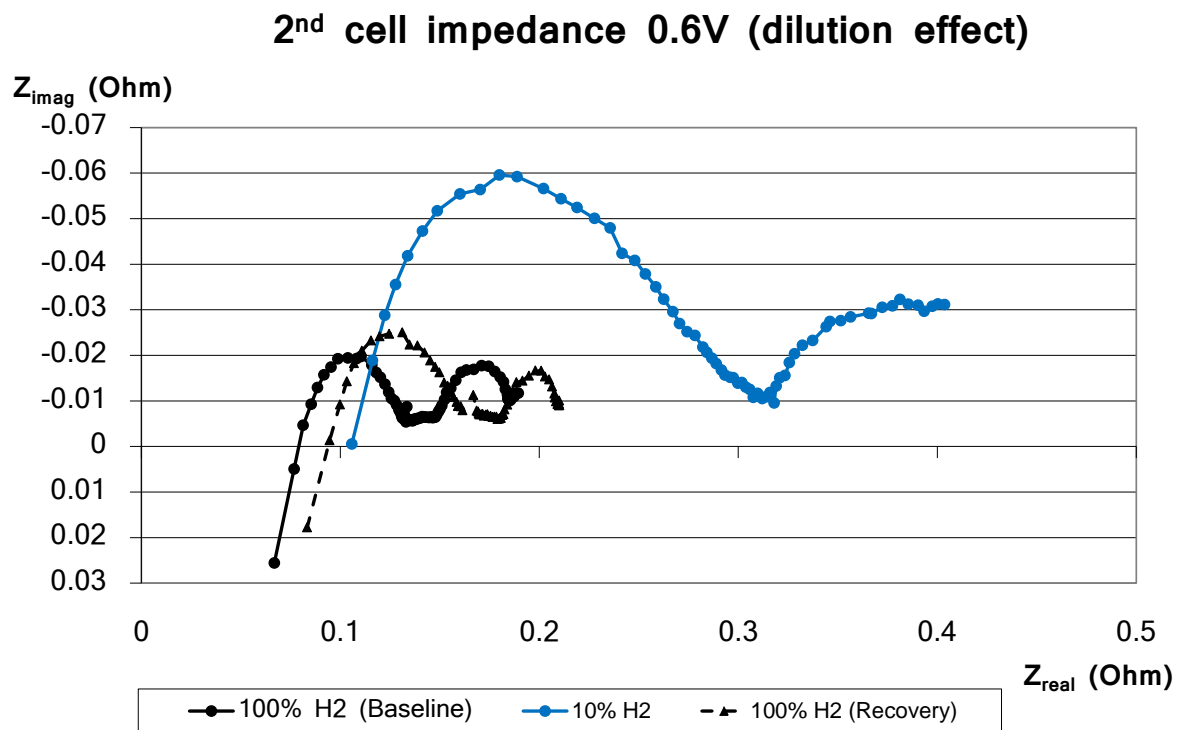


Figure 4.9: Impedance test 2nd fuel cell, 10% H₂ in Ar.

Larger differences can be observed in the case of the lower frequencies (right hand side of the diagram). These tend to point out that the kinetics of the reactions are not exactly the same for all cases. It can clearly be seen that the second semi-circle is much smaller in the diluted case which indicates that a reduction in the available ions or in the kinetics of the reaction is caused by the dilution process [11].

The steady state resistance does only increases slightly, so the overall effect is not too noticeable, as it was also proved with the transient analysis and the polarization curves.

Finally, a larger steady state resistance is also observed in the recovery curve (when dilution is removed), which means that the kinetic effects are permanent, indicating that some light damage may be caused to the catalyst by the dilution process.

Considering the geometry of the fuel cell (where the small holes really restrict the flow of hydrogen to the catalyst), it is possible that the addition

of argon may even make it more difficult for the hydrogen to reach the catalyst, which would cause that the local stoichiometry in some parts of the anode is smaller than the global one, leading to local starvation. This local starvation, along with the presence of oxygen ions might be promoting local oxidation of the nickel catalyst particles, which are not completely recovered once argon flow is removed. This effect is discussed more in depth in the following section.

From Figure 4.9, it can be seen that strong dilution does change the value of the high frequency intercept, that is, it changes the total resistance of the fuel cell. As the main contributor to the total resistance of a solid oxide fuel cell is the electrolyte, this result suggests that strong dilution may be cracking some parts of the electrolyte, reducing its electronic conductivity. This electronic conductivity is not completely recovered once argon flow is stopped.

The cracking of the electrolyte does make sense in the case of strong dilution. In that case, the total flow on the anode of the fuel cell is multiplied by ten. As the anode tube is really thin (1.59mm of exterior diameter), an increase in the flow means a high increase of the pressure, especially at the inlet of the fuel cell, which may be causing the cracking of the electrolyte.

Finally, another important factor that can be seen in Figure 4.9 is that the steady state resistance of the cell increases hugely when it works with diluted hydrogen compared to that when it works with pure hydrogen. As with the 50% dilution case, this effect is not completely recovered once dilution is removed, but like the 10% dilution case it is a small effect, especially compared with the increase in the electric resistance of the electrolyte.

4.5. Electrochemical Reactions

Table 4.4 shows a list of the reactions that are likely to take place inside the fuel cell under regular operating conditions with hydrogen as a fuel. The values of the potentials of all these reactions were calculated according to the procedure described in Appendix A2.

Since the values of the activities cannot be accurately determined, the following approach was used. First, a value without considering the activities of the different species ($E^{\circ}_{900^{\circ}\text{C}}$) was calculated and reported, although it does consider the temperature influence. Then a value corrected for the activities of the different elements ($E_{900^{\circ}\text{C}}$) was calculated. This value is calculated based on experimental results and conditions and it is reflected in the Table 4.4.

Then, the values for these two potentials ($E^{\circ}_{900^{\circ}\text{C}}$ and $E_{900^{\circ}\text{C}}$) are plotted in a current/potential plot. Since temperature is so high inside the fuel cell, it is assumed that kinetics are extremely fast, not producing any loses, and thus the limiting current can be achieved even at the real potential, producing the square shape that can be seen in Figures 4.10 ($E^{\circ}_{900^{\circ}\text{C}}$) and 4.11 ($E_{900^{\circ}\text{C}}$). In reality, these vertical lines would have a high slope (but not infinite) and they would reach the limiting current asymptotically. For simplicity, and given the expected fast kinetics of these reactions, it was chosen to represent it this way.

No values of the limiting current are reported in those graphs. The flow pattern is really complicated, due to the complex shape of the channel, and thus it is very difficult to calculate. In Appendix A1, two limiting cases were calculated, and they yield reasonable values, but with a large difference. Since the purpose of these graphs is to illustrate the reactions that may be taking place, we chose not to report any value of the current in the graphs. The proportions of the limiting current for each reaction were kept, according to the values calculated in Appendix A1.

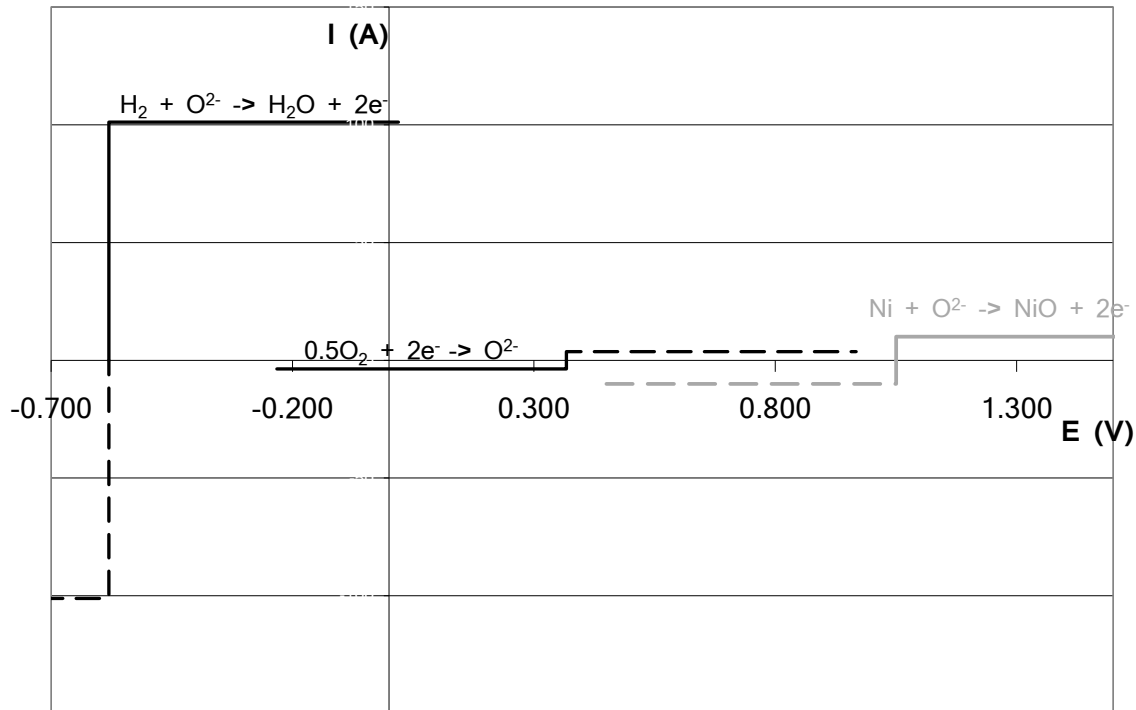
Table 4.4: Expected reactions when H₂ is used as fuel.

Reaction	Direction	E ^θ _{900°C} (V) *	E _{900°C} (V) **
Anode			
H ₂ O + 2e ⁻ → H ₂ + O ²⁻	Anodic	-0.581	-0.930
NiO + 2e ⁻ → Ni + O ²⁻	Anodic	+1.050	+1.050
Cathode			
0.5O ₂ + 2e ⁻ → O ²⁻	Cathodic	+0.367	+0.328

* Assuming all activities equal to one.

** Assuming the following activities:

$$a_{H_2} = 0.1, a_{NiO} = 1, a_{Ni} = 1, a_{H_2O} = 10^{-4}, a_{O_{ion}} = 1, a_{O_2} = 0.21$$

**Figure 4.10:** Expected reactions (not corrected w/ activities, E^θ_{900°C}), H₂ fuel, from [12].

As can be seen from the figures, this is a relatively simple system. It will certainly become more complicated when the fuel used is methane rather than hydrogen, as methane can produce many more species that need to be considered. The results with methane (pure and diluted) are shown in Chapter 5.

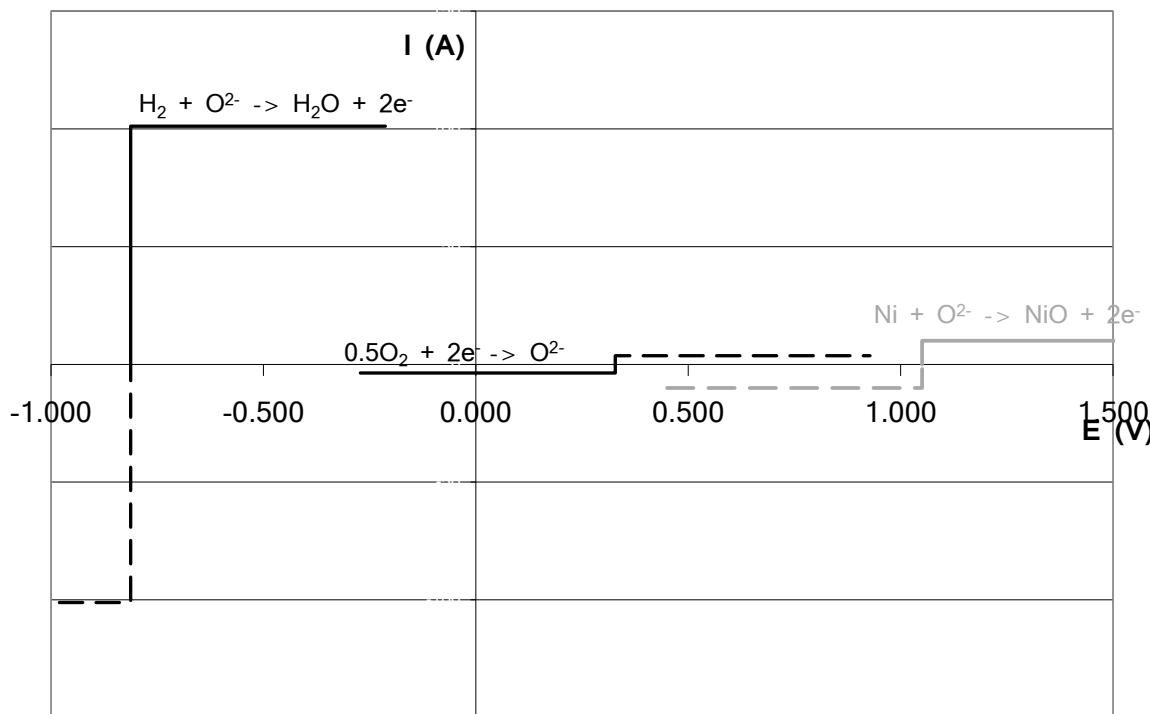


Figure 4.11: Expected reactions (corrected with activities, $E_{900^\circ C}$), H_2 fuel, from [12].

In this case, both graphs (considering and not considering the activities of different species) show the same trends. Hydrogen is the anodic reaction and will take place in the direction shown. Oxygen, as it has a higher potential and thus is located to the right of the hydrogen reaction, occurs in the cathodic direction (also shown in the graph). As the nickel reaction has a higher potential than the oxygen reaction, it means that it will not be oxidized as long as those conditions are maintained.

The difference in the limiting current of the hydrogen anodic reaction and the oxygen cathodic reaction is the theoretical maximum current that can be obtained from the cell. Ohmic losses should be discounted though. Please refer to Appendix A1 for actual limiting values of these limiting currents.

4.6. Analysis of the Results: Fuel Cell Structure

The fuel cell structure always plays an important role in the fuel cell behavior. In this particular case, it is believed that the influence of the structure is especially acute. The reason for this is the particular anode structure that these cells present, which was described in Chapter 3. The small holes (they represent about 1% of the total area of catalyst) present in the copper current collector combined with the tightly packed nickel oxide foam enormously difficult the flow of the gas fuel from the tube to the catalyst.

This fact could cause that, even if the flow is set to a value that should theoretically ensure proper working conditions (no cell starvation), due to the difficulties for the fuel to flow towards the catalyst, local starvation could happen in those areas of the catalyst that are located further away from the holes in the copper current collector of the anode side.

This local starvation would justify the reason why a rise in the current can be seen when the hydrogen flow is increased despite the fact that the global stoichiometry of the fuel cell is high enough. An increase in the hydrogen flow would cause an increase in the inner cell pressure, enhancing the flow to the catalyst. If no starvation occurred, then this would not affect the fuel cell performance. However if the cell is suffering from local starvation, an enhancement of the fuel flow to the catalyst would certainly reduce this hypothetical local starvation and increase the fuel cell performance, which in this case would be seen as an increase in the total electric current produced by the cell.

Also, from the results presented in this chapter, dilution with argon does not deeply affect the performance of the fuel cell, as long as certain limits are not exceeded. 50% is an acceptable level and nearly full cell recovery can be seen, while 10% is too extreme and a complete fuel cell recovery cannot be observed. The most reasonable explanation for this behavior appears to be the cracking of the electrolyte caused by the increase of

the total pressure produced by the increase in the flow inherent to the dilution process.

However, the fact that has been explained before - the short transient that could cause local fuel cell starvation when dilution is removed - could also account for some of the performance loss after dilution, especially in the stronger dilution case. As it was pointed out before, when dilution is removed, there is a short period of time (16 seconds approximately - the correspondent to the dead volume in front of the entrance of the fuel cell) when diluted hydrogen is flowing at a low rate - 50sccm. This means that for the higher dilution case (10%), only 5sccm of hydrogen will be flowing during those 16 seconds, which would certainly enhance the hypothetical local starvation, producing that some parts of the catalyst are oxidized and reducing the fuel cell performance. For the 50% dilution case, this effect would not be as strong, since 25sccm of hydrogen will flow during those 16 seconds.

Other alternative explanations, such as slower kinetics and degradation of the catalyst, were also considered to explain the fuel cell degradation seen after the dilution process, but they do not seem to have such a strong impact. The analysis of the impedance tests data completely confirms this hypothesis.

Also, from the results it can be seen that the fuel cell shows quite a slow response - both in the transients recorded with argon dilution, and also in the changes of potential. This might be due to the complex shape of the flow path for the hydrogen. Since it has holes that only cover about 1% of the total surface, it seems logical that the space that surrounds the catalyst is filled with hydrogen at open circuit potential. Once reaction starts, some current is produced, and some part of this hydrogen is consumed. This fact would also explain the reason why the first transients - when dilution is applied - are faster than those obtained when dilution is removed.

As the holes have such a small area compared with the catalyst area, it seems reasonable that maybe the hydrogen is not able to reach all the surface of catalyst, especially when it is diluted inside an inert gas like

argon. This would explain the high transitory peaks reached every time the potential is reduced and also the slow response that it presents to dilution (and removing the dilution, as then, hydrogen needs to fill in again the holes that it left before).

4.7. Summary in English

An electrochemical characterization of the SOFC was carried out using the electrochemical techniques described in the previous chapter. Hydrogen, as the universal fuel for fuel cells was used to perform this characterization. The results obtained are consistent with one another and with the reality as well.

The fuel cell shows a lower performance after dilution has been applied, compared to the one it had before. This effect is more acute in the stronger dilution cases, as expected. The reason for this behavior could be attributed to cracking of the electrolyte caused by the increase in the internal pressure due to the rise in the flow inherent to the dilution process. Another contributor to this performance loss could be the local starvation induced for a short period of time (16 seconds) when dilution is removed.

Also, the slow response that the fuel cell shows can be attributed to complicated shape that the flow path has. This complicated path for the fuel would also justify why the initial processes (dilution) are faster than the later (dilution removal).

This reflects how important the fuel cell structure is in the behavior of the fuel cell and it clearly suggests one possible improvement to these cells: increase the total area of the holes, so hydrogen does not have so many difficulties to reach the catalyst.

4.8. Summary in Spanish

Una caracterización electroquímica de la pila de combustible de óxido sólido (SOFC) ha sido llevada a cabo usando las técnicas electroquímicas descritas en el capítulo anterior. El hidrógeno, como combustible universal para las pilas de combustible fue empleado para realizar esta caracterización. Los resultados obtenidos son consistentes entre ellos y con lo esperado a priori.

La pila de combustible reduce su rendimiento tras el proceso de dilución, en comparación con el que tenía antes del mismo. Como se esperaba, este efecto es más acusado en los casos de dilución más fuertes. Las razones para este comportamiento pueden ser atribuidas a daños en electrolito causados por el aumento de la presión interna. Dicho aumento se produce debido al incrementar el flujo total del ánodo inherente al proceso de dilución. Otro factor que podría contribuir a disminuir el rendimiento de la pila podría ser una falta de combustible local y transitoria inducida durante un corto periodo de tiempo (16 segundos) cuando se retira la dilución.

Del mismo modo, la respuesta lenta que la pila de combustible presenta se puede atribuir a la compleja forma que el conducto de combustible del ánodo. Esto también justifica la razón por la que los procesos iniciales (la dilución) son más rápidos que los siguientes (al retirar la dilución).

Todos estos hechos reflejan la importancia que tiene la estructura de la pila de combustible en su comportamiento y sugiere de forma clara una posible mejora de las mismas: un incremento del área agujereada del colector del ánodo para facilitar la difusión del combustible hacia los centros activos del catalizador del ánodo.

4.9. References

- [1] Van herle, J., Membrez, Y., Bucheli, O., "Biogas as a fuel source for SOFC co-generators", Journal of Power Sources, Vol. 127, pages 300-312, 2004.
- [2] Yi, Y., Rao, A. D., Brouwer, J., Samuelsen, G. S., "Fuel flexibility study of an integrated 25kW SOFC reformer system", Journal of Power Sources, Vol. 144, pages 67-76, 2005.
- [3] Desclaux, P., Nürnberger, S., Rzepka, M., Stimming, U., "Investigation of direct carbon conversion at the surface of a YSZ electrolyte in a SOFC", International Journal of Hydrogen Energy, Vol. 36, pages 10278-10281, 2011.
- [4] Toonssen, R., Sollai, S., Aravind, P. V., Woudstra, N., Verkooijen, A. H. M., "Alternative system designs of biomass gasification SOFC/GT hybrid systems", International Journal of Hydrogen Energy, Vol. 36, pages 10414-10425, 2011.
- [5] Santori, G., Brunetti, E., Polonara, F., "Experimental characterization of an anode-supported tubular SOFC generator fueled with hydrogen, including a principal component analysis and a multi-linear regression", International Journal of Hydrogen Energy, Vol. 36, pages 8435-8449, 2011.
- [6] Santarelli, M., Leone, P., Calì, M., Orsello, G., "Experimental evaluation of the sensitivity to fuel utilization and air management on a 100kW SOFC system", Journal of Power Sources, Vol. 171, pages 155-168, 2007.

- [7] Gong, M., Bierschenk, D., Haag, J., Poeppelmeier, K. R., Barnett, S. A., Xu, C., Zondlo, J. W., Liu, X., "Degradation of LaSr₂Fe₂CrO_{9-δ} solid oxide fuel cell anodes in phosphine-containing fuels", Journal of Power Sources, Vol. 195, pages 4013-4021, 2010.
- [8] Kattke, K. J., Braun, R. J., "Characterization of a novel, highly integrated tubular solid oxide fuel cell system using high-fidelity simulation tools", Journal of Power Sources, Vol. 196, pages 6347-6355, 2011.
- [9] Sin, Y.-W., Galloway, K., Roy, B., Sammes, N. M., Song, J.-H., Suzuki, T., Awano, M., "The properties and performance of micro-tubular (less than 2.0mm O.D.) anode supported solid oxide fuel cell (SOFC)", International Journal of Hydrogen Energy, Vol. 36, pages 1882-1889, 2011.
- [10] Lay, E., Gauthier, G., Dessemond, L., "Preliminary studies of the new Ce-doped La/Sr chromo-manganite series as potential SOFC anode or SOEC cathode materials", Solid State Ionics, Vol. 189, pages 91-99, 2011.
- [11] Andres Lozano, C., Ohashi, M., Shimpalee, S., Van Zee, J. W., Aungkavattana, P., "Electrochemical Analysis of Microtubular SOFC under Fuel Contaminants". ECS Transactions, Vol. 33, pages 149-160, 2010.
- [12] Andres Lozano, C., Ohashi, M., Shimpalee, S., Van Zee, J. W., Aungkavattana, P., "Comparison of Hydrogen and Methane as fuel in Micro-Tubular SOFC using Electrochemical Analysis". J. Electrochem. Soc., Vol. 158, pages B1235-B1245, 2011.

CHAPTER 5

Experimental Characterization of the SOFC Using Methane

Contents

5.1. Introduction	123
5.2. Effect of Methane and Dilution on the Current	125
5.3. Polarization Curves	135
5.4. Electrochemical Impedance Spectroscopy	140
5.5. Carbon Mass Balance	146
5.6. Electrochemical Reactions	152
5.7. Summary in English	158
5.8. Summary in Spanish	160
5.9. References.....	161

5. Experimental Characterization of the SOFC Using Methane

5.1. Introduction

Methane is one of the main components of the coal gas, biomass gas and other alternative and renewable fuels. Therefore, in order to study the viability of the use of this type of fuels inside a SOFC, an evaluation of the behavior of this type of fuel cells when methane is used as a fuel is necessary. In order to obtain results which are easier to interpret, a characterization of the behavior of the SOFC when it is fed with pure and diluted methane was performed. The chemistry of methane is already very complex, so this characterization is necessary prior to any characterization that involves mixtures containing both hydrogen and methane. Those studies will be part of the future plans for this project.

In addition to this, methane reforming is currently the most widely used way to produce hydrogen, for it has proved to be the most cost-effective way to obtain it. In the long term future, expectations are that hydrogen is obtained from other type of resources, in a way that allows its production in a sustainable way, which will probably involve renewable and alternative fuels. Meanwhile, if a fuel cell is able to operate with pure methane rather than hydrogen, intermediate steps of the whole process will be no longer necessary (hydrogen production, distribution and storage), increasing the efficiency of the whole process and making this kind of fuel cells more competitive in comparison with other types of fuel cells.

Therefore, the study of the behavior of the fuel cell when methane is used as fuel is not just meaningful in relation to the behavior of the fuel cell with alternative/renewable fuels, but also it is meaningful by itself as it might prove to be a valid alternative to the use of pure hydrogen in the fuel cell.

There are plenty of studies of SOFC working with methane in the literature [5-8]. The unique characteristic of this study is the particular fuel cell structure (flow path in the anode) as well as the materials used.

Table 5.1: Flow conditions of the tests carried out.

Fuel Cell #	1 st	2 nd	3 rd
Anode flow H ₂ (set point, sccm)	50	50	50
Anode stoich H ₂ (0.6V)*	3.99	3.77	4.09
Anode flow Ar (for H ₂) (set point)	50	450	0
Anode dilution (real %H ₂)	52.95%	10.1%	0%
Anode flow CH ₄ (set point, sccm)	16.67	16.67	16.67
Anode stoich CH ₄ (0.6V, 8e ⁻)*	4.55	8.56	5.4
Anode stoich CH ₄ (0.6V, 6e ⁻)*	3.41	6.42	4.05
Anode flow Ar (for CH ₄) (set point)	16.67	150	0
Anode dilution (real %CH ₄)	54.5%	10.25%	0%
Cathode flow Air (set point, sccm)	300	300	300
Cathode stoich H ₂ (0.6V)**	~ 9.7	~ 9.2	~ 10
Cathode stoich CH ₄ (0.6V)**	~ 8.1	~ 15.2	~ 9.6

*min. stoich. for the anode side at 0.6V (max. current for this conditions used for the calculation).

** cathode theoretical stoich. calculated for same conditions. Actual stoich impossible to calculate.

The results obtained using pure methane as the fuel are presented in this chapter. Like in the previous chapter the impact that the dilution of methane with an inert gas has also been evaluated. The inert gas used for these studies was argon. The reason for using argon instead of nitrogen (more commonly used), as it was pointed out in previous chapters, was the mass spectrometer used to close the mass balance. Since the peak of the nitrogen is this equipment is located really close to the carbon monoxide peak (both having a molecular mass of 28), and carbon monoxide was one of the expected products at the outlet, the use

of large quantities of nitrogen as inert gas will interfere making the readings of the carbon monoxide peak impossible to read, or at least less accurate.

Three different cases were considered in order to analyze all those effects. Like before, the first one is the small dilution case to 50% fuel and 50% argon. In the second one, 10% fuel and 90% argon was used. Finally, the last case, only pure fuel was used. Again, so that the stoichiometry would not have an effect on the tests carried out, special care was taken to make sure that both the stoichiometry of the anode and the cathode was always over 2 both for the case of hydrogen and methane.

The results obtained are presented and analyzed in this chapter. Table 5.1 reflects the flow conditions for all three different fuel cells during the experiments performed with methane and hydrogen, both as pure and diluted gases.

5.2. Effect of Methane and Dilution on the Current

In this section, transitory analysis was used in order to understand the effect that changing the fuel from hydrogen to methane has for the three cells described in the introduction (0%, 10% and 50% of fuel diluted with argon). For consistency, those levels of dilution are the same as the ones studied in the previous chapter for pure hydrogen, and the additional case (of pure fuel) is also considered. In fact, for the first two cases (those involving dilution), the same cells as in the previous experiments were used (named first and second cell), and the third cell is added to study the case with no dilution.

As was pointed out in the introduction, Table 5.1 shows the flow conditions for all three cases. The reason why the flow set point changes when methane is used instead of hydrogen is to try to keep the stoichiometry as similar as possible in both cases. Every molecule of methane produces 8 electrons when it is completely oxidized while every molecule of hydrogen only produces 2. However, from the first experiments

with methane, it was found out that the main outlet product, when methane was used as fuel, was carbon monoxide rather than carbon dioxide. This means that every molecule of methane was actually producing six electrons rather than eight (see reactions 5.1, 5.2 and 5.3), which is three times as much as a hydrogen molecule.



As the proportion from molecules to volume (and thus volumetric flow) is maintained, when the inlet gas was switched from hydrogen to methane, the flow was reduced by a factor of three to try to keep the stoichiometry in both cases as similar as possible, but always preventing the fuel cell from starving.

The effect of the dilution of hydrogen with argon was already analyzed in Chapter 4 using the procedure indicated in that section, which consists of a transitory analysis. Two different levels of dilution were studied there, and they were reflected on Table 4.1. In the first case the transition from 100% hydrogen in the anode to 50% hydrogen diluted with argon was performed, while in the second one the transition was from 100% to 10% hydrogen. As it was pointed out in the previous chapter, the flow of hydrogen remained constant during the experiment, while the argon flow increased to achieve the desired dilution.

In these experiments an additional case was added (third cell, no dilution), so the expected transients are shown in Figures 5.1 (diluted case) and Figure 5.2 (non-diluted case), both in arbitrary scale. Like before a reduction in the current is expected to occur when dilution is applied, as is shown in Figure 5.1.

The cells used in these experiments proved to have a higher performance when they were fueled with methane than when they were fueled with hydrogen if both cases had a similar level of dilution. That is why an

increased current was expected when the fuel was switched from hydrogen to methane (Figures 5.1 and 5.2).

Similarly to what was presented in Chapter 4, Figure 5.3 shows the transient for the first fuel cell, (from 100% to 50% hydrogen and then to 50% methane), and then the subsequent recovery (from 50% methane to 50% hydrogen and then back to 100% hydrogen). Figure 5.4 was obtained for the second fuel cell (from 100% to 10% hydrogen, 10% methane and the subsequent recovery) and Figure 5.5 was obtained for the third fuel cell (no dilution, so simple transient from pure hydrogen to pure methane and then back to pure hydrogen).

Like experiments from the previous chapter, when the current reached steady state after the transient was performed, shorter experiments were performed (polarization curves and impedance tests) for the same flow conditions. They appear in the graphs as blank gaps in the transient trends.

Expected transients with diluted CH₄ (0.6V)

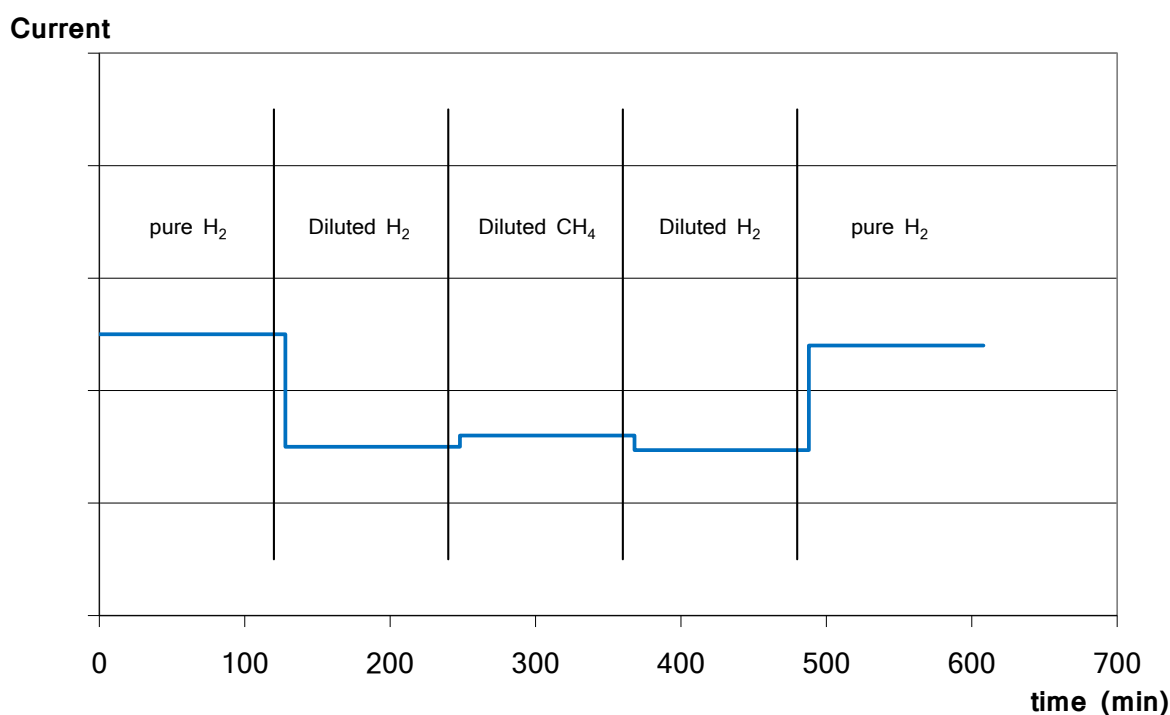


Figure 5.1: Transient expected for the diluted methane case.

Expected transients with pure CH₄ (0.6V)

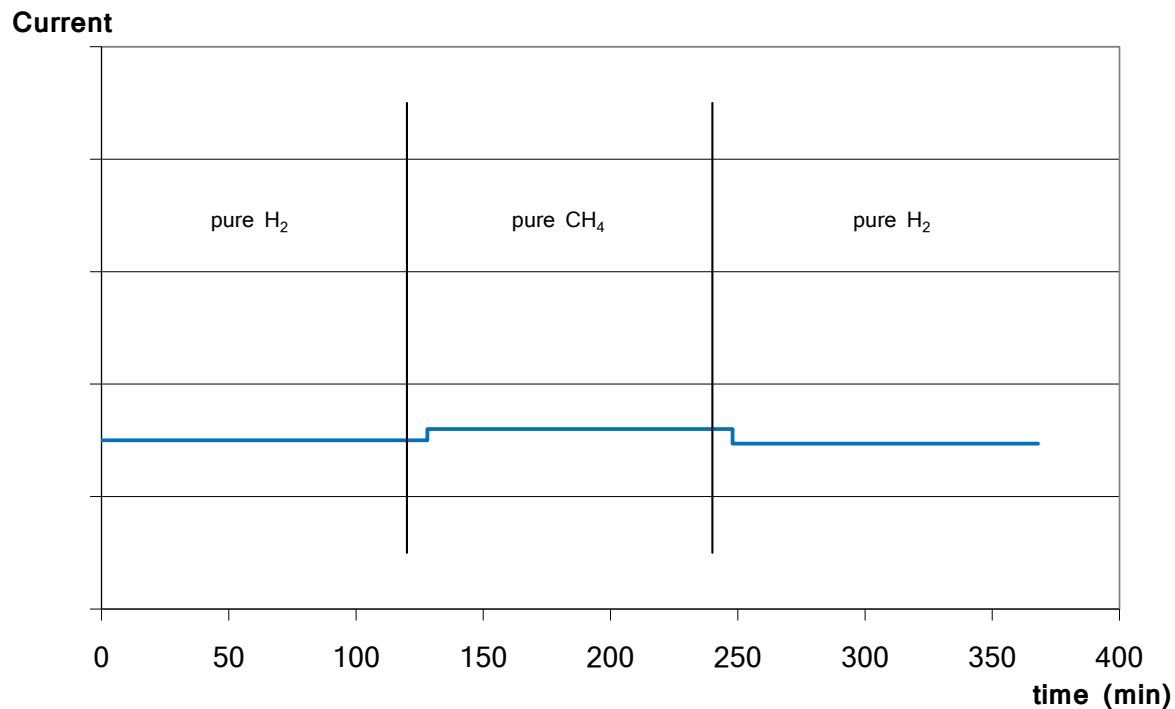


Figure 5.2: Transient expected for the pure methane case.

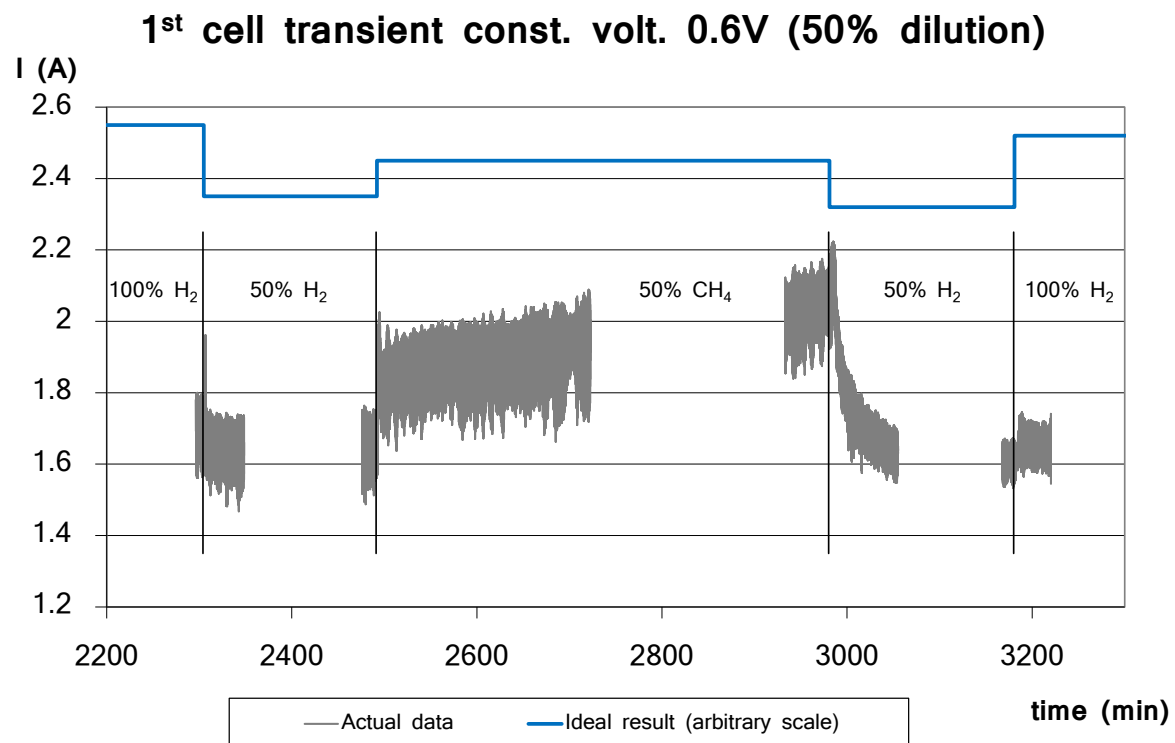


Figure 5.3: Transient 1st fuel cell, 50% H₂/CH₄ in Ar.

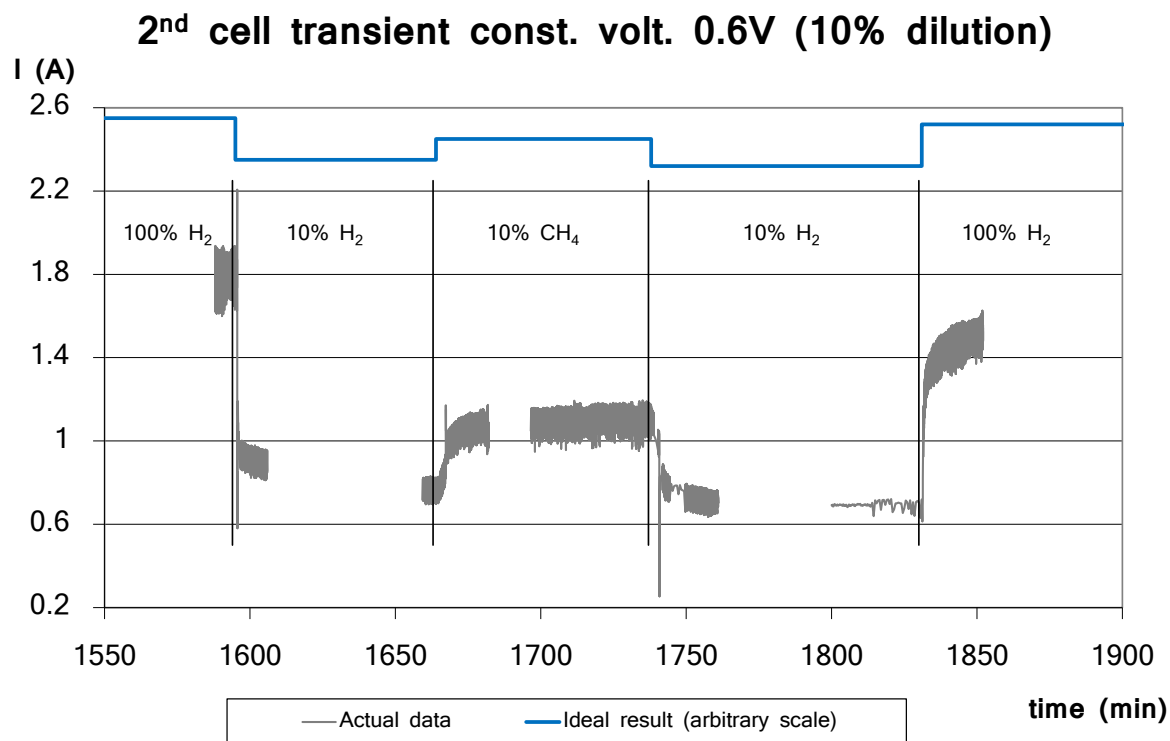


Figure 5.4: Transient 2nd fuel cell, 10% H₂/CH₄ in Ar.

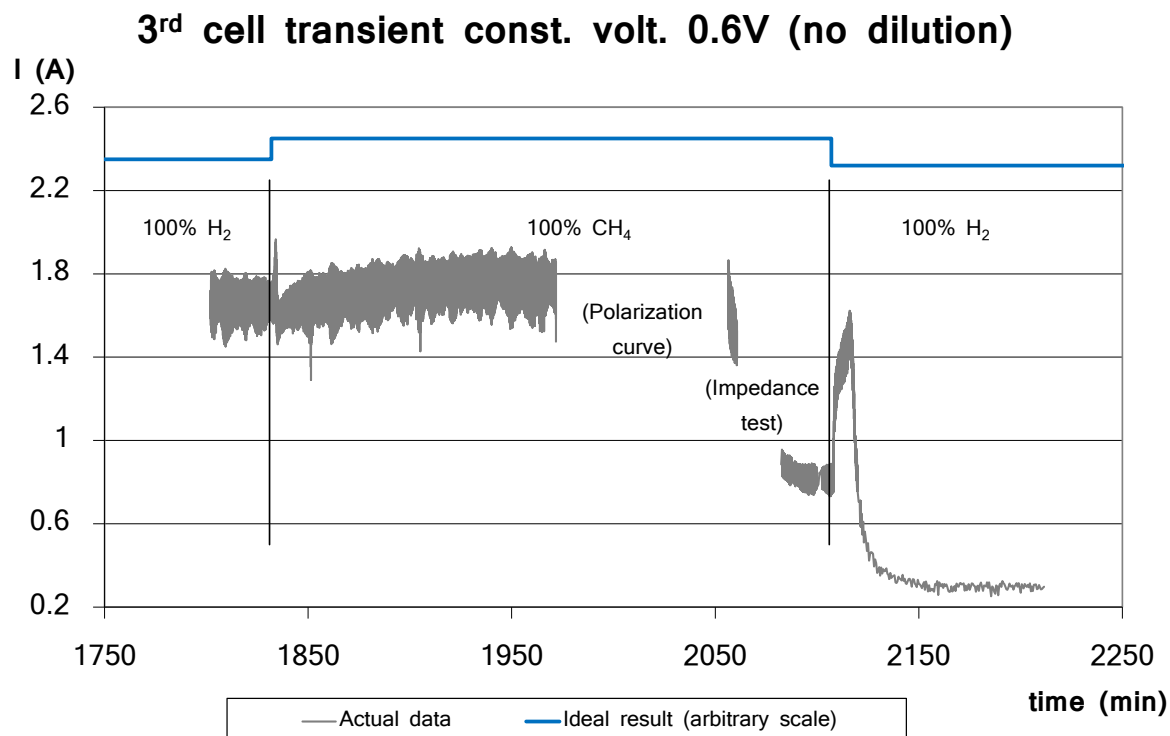


Figure 5.5: Transient 3rd fuel cell, no dilution with Ar.

In this case, all of the graphs present different trends, especially after methane has been applied. The reason for this behavior, as will be explained more in detail later in this chapter, is probably the different approach followed for each cell to perform the polarization curve while methane was used as the fuel. As was described in previous chapters, the polarization curve procedure includes the open circuit potential hold, but for these experiments, it was made differently for each cell.

The reason for this is that current (and thus potential) is an extremely important factor in carbon deposition when the cell is working with methane, as found in the literature [2, 3] and the C-H-O equilibrium diagram [1], see Figure 5.6. Some of the failures (like the one seen in the third cell) were caused by the potential hold at open circuit voltage (no current) during the measurement of the polarization curve. Therefore, the procedure was changed (hold time reduced, and eventually eliminated) for the rest of the cells.

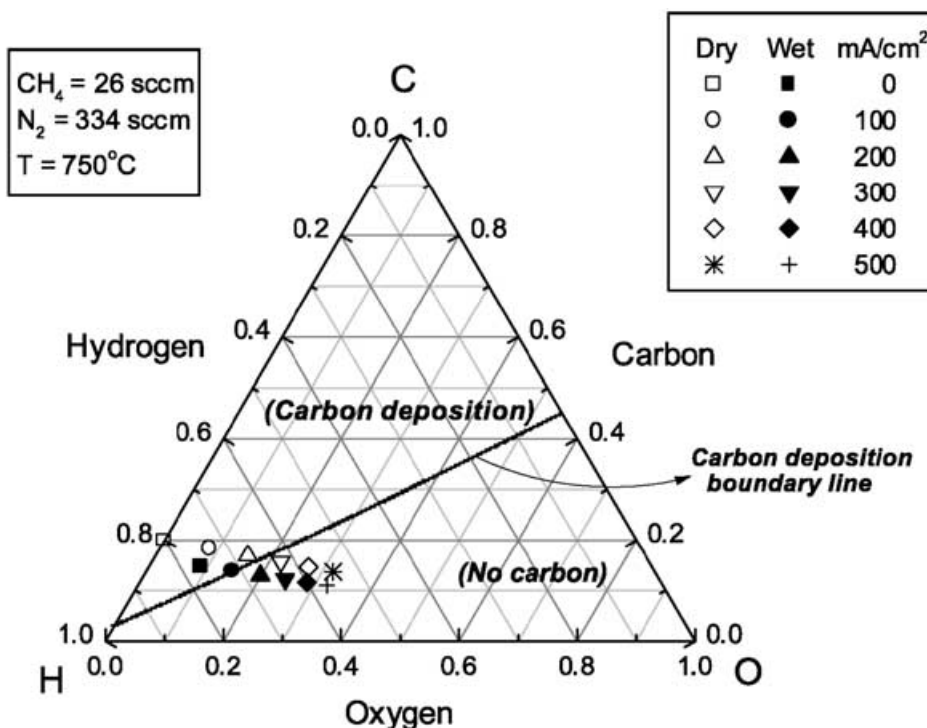


Figure 5.6: C-H-O equilibrium diagram at 750°C, from [1].

Figure 5.6 shows the equilibrium diagram for the C-H-O system. According to it, about 250mA/cm^2 (approximately 2.25A for the SOFC used in this project has a surface area of catalyst of 9cm^2) would be needed in order to prevent carbon deposition. However, from the results obtained it was observed that strong carbon deposition leading to cell failure only happened at open circuit voltage (no current). This behavior, better than expected can be attributed to the fact that the cell counts with a copper current collector.

According to literature [9-12], while nickel presents serious problems with carbon deposition, as it is able to activate and crack the hydrocarbons, copper shows a much better behavior towards coking, thus alloying the two of them can produce a catalyst with favorable properties towards coking. The high temperatures reached by the fuel cell can certainly cause diffusion of some part of the metallic copper from the current collector towards the nickel catalyst. Further studies that involve visual techniques, such as X-ray Photoelectron Spectroscopy (XPS) or Scanning Electron Microscopy (SEM), are required in order to determine if this is actually happening inside the fuel cell and that would justify the good behavior that the cell presents towards coking.

The hydrogen dilution cases, as was can be seen in Figures 5.3 and 5.4, show analogous trends that were discussed in the previous chapter, so it will not be discussed with the same level of detail here. As can be seen from Table 5.2, the characteristic values of the transients (time constant and percentage loss with respect to the baseline) are in accordance with the ones reported for the transients obtained with hydrogen (Table 4.2).

Also, higher differences can be found when the dilution is more extreme - second fuel cell, 10% fuel - compared to the case of low dilution - first fuel cell, 50% fuel, as was also seen in the experiments carried out in the previous chapter.

Actual current values in this case may be a little smaller than the ones shown in the previous chapter due to the performance reduction that the first dilution induced, since the cells used for these experiments are the same ones that were used for the experiments of the previous chapter,

both for the 50% and the 10% dilution cases. However, since a baseline using standard conditions is used at the beginning of each experiment, the results and conclusions are obtained taking this new baseline, and so the conclusion will still be valid.

Table 5.2: Summary of the results obtained with the transient analysis.

Condition	1 st cell - 50% dilution			2 nd cell - 10% dilution			3 rd cell - no dilution		
	I (A)	%	Γ (s)	I (A)	%	Γ (s)	I (A)	%	Γ (s)
Pure H ₂	1.72	-	-	1.80	-	-	1.66	-	-
Diluted H ₂	1.65	-4.07%	~27*	0.75	-56.4%	36	-	-	-
CH ₄	2.04	18.6%	~420*	1.09	-36.6%	180	1.73	0.58%	~540*
Diluted H ₂	1.61	-6.4%	~360*	0.69	-59.9%	102	-	-	-
Pure H ₂	1.66	-3.49%	~57*	1.58	-8.14%	54	**	**	~99**

* Imprecise value due to noise, fluctuations and small difference between the values.

** Cell failed once methane removed so values, if reported, are estimation on trends.

Also, like in Chapter 4, the first fluctuations observed (high and low peaks) should be discarded, for they are a consequence of the dead volume of gas that is in the tubing of the entrance of the fuel cell, as was explained in the previous chapter. This phenomenon can also be seen when methane starts being fed and also when it is removed, although not to such a big extent as in the case of the dilution with argon.

Another interesting point is that the current (and thus the power) of the fuel cell always increases when methane replaces hydrogen if the two cases are comparable (same level of dilution) and it happens with all the different cases of dilution studied. Hydrogen should have faster kinetics than methane [4] and thus it could lead to the conclusion that it would show a higher performance than methane. In order to explain this, the following considerations are taken: it is very likely that at those high temperatures (900°C) the kinetics of both molecules are extremely quick, so differences would be really small there. At the same time, the stoichiometry for the methane flow is larger than the one of the hydrogen when the stoichiometry of the methane is calculated for the full oxidation

case (8 electrons). Even though both cases present a large stoichiometry, and so it should not affect the performance in principle, the particular flow distribution of these fuel cells (described in chapter 3 and already discussed in chapter 4) - may cause a local fuel cell starvation and so small local stoichiometry maybe causing the stoichiometry to have an effect on the fuel cell performance.

Also, as the total flow of methane is much lower than the one of hydrogen to try to keep the stoichiometry of both cases as similar as possible, the pressure loss in the fuel cell and the velocity of the flow field will be much smaller in the methane case. This might be leading to a less guided flow in the case of methane, which would facilitate the fuel diffusion to the active sites in the anode catalyst. Hydrogen molecules are much smaller than methane molecules, but in this case the size of the molecule is not important: the holes in the copper tube that acts as the anode current collector are much larger than the typical size of molecules, so this effect should also be disregarded.

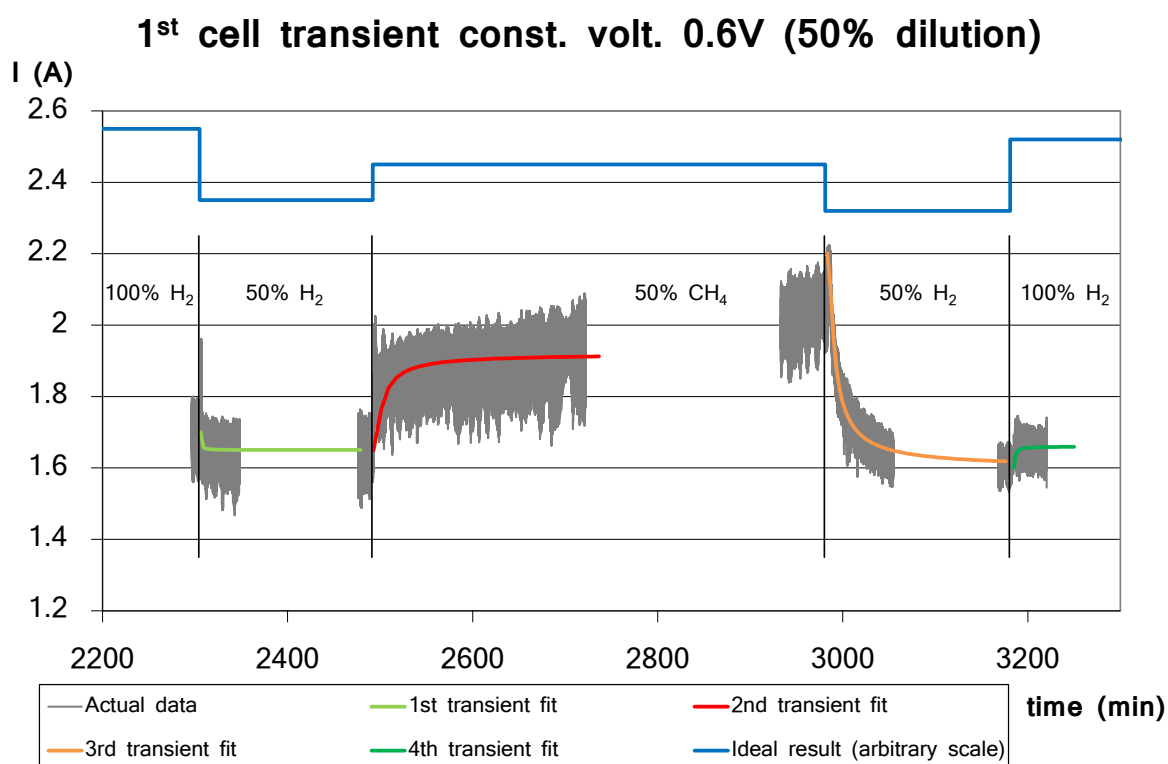


Figure 5.7: Transient adjusted with exponential function, 1st cell.

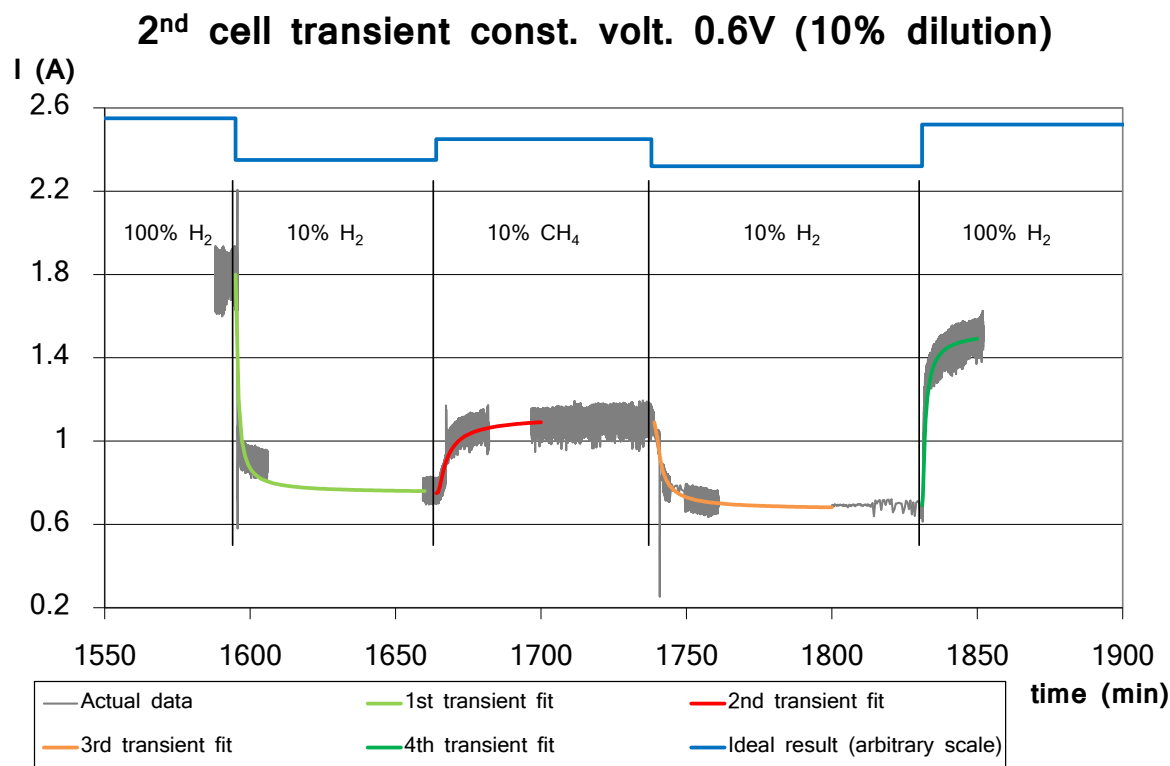


Figure 5.8: Transient adjusted with exponential function, 2nd cell.

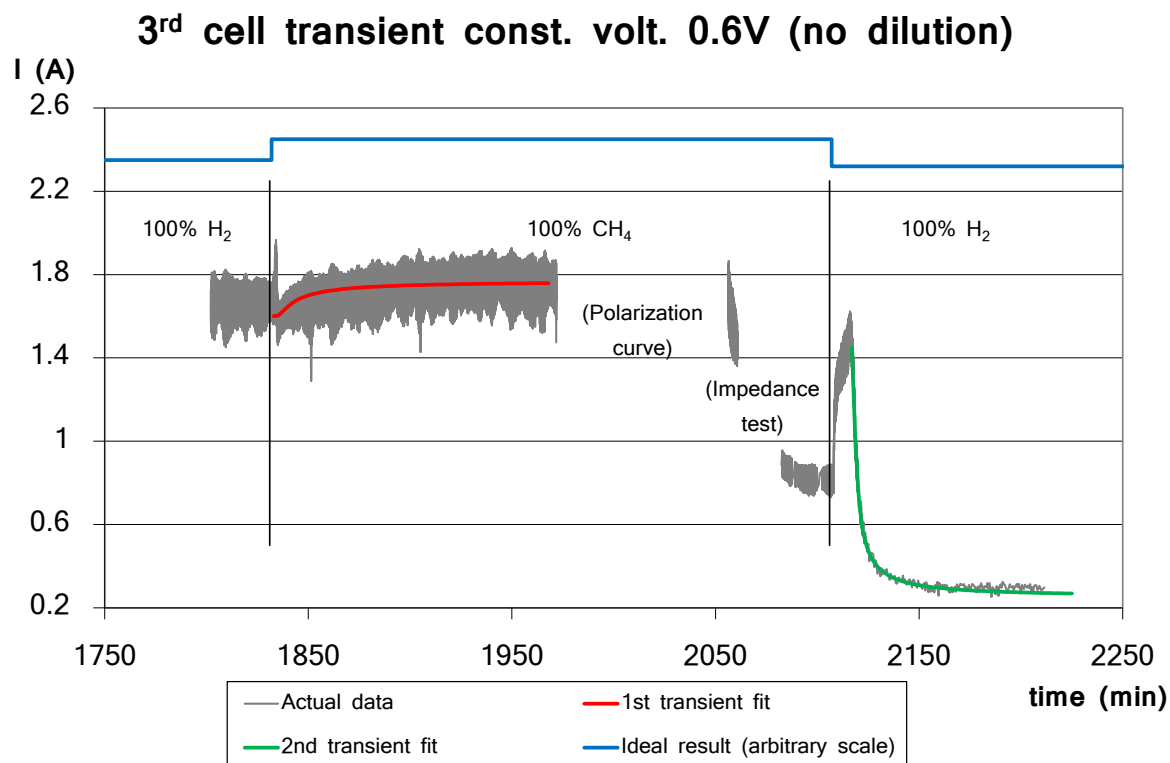


Figure 5.9: Transient adjusted with exponential function, 3rd cell.

Finally, the time constant for each transient was calculated the same way as they had been obtained in the previous chapter, that is, adjusting each of the transient recorded with an exponential function that follows the expression from equation 5.4:

$$I(t) = I_0 - (I_0 - I_{ss}) \cdot \exp\left(-\frac{\Gamma}{(t-t_0)}\right) \quad (5.4)$$

Figures 5.7, 5.8 and 5.9 show the curves that adjust each of the transients with the exponential function shown before. The value of the time constant for each transient can be found in Table 5.2.

Regarding the time constants, for the hydrogen cases, the response is quicker when the transient goes from pure to diluted hydrogen than when it goes in the opposite direction, as it was observed in the previous chapter. However, the response is slower when hydrogen is replaced with methane compared with the response when the transient follows the opposite direction (hydrogen replacing methane). In any case, the response to dilution is much quicker than the response to the change in the fuel type.

5.3. Polarization Curves

The procedure described in the third chapter was used again to perform the polarization curves for this set of experiments. The flow conditions for each polarization curve are identical to those used in the transient analysis and so they are reported in Table 5.1. Like before, the minimum stoichiometry calculated while performing the polarization curve is lower than the one reported for the transients. As the flows are fixed and the voltage is reduced to 0.35V (compared to the 0.6V at which the transients were performed), with the consequent increase in the current, the stoichiometry of the cell is reduced both for the anode and the cathode. The minimum stoichiometry while performing the polarization curves - which occurred at 0.35V - is reported on Table 5.3. Like before, in order

to prevent the starvation of the fuel cell that can occur due to poor flow distribution or non-uniformity of the current distribution due to non-uniform oxygen supply, the minimum stoichiometry is always above 2.

Table 5.3 Minimum stoichiometry while performing polarization curves.

Fuel Cell #	1 st	2 nd	3 rd
Minimum anode stoich H ₂ (0.35V)	3.99	3.77	4.09
Minimum anode stoich CH ₄ (0.35V - 8e ⁻)	2.69	7.24	6.57
Minimum anode stoich CH ₄ (0.35V - 6e ⁻)	2.02	5.43	4.93
Theoretical min. cath. stoich. H ₂ (0.35V)	~ 7.0	~ 6.0	~ 6.1
Theoretical min. cath. stoich. CH ₄ (0.35V)	~ 4.8	~ 12.8	~ 11.6

Similarly to the cases shown in the previous chapter, Figure 5.10 shows the polarization curve of the first cell, in this case using hydrogen and methane as the fuel. For this cell the fuel was diluted with argon to 50% and five different curves can be observed. The baseline is the first one taken and it was performed with pure hydrogen, before dilution started and also before the fuel was changed to methane. Then, the one performed during the first dilution with hydrogen is named as “(before)”. After that, the methane was applied, replacing the hydrogen, keeping the same dilution level. The curve obtained for those conditions is called “CH4”. Then, hydrogen replaced the methane as the fuel, but still it was diluted to the same extent. The curve obtained then was called “recovery” with the level of dilution indicated in the legend as well. Finally, the dilution was removed, and the fuel cell operated on pure hydrogen. That final curve is called as “pure H₂ (recovery)” in the legend.

Figure 5.11 shows the polarization curve for the second cell. In this case the fuel (either hydrogen or methane) was also diluted with argon, but to a much higher extent: the ratio was 10% of fuel to 90% argon. The nomenclature of the curves follows the same pattern as in the previous graph (Figure 5.10), but with the new level of dilution (10% instead of 50%) which appears in the legend of the graph.

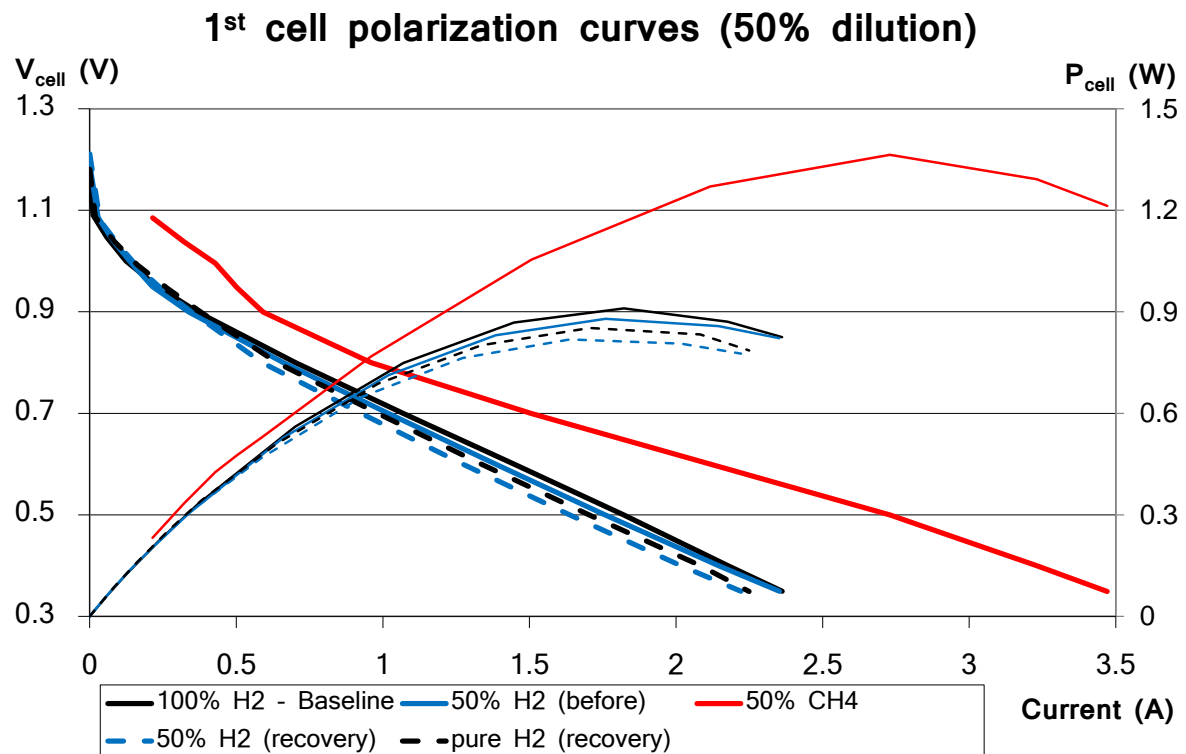


Figure 5.10: Polarization curves 1st fuel cell, 50% H_2/CH_4 in Ar.

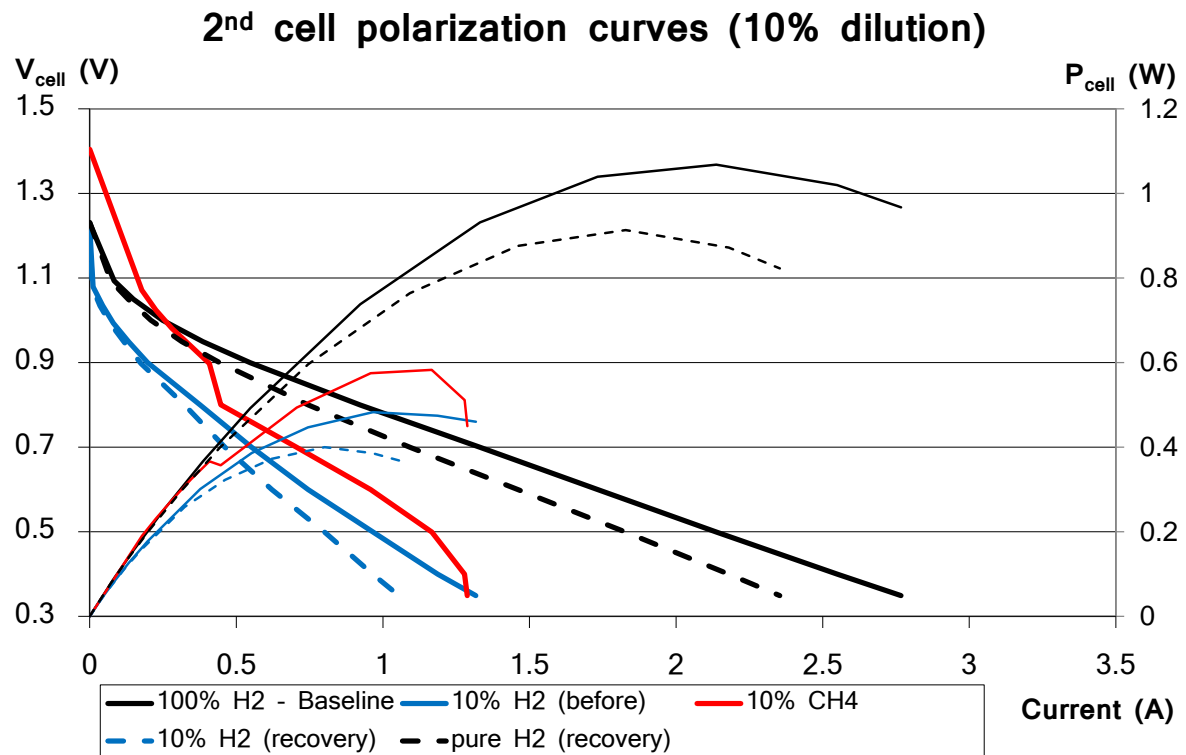


Figure 5.11: Polarization curves 2nd fuel cell, 10% H_2/CH_4 in Ar.

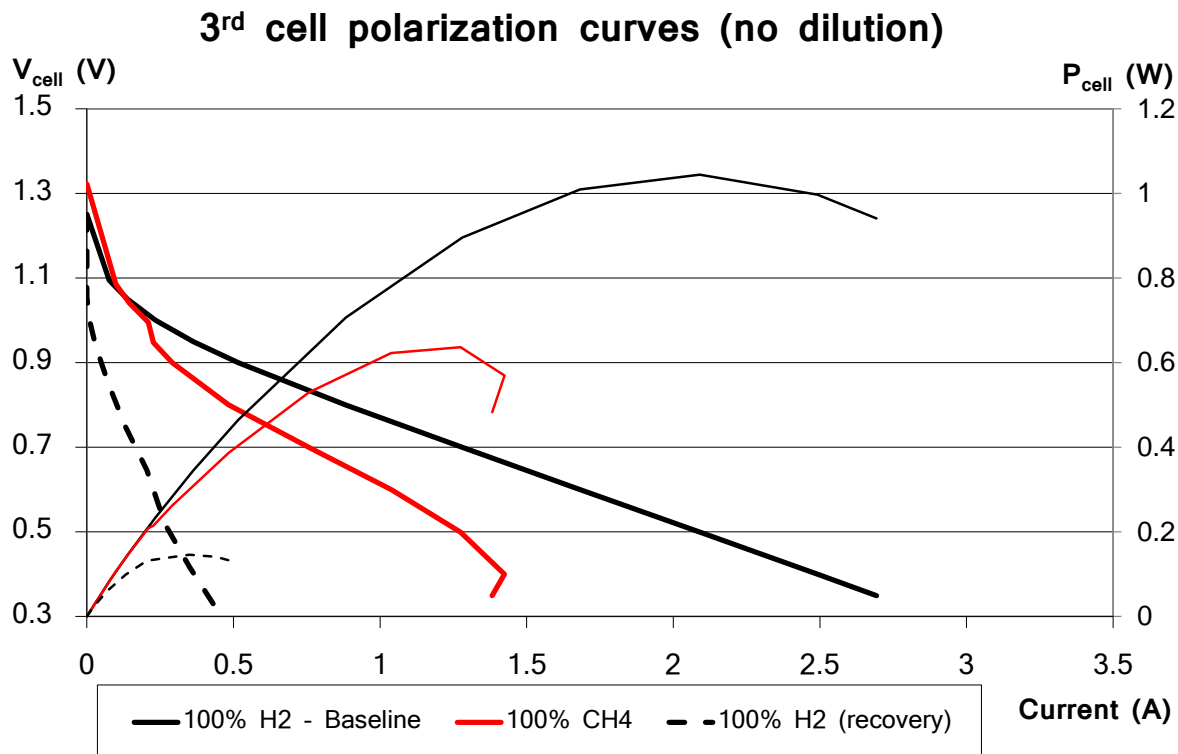


Figure 5.12: Polarization curves 3rd fuel cell, no dilution with Ar.

Figure 5.12 reflects the polarization curves obtain for the third cell, where no dilution was performed so only three different lines can be observed in the graph: the baseline performed with pure hydrogen before the cell was exposed to methane, the recovery line carried out with pure hydrogen after the cell had been exposed to methane and the one carried out while methane was used as the fuel (methane).

The results obtained are in accordance with the transient analysis. Like before, the trends are really similar, and also, the dilution has a bigger impact in the case where it is stronger (the one performed to 10% with the second cell).

Like before, the effect of the hydrogen dilution seems to be the same for every voltage: it reduces the current by a certain factor, and this factor is approximately the same for all voltages. This means that the cell behaves the same way for every potential when hydrogen is diluted with argon. Also, the open circuit voltage remains practically unaltered for all levels of

dilution studied, when hydrogen is used as the fuel, in accordance with what was explained in the previous chapter.

However, when methane is used as the fuel, an increase in the open circuit voltage can be observed (from 1.26 to over 1.32). The open circuit voltage was not recorded for the first fuel cell, for it was apparent that fuel cells failed when they were left at open circuit while methane was being flown. Even for the two fuel cells that were left at open circuit voltage, the hold time of each of them was different. It was longer for the third fuel cell (pure methane), when it was left at open circuit for over 10 minutes, while it was much shorter for the second fuel cell (10% methane) when it was left at open circuit voltage for just under 1 minute [12].

Those facts explain the different behavior shown by the three cells when methane was removed. This first fuel cell does not seem to be affected by the methane, as it shows a complete recovery when it is removed, as can be seen both in the transients (Figure 5.3) and the polarization curve (Figure 5.10). The second cell, shows a slight performance drop when methane is removed (about 4% compared with the diluted hydrogen case that was measured just before the flow of methane), and this performance drop is extended further (to about 8%) when the two cases of pure hydrogen are compared. Again, this fact can be observed both in the transitory analysis (Figure 5.4) and the polarization curve (Figure 5.11). This slight performance drop can be attributed to the minute that the cell spent at open circuit voltage while methane was flowing.

On the other hand, the third cell showed a larger decrease in the performance and it eventually failed after the methane was removed. The ten minute period that the cell was left at open circuit voltage while methane was flowing seems to be the reason for the cell performance drop and its eventual failure. This can clearly be seen in the transitory analysis (Figure 5.5), when right after the blank produced by the polarization curve, and before the impedance test and even before the methane was removed, a strong decrease in the current takes place. When methane is removed a first increase is seen, but it is quickly followed by another decrease.

This particular behavior can clearly be attributed to the cell being left at open circuit voltage for a longer period of time. Carbon deposition is likely to take place under those conditions and the longer those conditions are maintained, the larger the amount of carbon that will be deposited over the catalyst, which will decrease the performance of the cell and might lead to cell failure. A more detailed explanation of these facts will be given in sections 5.5 and 5.6.

The polarization curves of the third cell (Figure 5.12) relate to the transient curve as well. Even if the transient analysis shows that initially the performance increased when hydrogen was replaced with methane (like in the previous two cells), the polarization curve starts with a 3 minute period at open circuit. This induces a performance drop, and that is the reason why the polarization curve recorded for the methane is below the polarization curve of the comparable methane case (unlike the previous two cells). The recovery curve also shows the same as the transient: the cell showed an extremely small performance and was about to fail.

Unlike the dilution case - where the cell had the same behavior for all voltages - when the fuel is changed to methane, the cell does not show the same behavior for all voltages. Open circuit voltage is higher but the region between 0.9V and open circuit voltage (activation resistance region) shows a higher decrease than the correspondent hydrogen case. However, the ohmic resistance region (below 0.9V) show a smaller decrease when methane is used as the fuel than the correspondent hydrogen case. Thus it can be concluded that methane increases the open circuit voltage and reduces the ohmic losses, but it increases slightly the activation resistance of the fuel cell.

5.4. Electrochemical Impedance Spectroscopy

According to the procedure described in chapter 3, impedance tests were performed on the three cells. The conditions used for those experiments were the same as the ones used for the transient (one impedance test

was carried out for each set of conditions), and so they are reflected on Table 5.1.

The sinusoidal voltage applied had an averaged value of 0.6V - the same as the constant voltage at which the transients were performed - with perturbations of 20% in the current - which corresponded to about 0.1V. Thus, the maximum and minimum voltage during these experiments were 0.7V and 0.5V, and therefore the minimum stoichiometry of the cell was always over the values shown in Table 5.3 for the entire duration of the experiments, ensuring that the fuel cell always had enough fuel and oxidant for a normal working condition.

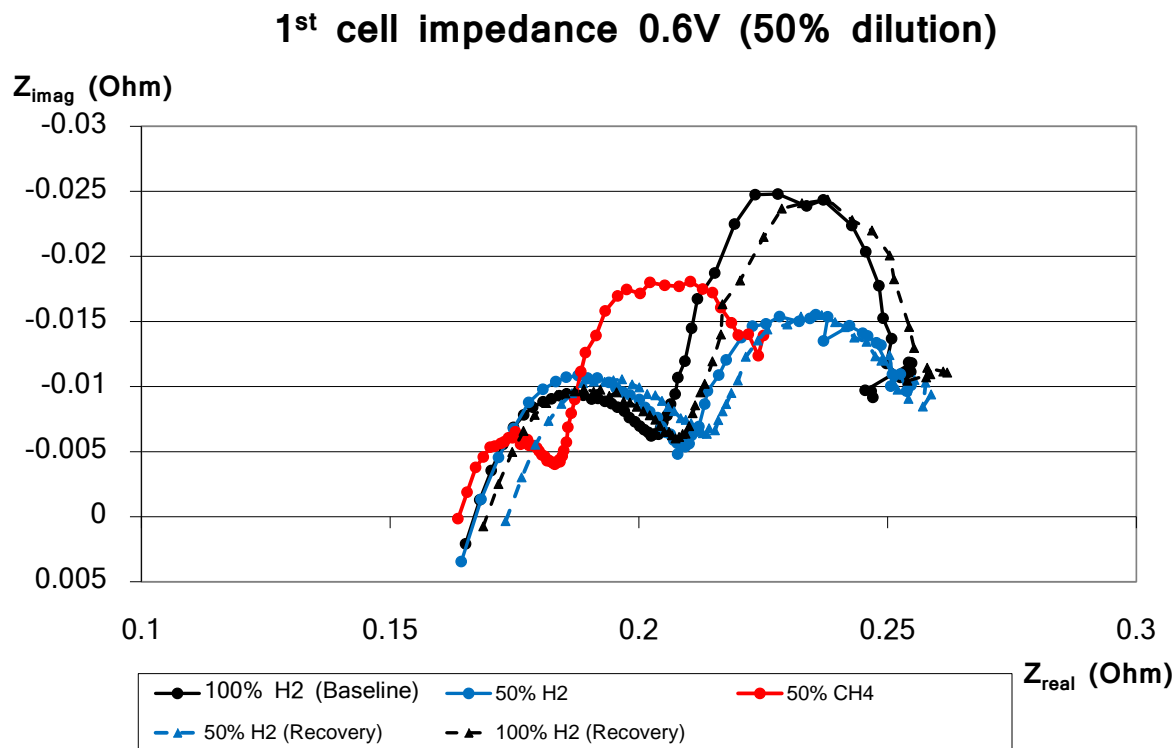


Figure 5.13: Impedance test 1st fuel cell, 50% H₂/CH₄ in Ar.

The results obtained following that procedure are reflected in Figures 5.13, 5.14 and 5.15. Figure 5.13 reflects the impedance test results for the first fuel cell, the one where small dilution (to 50%) was applied. Like in the correspondent polarization graph (Figure 5.10), five different lines can be observed, each corresponding to a different condition of the cell. The

baseline was carried out with pure hydrogen before dilution and methane were applied. Then, the curve labeled as “50% H₂” was obtained right after the hydrogen in the anode side was diluted to 50% with argon.

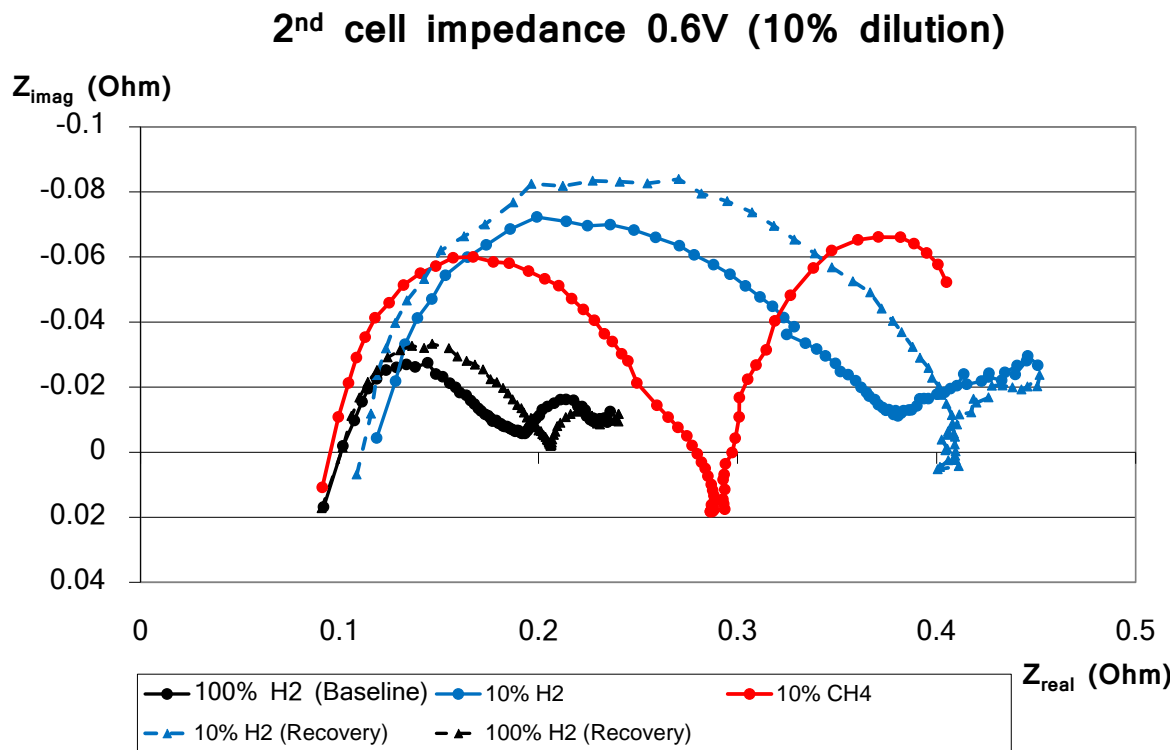


Figure 5.14: Impedance test 2nd fuel cell, 10% H₂/CH₄ in Ar.

After that, hydrogen was replaced with methane, with a smaller flow rate (for the reasons explained before), but with the same level of dilution. That curve is labeled as “50% CH₄” in the graph. After that, the methane was replaced by hydrogen again, increasing the flow rate but keeping the dilution constant, so that the conditions were exactly the same as they were before methane was applied, in order to see the recovery. The curve performed in that moment is labeled as “50% H₂ (Recovery)” in the graph. Finally dilution was removed and conditions were set back to the beginning of the experiment with pure hydrogen in order to see the global recovery. That curve is labeled as “100% H₂ (Recovery)” in the graph.

Figure 5.14 reflects the results obtained for the second fuel cell - where the dilution was taken to a more extreme value, 10%. The experimental

procedure is identical as the one followed for the first cell, with the difference in the level of dilution. For that reason, the nomenclature of the different curves is identical to the one followed for the previous cell, with the only difference in the level of dilution reflected in the labels.

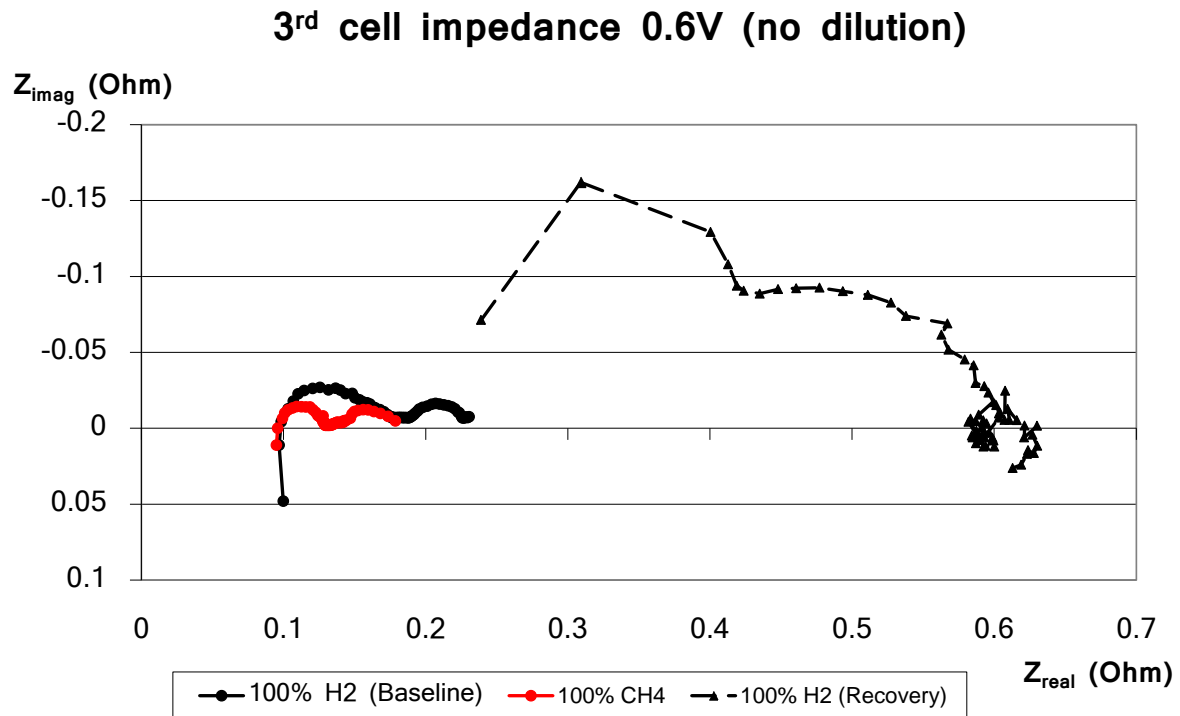


Figure 5.15: Impedance test 3rd fuel cell, no dilution with Ar.

Finally, Figure 5.15 shows the results obtained for the third cell - the one in which no dilution was performed. The procedure is the same as in the previous cells, with the only difference being that no diluted case were perform. Therefore, only three different lines can be observed: the baseline performed with pure hydrogen (labeled as “100% H₂ (Baseline)” in the graph), after that, hydrogen was replaced with methane, and the flow rate was reduced for the same reasons mentioned earlier in this chapter. The impedance curve performed during these conditions is labeled as “100% CH₄”. Finally when methane was replaced by hydrogen again, with the subsequent increase in the flow rate, the latest impedance test was

performed, and the curve obtained for those conditions was labeled as “100% H₂ (Recovery)”.

Low-frequency values of the impedance test (the ones located at the right hand side of the graph), should relate to the facts that were seen in both the transient and the polarization curves analysis, and they certainly do. For the first cell (Figure 5.13), all the values for the hydrogen case lie very close to one another (even the diluted cases), while the methane case shows a better behavior (the line shows lower values of impedance in the real axis for those low-frequency values).

In the case of the second cell (Figure 5.14), the non-diluted hydrogen cases show the lowest low-frequency impedance values (with the recovery line showing a larger value of the low-frequency impedance), and that perfectly correlates to the behavior observed in the polarization curves and the transient analysis for this cell (Figures 5.11 and 5.4) where the higher performance was shown by the hydrogen non-diluted cases, being the baseline the one with higher performance. The methane case shows a lower low-frequency than the comparable diluted hydrogen case, which is linked to the fact that it shows a better performance both in the polarization curve and in the transitory analysis. Finally, the diluted hydrogen recovery case shows a higher low-frequency impedance value compared to the original diluted hydrogen case, which corresponds to a worse performance shown both in the transitory analysis and the polarization curves of this cell.

For the third cell, the low-frequency values of the impedance also correlate closely to the transient analysis, but no so much with the polarization curves. The reason for this is that the polarization curve obtained for the pure methane case was obtained after the fuel cell had been left at open circuit voltage for a certain period of time, which means its performance was already lower than it should have been. On the other hand, the impedance test shown in Figure 5.15 had already been performed before the cell was left at open circuit voltage, and thus it shows a better behavior than the correspondent hydrogen case (in this case, the baseline). This is shown as an increase in the current recorded in the transient (Figure 5.5)

when methane started being flown, and also, as a lower low-frequency value for the impedance of the pure methane case, compared to the baseline. After methane was removed, the fuel cell showed an extremely low performance, and that is reflected in the transitory analysis with a strong decrease in the current (Figure 5.5) as well as in the polarization curve (Figure 5.12) and the impedance test (Figure 5.15), with an extremely high low-frequency value of the impedance.

Apart from this, impedance testing in the frequency domain provides extra information compared to that offered by the transient analysis and the polarization curves, like was explained in the previous chapter. In this case, it can be seen that dilution affects the impedance results the same way as it was described in the previous chapter, so the same conclusions could be drawn here [11].

Regarding the methane it can be seen that it does not affect the high frequency value compared to the hydrogen cases. This shows that the total resistance of the fuel cell is not affected when the fuel is changed to methane. This resistance results mainly by the electrolyte ion transport and so, it can be said that it is not changed by the change in the fuel.

However, the low frequency value of the impedance test is lower for the case when methane is used as the fuel compared to the hydrogen case that presents the same level of dilution. This justifies the higher performance that the fuel cell shows when it is fueled with methane. The reason for it might be an enhancement of the kinetics which is probably produced by the increment in the stoichiometry. Even if it seems high enough (and therefore should not affect the performance of the cell), due to the geometry of the anode of the fuel cell and the difficulties that it presents for the hydrogen to reach the catalyst, an increase in the stoichiometry is likely to produce an increase in the current.

Also, another interesting point that has not been discussed yet is that every molecule of methane produces three molecules of different gases (CO, CO₂, H₂O, H₂...). If the reaction happened in a single step, that is, CH₄ was completely oxidized in the first step and no intermediate species appeared, then this fact could be disregarded. The products of the

reaction will certainly have a larger volume than the reactants (three times larger for every molecule of methane that reacted), which means that the level of dilution (percentage of argon with respect to the rest of the species) will decrease, but this could be disregarded since the dilution of the reactants would not change.

However, that is not the case. As it will be shown in the next section, the reaction mechanism for this system is complex, and does not happen in a single step. This means that the dilution of the intermediate species formed in the reaction will be smaller than the one of the methane. If the reaction which forms the first intermediate species was reaction 5.5, then the level of dilution in terms of volume will decrease from $x/(x+1)$ to $x/(x+3)$, in our case from 90% to 75% (for the second cell) and from 50% to 25% (for the first cell), reducing the impact that dilution may have in the cell behavior.

This fact would also explain the reason why methane shows a higher current than hydrogen in the transients performed with dilution.



5.5. Carbon Mass Balance

As it was described in the third chapter, to close the carbon balance of the fuel cell, samples of the anodic outlet gas were collected by means of a plastic bag. This bag was taken both to a gas chromatograph and a mass spectrometer to determine its composition. The versatility of the mass spectrometer allowed determining not only the proportion of CH_4 to CO and CO_2 - like the gas chromatograph did - but also H_2 , N_2 and argon, which made it a more suitable tool to close the carbon balance at the anode of the fuel cell.

All these samples were collected with the second fuel cell, the one that was diluted to 10% with argon, while and after methane was being used as the fuel for this fuel cell. The system of the anode side can be seen as a black box, with several inputs and outputs, as shown in Figure 5.16.

In that system, the mass spectrometer determined the composition of the gases at the outlet of the fuel cell (CO, CO₂...)

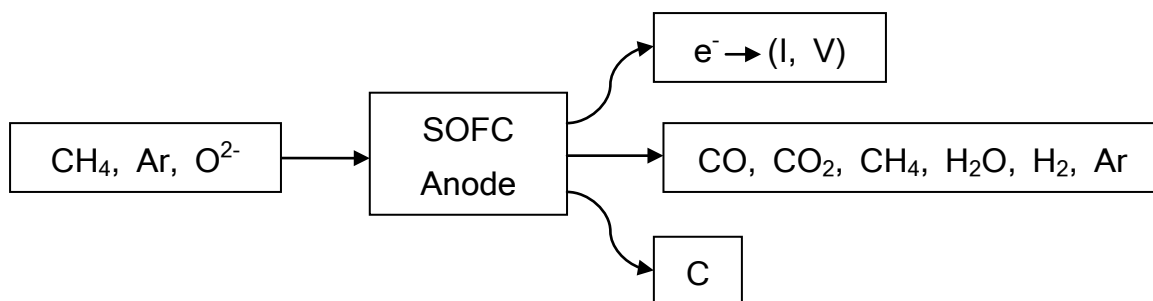


Figure 5.16: SOFC anode: Input and outputs.

This way, samples were taken for different flow and potential conditions, to characterize and understand the behavior of the fuel cell when methane was used as its fuel. The first sample was always taken during the first stages, when methane was starting to flow, that is, at the beginning of the transient when hydrogen was replaced with methane, at 0.6V.

Table 5.4: Conditions of each sample collected (2nd cell, 10% dilution in Ar).

Condition	Sample 1	Sample 2	Sample 3
Voltage (V)	0.6	1.1 - 0.9	0.6
Averaged Current (A)	1.016	0.301	0.638
Fuel	CH ₄	CH ₄	H ₂
Dilution with Ar (%Ar inlet)	89.7%	89.8%	90.5%
Stoich for CH ₄ (based on 8e ⁻)	9.3	31.3	-
Stoich for CH ₄ (based on 6e ⁻)	7.0	23.5	-
Stoich for H ₂	-	-	10.6

After that, another sample was collected during the measurement of the polarization curve with methane (which involved holding the potential at several different high values - from 1.1V to 0.9V concretely - during the time when the polarization curve for the methane case was performed), to see the influence of the voltage. Finally another sample was collected when the methane was replaced by hydrogen again (at 0.6V during the first stages of the transient) in order to see the products at the outlet of

the fuel cell during the recovery period. The conditions at which each of the samples was collected can be seen in Table 5.4.

The mass spectrometer was calibrated using bags that had known composition of the gases relevant to this study - Ar, H₂, CH₄, CO and CO₂. However, the mass spectrometer was unable to quantify the amount of two other species that were present in the anode reactions: H₂O (as it condensed inside the bag at room temperature) and carbon (as it is present in solid phase).

The spectrometer is able to give information on the proportion that each species has in the sample collected, but not of total flow, so a mere subtraction between the inlet products and the outlet products was not adequate to determine the carbon deposition, as the outlet flow does not have to be equal to the inlet flow (for every molecule of methane that is fully oxidized, three new molecules appear). Therefore, the outlet flow will be determined both by the inlet flow and by the extent of methane reaction. The electrochemical reactions are controlled by the current (electrons must be transferred so that the reaction occurs, and the amount of reaction is completely dependent on the amount of current applied) and thus they could be measured. However, the reforming reaction (one molecule of methane going to two molecules hydrogen and one atom of carbon, with no exchange of electrons through the external circuit) can occur without current being applied, so the total flow at the outlet of the fuel cell is not only dependent on the current applied.

Since the main objective of the mass balance is to determine the amount of carbon deposition that takes place while methane is being flown, a new approach had to be taken. From the data produced by the mass spectrometer, two different approaches were taken in order to determine the carbon deposition.

The first one is based on the fact that the proportion between the atoms of carbon and the atoms of argon has to remain constant from the inlet to the outlet. However, if carbon deposits inside the fuel cell, this proportion will not be maintained. Therefore, the difference between the C/Ar proportion at the inlet and at the outlet will be the proportion of carbon

that will deposit no matter if there are leaks in the system, or if the measurement of the flow (inlet and outlet) is not precise enough. In addition to this, given that the mass flow controllers will give a reasonably good estimation of the inlet flow at the fuel cell, the carbon deposition (in terms of mass per second) can be calculated.

Another alternative way to calculating the carbon deposition is using the proportion of atoms of carbon to atoms of hydrogen, which should also remain constant. In this case we would have an additional unknown, which is the concentration of water at the outlet. However, as the current that the fuel cell is producing is constantly measured throughout the experiments, and the extent of electrochemical reaction (oxidation - reduction) is controlled completely by the current, by solving the system with this additional variable, and this additional equation, not only the carbon deposition will be possible, but it will also make it possible to determine the proportion of water at the outlet of the fuel cell.

Table 5.5: Results obtained for each sample.

Flow (sccm)	Sample 1		Sample 2		Sample 3	
	C/Ar mth.	C/H mth.	C/Ar mth.	C/H mth.	C/Ar mth.	C/H mth.
H ₂	10.9	10.9	5.8	5.8	48.7	-
H ₂ O	-	1.8	-	0.1	-	-
C _{deposition}	1.1	0.9	1.7	0.8	-0.5	-
CH ₄	11.4	11.4	14.1	14.1	0.1	-
CO	5.1	5.1	2.1	2.1	0.3	-
CO ₂	0.4	0.4	0.0	0.0	0.0	-
Ar	157.1	157.1	157.2	157.2	491.0	-
C _{deposition} (g/h)	0.033		0.049		- 0.015	

The second method offers the advantage that it is able to determine the amount of water and also it does not need that the flow is diluted with an inert gas (it is based on the proportion C/H, not C/Ar). However since it makes use of more variables (current and inlet flow) it will definitely be less accurate to determine the carbon deposition, and therefore, the first method (C/Ar) will be preferred to use, especially in those cases where

either the current or the inlet flow cannot be determined accurately enough. However, in the non-diluted case it will be necessary to use the approach of the second method (C/H) for no argon will be present in the stream.

The results obtained for the second fuel cell (10% dilution with argon) at the conditions shown in Table 5.4, after the treatment previously described (for both methods) are reflected in Table 5.5.

From Table 5.5, it is remarkable how similar results obtained for the carbon deposition value are for the first sample with both methods, considering the different approach that they use. Therefore, both methods seem to be valid to determine the carbon deposition for the first sample conditions. Since the first method uses less variables, and will therefore be more precise, the value given by the first method is taken as the real one, and it is shown in the last row of Table 5.5.

However, it is not so for the second sample. The reason for this seems to be that, for the second sample, the measurement of the current was not so accurate. This sample was collected during the measurement of a polarization curve, and the data is collected at a much lower frequency in that case (0.1Hz compared to 1Hz in the first sample). In addition to that, the voltage (and therefore the current) changed during the experiment, and none of those transients were recorded, so the precision of the averaged current must be much smaller in this case. From calculations performed with the second method, it was discovered that the predicted carbon deposition is largely influenced by the value of the averaged current used. In fact a 5% difference in the current will produce more than a 20% change in the predicted value of the carbon deposition.

For those reasons, the second method does not seem to be valid in the case where the averaged current cannot be determined accurately, like the case of the second sample, and therefore the value obtained with the first method is probably closer to reality. In general, the first method is always preferred, for it has less sources of error and will always be more accurate than the second one. However, in the cases where the second method must be used (the fuel is not diluted with an inert gas, like the

third cell), stable conditions for the voltage and current are required in order to obtain an accurate value for the averaged current, and so, for the carbon deposition.

Finally, for the latest sample, the one collected with hydrogen at 0.6V, the C/H ratio at the inlet is zero. The C-based molecules which are present at the outlet (CH_4 , CO and CO_2) come from the carbon that was deposited inside the fuel cell while methane was being flown, and that reacts with the hydrogen for the conditions given to form those C-based molecules. Therefore, the second method (the one based on the C/H ratio) cannot be applied in order to determine the carbon deposition, for it would also need an accurate value for the total flow at the outlet of the fuel cell. Therefore, the column for that method in Table 5.5 is left blank and the value taken for the carbon deposition in this case is first one (the one based on the C/Ar ratio), and shown on the last row of the table. Since no carbon is being deposited in this case, but the opposite is happening (carbon is being released from the inner surface of the fuel cell), the value obtained for the carbon deposition is negative, which indicates carbon release.

According to these results obtained with the first method, carbon deposition seems to happen even at the lower voltages, even though it does not produce a reduction in the performance of the fuel cell, so this value of the carbon deposition is probably reduced over time. When the potential increases (and therefore the current decreases), the value of the carbon deposition increases, as it was expected. However, this carbon deposition at potentials lower than open circuit voltage, is small and reversible (proved by the negative value of the carbon deposition obtained for the third sample), and does not affect the overall performance of the fuel cell.

On the other hand, cell failure occurred when the cell was left at open circuit voltage while methane was flown, which seems to indicate that the carbon deposition produced under these conditions (no current applied), is not only larger than when current is applied, but it is also irreversible, but those issues will be discussed more deeply in the following section.

5.6. Electrochemical Reactions

Table 5.6 summarizes all the possible reactions that may take place inside the SOFC when methane is used as the fuel. Similarly to the previous chapter, the potential at which each reaction occurs was calculated following the approach described in Appendix A2,.

Table 5.6: Reactions when CH₄ is used as fuel.

#	Reaction	Direction	E° _{900°C} (V) *	E _{900°C} (V) **
Anode				
6	CO + 2H ₂ + 2e ⁻ → CH ₄ + O ²⁻	Anodic	-0.949	-1.269
7	C + H ₂ + H ₂ O + 2e ⁻ → CH ₄ + O ²⁻	-	-0.780	-1.245
9	CO + H ₂ + H ₂ O + 4e ⁻ → CH ₄ + 2O ²⁻	-	-0.765	-1.086
8	CO ₂ + 2H ₂ + 4e ⁻ → CH ₄ + 2O ²⁻	-	-0.759	-0.987
3	CO + 2e ⁻ → C + O ²⁻	Cathodic	-0.750	-0.927
12	CO + 2H ₂ O + 6e ⁻ → CH ₄ + 3O ²⁻	-	-0.703	-1.026
11	CO ₂ + H ₂ + H ₂ O + 6e ⁻ → CH ₄ + 3O ²⁻	-	-0.699	-0.959
10	C + 2H ₂ O + 4e ⁻ → CH ₄ + 2O ²⁻	-	-0.680	-1.075
13	CO ₂ + 2H ₂ O + 8e ⁻ → CH ₄ + 4O ²⁻	-	-0.670	-0.945
4	CO ₂ + 4e ⁻ → C + 2O ²⁻	-	-0.659	-0.816
2	H ₂ O + 2e ⁻ → H ₂ + O ²⁻	Anodic	-0.581	-0.904
5	CO ₂ + 2e ⁻ → CO + O ²⁻	Anodic	-0.569	-0.705
	NiO + 2e ⁻ → Ni + O ²⁻	Anodic	+1.050	+1.050
Cathode				
	0.5O ₂ + 2e ⁻ → O ²⁻	Cathodic	+0.367	+0.328

* Assuming all the activities are equal to one.

** Assuming the following activities:

$$a_{H_2} = 0.1, a_{NiO} = 1, a_Ni = 1, a_{H_2O} = 10^{-4}, a_{O_{ion}} = 1, a_{O_2} = 0.21$$

Like in the previous chapter, the values for the activities of each species cannot be determined accurately. For that reason, two different values are reported here: one without activity correction (named E°_{900°C} in Table 5.6) and another one considering the concentration of each species that is

measured at the outlet of the fuel cell at 0.6V, from the mass spectroscopy results (named $E_{900^\circ\text{C}}$ in Table 5.6). Obviously, the concentration of those species will vary along the tube and also if the conditions of the cell change (potential applied, dilution...), so these values are shown here just for illustration.

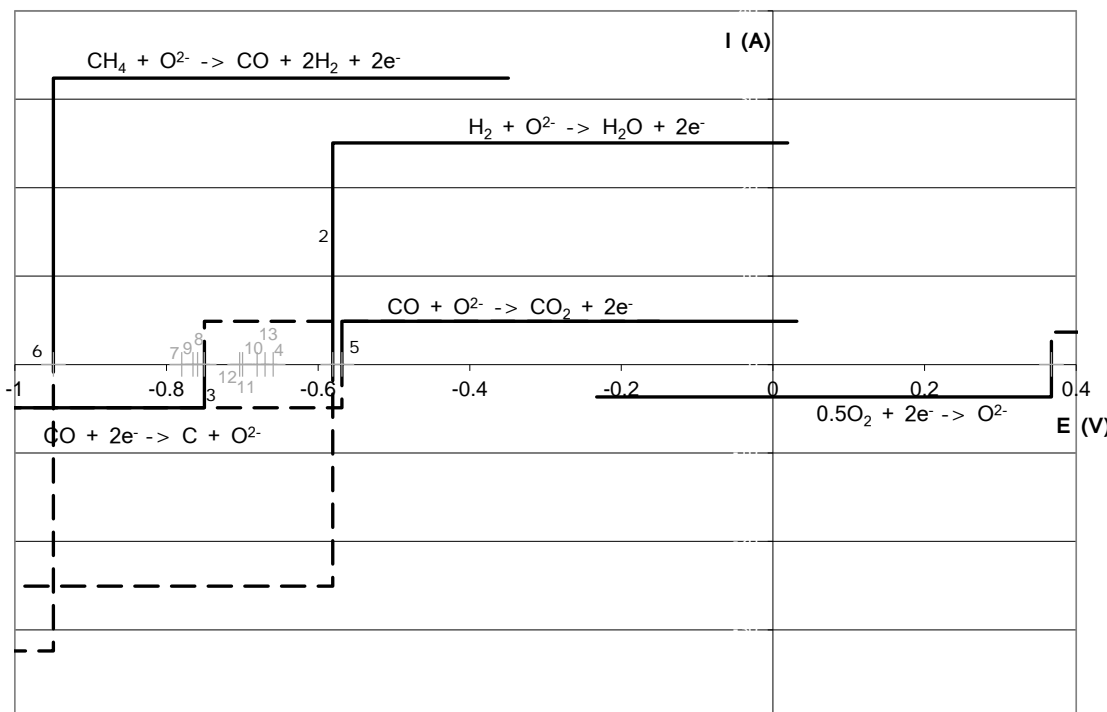


Figure 5.17: Expected reactions ($E_{900^\circ\text{C}}$, not corrected w/ activities), CH_4 fuel, [14].

The values of the potential of each reaction are plotted in a current/potential plot. Like before, all reactions are supposed to have extremely quick kinetics due to the high operating temperature, and therefore the current can increase up to its limiting value without any loss, creating the square-shaped diagram that can be seen (Figures 5.17 and 5.18). In reality, these lines will present a certain slope (losses), but since the objective of these graphs is to illustrate the possible reaction mechanisms that take place inside the fuel cell, they are represented by a vertical line.

Also, as the flow pattern is really complex, the limiting current is very hard to determine. In Appendix A1, the two limiting cases that have been explained in previous chapters are calculated for the methane case too, but due to the graph purpose (illustration), no values for that limiting current is reported. The proportion of the limiting current for all reactions is kept according to the values reported in Appendix A1.

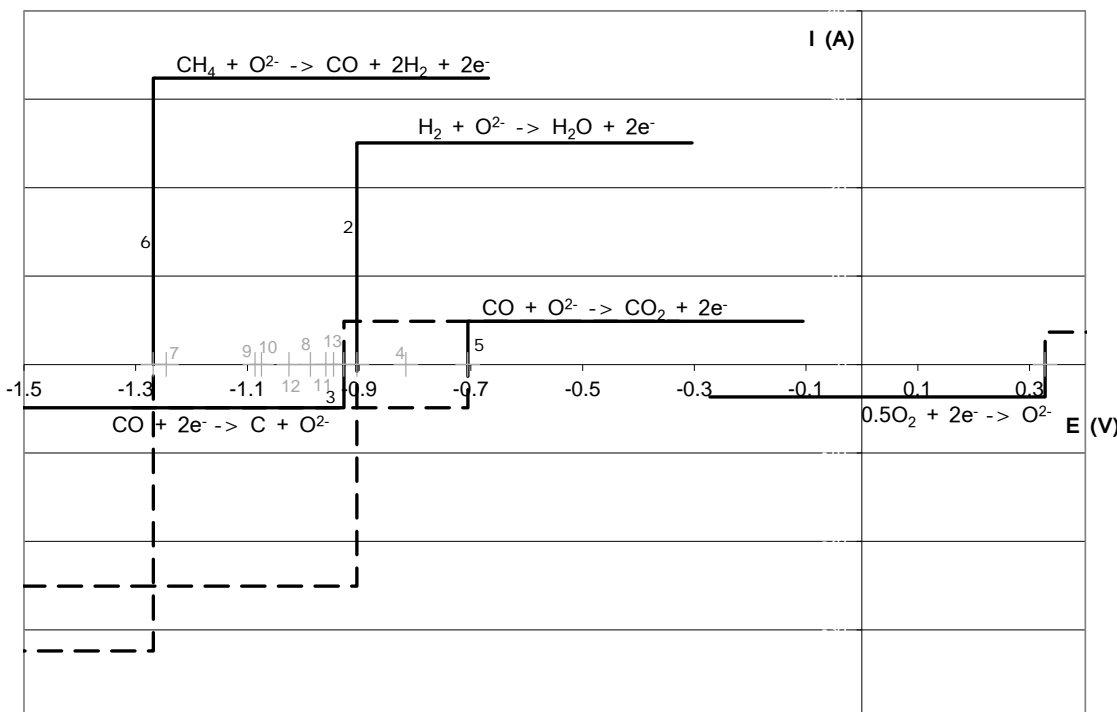


Figure 5.18: Expected reactions ($E_{900^\circ\text{C}}$, corrected with activities), CH_4 fuel, from [14].

Once methane substitutes hydrogen as the fuel, the system becomes much more complex, as can be seen by the large number of possible reactions. From experience, it is believed that only a few of those reactions will actually take place in the anode of the fuel cell. Those are the only reactions shown in Figures 5.17 and 5.18, and also they are highlighted (in black color) in Table 5.6. The rest of the reactions in Table 5.6 are included for reference, in gray color. Also, those reactions that are not expected to take place are shown as gray number next to a small gray cross in the x-axis in Figures 5.17 and 5.18.

The criterion used to decide if a reaction would take place or not is explained here. First, the reaction with the lowest potential will always occur, reaction number 6 in this case. Also, from equilibrium conditions, it is assumed that methane is only consumed inside the fuel cell, that is, it cannot be generated inside the fuel cell, and thus it cannot be the product of any reaction. Finally, the only way that a reaction can take place is that all of its reactants are present in the system. If one is missing it will not occur.

With this approach, reaction 6 will take place at first to a certain extent. This way some CH₄ will be consumed, producing the correspondent quantity of H₂ and CO. Next reactions that appear in the non-corrected case ($E^{\circ}_{900^{\circ}C}$) by going to less negative potentials are number 7, 9 and 8. However, they involve H₂O, C or CO₂ and neither of them has been generated by reaction 6. This means that they are still not present in the system, so those reactions will not take place.

The next reaction, in the non-corrected case, that has a less negative potential than number 8 is reaction 3. As CO was already generated by reaction 6, it will be present in the system and therefore reaction 3 can take place in the opposite direction - cathodic rather than anodic, where C will be produced from CO. Reactions 12, 11, 10 and 13 follow reaction 3 with increasing potentials in the non-corrected case. However, since they all involve H₂O - which has not been produced yet by any reaction - they will not take place.

The reaction that follow in the less negative potentials for the non-corrected case, number 4, could take place in the anodic direction, where CO₂ would be produced from C. However, according to the results obtained from the correspondent mass balance, the amount of carbon generated is extremely small, and it is believed that the amount of CO₂ that can be found at the outlet (which is small, but larger than the amount of C) is produced directly from CO, through reaction 5 in the anodic reaction as well. Also, the fact that reaction 4 involves more electrons than the other reactions considered (four instead of two) makes it less likely to occur. Therefore, reaction 4 was not considered in the analysis.

Finally, both reaction 2 and reaction 5 can occur in the anodic direction, as all of their reactants are present in the flow. Using reaction 2, H₂O will be produced from H₂, and from reaction 5, CO₂ will be produced from CO, as was explained before. Again, the nickel oxidation reaction (Table 5.6) has a higher potential than the main reactions considered for the anode and cathode of the system, which means that it will not take place. To make these graphs easier to understand, this reaction was plotted neither in Figure 5.17 nor in Figure 5.18.

From the information reflected on Table 5.6 and its representation in Figures 5.17 and 5.18, it can be seen how all the anodic reactions interact with one another. The fact that oxidizing and reducing reactions take place simultaneously leads to the mixed potential seen when these cells are tested experimentally. Similarly to what happened in the hydrogen case, when the potentials are corrected with the activity of each species, the values obtained are much close to those observed during the real experiments of the fuel cells, especially the open circuit voltage.

From Figure 5.18 it can be observed that the operating cell voltage should be below 0.35V (potential of reaction 3 minus potential of reaction 6, that is, -0.927V - (-1.269) = 0.342) in order to completely prevent carbon deposition from happening, as carbon deposition occurs due to reaction 3 happening in the reduction direction, and this reaction takes place at that voltage. This agrees with the results produced by the mass spectrometer, as small carbon deposition could be seen both at 0.6V and 0.9V. Also, from Figures 5.17 and 5.18, a larger carbon deposition should be seen with a larger polarization. The results obtained from the mass spectrometer certainly show this trend.

The different behavior of the cell observed when the experiments take place at open circuit voltage (complete cell failure) compared to the one observed when it is not left at open circuit voltage while methane is fed (complete recovery) seems to be related to the reversibility of the carbon deposition to a greater extent than the value of the actual carbon deposition. This can explain why the reaction graphs of open-circuit

voltage and 0.6V look so similar while the cell presents a completely different behavior in each case.

A possible explanation to the different behavior shown by the cell at different potentials when methane is used as the fuel could be a critical potential - around 1.1V according to the experiments. A reaction that deposits carbon over the catalyst in a non-reversible way might take place above that critical potential. Below it, the reactions shown by Figures 5.17 and 5.18 would take place causing smaller carbon deposition in a reversible way.

An alternative hypothesis that would explain this phenomenon is related to the water formation inside the fuel cell. Oxygen is not fed in the anode of the fuel cell. Therefore all oxygen atoms that arrive to the anode of the fuel cell come from the cathode side, as ions, and so they are only involved in electrochemical reactions. No electrochemical reaction can take place while current is not applied, thus no oxygen ion will react while no current is applied to the cell. Since water can only be formed when oxygen ions react, no water will be formed as long as the cell is kept at open circuit voltage. However, as current increases (when voltage decreases), so will water formation inside the anode of the fuel cell.

Similarly to the processes that take place inside a reformer (the water-gas-shift (WGS) reaction), when water is not formed inside the cell, the equilibrium of the local reactions that take place there is shifted causing larger carbon deposition, which seems to be irreversible. On the contrary, when current is applied, the electrochemical reaction that involves the oxygen ions takes place, forming water and shifting the rest of the reactions and reducing the amount of carbon deposition. This smaller carbon formation seems to be reversible unlike the open-circuit case.

Another result that can be derived from the composition of the gases at the outlet of the fuel cell obtained from the mass spectrometer is the reaction path as well as the percentage of reaction for each of them. Table 5.7 shows those results. For reference, it is included in Table 5.8 the concentrations - both absolute and relative to 100sccm inlet flow -

found using the mass spectrometer. The water concentration was calculated using the C/H method described before.

Since the sample that produced those results was collected when the cell was polarized to 0.6V, the results shown in Table 5.7 and 5.8 are only valid for a polarization of 0.6V.

Table 5.7: Percentage of reaction from outlet composition (for CH₄ fuel, 0.6V).

Reaction	% Reac.	Products (based on 100sccm inlet flow)					
		H ₂	H ₂ O	C	CH ₄	CO	CO ₂
6 CH ₄ + O ²⁻ → CO + 2H ₂ + 2e ⁻	36%	72	-	-	64	36	-
3 CO + 2e ⁻ → C + O ²⁻	3%	72	-	3	64	33	-
2 H ₂ + O ²⁻ → H ₂ O + 2e ⁻	10%	62	10	3	64	33	-
5 CO + O ²⁻ → CO ₂ + 2e ⁻	3%	62	10	3	64	30	3

Table 5.8: Concentration of each species found at the outlet of the SOFC at 0.6V.

	H ₂	H ₂ O	C	CH ₄	CO	CO ₂
Absolute Concentration	35.7%	5.9%	2.95%	37.4%	16.7%	1.31%
Con. based on 100sccm inlet flow	61.24	10.11	5.06	64.04	28.65	2.25

5.7. Summary in English

An electrochemical characterization of the SOFC was carried out using the electrochemical techniques described in previous chapters. Methane and hydrogen (to compare the results with the ones obtained in the previous chapter) were used to perform this characterization. The results obtained are in complete agreement with one another, and with the ones reported in the previous chapter as all the discrepancies observed seem to have a logical explanation.

Methane, in comparison with hydrogen, increased the performance of the cell and as long as current was applied no signs of degradation were seen while methane was being flown. A possible explanation is a higher local stoichiometry caused by the particular flow distribution of the cell

explained in the previous chapters. However, in case no current was applied a quick cell failure was observed. As it was pointed out before, a copper tube is used as the current collector for the anode side, and that might be the reason that the cells present an exceptionally good behavior towards coking - even better than it would be expected using the C-H-O equilibrium diagram.

When the mass balance was closed using mass spectroscopy an estimation of the value of the carbon deposition was obtained using two different methods. Both of them yield similar results as long as all variables are measured accurately. However, the second method (C/H ratio) is extremely sensitive to the value of the averaged current used, and therefore it is less precise. For that reason, it is recommended to use the first method (C/Ar ratio) as far as possible. In case the second method should be used (for the non-diluted case, for example), an accurate value for the averaged current should be used in order to get reliable results.

The values of carbon deposition obtained were smaller when the voltage was lower (higher currents), which is in accordance with the equilibrium diagram. For both cases this carbon deposition is reversible as long as some current is applied to cell while methane is flowing. This is proved by the negative value of the carbon deposition obtained when methane was removed, and also by the fact that no performance loss was appreciated while methane was flowing.

On the other hand, when no current was applied to cell while methane was flowing, it was observed larger carbon deposition and eventual cell failure when those conditions were kept for more than ten minutes. A strong performance decrease was observed even if those conditions were kept for just one minute. From the experiments carried out, this carbon deposition that occurs at open circuit voltage seems to be non-reversible as both mass balance and electrochemical techniques point to that direction.

5.8. Summary in Spanish

Siguiendo la metodología descrita en capítulos previos, se ha llevado a cabo una caracterización electroquímica de la pila de óxido sólido (SOFC). Como combustibles fueron usados tanto metano como hidrógeno (para comparar los resultados obtenidos en esta serie de experimentos con los del capítulo previo). Los resultados obtenidos están en concordancia entre ellos y con los que han sido descritos en el capítulo anterior, dado que las discrepancias encontradas parecen tener una explicación razonable.

Se encontró que el metano incrementaba el rendimiento de la pila en comparación con el hidrógeno, y no se encontraron signos de degradación en la pila siempre y cuando la corriente eléctrica aplicada fuera mayor de cero mientras el metano era utilizado. Una posible explicación para este fenómeno sería que el metano provoca una alta estequiometría local debido a particular distribución del flujo que tiene lugar en el ánodo de la pila de combustible como se describió en el capítulo anterior. Sin embargo, cuando la pila fue dejada a circuito abierto (sin corriente aplicada), una rápida degradación ocurría que provocaba el fallo de la pila. Como se ha señalado anteriormente, el hecho de que el colector de corriente del ánodo esté hecho de cobre es una posible razón para explicar el buen comportamiento que este tipo de pilas presenta frente a la deposición de carbono - incluso mejor del que sería esperado del diagrama de equilibrio CHO (carbono - hidrógeno - oxígeno).

A través de un espectrómetro de masas y usando dos métodos distintos, se obtuvo una estimación de la deposición de carbono en el ánodo de la pila de combustible. Ambos métodos producen resultados similares siempre que todas las variables de las que hacen uso sean medidas con precisión. Se encontró que el segundo método (basado en la proporción carbono/hidrógeno) es extremadamente sensible al valor de la corriente eléctrica promedio que se utilice y por tanto es menos preciso que el primero - basado en la proporción carbono/argón. Por esta razón se recomienda el empleo del primer método siempre que sea posible. En los

casos en los que el segundo método deba ser utilizado (por ejemplo, para el caso de combustibles no diluidos), un valor muy preciso de la corriente eléctrica promedio deberá ser utilizado para que los resultados sean fiables.

Los valores de deposición de carbono que se obtuvieron para voltajes más bajos (más altas corrientes eléctricas) fueron menores que los obtenidos para mayores voltajes, lo que está en concordancia con el diagrama de equilibrio. En ambos casos, la deposición de carbono es reversible siempre que algo de corriente circule por la pila mientras se utiliza metano. Esta afirmación viene soportada por el valor negativo de la deposición de carbono obtenido cuando el metano era reemplazado por hidrógeno y también por el hecho de que no se pudo apreciar ninguna caída en el rendimiento de la pila mientras el metano fluía por ella.

Por otro lado, cuando ninguna corriente circula por la pila mientras se usaba metano, se pudo observar una mayor deposición de carbono y un eventual fallo en la pila de combustible cuando dichas condiciones eran mantenidas por más de diez minutos. Un gran decremento en el rendimiento de la pila de combustible se podía observar incluso cuando dichas condiciones se mantenían por tan solo un minuto. Por posteriores experimentos llevados a cabo posteriormente, la deposición de carbono que ocurre a circuito abierto cuando metano se usa como combustible parece ser irreversible, dado que tanto el balance de masa como las técnicas electroquímicas apuntan en esa dirección.

5.9. References

- [1] Koh, J. H., Yoo, Y. S., Park J. W., Lim, H. C., "Carbon deposition and cell performance of Ni-YSZ anode support SOFC with methane fuel", Solid State Ionics, Vol. 149, pages 157-166, 2002.
- [2] Alzate-Restrepo, V., Hill, J. M., "Effect of anodic polarization on carbon deposition on Ni/YSZ anodes exposed to methane", Applied Catalysis A: General, Vol. 342, pages 49-55, 2008.

- [3] He, H., Hill, J. M., "Carbon deposition on Ni/YSZ composites exposed to humidified methane", *Applied Catalysis A: General*, Vol. 317, pages 284-292, 2007.
- [4] Kim, T., Liu, G., Boaro, M., Lee, S. I., Vohs, J. M., Gorte, R. J., Al-Madhi, O. H., Dabbousi, B. O., "A study of carbon formation and prevention in hydrocarbon-fueled SOFC", *J. Power Sources*, Vol. 155, pages 231-238, 2006.
- [5] Kendall, K., Finnerty, C. M., Saunders, G., Chung, J. T., "Effects of dilution on methane entering an SOFC anode", *Journal of Power Sources*, Vol. 106, pages 323-327, 2002.
- [6] Laosiripojana, N., Assabumrungrat, S., "Catalytic steam reforming of methane, methanol, and ethanol over Ni/YSZ: The possible use of these fuels in internal reforming SOFC", *Journal of Power Sources*, Vol. 163, pages 943-951, 2007.
- [7] Vakouftsi, E., Marnellos, G., Athanasiou, C., Coutelieris, F. A., "A detailed model for transport processes in a methane fed planar SOFC", *Chemical Engineering Research and Design*, Vol. 89, pages 224-229, 2011.
- [8] Klein, J.-M., Bultel, Y., Georges, S., Pons, M., "Modeling of a SOFC fuelled by methane: From direct internal reforming to gradual internal reforming", *Chemical Engineering Science*, Vol. 62, pages 1636-1649, 2007.
- [9] Hornés, A., Gamarra, D., Munuera, G., Conesa, J. C., Martínez-Arias, A., "Catalytic properties of monometallic copper and bimetallic copper-nickel systems combined with ceria and Ce-X (X = Gd, Tb) mixed oxides applicable as SOFC anodes for direct oxidation of methane", *Journal of Power Sources*, Vol. 169, pages 9-16, 2007.

- [10] Huang, T.-J., Jhao, S.-Y., "Ni-Cu/samaria-doped ceria catalysts for steam reforming of methane in the presence of carbon dioxide", Applied Catalysis A: General, Vol. 302, pages 325-332, 2006.
- [11] Maček, J., Novosel, B., Marinšek, M., "Ni-YSZ SOFC anodes—Minimization of carbon deposition", Journal of the European Ceramic Society, Vol. 27, pages 487-491, 2007.
- [12] Boder, M., Dittmeyer, R., "Catalytic modification of conventional SOFC anodes with a view to reducing their activity for direct internal reforming of natural gas", Journal of Power Sources, Vol. 155, pages 13-22, 2006.
- [13] Andres Lozano, C., Ohashi, M., Shimpalee, S., Van Zee, J. W., Aungkavattana, P., "Electrochemical Analysis of Microtubular SOFC under Fuel Contaminants". ECS Transactions, Vol. 33, pages 149-160, 2010.
- [14] Andres Lozano, C., Ohashi, M., Shimpalee, S., Van Zee, J. W., Aungkavattana, P., "Comparison of Hydrogen and Methane as fuel in Micro-Tubular SOFC using Electrochemical Analysis". J. Electrochem. Soc., Vol. 158, pages B1235-B1245, 2011.

CHAPTER 6

Preliminary Characterization of the SOFC Contamination with Hydrogen Sulfide

Contents

6.1. Introduction	167
6.2. Effect of Hydrogen Sulfide on the Current.....	169
6.3. Polarization Curves	177
6.4. Electrochemical Impedance Spectroscopy	179
6.5. Summary in English	181
6.6. Summary in Spanish	183
6.7. References.....	185

6. Preliminary Characterization of the SOFC Contamination with Hydrogen Sulfide

6.1. Introduction

Although SOFCs seem to be more tolerant to contaminants compared to PEMFCs, they are sensible to several contaminants that may be present in the renewable/alternative fuels. According to literature phosphorous and sulfurous components seem to have a strong impact on the SOFC performance as well as those molecules containing chlorine atoms and some metals like chromium [1], [7], [8], [9].

Hydrogen sulfide is one of those kinds of contaminants, and it seems to affect the fuel cell performance even at low concentrations. Since hydrogen sulfide can appear in the coal gas when the coal used to produce it contains a certain percentage of sulfur, and it is also a common contaminant that can be present in other renewable fuels, its study is considered really important in order to evaluate the impact that it has on the fuel cell performance (depending on its concentration), and also to evaluate the feasibility of the use of those kinds of fuels with the SOFC.

In this chapter, the preliminary results obtained with hydrogen sulfide, diluted with hydrogen, are presented. The procedure followed changes slightly from the one followed in the previous cases (pure hydrogen and methane). The transient was performed at 0.9V (rather than 0.6V) to try to minimize the polarization kinetics effect. The baseline was performed with pure hydrogen, the same way it was performed previously. Then, the contaminant (H_2S) was applied diluted to 25ppm in hydrogen and the results were recorded. Unlike the previous cases, no polarization curves and no impedance tests were performed during contamination. Therefore, the polarization and impedance curves presented in this chapter were all performed with hydrogen, and they show the different behavior that the

cell has before and after the contamination with hydrogen sulfide was induced.

The transient from pure hydrogen to hydrogen sulfide diluted with hydrogen was performed three times - with their subsequent recovery periods - in order to see the effect of cyclic contamination. Only one cell was used to perform the tests described in this chapter and it is called “fourth cell” in order to distinguish it from the cell used in the methane case.

Ideal expected transients with H₂S (0.9V)

Current

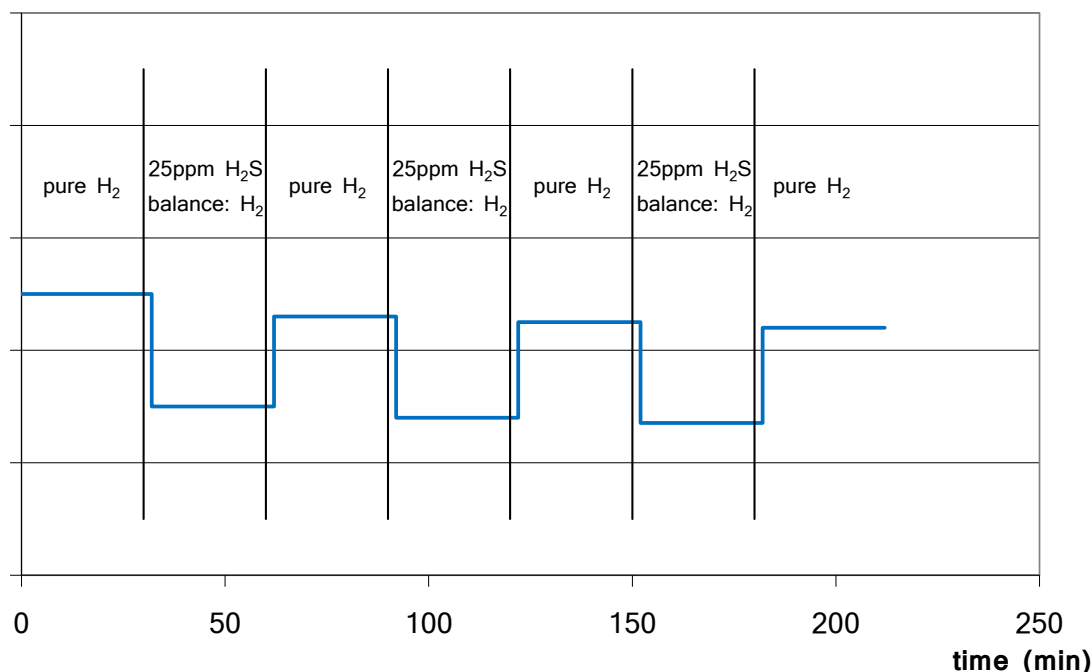


Figure 6.1: Ideal transient expected for H₂S contamination at 0.9V.

The schematic of the expected result in the transient at constant voltage is shown in Figure 6.1. As it is shown in that figure, an initial decrease in the current is expected to be seen as H₂S starts flowing. A recovery (not complete) is expected to be seen as the H₂S is removed, and it was expected to see a similar behavior for the rest of the cycles, from what was found in the literature [1]. The actual values of irreversible current loss and transitory current loss will depend on the working conditions and the fuel cell itself, according to literature [2], [6], [3].

All the preliminary results obtained with hydrogen sulfide as a contaminant for the hydrogen flowing in the anode side of the fuel cell are presented and analyzed in this chapter. The flow conditions for the cell used in this case are shown in Table 6.1.

Table 6.1: Flow conditions of the tests carried out.

Fuel Cell #	4 th
Anode flow H ₂ (set point, sccm)	50
Anode stoich. (0.9V)*	12.33
Anode stoich. (0.6V)*	3.46
Anode stoich. (0.35V)*	2.01
H ₂ S dilution (ppm)	25
Cathode flow Air (set point, sccm)	300
Cathode stoich. (0.9V)**	~ 30.1
Cathode stoich. (0.6V)**	~ 8.5
Cathode stoich. (0.35V)**	~ 4.9

*min. stoich. for the anode side (max. current for this conditions used for the calculation).

** cathode theoretical stoich. calculated for same conditions. Actual stoich impossible to calculate.

Unlike previous experiments with methane and hydrogen, where several cells were used, only one fuel cell was used here (labeled as the fourth fuel cell). The reason for this is that these are only the preliminary results obtained with this contaminant.

6.2. Effect of Hydrogen Sulfide on the Current

As it was described in the introduction, the transitory analysis was carried out slightly differently for the hydrogen sulfide contamination than it was for the previous cases. The voltage was held at 0.9V (instead of the 0.6V that was used previously) in order to minimize the effect that such a big polarization could have on the kinetics of the fuel cell, especially those in

the anode side since that is where the contaminant was introduced. Also no other test (neither polarization curves nor impedance tests) were performed during the transient, and so no blank gaps can be appreciated in the graph. Like before, the value of the current was constantly recorded and it represents the main result of this transitory.

The reason why no other tests were performed during the transient was to make sure that neither other factors nor other conditions that generally take place during those tests (such as open circuit voltage) affected the results obtained in any way. Polarization and impedance tests during the contamination with H_2S are part of the future work in relation to this project.

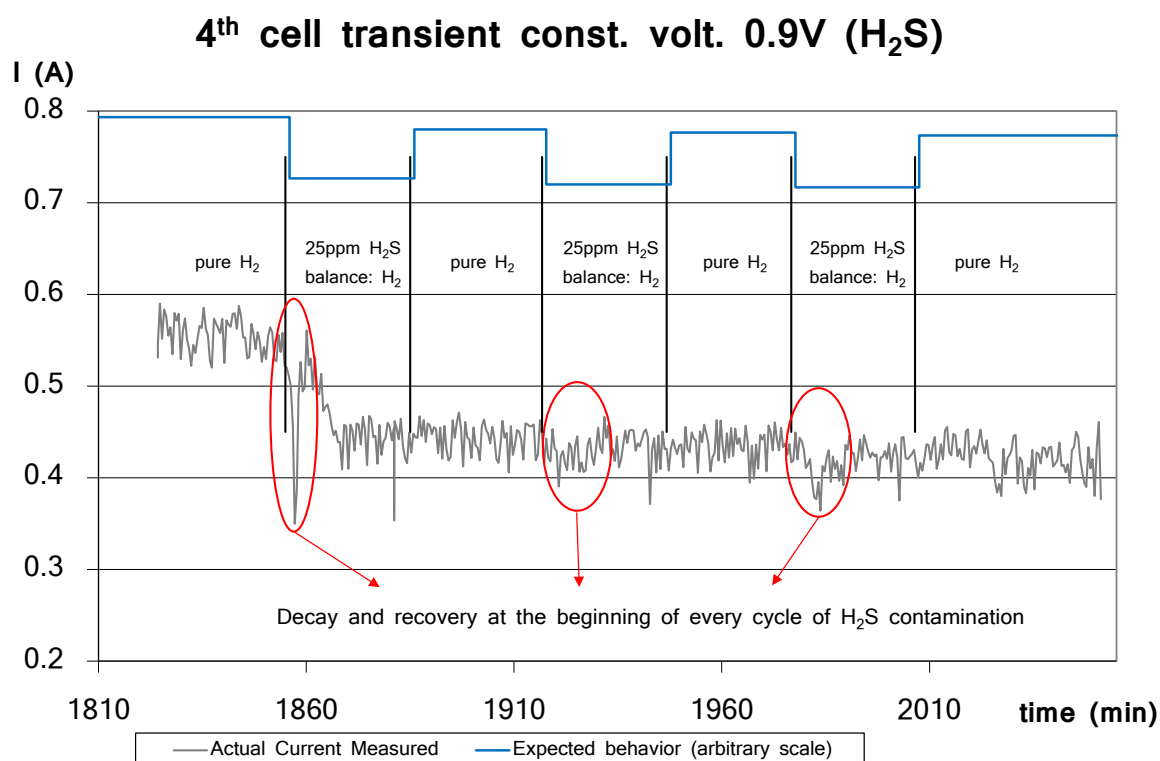


Figure 6.2: Transient during 25ppm H_2S cyclic contamination.

Also, it is interesting to point out that most of the studies found in the literature [1, 3, 5, 6, 10] used the opposite approach to the one used here, that is, keeping a constant value for the current and recording the voltage. Although both methods should in principle lead to the same result,

it was preferred to keep the voltage constant rather than the current because, as it was explained in previous chapters, current is linked to the electrons transferred and thus a rate of reaction. Therefore controlling the current means controlling the rate of reaction, and this is something that should be prevented, especially when transients are measured, since one of the results that they produce is the time constant of a process - how fast that process happens.

The flow conditions that were maintained during the transient analysis - all of them constant except for the 25ppm that were added and removed from the inlet flow in intervals of 30 minutes and that generated the transitory response - are part of the conditions included in Table 6.1. The actual results obtained from this transient analysis are shown in Figure 6.2. The expected result from this analysis described previously is also shown in the figure for reference.

In order to characterize these processes, these transitory responses were adjusted using an exponential expression (equation 6.1) like it has been done in previous chapters. The results of the adjustment are shown in Figure 6.3. Like in Figure 6.2, the expected result of the experiment is shown in blue inside the figure for reference.

$$I(t) = I_0 - (I_0 - I_{ss}) \cdot \exp\left(-\frac{\Gamma}{(t - t_0)}\right) \quad (6.1)$$

From the transient observed during the cyclic H₂S contamination (Figure 6.2), several conclusions can be remarked. Firstly, the contamination with 25ppm of H₂S causes a performance drop of about 18.2% in the current during the first 15 minutes of contamination. After that initial drop, the performance remains stable and constant, both with and without contamination. Thus, it can be concluded that it is during those initial stages of contamination with H₂S when the anode of the fuel cell is affected - through a mechanism which will be discussed further in this chapter - in an irreversible way, as no recovery can be seen after H₂S is removed and the deterioration is permanent.

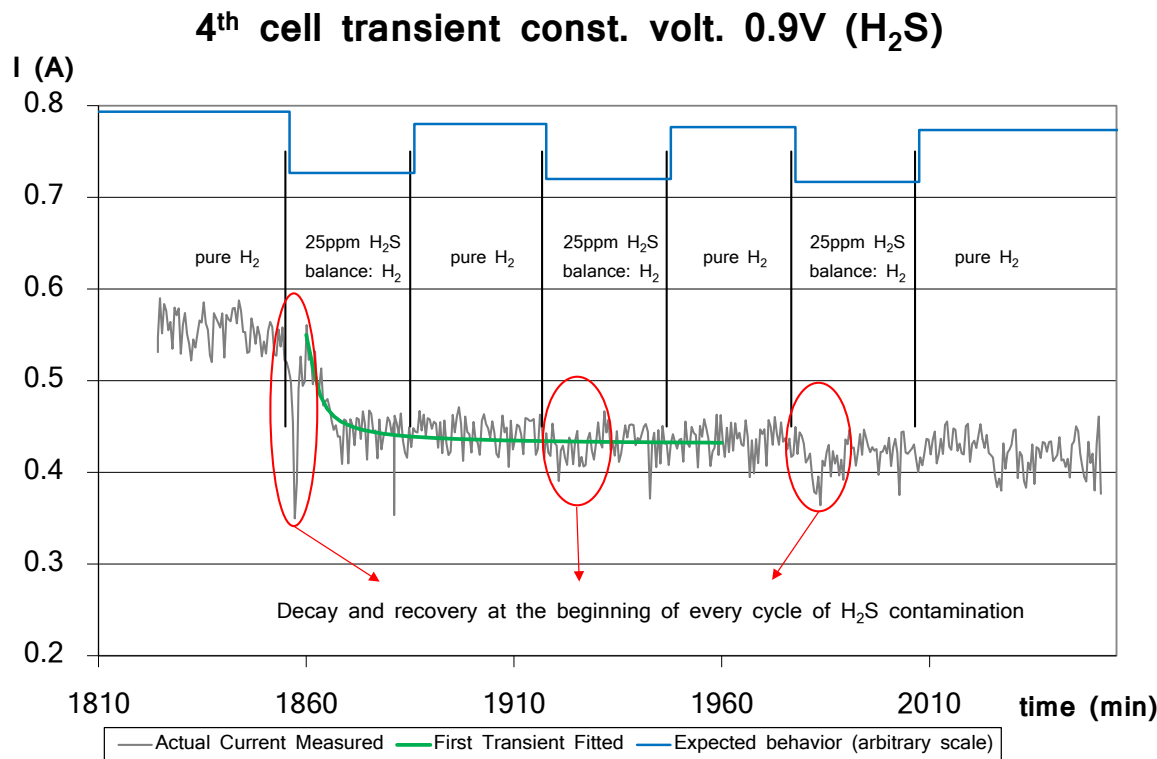


Figure 6.3: Transient during 25ppm H₂S cyclic contamination (adjusted).

Another interesting fact that has to be pointed out is that a sharp performance drop followed by a quick recovery could be observed during the first minutes for each cycle of contamination (circled in red in Figure 6.2). This drop was extremely acute on the first cycle (quick and with a big change in the current) whereas it was less noticeable during the other two cycles (slightly slower and with a smaller value).

Therefore, it looks like there are in fact two different contamination mechanism taking place simultaneously when this kind of cell is contaminated with H₂S, one of them being reversible (the one that can be seen at the beginning of every cycle of contamination) and another one which is irreversible (the one that happens only at the beginning of the first cycle of contamination), as no recovery can be seen after the first cycle even when H₂S is removed.

Although plenty of studies related to H₂S contamination of SOFC can be found in the literature [2, 3, 6, 12], it is difficult to get a clear idea of the

real contamination mechanisms of H₂S for this type of fuel cells since all of them point to different mechanisms even for cells that have the same composition. Those mechanisms try to explain both reversible and irreversible performance drops and different. Some authors suggest a mechanism to be causing one kind of performance drop (reversible - irreversible), while other use the same mechanism to justify a different kind of performance drop (irreversible - reversible).

The reasons behind those apparent contradictions seem to be the different conditions at which the tests are carried out (different value of the current density which is kept constant, different H₂S concentration, different time of exposition, different operating temperature) that according to some authors may greatly influence the extent of the damage caused by a certain mechanism, and even if those effects are reversible or not [1], [3].

Also differences in the internal structure (caused by different assembly mechanisms) of the cells may have a great impact on those result even if the cells are supposed to have the same theoretical composition. Since SOFC is a new technology and they are still in a developmental stage, they are manufactured individually and this manufacture process will induce certain variability from one laboratory to another, and even inside the same laboratory from one cell to the next. Thus, the internal structure may change significantly from the cell used in one paper to the one used in a different one.

Also, it was found in the literature a wide range of results that are difficult to justify as they seem to draw opposite conclusions. It is clear that different conditions, different cell materials and different cell fabrication and assembly processes hugely affect cell behavior and performance, leading to these apparently contradictory results.

Therefore, certain standards should be established in order to facilitate the comparison of different experiments and different cells. Some of them related to the fabrication process and intimate cell structure (which is not always reported in the articles found in the literature), and others related with cell performance. It could perfectly happen that two cells tested at the same current density (current divided by the surface area of the catalyst),

showed different results because they were not manufactured in the same way and therefore they do not have the same maximum current density. In this case, it would probably make more sense, to compare them if the constant density current at which the experiments are carried out was normalized with the maximum current density that the cell is able to produce, producing a dimensionless parameter. However, the maximum current density is usually a difficult value to calculate (the voltage needs to be reduced to a value as low as possible, and that produces new technical difficulties such as cell failure) and it is generally not reported which makes it impossible to relate some of the experiments reported in the literature.

Also, as this is a promising technology at a development stage and not many patents have been produced, it could be that researchers try to report the minimal information possible regarding their manufacturing and assembly processes, to protect their work with the hope this technology will become commercially viable in the near future. This fact complicates even more all the difficulties explained above.

An example of all this apparent inconsistencies is that, unlike what the transient presented here (Figure 6.2) shows, Hagen et al [6] conclude that H_2S had a reversible effect on the fuel cell for the conditions of the test they carried out (2-100 ppm of H_2S , exposure times of 24 hours and constant current of $1\text{A}/\text{cm}^2$, which would be equivalent to 9A in the cells used in this project). They report that the transitory decrease in the performance was caused by chemisorption of the sulfur particles that were dechemisorbed when the H_2S flow was removed. They do not report any significant change in the microstructure of the anode, neither any chemical reaction that was irreversible.

Several factors can justify the differences seen with the study presented here, including different operating conditions (longer exposition time in their case, constant current vs. constant voltage, and still their experiments presented a much a high current), different SOFC design (planar vs. microtubular) and even different materials used - as was pointed out in

previous chapters, the copper tube that functions as a current collector might be affecting the reaction paths and reaction reversibility.

On the other hand, Lussier et al. [2] used a planar SOFC with a constant voltage approach (like was done in this thesis). The duration of the transients was also closer to the one used in this study (1 hour vs. the 30 minutes used here). However, they use larger concentrations of H₂S (200-500ppm vs. 25ppm used in this study). Also, the polarization that they used in their study is much larger than the one used in this study (0.5V vs 0.9V used here), which is translated into a larger influence of the polarization in the kinetics of the reaction which is something that we tried to avoid in the present study.

Lussier et al. report permanent performance drop - as in our study - as well as an additional transitory performance drop that was maintained as long as H₂S was flowing through the anode (in our case that transitory was quickly recovered). They used several surface techniques, like XPS (X-ray photoelectron spectroscopy), to determine the composition of the anodes after H₂S had been flown. Since they were unable to detect any sign of sulfur compounds, and the nickel appeared in the conductive metallic phase.

However, as they did see changes in the structure of anode (nickel migration) they concluded that the nickel mobility mechanism (possibly caused by the alloying of the nickel particles with the sulfur while it was fed) should be responsible for the irreversible performance drop seen. The reversible performance drop was not discussed in detail, but some kind of reaction of the sulfur atoms with the active nickel sites should be the cause of that transitory performance drop that was observed. The other alternative, the absorption of sulfur in the anode matrix, should only show a transitory decrease while this process takes place (like the one seen in our case), rather than taking place while H₂S is fed - as seen in their case.

Finally Brightman et al. [3] also work with planar SOFC, at slightly lower temperatures and a wide range of current densities. They do not present the transients in terms of current, but impedance and cell resistance. Their

conclusion is that even if the cell performance is reduced while H₂S flows, this effect is not permanent as the cell recovers its initial performance once H₂S is removed - as long as the H₂S concentrations are below 1ppm.

With concentrations up to 3ppm some permanent performance drop starts to be seen. Like Lussier et al. [2] they hypothesize that this permanent performance drop might be caused by microstructural changes in the surface of the anode of the fuel cell.

Table 6.2: Summary of the results obtained with the transient analysis (0.9V).

Condition	4 th cell - 25ppm H ₂ S		
	I (A)	% change	Γ. (s)
Pure H ₂	0.54	-	-
25ppm H ₂ S diluted with H ₂	0.43	-20%	120
Pure H ₂	0.43	~0%	-
25ppm H ₂ S diluted with H ₂	0.43	~0%	-
Pure H ₂	0.43	~0%	-
25ppm H ₂ S diluted with H ₂	0.43	~0%	-
Pure H ₂	0.43	~0%	-

The numerical results obtained with this transitory analysis are reflected in Table 6.2. As was said before, an initial 20% decrease in the first transient was measured whereas no decrease or recovery could be measured in the following transients. This 20% is in the range of the results obtained by some of the authors [2], although the comparison is very complicated due to different testing conditions and different cell structure.

The time constant calculated for that first transient is of 120s. It looks really distant from some other studies [6], which are in the order of hours instead of seconds. The closest ones of those experiments found in literature where the ones carried out by Lussier et al. [2] which are in the same order as the ones reported here. The reason for this, might be the different hold time for the H₂S contamination, as Lussier et al. used

similar time lengths for their transients as the ones used for this study. Again, the diverse conditions of all the experiments found in the literature complicate this comparison to a great extent.

6.3. Polarization Curves

Unlike previous chapters, where polarization curves were performed during the transitory experiment for each set of conditions, in this case polarization curves were only performed before the experiment started and when the experiment finished once the H₂S had been removed, in both cases with pure hydrogen and the same conditions.

The results that were obtained this way are presented in this section. The information about the conditions of the flow, both anode and cathode, are reflected in Table 6.1 as they are the same ones which were used for the transitory analysis.

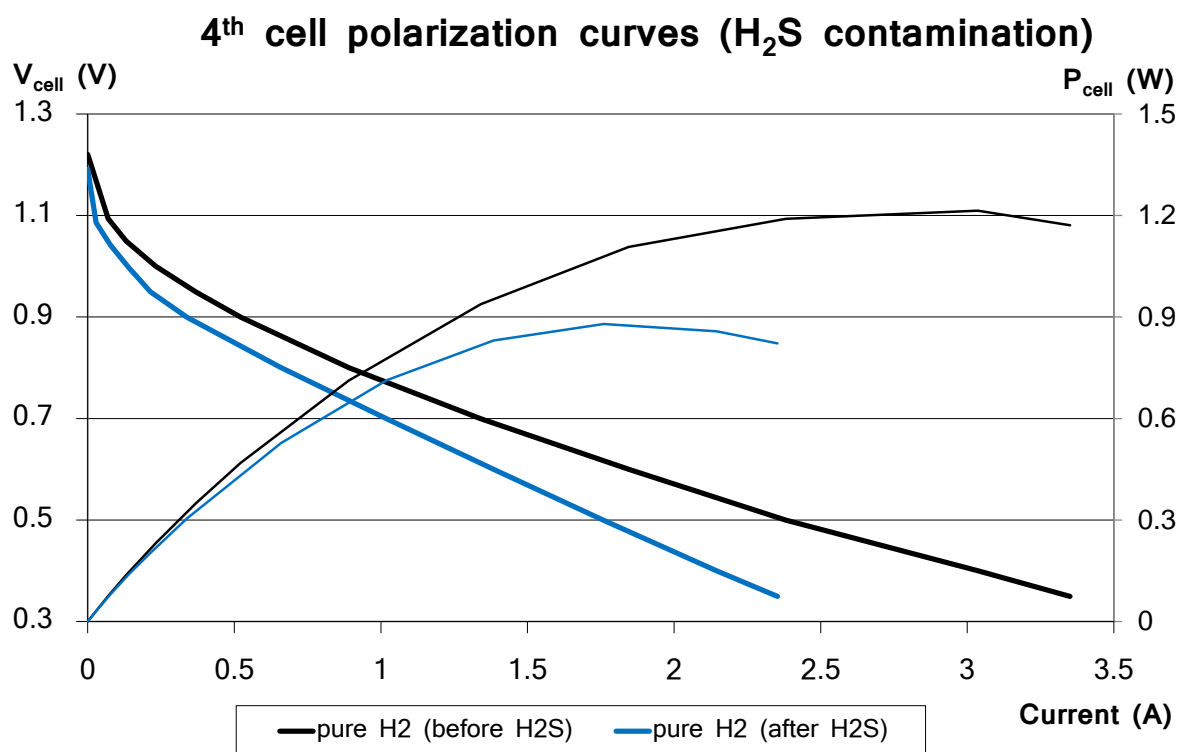


Figure 6.4: Polarization curves and power showing the irreversible effect of H₂S.

However, the minimum stoichiometry, both for the anode and cathode sides, is reduced as polarization curve involves higher levels of polarization (down to 0.35V), and thus higher currents with the correspondent stoichiometry decrease as the cell is run at constant flow both for the anode and cathode sides.

Table 6.1 also shows the minimum stoichiometry both for the anode and cathode sides. Like previous cases, the condition for minimum stoichiometry occurs when the current has its maximum value. In this case, that corresponds with the conditions that took place before the cell was contaminated with H₂S and at voltage of 0.35V (minimum cell voltage).

Figure 6.4 shows both the polarization curves before and after the fuel cell was contaminated with H₂S.

The information that can be obtained from this diagram is very similar to the one provided by the transient analysis for both of them rely on the same principles: polarization techniques. Therefore, Figure 6.4 shows a similar trend as the one obtained for the transitory analysis: a strong performance loss after the fuel cell was contaminated with H₂S.

The additional information that can be obtained from Figure 6.4 has to do with the variety of potentials at which the polarization curve is performed. It can be seen that all potentials follow approximately the same trend (about a 20% decrease in the current) and the open circuit potential is not altered. Therefore it looks like contamination with H₂S at a single potential (0.9V) affects all voltages in a similar way, once H₂S is removed.

However, it might not be correct to conclude that H₂S affects equally regardless the potential at which the cell is kept while it is being contaminated with this gas. According to literature, different levels of polarization may affect the local equilibrium [2], as shown clearly by Brightman et al. [3]. Therefore, it would be extremely interesting to perform the polarization curve while H₂S is flowing and compare it with the current case.

6.4. Electrochemical Impedance Spectroscopy

The electrochemical impedance spectroscopy tests were performed according to the procedure described in chapter 3, but not during H₂S contamination. They were performed before and after for the reasons explained in the introduction of this chapter.

Also, two different tests were carried out (two before and two after the cell was contaminated with H₂S). One at 0.9V for consistency with the transient (and the minimum stoichiometry is obviously the same one as the one calculated for the transitory analysis and thus it is reflected in Table 6.1) and another one at 0.6V so that the results could be compared with the ones obtained with pure hydrogen (Chapter 4) and with methane (Chapter 5).

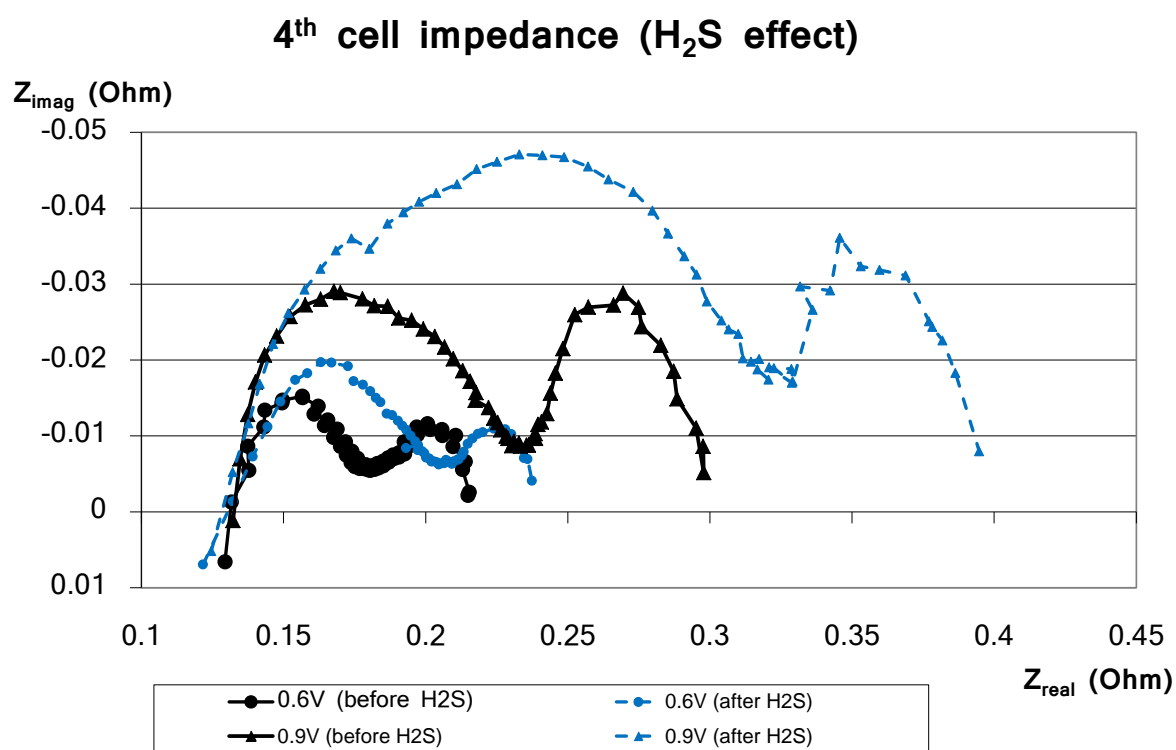


Figure 6.5: Impedance curves showing the irreversible effect of H₂S.

In this second case (0.6V), the stoichiometry will obviously be decreased, since the cell operates at higher currents. The flow conditions though are

reflected in Table 6.1, as it would be clearer to show all the conditions related with the flows in a single Table for all the tests carried out in this chapter.

The sinusoidal voltage that was applied in this case averaged 0.6V in two cases and 0.9V in the other two. However, the perturbations in the current were the same in both cases (20% in the current - which corresponds to perturbations of about 0.1V in the 0.6V case slightly smaller for the 0.9V case). The results obtained both for the 0.6V case and 0.9V case are reflected in Figure 6.5.

The results obtained are in accordance to what was expected. Both potentials show similar trends. Like before, it does not mean that H₂S affects the fuel cell in the same way, regardless its polarization (studies have shown the opposite [3]), it rather means that once H₂S is removed, those two potentials (0.6V and 0.9V) show the same trends.

In both cases, the impedance increases after the contamination with H₂S and in both cases the high frequency range values (the values located at the left hand side of the graph) do not change, which means that the internal resistance of the electrolyte is not altered in an irreversible way during the contamination with H₂S. It might be altered transitorily in a reversible way during contamination, but in order to determine if that happens, some impedance measurements should have been performed during contamination with hydrogen sulfide. However, since those tests were not performed, it is impossible to determine with the available information.

The low frequency values (the ones in the right hand side of the impedance graph) increase after the contamination with H₂S, and this justifies the performance decrease seen after the contamination. The reasons for this performance decrease are not clear from this diagram either. An impedance measurement performed during the contamination would certainly enlighten what is really happening, and so would some kind of surface analysis of the anode after the contamination process.

Brightman et al. [3] also performed impedance test under similar (not identical though) conditions with planar SOFC, which were explained in

section 6.2. They did not carry out any surface testing on the contaminated anodes. However, their explanation of the performance drop - similar to that presented by Lussier et al. [2], which is based on an structural reorganization of the nickel metal atoms - can also be applied in this case.

Also, both cases (0.6V and 0.9V) show increases in the capacitive area of the graph (the humps) after the contamination, which means that the response of the fuel cell will also be slower after the H₂S contamination.

Finally, it can be noted that the cell resistance increases when the polarization is reduced (higher voltages, i. e. 0.9V), which is in complete agreement with what should be expected from this procedure.

6.5. Summary in English

A preliminary analysis of the behavior of the cell when it is contaminated with H₂S was performed. The results were in general accordance with those found in the literature, considering all the apparent contradictions that seem to be among different authors.

Interestingly, and differently to all that was found in the literature, the SOFC used show an initial fast decrease in the performance as soon as H₂S was introduced, and neither a further decrease, nor a recovery could be seen afterwards, regardless the conditions (pure and contaminated hydrogen) used.

The main reason for this different behavior found can be attributed both to the different conditions used in our experiments, compared to those used in the experiments found in the literature (different hold time, different H₂S concentration, experiments carried out at constant voltage rather than constant current...) and also internal differences in the fuel cell structure caused by the assembly and manufacture processes (Cu present in the anode...).

In spite of these facts, some of the explanations found in the literature could also be applied in our case (a quick redistribution in the nickel

distribution in the surface area of the anode of the fuel cell, some chemical reaction of the sulfur that comes from the H₂S with catalytically active nickel sites...), but it is impossible to determine without any further testing.

Polarization curves and electrochemical impedance spectroscopy also showed that after the cell was contaminated, the behavior of the cell was maintained for all different potentials. However, it does not mean that the behavior of the contaminant will be the same as observed if the polarization conditions of the fuel cell changed. In fact, it is clear from the literature that polarization clearly affects the mechanism by which the performance of the cell changes.

Also, electrochemical impedance spectroscopy showed that the response of the fuel cell may become slower after the contamination with H₂S, for a larger capacitive region could be seen in the graph, both at large (0.6V) and small (0.9V) polarization.

In order to determine the nature of these contamination mechanisms and whether they are reversible or irreversible, further studies should be carried out. Those tests should include electrochemical impedance spectroscopy and polarization curves while the H₂S is being flown, and also some kind of surface analysis technique (Scanning Electron Microscope, X-ray Photoelectron Spectroscopy...) that could provide some information of the composition and distribution of the fuel cell's anode surface (if sulfur reacts and stays, if it is just absorbed or if it simply changes the structure of the nickel and/or nickel particles distribution).

Finally, it has to be pointed out that these preliminary results obtained with hydrogen sulfide are extremely interesting and set the base for further studies that should clarify the nature of the processes that take place inside the fuel cell during H₂S contamination, and will hopefully enable to find a way to remove, or at least minimize, the effect that this contaminant has on this type of fuel cell.

6.6. Summary in Spanish

Un análisis preliminar del comportamiento de la pila de combustible cuando ésta es contaminada con H₂S ha sido llevado a cabo en este capítulo. En general, los resultados obtenidos son consistentes con los encontrados en la literatura, considerando las aparentes contradicciones que fueron encontradas entre distintos artículos y autores disponibles para la contaminación con H₂S.

Sorprendentemente, y al contrario a todo lo encontrado en la literatura, la pila de óxido sólido usada en este caso mostró una aguda disminución (de alrededor de un 18%) al comienzo de cada ciclo de contaminación con ácido sulfídrico, pero ninguna disminución posterior ni en el primer periodo de contaminación, ni en los subsiguientes. Tampoco se observó ninguna recuperación posterior independientemente de si el ácido sulfídrico era aplicado o no.

La principal razón para este diferente comportamiento encontrado se puede atribuir tanto a las distintas condiciones experimentales usadas (diferentes tiempos de mantenimiento, diferente concentración del contaminante, experimentos a voltaje constante en lugar de corriente constante...) así como diferencias internas en la estructura de la pila causada por diferentes procesos de montaje y manufactura (presencia de cobre en el ánodo de la pila de combustible...).

A pesar de ello, algunas de las explicaciones encontradas en la literatura para justificar el comportamiento de la pila de combustible pueden ser aplicadas en este caso también (rápida redistribución de la estructura de níquel en el área de catalizador, alguna reacción química causada por el azufre procedente del ácido sulfídrico con los centros catalíticos activos de níquel...), pero es imposible determinar cuál de todas ellas es la correcta en nuestro caso sin experimentación adicional.

Los ensayos correspondientes a las curvas de polarización y la espectroscopía en el dominio de la frecuencia mostraron que el comportamiento de la pila tras la contaminación era similar para los

distintos potenciales (mismo porcentaje de disminución en la corriente a potencial constante). Sin embargo, eso no quiere decir que el comportamiento de la pila durante la contaminación sea igual a todos los niveles de polarización. De hecho, queda patente por los experimentos encontrados en la literatura que la polarización afecta en gran medida el mecanismo por el que el ácido sulfídrico afecta las propiedades y el comportamiento de la pila de combustible.

Además, los ensayos de espectroscopía en el dominio de la frecuencia mostraron que la respuesta de la pila de combustible podría ser más lenta tras la contaminación con ácido sulfídrico, dado que una mayor región capacitiva puede observarse en el gráfico, tanto a polarizaciones grandes (0.6V) como a pequeñas (0.6V).

Para determinar la naturaleza de estos mecanismos de contaminación y si son reversibles o no, estudios y experimentos adicionales deberán llevarse a cabo. Dichos experimentos deberán incluir espectroscopía en el dominio de la frecuencia y curvas de polarización mientras el ácido sulfídrico fluye por la pila, así como algún tipo de técnica de análisis superficial como Microscopía Electrónica de Escaneo (SEM de sus iniciales en inglés: Scanning Electron Microscopy), Espectroscopía de Fotoelectrones de Rayos X (XPS de sus iniciales en inglés: X-ray Photoelectron Spectroscopy) que pudiera proporcionar alguna información sobre la composición y distribución del ánodo de la pila de combustible (si el sulfuro reacciona y se queda formando un nuevo compuesto, si es simplemente absorbido reduciendo la disponibilidad de espacio para sitios activos de níquel, o si simplemente cambia la estructura del níquel y/o la distribución de las partículas de níquel).

Por último, cabe destacar que estos resultados preliminares obtenidos con ácido sulfídrico son extremadamente interesantes y sientan la base para posteriores estudios que deberían clarificar la naturaleza de los procesos que tienen lugar dentro de la pila de combustible durante la contaminación con H₂S, y que podrían proporcionar las claves para eliminar, o al menos minimizar, el efecto que este contaminante tiene sobre este tipo de pilas de combustible.

6.7. References

- [1] Bao, J., Krishnan, G. N., Jayaweera, P., Lau, K.-H., Sanjurjo, A., "Effect of various coal contaminants on the performance of solid oxide fuel cells: Part II. ppm and sub-ppm level testing", Journal of Power Sources, Vol. 193, pages 617-624, 2009.
- [2] Lussier, A., Sofie, S., Dvorak, J., Idzerda, Y. U., "Mechanism for SOFC anode degradation from hydrogen sulfide exposure", International Journal of Hydrogen Energy, Vol. 33, pages 3945-3951, 2008.
- [3] Brightman, E., Ivey, D. G., Brett, D. J. L., Brandon, N. P., "The effect of current density on H₂S-poisoning of nickel-based solid oxide fuel cell anodes", Journal of Power Sources, Vol. 196, Issue 17, pages 7182-7187, 2011.
- [4] Grgicak, C. M., Green, R. G., Giorgi, J. B., "SOFC anodes for direct oxidation of hydrogen and methane fuels containing H₂S", Journal of Power Sources, Volume 179, pages 317-328, 2008.
- [5] Rasmussen, J. F. B., Hagen, A., "The effect of H₂S on the performance of Ni-YSZ anodes in solid oxide fuel cells", Journal of Power Sources, Volume 191, pages 534-541, 2009.
- [6] Hagen, A., Rasmussen, J. F. B., Thyden, K., "Durability of solid oxide fuel cells using sulfur containing fuels", Journal of Power Sources, Vol. 196, pages 7271-7276, 2011.
- [7] Liu, D.-J., Almer, J., "Phase and Strain Distributions Associated with Reactive Contaminants inside of a Solid Oxide Fuel Cell", Applied Physics Letters, Vol. 94, 224106, 2009.

- [8] Offer, G. J., Mermelstein, J., Brightman, E., Brandon, N. P., "Thermodynamics and Kinetics of the Interaction of Carbon and Sulfur with Solid Oxide fuel Cell Anodes", *J. Am. Ceram. Soc.*, Vol. 92, pages 763-780, 2009.
- [9] Galea, N. M., Kadantsev, E. S., Ziegler, T., "Studying Reduction in Solid Oxide Fuel Cell Activity with Density Functional Theory-Effects of Hydrogen Sulfide Adsorption on Nickel Anode Surface", *J. Phys. Chem. C.*, Vol. 111, pages 14457-14468, 2007.
- [10] Zhang, L., Jiang, S. P., He, H. Q., Chen, X., Ma, J., Song, X. C., "A comparative study of H₂S poisoning on electrode behavior of Ni/YSZ and Ni/GDC anodes of solid oxide fuel cells", *International Journal of Hydrogen Energy*, Vol. 35, pages 12359-12368, 2010.
- [11] Yokokawa, H., Tu, H., Iwanschitz, B., Mai, A., "Fundamental mechanisms limiting solid oxide fuel cell durability", *Journal of Power Sources*, Vol. 182, pages 400-412, 2008.

CHAPTER 7

Conclusions and Future Research

Contents

7.1. Conclusions	191
7.1.1. General Conclusions.....	191
7.1.2. Specific Conclusions.....	192
7.2. Future Research.....	196

7. Conclusions and Future Research

7.1. Conclusions

In this chapter, the conclusions related to the work carried out in this project - which has been described in this dissertation - are presented. These conclusions can be classified into two different types according to their character: the general conclusions and the specific conclusions.

7.1.1. General Conclusions

The first main objective of this work, the acquisition of the abilities and skills to develop research at the highest level, has been achieved since the project in which this PhD was involved tested all those skills and abilities: It required problem identification - like, for example, why Cyclic Voltammetry (CV) could not be applied to this kind of fuel cell, as well as experimental design to overcome the problems found. Once experimental design was finished, it was necessary to learn the different experimental procedures in order to obtain adequate results. Finally, the results were analyzed using several tools. Those results were used as feedback for new problem identification and experimental design. As it was pointed out in Chapter 1, staying at one of the best fuel cell research centers in the world certainly helped achieving this objective.

In order to meet the general objectives of the Thesis, it was necessary to acquire a deep knowledge base related to the field of study, both in general terms (basic electrochemistry) as well as in more particular terms: fuel cells and concretely Solid Oxide Fuel Cells. This is reflected in the literature review that can be found in Chapter 2.

Finally, it must be remarked that the fuel cell research group in which this project was carried out has a strong relationship with several companies

through a program of the *National Science Foundation* (NSF) of the government of the United States. This fact really emphasized the importance of applying the knowledge acquired in the laboratory to the real world.

7.1.2. Specific Conclusions

The specific conclusions that can be drawn from this project are the following ones:

- An **electrochemical characterization** of the SOFC has been carried out using different techniques such as impedance and polarization techniques.
- **Two different fuels** have been used to perform this characterization: **hydrogen**, as the universal fuel with simpler chemistry has been used to understand the fuel cell behavior while **methane**, as one of the main components of the coal gas, has been used to see how the cell could change its behavior.
- The results obtained with those different techniques are in **agreement** with one another and with the ones found in the literature.
- When hydrogen is **diluted** with argon, it causes a **performance drop** that is not fully recovered.
- As expected, **the stronger the dilution, the higher the impact** it has on the SOFC performance. If the value of the dilution is below 75% argon, the dilution effect can hardly be seen. However, when the dilution reaches 90% argon, the effect is strong causing a descent in the current of over 60% at 0.6V constant voltage.

- **Mechanical cracking of the electrolyte** seems to be the most reasonable explanation for this effect, according to the results obtained. The cracking of the electrolyte could be caused by the increase of the total pressure produced by the rise in the anode flow inherent to the dilution process.
- **Methane slightly increases the performance** of the SOFC compared to the correspondent hydrogen case for the same apparent stoichiometry..
 - o The reason for this unexpected behavior could be related to the **increase in the stoichiometry** in the anodic catalyst caused by the particular fuel cell structure.
 - o This increase in the performance seems to be **stronger at higher potentials** - low currents - as the fuel cell shows a much **higher open circuit voltage** when methane is used compared with hydrogen, and it is less noticeable at higher polarization levels (higher current).
 - o If the cell is left at **open circuit** potential while feeding methane, a quick performance drop and **cell failure** is observed, probably as a result of carbon deposition on the anode nickel catalyst.
 - o At any **other level of polarization**, the **performance of the cell is not affected** and fully recovery can be seen.
 - o From the carbon mass balance, it was discovered that with **current applied very small carbon deposition** can be seen and it is reversible (negative value of the carbon deposition when hydrogen applied after the methane and also **fully recovery** can be seen, 1st cell)

- As expected, the **higher the current, the smaller the carbon deposition.**
- The difference between open circuit and the rest of polarization levels seems to be related to the reversibility of the carbon deposition observed: at open circuit the carbon deposition is irreversible, leading to quick cell failure while the rest of the levels of polarization this carbon deposition is reversible.
- The behavior of this SOFC towards **coking is better than the one predicted by the C-H-O diagram**. The reason for this could be related to the fact that the current collector is made of copper. According to literature, **copper improves the behavior of the nickel catalyst towards coking**. At high temperatures some of the copper from the anode current collector could diffuse through to the catalyst causing this good behavior towards cocking.
- The preliminary results of **hydrogen sulfide contamination** shown that the cell is affected even at concentrations of **25ppm** with a **decrease of about 20%** during the initial stages of contamination, and **no recovery** could be found when the hydrogen sulfide was removed. **No further decrease** in the performance could be observed in the subsequent cycles of contamination applied.
- **Further studies are required** in order to establish the mechanism of contamination more precisely. Some of the possibilities include some **chemical reaction** of the sulfur that comes from the H₂S with catalytically active nickel sites, a **quick redistribution** of the nickel structure in the surface area of the anode of the fuel cell or **simple absorption** of the sulfur in the surface area of the anode of the fuel cell, leaving less available space for the nickel active sites.

- All the results obtained seem to point out that the gas flowing in the anode - regardless if it is pure hydrogen, methane or a mixture of gases - encounters **serious difficulties to reach the nickel catalyst** due to the cell structure. **Small holes** compared to the area of the catalyst and **compactly packed nickel oxide foam** in the anode side seem to be the reason for this behavior.
- All those results suggest that a clear improvement for this kind of Solid Oxide Fuel Cell would be to **increase the area of the holes** so that the fuel can reach the catalyst more easily. The reduction in the area of current collector would probably not have an effect since it would still be big enough.
- Another possible improvement that could be tested would be **not to pack the nickel oxide foam so tightly**, thus allowing the fuel to reach the catalyst in the anode side more easily. However, this second possible improvement would reduce the electrical conductivity of the nickel oxide, increasing the whole cell resistance. Therefore an optimal compromise between those two quantities should be achieved for optimal fuel cell performance.
- Using a completely **electrochemical approach** (opposed to the material-science approach that most of the publications about SOFC use) for this kind of fuel cells along with the **particular fuel cell structure**, is one of the **innovative** parts of this thesis and what differences it from the rest of SOFC studies that can be found in the literature.

7.2. Future Research

In order to complete the electrochemical analysis with hydrogen sulfide contamination, new experiments should be carried out during contamination with hydrogen sulfide. As it was pointed out in previous chapters, in the preliminary results presented here no test was carried out during the contamination, as the objective of this experiment was to evaluate the global effect of several cycles of contamination at a constant voltage of 0.9V.

However, performing polarization curves and impedance tests during hydrogen sulfide contamination will certainly clarify the processes that take place during contamination and it will help understand the contamination mechanism of the hydrogen sulfide for this type of fuel cell, closing the electrochemical analysis of the cell with H₂S.

Also, another interesting set of experiments that will be done in this project includes some kind of surface analysis technique to analyze the anode (catalyst, current collector and electrolyte) of the fuel cell. Scanning Electron Microscopy (SEM) and X-ray Photoelectron Spectroscopy (XPS) are two possible alternatives.

Applying these techniques to the cell in several states (before use, after regular working conditions with hydrogen, after working with methane and after contamination with hydrogen sulfide) will clarify certain aspects like the contamination mechanism of H₂S and if copper diffuses from the current collector to the nickel catalyst at the high temperatures reached inside the fuel cell.

On a different level, further experimentation with other potential contaminants should be carried out in order to assess the viability of using

this kind of fuel cell with renewable or alternative fuels, like coal gas. As it was pointed out in the literature review, coal gas can have traces of CH₃Cl, PH₃, AsH₃ and some other gasses and metals, so the future research of the project should focus on those contaminants. In an initial stage, they should be studied one at a time, to evaluate their influence on the fuel cell, similarly to the process followed with hydrogen sulfide. On a second stage, new experiments should be designed in order to evaluate the effect when more than one is present in the fuel stream.

CAPÍTULO 7

Conclusiones y Trabajo Futuro

Contenido

7.1. Conclusiones	201
7.1.1. Conclusiones Generales.....	201
7.1.2. Conclusiones Particulares	202
7.2. Trabajo Futuro.....	206

7. Conclusiones y Trabajo Futuro

7.1. Conclusiones

En este capítulo las conclusiones relacionadas con el trabajo llevado a cabo en este proyecto - que ha sido descrito en esta memoria - serán presentadas. Dichas conclusiones se pueden clasificar atendiendo a su carácter en conclusiones generales y conclusiones particulares.

7.1.1. Conclusiones Generales

El primer gran objetivo de este trabajo, la adquisición de las habilidades para desarrollar investigación al más alto nivel, ha sido conseguido, dado que el proyecto en el que esta tesis doctoral fue realizada, requería todas esas habilidades. Requería de identificación de problemas - como por ejemplo estudiar la razón por la que la voltametría cíclica (CV, de sus siglas en inglés) no podía ser aplicada a esta clase de pila de combustible - así como el diseño de experimentos para resolver los problemas encontrados. Una vez el diseño de experimentos fue terminado, el aprendizaje de diferentes técnicas experimentales era necesario para llevar a cabo los experimentos planteados y obtener resultados adecuados. Finalmente, los resultados fueron analizados usando distintas herramientas. Dichos resultados fueron la base para una nueva identificación de problemas y diseño de nuevos experimentos. Como se indicó en el primer capítulo, la estancia en uno de los mejores centros de investigación de pilas de combustible a nivel mundial ayudó enormemente a cumplir este objetivo.

Para poder cumplir los objetivos generales de la Tesis, fue necesario adquirir una profunda base de conocimientos relacionadas con el campo de estudio, tanto en términos generales (electroquímica básica) como en

términos más particulares: pilas de combustible y en concreto Pilas de Combustible de Óxido Sólido. Esto ha sido reflejado en la revisión bibliográfica del segundo capítulo.

Por último, debe ser puesto de relieve que el grupo de investigación en el que este proyecto fue desarrollado tiene una fuerte relación con varias empresas privadas a través de un programa de la *National Science Foundation* (NSF) del gobierno de los Estados Unidos. Este hecho realmente enfatizó la importancia de llevar los conocimientos adquiridos en el laboratorio al mundo real.

7.1.2. Conclusiones Particulares

Las conclusiones particulares que se pueden sacar de este proyecto son las siguientes:

- Una **caracterización electroquímica** de la pila de Óxido Sólido ha sido llevada a cabo usando una variedad de técnicas como impedancia y técnicas de polarización.
- **Dos combustibles distintos** han sido empleados para esta caracterización: **hidrógeno**, como el combustible universal para pilas de combustible, con una química relativamente simple ha sido empleado para caracterizar el comportamiento de la pila. Por otro lado, **metano**, como uno de los principales componentes del gas procedente del carbón entre otros combustibles renovables, ha sido usado para ver de qué forma la pila cambiaba su comportamiento.
- Los resultados obtenidos con estas diferentes técnicas están en **concordancia** entre ellos y con los encontrados en la literatura.
- Cuando el hidrógeno se **diluye** con argón, se puede observar una **caída en el rendimiento** de la pila que no es completamente recuperada cuando el argón se elimina del flujo del ánodo.

- Como se esperaba, **cuanto más grande es la dilución, mayor impacto** tiene en el rendimiento de la pila. Si el valor de la dilución es de hasta el 75% de argón, el efecto de la dilución apenas puede apreciarse. Sin embargo, para un valor de dilución del 90% de argón, el efecto es fuerte, causando una reducción de más de 60% en la corriente eléctrica a 0.6V.
- **Daños mecánicos en el electrolito** causados por el incremento de la presión total (debido al aumento del caudal del ánodo inherente al proceso de dilución), parecen ser la explicación más razonable para este efecto, de acuerdo con los resultados obtenidos.
- **El metano incrementa de forma leve el rendimiento** de la pila, en comparación con el caso de hidrógeno correspondiente, para la misma estequiométria aparente.
 - La razón de este comportamiento inesperado podría ser debido a un **incremento en la estequiometría** del catalizador del ánodo, causado por la particular estructura del ánodo.
 - Este incremento de rendimiento parece ser **más acusado a altos potenciales** - bajas corrientes eléctricas - dado que la pila presenta un **voltaje a circuito abierto mayor** cuando se emplea metano en lugar de hidrógeno, y es menos apreciable a altos niveles de polarización (más altas corrientes eléctricas).
 - Una rápida **caída del rendimiento** de la pila, y su posterior **fallo** se puede observar si se deja la pila a **circuito abierto** mientras circula metano por ella, probablemente debido a la deposición de carbón sobre el catalizador de níquel del ánodo.

- A cualquier otro nivel de polarización el rendimiento no se ve afectado y una recuperación completa se puede observar.
 - Del balance del carbono, se descubrió que cuando **corriente eléctrica circula por la pila, una pequeña deposición de carbón** se puede observar, y que dicha deposición es reversible (dado que una completa recuperación se puede apreciar al retirar el metano de la pila y además se obtiene un valor negativo de la deposición de carbono en las muestras con hidrógeno tomadas tras el uso de metano).
 - Como se esperaba, a mayor **corriente menor deposición de carbón**.
- La diferencia del comportamiento que presenta la pila entre circuito abierto y el resto de los niveles de polarización cuando el metano es usado como combustible, parece estar relacionada con la reversibilidad del carbón depositado: a circuito abierto la deposición de carbón es irreversible lo que provoca un rápido fallo en la pila de combustible, mientras que al resto de niveles de polarización, la deposición de carbono es reversible.
- El **comportamiento de la pila frente a la deposición de carbón es mejor del predicho por el diagrama de equilibrio C-H-O**. La razón que explica este fenómeno podría estar relacionada con el hecho de que el colector de corriente del ánodo está hecho de cobre. De acuerdo con la literatura, el **cobre mejora el comportamiento del catalizador de níquel frente a la deposición de carbono**. A altas temperaturas, algo del cobre presente el colector de corriente podría difundir hasta el catalizador provocando este buen comportamiento.
- Los resultados preliminares de la **contaminación con ácido sulfídrico** muestran que la pila es afectada por este contaminante

incluso a concentraciones de **25ppm**, con una **disminución de la corriente de sobre el 20%** con respecto a los valores iniciales obtenidos antes de la contaminación. Además, **no se pudo recuperar el rendimiento** de la pila una vez que el ácido fue quitado. Eso sí, **tampoco se pudo observar un mayor decremento** del rendimiento de la pila con los siguientes ciclos de contaminación con ácido sulfídrico.

- **Nuevos estudios** son necesarios para establecer los mecanismos de contaminación de forma más precisa. Algunos de estos posibles mecanismos son **reacciones químicas** del azufre procedente del ácido sulfídrico con los centros activos del catalizador de níquel, **una rápida redistribución de la estructura del níquel** en el área superficial del ánodo de la pila de combustible, o **simple absorción** del azufre en la superficie, dejando menos huecos disponibles para los centros activos del níquel.
- Todos los resultados obtenidos parecen indicar que el gas que fluye por el ánodo - independientemente de si es hidrógeno puro, metano puro o una mezcla de gases - encuentra **serias dificultades para alcanzar el catalizador de níquel** debido a la estructura de la pila. **Huecos muy pequeños** en comparación con el tamaño total del área de catalizador y una **espuma de óxido de níquel empaquetada de forma muy compacta** en el ánodo de la pila parecen ser la razón fundamental para este comportamiento.
- Todos estos resultados sugieren que una mejora para esta clase de pilas de combustible: podría ser **incrementar el área de los agujeros del tubo de cobre** (colector de la corriente del ánodo) para que el combustible pueda llegar al catalizador de forma más sencilla. El efecto negativo de la reducción del área del colector de

corriente seguramente sea completamente despreciable, dado que el área del tubo seguirá siendo suficiente mente grande aún.

- Otra posible mejora que podría aplicarse, sería **no compactar tanto la espuma de óxido de níquel**, para que el combustible pueda llegar al catalizador sin problemas. Sin embargo, esta opción podría reducir la conductividad eléctrica del óxido de níquel, incrementando la resistencia eléctrica del conjunto de la pila. Por ello, un compromiso óptimo entre las dos opciones debería ser conseguido para un rendimiento óptimo de la pila.
- El hecho de usar un **enfoque completamente electroquímico** para este tipo de pilas (en contraste con el enfoque de ciencia de materiales que la mayoría de las publicaciones de Pilas de Óxido Sólido emplean) así como la **estructura tan particular** que presenta la pila, dan el carácter **innovador** y único que diferencia éste del resto de estudios sobre SOFC que pueden encontrarse en la literatura.

7.2. Trabajo Futuro

Para completar el análisis electroquímico de los resultados de la contaminación con ácido sulfídrico, nuevos experimentos deberán ser realizados durante la contaminación con este gas. Como se ha remarcado en capítulos anteriores, durante los experimentos preliminares llevados a cabo, ningún ensayo fue llevado a cabo durante la contaminación, ya que el objetivo de estos experimentos era evaluar el efecto global de varios ciclos de contaminación a un determinado nivel de polarización constante, en concreto a un voltaje constante de 0.9V.

Sin embargo, la realización de test de impedancia y curvas de polarización durante la contaminación con ácido sulfídrico aclarará de forma importante los procesos que tienen lugar dentro de la pila de combustible y ayudará a comprender el mecanismo de contaminación del ácido sulfídrico, para este tipo de pilas, cerrando así el análisis electroquímico de la pila con H₂S.

También, otro set de experimentos que serán realizadas por este proyecto consiste en el uso de alguna técnica superficial para analizar el ánodo (catalizador, colector de corriente y electrolito) de la pila de combustible. Microscopía Electrónica de Escaneo (SEM, de sus iniciales en inglés:), Espectroscopía de Fotoelectrones de Rayos X (XPS de sus iniciales en inglés) son dos posibles alternativas.

La aplicación de estas técnicas a la pila en diversos estados (antes de su uso, después de condiciones de trabajo normales con hidrógeno, tras la aplicación de metano y tras una combinación de hidrógeno y ácido sulfídrico, clarificarán aspectos claves del comportamiento de la pila, como el mecanismo de contaminación del H₂S, y si el cobre difunde desde el colector de corriente hasta los centros activos del catalizador de níquel cuando se encuentra a temperaturas tan altas como las que se dan dentro de pila.

A otro nivel, nuevos experimentos con otros contaminantes potenciales deberán ser llevados a cabo para determinar la viabilidad del empleo de este tipo de pila de combustible con combustibles renovables, como el gas obtenidos a partir del carbón. Éste tipo de gas presenta niveles bajos (del orden de ppm) de CH₃Cl, PH₃, AsH₃ y otros metales, por lo que los próximos estudios del proyecto deberán concentrarse en estos

contaminantes. En una etapa inicial, deberán ser estudiados de forma individual, para evaluar su influencia en la pila de forma análoga al proceso seguido con ácido sulfídrico. En una segunda etapa, nuevos experimentos deberán ser diseñados para evaluar el efecto que tienen sobre la pila cuando más de uno está presente el flujo de combustible.

REFERENCES

- ◊ Alston, T., Kendall, K., Palin, M., Prica, M., Windibank,P., "A 1000-cell SOFC reactor for domestic cogeneration", Journal of Power Sources, Vol. 71, páginas 271-274, 1998.
- ◊ Alzate-Restrepo, V., Hill, J. M., "Effect of anodic polarization on carbon deposition on Ni/YSZ anodes exposed to methane", Applied Catalysis A: General, Vol. 342, pages 49-55, 2008.
- ◊ Andres Lozano, C., Ohashi, M., Shimpalee, S., Van Zee, J. W., Aungkavattana, P., "Electrochemical Analysis of Microtubular SOFC under Fuel Contaminants". ECS Transactions, Vol. 33, pages 149-160, 2010.
- ◊ Andres Lozano, C., Ohashi, M., Shimpalee, S., Van Zee, J. W., Aungkavattana, P., "Comparison of Hydrogen and Methane as fuel in Micro-Tubular SOFC using Electrochemical Analysis". J. Electrochem. Soc., Vol. 158, pages B1235-B1245, 2011.
- ◊ Andújar, J. M., Segura, F., "Fuel cells: History and updating. A walk along two centuries", Renewable and Sustainable Energy Reviews, Vol. 13, pages 2309-2322, 2009.

- ◊ Antolini, E., Salgado, J. R. C., Gonzalez, E. R., "The stability of Pt-M (M = first row transition metal) alloy catalysts and its effect on the activity in low temperature fuel cells: A literature review and tests on a Pt-Co catalyst", *Journal of Power Sources*, Vol. 160, pages 957-968, 2006.
- ◊ Appleby, A. J., Foulkes, F. R., *Fuel Cell Handbook*, Van Nostrand Reinhold, New York, NY, 1989.
- ◊ Aungkavattana, P., Timakul, P., Atong, D., Mongkolkachit, C., Wanakitti, S., Lertwittayanon, K., Hills, M., Henson, M., "Component Materials and Design for Tubular Solid Oxide Fuel Cell", Annual Meeting of The Ceramic Society of Japan, Invited lecture, Nagaoka, Japan, 2008.
- ◊ Bao, J., Krishnan, G. N., Jayaweera, P., Lau, K.-H., Sanjurjo, A., "Effect of various coal contaminants on the performance of solid oxide fuel cells: Part II. Ppm and sub-pmm level testing", *Journal of Power Sources*, Vol. 193, pages 617-624, 2009.
- ◊ Bard, A., Faulkner, L., *Electrochemical Methods. Fundamentals and Applications*. 2nd edition, John Wiley and Sons, Inc., 2001.
- ◊ Barrera, R., De Biase, S., Ginocchio, S., Bedogni, S., Montelatici, L., "Performance and life time test on a 5kW SOFC system for distributed cogeneration, *International Journal of Hydrogen Energy*, Vol. 33, páginas 3193-3196, 2008.
- ◊ Beard, K. D., Schaal, M. T., Van Zee, J. W., Monnier, J. R., "Preparation of highly dispersed PEM fuel cell catalysts using electroless deposition methods", *Applied Catalysis B: Environmental*, Vol. 72, pages 262-271, 2007.

- ◊ Bedogni, S., Campanari, S., Iora, P., Montelatici, L., Silva, P., "Experimental analysis and modeling for a circular-planar type IT-SOFC", *Journal of Power Sources*, Vol. 171, pages 617-625, 2007.
- ◊ Bessler, W. G., "Rapid Impedance Modeling via Potential Step and Current Relaxation Simulations", *J. Electrochem. Soc.*, Vol. 154 pages B1186-B1191, 2007.
- ◊ Boder, M., Dittmeyer, R., "Catalytic modification of conventional SOFC anodes with a view to reducing their activity for direct internal reforming of natural gas", *Journal of Power Sources*, Vol. 155, pages 13-22, 2006.
- ◊ Brightman, E., Ivey, D. G., Brett, D. J. L., Brandon, N. P., "The effect of current density on H₂S-poisoning of nickel-based solid oxide fuel cell anodes", *Journal of Power Sources*, Vol. 196, Issue 17, pages 7182-7187, 2011.
- ◊ Burstein, G. T., "A Century of Tafel's Equation: 1905-2005 A Commemorative Issue of Corrosion Science". *Corrosion Science*, Vol. 47, pages 2858-2870, 2005.
- ◊ Bussayajarn, N., Han Ming, H., Hoong, K. K., Stephen, W. Y. M., Hwa, C. S., "Planar air breathing PEMFC with self-humidifying MEA and open cathode geometry design for portable applications", *International Journal of Hydrogen Energy*, Vol. 34, pages 7761-7767, 2009.
- ◊ Calì, M., Santarelli, M. G. L., Leone, P., "Design of experiments for fitting regression models on the tubular SOFC: Screening test, response surface analysis and optimization", *International Journal of Hydrogen Energy*, Vol. 32, pages 343-358, 2007.

- ◊ Campana, R., Merino, R. I., Larrea, A., Villarreal, I., Orera, V. M., "Fabrication, electrochemical characterization and thermal cycling of anode supported microtubular solid oxide fuel cells", Journal of Power Sources, Vol. 192, pages 120-125, 2009.
- ◊ Carvalho, L., Scott, L., Jeffery, R., "An exploratory study into the use of qualitative research methods in descriptive process modeling", Information and Software Technology, Vol. 47, pages 113-127, 2005.
- ◊ Channa K, De Silva, R., Kaseman, B. J., Bayless, D. J., "Accelerated anode failure of a high temperature planar SOFC operated with reduced moisture and increased PH₃ concentrations in coal syngas", International Journal of Hydrogen Energy, Vol. 36, pages 9945-9955, 2011.
- ◊ Chao Xu, C., Faghri, A., Li, X., Ward, T., "Methanol and water crossover in a passive liquid-feed direct methanol fuel cell", International Journal of Hydrogen Energy, Vol. 35, pages 1769-1777, 2010.
- ◊ Chapman, S., Cowling, T. G., *The mathematical theory of non-uniform gases: an account of the kinetic theory of viscosity, thermal conduction, and diffusion in gases*, Cambridge University Press, 1990.
- ◊ Chen, K., Lü, Z., Ai, N., Huang, X., Zhang, Y., Ge, X., Xin, X., Chen, X., Su, W., "Fabrication and performance of anode-supported YSZ films by slurry spin coating", Solid State Ionics, Vol. 177, pages 3455-3460, 2007.
- ◊ De Silva, K. C. R., Kaseman, B. J., Bayless, D. J., "Silver (Ag) as anode and cathode current collectors in high temperature planar solid oxide fuel cells", International Journal of Hydrogen Energy, Vol. 36, pages 779-786, 2011.

- ◊ Desclaux, P., Nürnberg, S., Rzepka, M., Stimming, U., "Investigation of direct carbon conversion at the surface of a YSZ electrolyte in a SOFC", International Journal of Hydrogen Energy, Vol. 36, pages 10278-10281, 2011.
- ◊ Donckels, B. M. R., De Pauw, D. J. W., Vanrolleghem, P. A., De Baets, B., "An ideal point method for the design of compromise experiments to simultaneously estimate the parameters of rival mathematical models", Chemical Engineering Science, Vol. 65, pages 1705-1719, 2010.
- ◊ Esquirol, A., Brandon, N. P., Kilner, J. A., Mogensen, M., "Electrochemical Characterization of $\text{La}_{0.6}\text{Sr}_{0.4}\text{Co}_{0.2}\text{Fe}_{0.8}\text{O}_3$ Cathodes for Intermediate-Temperature SOFCs", J. Electrochem. Soc., Vol. 151, pages A1847-A1855, 2004.
- ◊ Fiúza, R. da P., da Silva, M. A., Boaventura, J. S.; "Development of Fe-Ni/YSZ-GDC electrocatalysts for application as SOFC anodes: XRD and TPR characterization and evaluation in the ethanol steam reforming reaction", International Journal of Hydrogen Energy, Vol. 35, pages 11216-11228, 2010.
- ◊ Francia, C., Ijeri, V. S., Specchia, S., Spinelli, P., "Estimation of hydrogen crossover through Nafionl membranes in PEMFCs", Journal of Power Sources, Vol. 196, pages 1833-1839, 2011.
- ◊ Fu, C., Sun, K., Zhang, N., Chen, X., Zhou, D., "Electrochemical characteristics of LSCF-SDC composite cathode for intermediate temperature SOFC", Electrochimica Acta, Vol. 52, pages 4589-4594, 2007.

- ◊ Galea, N. M., Kadantsev, E. S., Ziegler, T., "Studying Reduction in Solid Oxide Fuel Cell Activity with Density Functional Theory-Effects of Hydrogen Sulfide Adsorption on Nickel Anode Surface", *J. Phys. Chem. C.*, Vol. 111, pages 14457-14468, 2007.
- ◊ Gansor, P., Xu, C., Sabolsky, K., Zondlo, J. W., Sabolsky, E. M., "Phosphine impurity tolerance of Sr₂MgMoO_{6-δ} composite SOFC anodes", *Journal of Power Sources*, Vol. 198, pages 7-13, 2012.
- ◊ Gasteiger, H. A., Markovic, N. M., Ross Jr., P. N., "Electrooxidation of CO and H₂/CO Mixtures on a Well-Characterized Pt₃Sn Electrode Surface", *J. Phys. Chem. Vol.* 99, pages 8945-8949, 1995.
- ◊ Gong, M., Bierschenk, D., Haag, J., Poeppelmeier, K. R., Barnett, S. A., Xu, C., Zondlo, J. W., Liu, X., "Degradation of LaSr₂Fe₂CrO_{9-δ} solid oxide fuel cell anodes in phosphine-containing fuels", *Journal of Power Sources*, Vol. 195, pages 4013-4021, 2010.
- ◊ Grgicak, C. M., Green, R. G., Giorgi, J. B., "SOFC anodes for direct oxidation of hydrogen and methane fuels containing H₂S", *Journal of Power Sources*, Volume 179, pages 317-328, 2008.
- ◊ Hagen, A., Rasmussen, J. F. B., Thyden, K., "Durability of solid oxide fuel cells using sulfur containing fuels", *Journal of Power Sources*, Vol. 196, pages 7271-7276, 2011.
- ◊ Haraldsson, K., Folkesson, A., Alvfors, P., "Fuel cell buses in the Stockholm CUTE project—First experiences from a climate perspective", *Journal of Power Sources*, Vol. 145, pages 620-631, 2005.
- ◊ He, H., Hill, J. M., "Carbon deposition on Ni/YSZ composites exposed to humidified methane", *Applied Catalysis A: General*, Vol. 317, pages 284-292, 2007.

- ◊ He, H., Vohs, J. M., Gorte, R. J., "Carbonaceous deposits in direct utilization hydrocarbon SOFC anode", *Journal of Power Sources*, Vol. 144, pages 135-140, 2005.
- ◊ Hernández, A. M., Mogni, L., Caneiro, A., "La₂NiO_{4+δ} as cathode for SOFC: Reactivity study with YSZ and CGO electrolytes", *International Journal of Hydrogen Energy*, Vol. 35, pages 6031-6036, 2010.
- ◊ Heywood, J. B., *Internal Combustion Engine Fundamentals*, McGraw-Hill, 1988.
- ◊ Hirschenhofer, J.H., Stauffer, D.B., Engleman, R.R., and Klett, M.G., *Fuel Cell Handbook*. DOE/FETC-99/1076, Cap 1. (2008).
- ◊ Hofmann, Ph., Panopoulos, K. D., Aravind, P. V., Siedlecki, M., Schweiger, A., Karl, J., Ouweltjes, J. P., Kakaras, E., "Operation of solid oxide fuel cell on biomass product gas with tar levels >10 g Nm⁻³", *International Journal of Hydrogen Energy*, Vol. 34, pages 9203-9212, 2009.
- ◊ Hornés, A., Gamarra, D., Munuera, G., Conesa, J. C., Martínez-Arias, A., "Catalytic properties of monometallic copper and bimetallic copper-nickel systems combined with ceria and Ce-X (X = Gd, Tb) mixed oxides applicable as SOFC anodes for direct oxidation of methane", *Journal of Power Sources*, Vol. 169, pages 9-16, 2007.
- ◊ Howe, K. S., Thompson, G. J., Kendall, K., "Micro-tubular solid oxide fuel cells and stacks", *Journal of Power Sources*, Vol. 196, pages 1677-1686, 2011.
- ◊ Huang, Q.-A., Hui, R., Wang, B., Zhang, J., "A review of AC impedance modeling and validation in SOFC diagnosis", *Electrochimica Acta*, Vol. 52, pages 8144-8164, 2007.

- ◊ Huang, T.-J., Jhao, S.-Y., "Ni-Cu/samaria-doped ceria catalysts for steam reforming of methane in the presence of carbon dioxide", *Applied Catalysis A: General*, Vol. 302, pages 325-332, 2006.
- ◊ Huijsmans, J. P. P., van Berkel, F. P. F., Christie, G. M., "Intermediate temperature SOFC - a promise for the 21st century", *Journal of Power Sources*, Vol. 71, pages 107-110, 1998.
- ◊ Jardiel, T., Caldes, M. T., Moser, F., Hamon, J., Gauthier, G., Joubert, O., "New SOFC electrode materials: The Ni-substituted LSCM-based compounds $(La_{0.75}Sr_{0.25})(Cr_{0.5}Mn_{0.5-x}Ni_x)O_{3-\delta}$ and $(La_{0.75}Sr_{0.25})(Cr_{0.5-x}Ni_xMn_{0.5})O_{3-\delta}$ " *Solid State Ionics*, Vol. 181, pages 894-901, 2010.
- ◊ Jones, D. A. *Principles and Prevention of Corrosion*. Ed. Prentice Hall, 1995.
- ◊ Joon, K., "Fuel cells - a 21st century power system", *Journal of Power Sources*, Vol. 71, pages 12-18, 1998.
- ◊ Kattke, K. J., Braun, R. J., "Characterization of a novel, highly integrated tubular solid oxide fuel cell system using high-fidelity simulation tools", *Journal of Power Sources*, Vol. 196, pages 6347-6355, 2011.
- ◊ Kendall, K., Finnerty, C. M., Saunders, G., Chung, J. T., "Effects of dilution on methane entering an SOFC anode", *Journal of Power Sources*, Vol. 106, pages 323-327, 2002.
- ◊ Kim, S.-H., Shimpalee, S., Van Zee, J. W., "The Effect of Flow Field Design and Voltage Change Range on the Dynamic Behavior of a PEMFC", *J. of Electrochem. Soc.*, Vol. 152, pages A1265-A1271, 2005.

- ◊ Kim, S-H., Shimpalee, S., and Van Zee, J. W., "The effect of stoichiometry on dynamic behavior of a PEMFC during load change", *J. of Power Source*, Vol. 135, pages 110-121, 2004.
- ◊ Kim, T., Liu, G., Boaro, M., Lee, S. I., Vohs, J. M., Gorte, R. J., Al-Madhi, O. H., Dabbousi, B. O., "A study of carbon formation and prevention in hydrocarbon-fueled SOFC", *J. Power Sources*, Vol. 155, pages 231-238, 2006.
- ◊ Kirubakaran, A., Jain, S., Nema, R. K., "A review on fuel cell technologies and power electronic interface", *J. of Renewable and Sustainable Energy Reviews*, Vol. 13, pages 2430-2440, 2009.
- ◊ Klein, J.-M., Bultel, Y., Georges, S., Pons, M., "Modeling of a SOFC fuelled by methane: From direct internal reforming to gradual internal reforming", *Chemical Engineering Science*, Vol. 62, pages 1636-1649, 2007.
- ◊ Koh, J. H., Yoo, Y. S., Park J. W., Lim, H. C., "Carbon deposition and cell performance of Ni-YSZ anode support SOFC with methane fuel", *Solid State Ionics*, Vol. 149, pages 157-166, 2002.
- ◊ Kournoutis, V. Ch., Tietz, F., Bebelis, S., "Cyclic voltammetry characterization of a $\text{La}_{0.8}\text{Sr}_{0.2}\text{Co}_{0.2}\text{Fe}_{0.8}\text{O}_{3-\delta}$ electrode interfaced to CGO/YSZ", *Solid State Ionics*, Vol. 197, pages 13-17, 2011.
- ◊ Laosiripojana, N., Assabumrungrat, S., "Catalytic steam reforming of methane, methanol, and ethanol over Ni/YSZ: The possible use of these fuels in internal reforming SOFC", *Journal of Power Sources*, Vol. 163, pages 943-951, 2007.

- ◊ Lay, E., Gauthier, G., Dessemond, L., "Preliminary studies of the new Ce-doped La/Sr chromo-manganite series as potential SOFC anode or SOEC cathode materials", *Solid State Ionics*, Vol. 189, pages 91-99, 2011.
- ◊ Lee, K. H., Strand, R. K., "SOFC cogeneration system for building applications, part 1: Development of SOFC system-level model and the parametric study", *Renewable Energy*, Vol. 34, páginas 2831-2838, 2008.
- ◊ Li, X., Li, J., Xu, L., Yang, F., Hua, J., Ouyang, M., "Performance analysis of proton-exchange membrane fuel cell stacks used in Beijing urban-route buses trial project", *International Journal of Hydrogen Energy*, Vol. 35, pages 3841-3847, 2010.
- ◊ Lin, C.-W., Chien, C.-H., Tan, J., Chao, Y. J., Van Zee, J. W., "Chemical degradation of five elastomeric seal materials in a simulated and an accelerated PEM fuel cell environment", *Journal of Power Sources*, Vol. 196, pages 1955-1966, 2011.
- ◊ Liu, D.-J., Almer, J., "Phase and Strain Distributions Associated with Reactive Contaminants inside of a Solid Oxide Fuel Cell", *Applied Physics Letters*, Vol. 94, 224106, 2009.
- ◊ Lussier, A., Sofie, S., Dvorak, J., Idzerda, Y. U., "Mechanism for SOFC anode degradation from hydrogen sulfide exposure", *International Journal of Hydrogen Energy*, Vol. 33, pages 3945-3951, 2008.
- ◊ Lutz, A. E., Larson, R. S., Keller, J. O., "Thermodynamic comparison of fuel cells to the Carnot cycle", *International Journal of Hydrogen Energy*, Vol. 27, páginas 1103-1111, 2002.

- ◊ Maček, J., Novosel, B., Marinšek, M., "Ni-YSZ SOFC anodes–Minimization of carbon deposition", Journal of the European Ceramic Society, Vol. 27, pages 487-491, 2007.
- ◊ Maheshwari, P. H., Mathur, R. B., Dhami, T. L., "The influence of the pore size and its distribution in a carbon paper electrode on the performance of a PEM Fuel cell", Electrochimica Acta, Vol. 54, pages 655-659, 2008.
- ◊ Maier, J., "Ionic transport in nano-sized systems", Solid State Ionics, Vol.175, pages 7-12, 2004.
- ◊ Mangalaraja, R. V., Ananthakumar, S., Paulraj, M., Pesenti, H., López, M., Camurri, C. P., Barcos, L. A., Avila, R. E., "Electrical and thermal characterization of Sm³⁺ doped ceria electrolytes synthesized by combustion technique", Journal of Alloys and Compounds, Vol. 510, pages 134-140, 2012.
- ◊ Marina, O. A., Pederson, L. R., Thomsen, E. C., Coyle, C. A., Yoon, K. J., "Reversible poisoning of nickel/zirconia solid oxide fuel cell anodes by hydrogen chloride in coal gas", Journal of Power Sources, Vol. 195, pages 7033-7037, 2010.
- ◊ Masel, R. I., "Chemical Kinetics and Catalysis" Wiley-Interscience, New York, 2001.
- ◊ Mekhilef S, Saidur, R., Safari, A., "Comparative study of different fuel cell technologies", Renew. Sustain. Energy Rev., 2011.
- ◊ Merriam Webster online dictionary.

<http://www.merriam-webster.com>

Consulted on 02/22/2011.

- ◊ Milliken, J. FY 2007 Annual Progress Report, DOE Hydrogen Program.
<http://www.hydrogen.energy.gov/pdfs/progress07/introduction.pdf>
Consulted on 15/02/2009.
- ◊ Minh, N. Q., "Ceramic Fuel-Cells", Journal of the American Ceramic Society, Vol. 76, pages 563-588, 1993
- ◊ Mohtadi, R., Lee, W.-K., Van Zee, J. W., "The Effect of Temperature on the Adsorption Rate of Hydrogen Sulfide on Pt Anodes in a PEMFC", J. of Applied Catalysis B, Environmental, Vol. 56, pages 37-42, 2005.
- ◊ Morel, B., Roberge, R., Savoie, S., Napporn, T. W., Meunier, M., "Catalytic activity and performance of LSM cathode materials in single chamber SOFC", Applied Catalysis A: General, Vol. 323, pages 181-187, 2007.
- ◊ Mourits F. M., Rummens, F. H. A., "A critical evaluation of Lennard-Jones and Stockmayer potential parameters and of some correlation methods", Canadian Journal of Chemistry, Vol. 55, pages 3007-3020, 1977.
- ◊ National Institute of Standards and Technology (NIST), web database.
<http://webbook.nist.gov/>
Consulted on 18/05/2011.
- ◊ O'Hayre, R., Cha, S.W., Colella, W., Prinz, F. B., *Fuel Cell Fundamentals*. Wiley, Cap. 1. (2009).
- ◊ Offer, G. J., Mermelstein, J., Brightman, E., Brandon, N. P., "Thermodynamics and Kinetics of the Interaction of Carbon and Sulfur with Solid Oxide fuel Cell Anodes", J. Am. Ceram. Soc, Vol. 92, pages 763-780, 2009.

- ◊ Panteix, P. J., Baco-Carles, V., Tailhades, Ph., Rieu, M., Lenormand, P., Ansart, F., Fontaine, M. L., "Elaboration of metallic compacts with high porosity for mechanical supports of SOFC", Solid State Sciences, Vol. 11, pages 444-450, 2009.
- ◊ Park, E. W., Moon, H., Park, M.-S., Hyun, S. H., "Fabrication and characterization of Cu-Ni-YSZ SOFC anodes for direct use of methane via Cu-electroplating", International Journal of Hydrogen Energy, Vol. 34, pages 5537-5545, 2009.
- ◊ Peña-Martínez, J., Marrero-López, D., Pérez-Coll, D., Ruiz-Morales, J. C., Núñez, P., "Performance of XSCoF (X = Ba, La and Sm) and LSCrX' (X' = Mn, Fe and Al) perovskite-structure materials on LSMG electrolyte for IT-SOFC", Electrochimica Acta, Vol. 52, pages 2950-2958, 2007.
- ◊ Pérez-Flores, J. C., Ritter, C., Pérez-Coll, D., Mather, G. C., Canales-Vázquez, J., Gálvez-Sánchez, M., García-Alvarado, F., Amador, U., "Structural and electrochemical characterization of $\text{La}_{2-x}\text{Sr}_x\text{NiTiO}_{6-\delta}$ ", International Journal of Hydrogen Energy, Available online 25 November 2011.
- ◊ Piao, J., Sun, K., Chen, X., "Compatibility between glass sealants and electrode materials of solid oxide fuel cells", Rare Metals, Vol. 27, pages 378-383, 2008.
- ◊ Punyawudho, K., Blom, D. A., Van Zee, J. W., Monnier, J. R., "Comparison of different methods for determination of Pt surface site concentrations for supported Pt electrocatalysts", Electrochimica Acta, Vol. 55, pages 5349-5356, 2010.

- ◊ Rambabu, B., Ghosh, S., Zhao, W., Jena, H., "Innovative processing of dense LSGM electrolytes for IT-SOFC's", Journal of Power Sources, Vol. 159, pages 21-28, 2006.
- ◊ Rasmussen, J. F. B., Hagen, A., "The effect of H₂S on the performance of Ni-YSZ anodes in solid oxide fuel cells", Journal of Power Sources, Volume 191, pages 534-541, 2009.
- ◊ Recknagle, K. P., Ryan, E. M., Koeppl, B. J., Mahoney, L. A., Khaleel, M. A., "Modeling of electrochemistry and steam-methane reforming performance for simulating pressurized solid oxide fuel cell stacks", J. Power Sources, Vol. 195 pages 6637-6644, 2010.
- ◊ Santarelli, M., Leone, P., Calì, M., Orsello, G., "Experimental evaluation of the sensitivity to fuel utilization and air management on a 100kW SOFC system", Journal of Power Sources, Vol. 171, pages 155-168, 2007.
- ◊ Santori, G., Brunetti, E., Polonara, F., "Experimental characterization of an anode-supported tubular SOFC generator fueled with hydrogen, including a principal component analysis and a multi-linear regression", International Journal of Hydrogen Energy, Vol. 36, pages 8435-8449, 2011.
- ◊ Satyapal, S., FY 2010 Annual Progress Report, DOE Hydrogen Program.
http://www.hydrogen.energy.gov/pdfs/progress10/i_introduction.pdf
Consulted on 15/11/2011.
- ◊ Secanell, M., Djilali, N., Suleman, A., "Optimization of a planar self-breathing PEM fuel cell cathode". 11th AIAA/ISSMO Multidisciplinary Analysis and Optimization Conference, Portsmouth, Virginia, 2006.

- ◊ Selman, J. R., Tobias, C. W., "Mass-Transfer Measurements by the Limiting Current Technique", *Advances in Chemical Engineering*, Vol. 10, pages 211-318, 1978.
- ◊ Shang, J. L., Pollet, B. G., "Hydrogen fuel cell hybrid scooter (HFCHS) with plug-in features on Birmingham campus", *International Journal of Hydrogen Energy*, Vol. 35, pages 12709-12715, 2010.
- ◊ Shao, Z., Haile, S. M., "A High Performance Cathode for the Next Generation Solid-Oxide Fuel Cells", *Nature*, Vol. 431, pages 170-173, 2004.
- ◊ Shimpalee, S., Greenway, S., Spuckler, D., Van Zee, J. W., "Predicting water and current distributions in a commercial-size PEMFC", *Journal of Power Sources*, Vol. 135, pages 79-87, 2004.
- ◊ Simner, S. P., Anderson, M. D., Coleman, J. E., Stevenson, J. W., "Performance of a novel La(Sr)Fe(Co)O₃-Ag SOFC cathode", *Journal of Power Sources*, Vol. 161, pages 115-122, 2006.
- ◊ Sin, Y.-W., Galloway, K., Roy, B., Sammes, N. M., Song, J.-H., Suzuki, T., Awano, M., "The properties and performance of micro-tubular (less than 2.0mm O.D.) anode supported solid oxide fuel cell (SOFC)", *International Journal of Hydrogen Energy*, Vol. 36, pages 1882-1889, 2011.
- ◊ Song, R.-H., Shin, D. R., "Influence of CO concentration and reactant gas pressure on cell performance in PAFC", *International Journal of Hydrogen Energy*, Vol. 26, pages 1259-1262, 2001.
- ◊ Sonntag, R. E., Borgnakke, C., Van Wylen , G. J., *Fundamentals of Thermodynamics*, 6th edition, John Wiley and Sons, Inc., 2002.

- ◊ Souza, S. de, Visco, S. J., Jonghe, L. C. De, "Reduced-Temperature Solid Oxide Fuel Cell Based on YSZ Thin-Film Electrolyte", *J. Electrochem. Soc.*, Vol. 144, pages L35-L37, 1997.
- ◊ Springer, T. E., Rockward, T., Zawodzinski, T. A., Gottesfeld, S., "Model for Polymer Electrolyte Fuel Cell Operation on Reformate Feed. Effects of CO, H₂ Dilution and High Fuel Utilization", *J. Electrochem. Soc.*, Vol. 148, pages A11-A23, 2001.
- ◊ Stambouli, A. B., Traversa, E., "Fuel cells, an alternative to standard sources of energy", *Renewable and Sustainable Energy Reviews*, Vol. 6, pages 295-304, 2002.
- ◊ Stöver, D., Buchkremer, H. P., Uhlenbruck, S., "Processing and properties of the ceramic conductive multilayer device solid oxide fuel cell (SOFC)", *Ceramics International*, Vol. 30, pages 1107-1113, 2004.
- ◊ Strong, F. C., "Faraday's laws in one equation", *J. Chem. Educ.*, Vol. 38, page 98, 1961.
- ◊ Studer, R., Benjamins, V. R., Fensel, D., "Knowledge engineering: Principles and methods, Data & Knowledge Engineering", Vol. 25, pages 161-197, 1998.
- ◊ Sumi, H., Puengjinda, P., Muroyama, H., Matsui, T., Eguchi, K., "Effects of crystal Structure of yttria- and scandia-stabilized zirconia in nickel-based SOFC anodes on carbon deposition and oxidation behavior", *Journal of Power Sources*, Vol. 196, pages 6048-6054, 2011.
- ◊ Suzuki, T., Yamaguchi, T., Fujishiro, Y., Awano, M., "Improvement of SOFC Performance Using a Microtubular, Anode-Supported SOFC", *J. Electrochem. Soc.*, Vol. 153, pages A925-A928, 2006.

- ◊ Tan, J., Chao, Y. J., Van Zee, J. W., Lee, W. K., "Degradation of elastomeric gasket materials in PEM fuel cells", Materials Science and Engineering: A, Vols. 445-446, pages 669-675, 2007.
- ◊ Tikhonovich, V. N., Kharton, V. V., Naumovich, E. N., Savitsky, A. A., "Surface modification of La(Sr)MnO₃ electrodes" Solid State Ionics, Vol. 106, pages 197-206, 1998.
- ◊ Toonssen, R., Sollai, S., Aravind, P. V., Woudstra, N., Verkooijen, A. H. M., "Alternative system designs of biomass gasification SOFC/GT hybrid systems", International Journal of Hydrogen Energy, Vol. 36, pages 10414-10425, 2011.
- ◊ Vakouftsi, E., Marnellos, G., Athanasiou, C., Coutelieris, F. A., "A detailed model for transport processes in a methane fed planar SOFC", Chemical Engineering Research and Design, Vol. 89, pages 224-229, 2011.
- ◊ Van herle, J., Membrez, Y., Bucheli, O., "Biogas as a fuel source for SOFC co-generators", Journal of Power Sources, Vol. 127, pages 300-312, 2004.
- ◊ Vert, V. B., Serra, J. M., Jordá, J. L., "Electrochemical characterization of MBaCo₃ZnO_{7+d} (M = Y, Er, Tb) as SOFC cathode material with low thermal expansion coefficient", Electrochemistry Communications, Vol. 12, pages 278-281, 2010.
- ◊ Vilekar, S. A., Datta, R., "The effect of hydrogen crossover on open-circuit voltage in polymer electrolyte membrane fuel cells", Journal of Power Sources, Vol. 195, pages 2241-2247, 2010.

- ◊ Vivet, N., Chupin, S., Estrade, E., Richard, A., Bonnamy, S., Rochais, D., Bruneton, E., "Effect of Ni content in SOFC Ni-YSZ cermets: A three-dimensional study by FIB-SEM tomography", Journal of Power Sources, Vol. 196, pages 9989-9997, 2011.
- ◊ Will, J., Mitterdorfer, A., Kleinlogel, C., Perednis, D., Gauckler, L. J., "Fabrication of thin electrolytes for second-generation solid oxide fuel cells", Solid State Ionics, Vol. 131, pages 79-96, 2000.
- ◊ Wincewicz, K. C., Cooper, J. S., "Taxonomies of SOFC material and manufacturing alternatives", Journal of Power Sources, Vol. 140, pages 280-296, 2005.
- ◊ Yamaguchi, T., Shimizu, S., Suzuki, T., Fujishiro, Y., Awano, M., "Fabrication and characterization of high performance cathode supported small-scale SOFC for intermediate temperature operation", Electrochemistry Communications, Vol. 10, pages 1381-1383, 2008.
- ◊ Yan, A., Maragou, V., Arico, A., Cheng, M., "Panagiotis Tsiakaras, Investigation of a Ba_{0.5}Sr_{0.5}Co_{0.8}Fe_{0.2}O_{3-δ} based cathode SOFC: II. The effect of CO₂ on the chemical stability", Applied Catalysis B: Environmental, Vol. 76, pages 320-327, 2007.
- ◊ Yi, Y., Rao, A. D., Brouwer, J., Samuelsen, G. S., "Fuel flexibility study of an integrated 25kW SOFC reformer system", Journal of Power Sources, Vol. 144, pages 67-76, 2005.
- ◊ Yokokawa, H., Tu, H., Iwanschitz, B., Mai, A., "Fundamental mechanisms limiting solid oxide fuel cell durability", Journal of Power Sources, Vol. 182, pages 400-412, 2008.

- ◊ Zegers, P., "Fuel cell commercialization: The key to a hydrogen economy", *Journal of Power Sources*, Vol. 154, pages 497-502, 2006.
- ◊ Zhang, L., Jiang, S. P., He, H. Q., Chen, X., Ma, J., Song, X. C., "A comparative study of H₂S poisoning on electrode behavior of Ni/YSZ and Ni/GDC anodes of solid oxide fuel cells", *International Journal of Hydrogen Energy*, Vol. 35, pages 12359-12368, 2010.
- ◊ Zhang, S., Yuan, X., Wang, H., Mérida, W., Zhu, H., Shen, J., Wu, S., Zhang, J., "A review of accelerated stress tests of MEA durability in PEM fuel cells", *International Journal of Hydrogen Energy*, Vol. 34, pages 388-404, 2009.
- ◊ Zhao, F., Virkar, A. V., "Effect of morphology and space charge on conduction through porous doped ceria", *Journal of Power Sources*, Vol. 195, pages 6268-6279, 2010.
- ◊ Zhu, H., Kee, R. J., Janardhanan, V. M., Deutschmann, O., Goodwin, D. G., "Modeling Elementary Heterogeneous Chemistry and Electrochemistry in Solid-Oxide Fuel Cells", *J. Electrochem. Soc.*, Vol. 152, pages A2427-A2440, 2005.
- ◊ Zidansek, A., Ambrozic, M., Milfelner, M., Blinc, R., Lior, N., "Solar orbital power: Sustainability analysis", *Energy*, Vol. 36, pages 1986-1995, 2011.

APPENDIX A1

Limiting Current Calculation

Contents

A1.1. Introduction	233
A1.2. Model Used	233
A1.3. Calculation and Results	235
A1.4. References	239

A1. Limiting Current Calculation

A1.1. Introduction

Due to the complex flow path of the fuel in the anode side of the fuel cell, it is very difficult to get an accurate value for the limiting current using the traditional correlations. Since the purpose of the figures presented for the reactions (Figures 4.10, 411, 5.17 and 5.18) is simply to illustrate the possible reactions that could take place in the anode of the fuel cell and the voltage at which they take place, the approach described in this appendix was used.

A1.2. Model Used

To calculate the limiting current for each reaction, a traditional correlation for laminar forced convection mass transport on tubular ducts, taken from Selman and Tobias [1], was used. This correlation is given by equation A1.1:

$$Sh = 1.94 \cdot \left(Re \cdot Sc \cdot \frac{d_e}{L} \right)^{1/3} = 2.103 \cdot \left(\frac{Q}{D \cdot L} \right)^{1/3} \quad (A1.1)$$

The flow pattern correspondent to this correlation is represented in Figure A1.1. This is an approximation of the actual flow pattern expected for the anode of the SOFC, represented in Figure A1.2.

No matter how different these two flow fields look, the real flow pattern could be considered as an intermediate case of two cases that can be described with the flow field of the correlation. The first one, the upper

limit, would be described considering the flow pattern of the correlation with the catalyst surface area of the real fuel cell (9cm^2). Since the real flow would be equivalent to the flow of the correlation with some obstacles added, the real limiting current would never be greater than the one predicted by the correlation, and thus it would mark the upper limit.

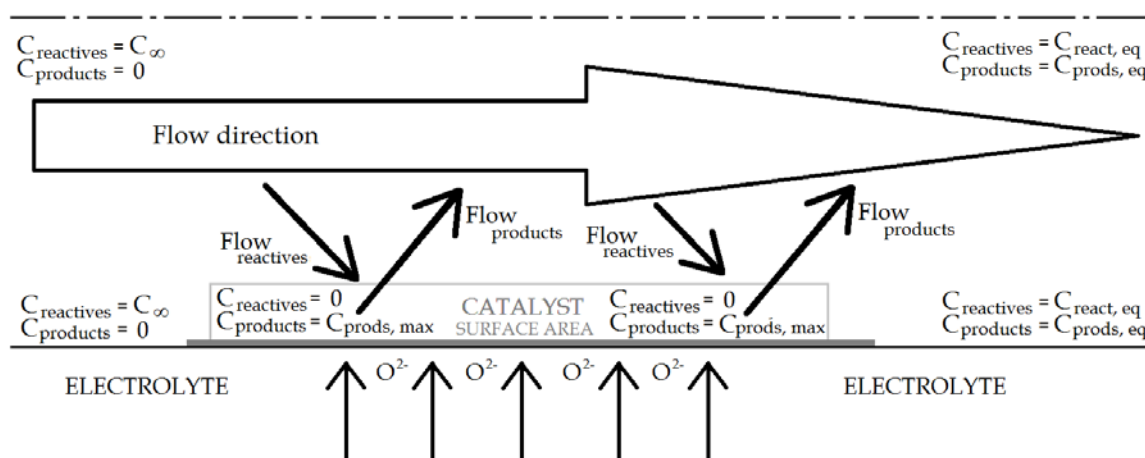


Figure A1.1: Flow pattern for the correlation used (anode side).

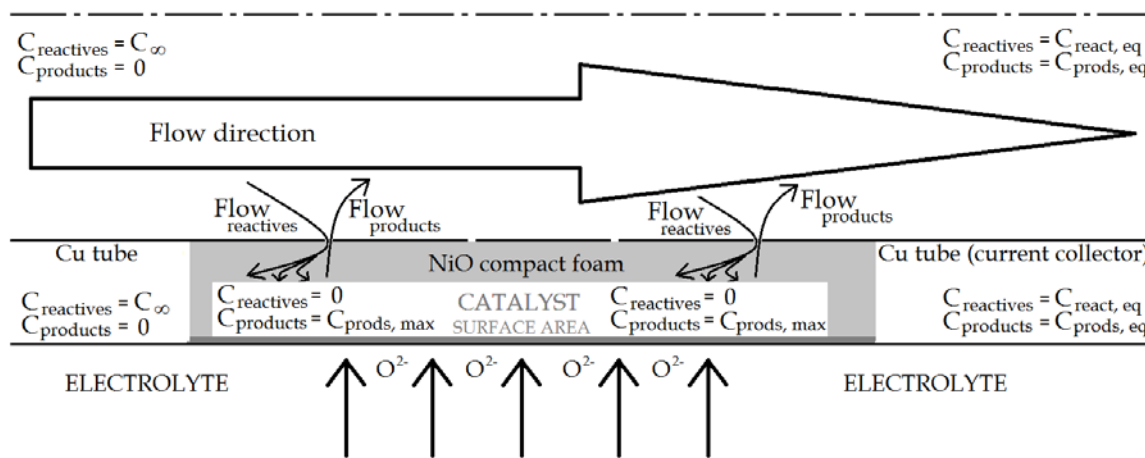


Figure A1.2: Real flow pattern of the fuel cell (anode side).

Regarding the lower limit, it is clear that if the fuel did not reach the catalysts, it would not react and it would start accumulating inside the

foam. Obviously, in the steady state, no accumulation can occur, so all the fuel entering the foam should react, thus the lower limit for the limiting current is given by the case of a flow pattern of the correlation with a catalyst surface area equivalent to the area of the holes in the copper current collector (which is a hundredth of the area of the catalyst, that is 0.09cm^2).

These two cases constitute the two reference limits and they mark the two extremes of the range where the real limiting current should be contained. It is a large window as the lower limiting current will be two orders of magnitude smaller than the upper limiting current. However, as it was pointed out before, the purpose of this study is simply to illustrate the reactions happening in the anode of the fuel cell and the potentials at which they occur. This approach gives a rough idea of the value of the current that can be expected, and also the proportions of the limiting currents at different conditions and gases should also be maintained in the real cell.

A1.3. Calculation and Results

In this section, the calculations and the results obtained using equation A1.1 are presented. Table A1.5, located at the end of this chapter, reflects the results obtained, both considering a catalyst surface area of 9cm^2 - which produces the upper limit for the value of the limiting current of the reaction (" $I_{\text{lim}} \text{ (max)}$ " in Table A1.5) - and an area of 0.09cm^2 - which produces the lower limit for the value of the limiting current (" $I_{\text{lim}} \text{ (min)}$ " in Table A1.5), using the approach described previously.

Since the following dimensionless numbers are involved in the correlation, they were calculated for all the conditions of the anode side (different flow and different gases):

$$\text{Sherwood number: } \text{Sh} = \frac{i_L \cdot d_e}{n \cdot F \cdot D \cdot c} \quad (\text{A1.2})$$

$$\text{Reynolds number: } \text{Re} = \frac{v_{\text{avg}} \cdot d_e}{\nu} = \frac{4 \cdot Q}{\pi \cdot d_e \cdot \nu} \quad (\text{A1.3})$$

$$\text{Schmidt number: } \text{Sc} = \frac{\nu}{D} \quad (\text{A1.4})$$

Table A1.1 shows the values used for the kinematic viscosity (ν) for all the different gas combinations that were used in the fuel cell, at 900°C.

Table A1.1: Kinematic viscosity (ν) at 900°C for all different species, in m²/s.

H ₂	CO	CH ₄	CO ₂
9.88·10 ⁻⁴	1.53·10 ⁻⁴	1.68·10 ⁻⁴	9.78·10 ⁻⁵

The Chapman-Enskog Theory (equation A1.5) [3] was used to determine the diffusivities (D_{ab}) for the different conditions and gases. Table A1.3 shows the values obtained for each of the possible working conditions that occurred at the anode of the fuel cell.

$$D_{12} = \frac{1.86 \cdot 10^{-3} \cdot T^{3/2} \cdot \sqrt{\frac{1}{M_1} + \frac{1}{M_2}}}{P \cdot \sigma_{12} \cdot \Omega} \quad (\text{A1.5})$$

From that equation, the collision integral parameter (Ω) is assumed to be equal to 1 and the values for the averaged collision diameter (σ_{12}) must be calculated for each set of gases.

To do so, the averaged collision diameter (σ_{12}) is calculated following equation A1.6 as an average of the values of the averaged-pure-specie diameter (σ_1) involved.

$$\sigma_{12} = \frac{1}{2} \cdot (\sigma_1 + \sigma_2) \quad (\text{A1.6})$$

The values for the averaged-pure-specie diameters are shown in Table A1.2, and were taken from Mourits and Rummens [2]:

Table A1.2: Averaged molecule diameter (σ) in Å.

H ₂	CO	CH ₄	CO ₂	Ar	N ₂
3.255	4.151	4.254	4.426	3.889	4.195

Table A1.3: Calculated diffusivities (Chapman-Enskog Theory).

Species	Diluted in	D ₁₂ (m ² /s)
H ₂	H ₂	7.054·10 ⁻⁴
H ₂	Ar	4.244·10 ⁻⁴
H ₂	CH ₄	3.976·10 ⁻⁴
CH ₄	CH ₄	1.460·10 ⁻⁴
CH ₄	Ar	1.334·10 ⁻⁴
CO	CO	1.159·10 ⁻⁴
CO	Ar	1.140·10 ⁻⁴
CO	CH ₄	1.326·10 ⁻⁴

Now that all these values have been obtained, it must be verified if the flux is laminar or turbulent. The correlation used (equation A1.1) is only applicable with laminar flow, so the less favorable case (the one with highest Reynolds number) should be considered. The greatest volumetric flux (Q) used occurred with the most extreme dilution - 10% hydrogen in argon, so it is this flux - 500sccm (which is equivalent to 3.28·10⁻⁵ m³/s at

the working conditions of temperature and pressure, assuming ideal gas) - the one that will be used. Equation A1.7 is the general expression to calculate the Reynolds number as a function of the volumetric flux (Q). The geometric characteristics of the cell used for this calculation are shown in Table A1.4.

$$Re_{MAX} = \frac{4 \cdot Q}{\pi \cdot d_e \cdot v} = \frac{4 \cdot 3.28 \cdot 10^{-5}}{\pi \cdot 0.00127 \cdot 9.78 \cdot 10^{-5}} = 336 \quad (A1.7)$$

Table A1.4: Geometric characteristics of the fuel cell.

Diameter - d_e (m)	Catalyst Length - L (m)	Active area - A (m^2)
0.00127	0.1524	0.0009

Since the maximum Reynolds number, 336, is below the laminar limit (2800), the correlation used for the calculation of the limiting current (equation A1.1) is valid for all the cases considered.

Table A1.5: Limiting currents calculated for all different reactions.

Fuel	Pure H ₂	Diluted H ₂	Pure CH ₄			Diluted CH ₄		
Reaction	pure H ₂	H ₂ in Ar	pure CH ₄	H ₂ in CH ₄	CO in CH ₄	CH ₄ in Ar	H ₂ in Ar	CO in Ar
Q (scmm)	50.00	500.00	16.67	16.67	16.67	166.67	166.67	166.67
Q _{900°C} (cm ³ /min)	196.74	1967.38	65.58	65.58	65.58	655.79	655.79	655.79
Q _{900°C} (m ³ /s)	3.3·10 ⁻⁶	3.3·10 ⁻⁵	1.1·10 ⁻⁶	1.1·10 ⁻⁶	1.1·10 ⁻⁶	1.1·10 ⁻⁵	1.1·10 ⁻⁵	1.1·10 ⁻⁵
v (m ² /s)	9.9·10 ⁻⁴	9.9·10 ⁻⁴	1.7·10 ⁻⁴	9.9·10 ⁻⁴	1.5·10 ⁻⁴	1.7·10 ⁻⁴	9.9·10 ⁻⁴	1.5·10 ⁻⁴
Re	3.33	33.26	6.50	1.11	7.17	65.04	11.09	71.69
D (m ² /s)	7.05·10 ⁻⁴	4.24·10 ⁻⁴	1.46·10 ⁻⁴	3.98·10 ⁻⁴	1.33·10 ⁻⁴	1.33·10 ⁻⁴	4.24·10 ⁻⁴	1.14·10 ⁻⁴
Sh	0.657	1.677	0.770	0.551	0.795	1.710	1.162	1.802
c (mol/mol)	1.00	0.10	1.00	0.36	0.17	0.10	0.036	0.017
c (mol/m ³)	10.39	1.04	10.39	3.71	1.74	1.04	0.37	0.17
n	2	2	2	2	2	2	2	2
I (A/m ²)	731600	112300	177500	123700	27830	36000	27840	5420
I _{lim} (A) (max)	658.43	101.10	159.75	111.34	25.05	32.40	25.05	4.88
I _{lim} (A) (min)	6.58	1.01	1.59	1.11	0.25	0.32	0.25	0.05

Table A1.5 shows both the upper and the lower limits calculated for the limiting current at different conditions inside the SOFC and for all the different reactions considered. Please note that the values of the concentration of the sub-products were calculated using the efficiency of the initial reaction (Table 5.7), which is calculated in Chapter 5 using the data obtained from the mass spectrometer at 0.6V.

A1.4. References

- [1] Selman, J. R., Tobias, C. W., "Mass-Transfer Measurements by the Limiting Current Technique", *Advances in Chemical Engineering*, Vol. 10, pages 211-318, 1978.
- [2] Mourits F. M., Rummens, F. H. A., "A critical evaluation of Lennard-Jones and Stockmayer potential parameters and of some correlation methods", *Canadian Journal of Chemistry*, Vol. 55, pages 3007-3020, 1977.
- [3] Chapman, S., Cowling, T. G., *The mathematical theory of non-uniform gases: an account of the kinetic theory of viscosity, thermal conduction, and diffusion in gases*, Cambridge University Press, 1990.

APPENDIX A2

Reaction Potential Calculation

Contents

A2.1. Introduction	243
A2.2. Procedure	243
A2.3. References	245

A2. Reaction Potential Calculation

A2.1. Introduction

In this chapter, the method used to obtain the potential for each reaction reported in Chapters 4 and 5 is described. Since the fuel cell operates at high temperatures (900°C), the traditional approach, which uses the tables of standard electrode potential along with the Gibbs equation, are no longer valid since a correction for the temperature is necessary to the standard potential.

The approach used considers both electrochemical and thermodynamic relationships.

A2.2. Procedure

In order to calculate the potential at which any electrochemical reaction takes place (E), the Nernst equation was derived to correct the standard value (E°) with the activities of each species involved in the reaction. Equation A2.1 shows the general reduction reaction and equation A2.2 the correspondent Nernst equation:



$$V = V^{\circ} - \frac{R \cdot T}{n \cdot F} \ln \left(\frac{[C]^c \cdot [D]^d}{[A]^a \cdot [B]^b} \right) \quad (\text{A2.2})$$

The Nernst equation corrects the standard potential (E°) with the activity of each species (the term inside the logarithm). Under certain conditions the

activity term can be replaced by the concentration (in square brackets, as shown in equation A2.2) or the partial pressure in case of gases.

The standard potentials at standard temperature can be found in electrochemistry books for a wide range of reactions, but it is not as common to find them calculated at other temperatures. Just for clarification, the temperature term that appears in the Nernst equation (equation A2.2) does not correct the standard potential with temperature. It simply modulates the impact that the activity term has: with higher temperatures, the activity correction has a higher influence. For that reason, the standard potential at 900°C (the working temperature of the SOFC) must be calculated using the Gibbs free energy of the reaction (at that temperature) and the relation of the Gibbs free energy with the standard potential of the reaction (equation A2.3):

$$V_T^0 = -\frac{\Delta_R G_T^0}{n \cdot F} \quad (\text{A2.3})$$

To obtain the Gibbs free energy of the reaction at a certain temperature, the Gibbs free energy of each species was considered at that same temperature, following equation A2.4 (when the general reduction reaction given by equation A2.1 is considered):

$$\Delta_R G_T^0 = c \cdot G_C^T + d \cdot G_D^T - a \cdot G_A^T - b \cdot G_B^T \quad (\text{A2.4})$$

In order to calculate the Gibbs free energy of each species at the temperature of interest, the following thermodynamic relationship was used (given by equation A2.5, where “x” denotes any of the species involved in the reaction):

$$G_x^T = H_x^T - T \cdot S_x^T \quad (\text{A2.4})$$

Finally, to calculate the properties at the desired temperature, T, the general thermodynamic equations A2.5 and A2.6 were used:

$$H_x^T = H_x^{T_0} + \int_{T_0}^T C_{p,x} \cdot dT \quad (A2.5)$$

$$S_x^T = S_x^{T_0} + \int_{T_0}^T \frac{C_{p,x}}{T} \cdot dT \quad (A2.6)$$

With this approach, it is possible to obtain the standard reaction potential at any temperature, given that both the enthalpy and the entropy at the standard state for each species - $H_x^{T_0}$, $S_x^{T_0}$ - as well as a temperature-dependent correlation for the constant pressure heat capacity for each species - $C_{p,x}(T)$ are available. Those values were taken from [1] for all the species involved in all the reactions considered throughout this dissertation. After that, the real reaction potential will be calculated using the correction for the activities of all species given by Nernst equation (equation A2.2) and the activities considered in each chapter.

The results obtained with this approach are reflected in Table 4.4, and Figures 4.10 and 4.11 in Chapter 4, as well as Table 5.6 and Figures 5.17 and 5.18 in Chapter 5.

A2.3. References

- [1] National Institute of Standards and Technology (NIST), web database.
<http://webbook.nist.gov/>

Consulted on 18/05/2011.

